Block and Graft Copolymers Containing Carboxylate or Phosphonate Anions

Nan Hu

Dissertation submitted to the faculty of the Virginia Polytechnic Institute and State University in partial fulfillment of the requirements for the degree of

Doctor of Philosophy

in

Chemistry

Judy S. Riffle
S. Richard Turner
Richey M. Davis
Kevin J. Edgar

September 26, 2014
Blacksburg, VA

Keywords: phosphonate, graft copolymers, polyelectrolytes, polyphosphonate, poly(acrylic acid), polyamide, poly(ethylene oxide), radical polymerization, ring-opening polymerization, ATRP

Block and Graft Copolymers Containing Carboxylate or Phosphonate Anions

Nan Hu
Department of Chemistry and the Macromolecules and Interfaces Institute,
Virginia Polytechnic Institute and State University,
Blacksburg, VA 24061, USA

Abstract

This dissertation focuses on synthesis and characterization of graft and block copolymers containing carboxylate or phosphonate anions that are potential candidates for biomedical applications such as drug delivery and dental adhesives.

Ammonium bisdiethylphosphonate (meth)acrylate and acrylamide phosphonate monomers were synthesized based on aza-Michael addition reactions. Free radical copolymerizations of these monomers with an acrylate-functional poly(ethylene oxide) (PEO) macromonomer produced graft copolymers. Quantitative deprotection of the alkylphosphonate groups afforded graft copolymers with zwitterionic ammonium bisphosphonate or anionic phosphonate backbones and PEO grafts. The zwitterionic copolymers spontaneously assembled into aggregates in aqueous media. The anionic copolymers formed aggregates in DMF and DMSO, while only small amounts of aggregates were present in copolymer/methanol or copolymer/water solutions. Binding capabilities of the acrylamide phosphonic acids were investigated through interactions with hydroxyapatite.

Previously our group has prepared poly(ethylene oxide)-*b*-poly(acrylic acid) (PEO-*b*-PAA) copolymers and used these polymers as carriers for both MRI imaging agents and cationic drugs. To enhance the capabilities of those carriers in tracking and crosslinking, we have designed, synthesized and characterized amine functionalized PEO-*b*-PAA copolymers. First, heterobifunctional poly(ethylene oxide) (PEO) with three different molecular weights were

synthesized. Modification on one of these afforded a PEO macroinitiator with a bromide on one end and a protected amine on the other end. ATRP polymerization of *tert*-butyl acrylate (*t*BuA) in the presence of this initiator and a copper (I) bromide (CuBr) catalyst yielded a diblock copolymer. The copolymer was deprotected by reaction with trifluoroacetic acid (TFA) and formed an amine terminated H_2N-PEO-*b*-PAA.

Recently our group has utilized the novel ammonium bisdiethylphosphonate (meth)acrylate and acrylamide phosphonate copolymers to incorporate Carboplatin. The resulting complexes exhibited excellent anticancer activity against MCF-7 breast cancer cells which might be related to ligand exchange of the dicarboxylate group of Carboplatin with the phosphonic acid moieties in the copolymer. Hence, complexation of small-molecule phosphonic acids with Carboplatin was investigated. Three compounds, vinylphosphonic acid, 3-hydroxypropyl ammonium bisphosphonic acid and 2-hydroxyethyl ammonium phosphonic acid were complexed with Carboplatin under acidic and neutral conditions. Covalent bonding of these acids to carboplatin was only observed under acidic pH. The covalently bonded percentage was 17%, 37% and 34%, respectively. More in-depth investigation was of great importance to further understand this complexation behavior.

This work is dedicated to my husband:

Chen Qian

My parents:

Yunpeng Li and Linshan Hu

and

My parents-in-law:

Jianhua Wang and Junhua Qian

Table of Contents

Acknowledgement

First, I would like to express my deepest thanks to my advisor, Dr. Judy S. Riffle, for her guidance and support during my time here at Virginia Tech. I appreciate her patience and confidence in me through my entire graduate career. She is an amazing, understanding and accommodating advisor. I am also thankful for my committee members, Dr. S. Richard Turner, Dr. Richey M. Davis and Dr. Kevin J. Edgar for their time and kind suggestions.

Recognition is definitely deserved for my collaborators who significantly contributed to this work; Dr. Yinnian Lin, Dr. Nikorn Pothayee, Dr. Nipon Pothayee, Rui Zhang, Lindsay M. Johnson, Shreya Roy Choudhury and Ashley Peralta. I would like to thank my dear colleagues and friends: Dr. Sharavanan Balasubramaniam, Dr. Oguzhan Celebi, Dr. Jue Liang, Ran Liu, Sanem Kayandan, Alfred Chen, Gurtej Narang, Greg Miller, Suzanne Barnes and Dr. Sue Mecham.

Thanks are also extended to the secretaries in Dr. Riffle's group, Angie Flynn, Mary Jane Smith and Cyndy Graham for keeping the daily activities of our group moving along smoothly.

Abbreviations

AHM 3-(acryloyloxy)-2-hydroxypropyl methacrylate

AIBN 2,2-azobis(2-methylpropionitrile)

AMG ammonium glycyrrhizinate

AMP adenosine monophosphate

antisense-ODN antisense-oligodeoxynucleotides

ATRP atom transfer radical polymerization

ATP adenosine triphosphate

BHT 2,6-di-*tert*-butyl-4-methylphenol

Bis-GMA 2,2-bis[4-(2-hydroxy-3-methacryloyloxy propyloxy) phenyl] propane

CaP calcium phosphate

CBPt carboplatin

ε-CL ε-caprolactone

CMP cyanomethyl potassium

CPt cisplatin

DABCO 1,4-diazabicyclo[2.2.2]octane

DEBAAP *N,N'*-diethyl-1,3-bis(acrylamido)propane

DLS dynamic light scattering

DMAP 4-dimethylaminopyridine

DMF dimethylformamide

DMSO dimethylsulfoxide

EO ethylene oxide

GDMA glycerol dimethacrylate

HAP hydroxyapatite

HMPA hexamethylphosphoramide

LDA lithium diisopropylamine

MEK methyl ethyl ketone

MMA methyl methacrylate

mPEO monomethoxy PEO

N-BPs nitrogen-containing bisphosphonic acids

NMR nuclear magnetic resonance spectroscopy

*Nn*PAAm *N*-*n*-propylacrylamide

ODN oligodeoxynucleotide

PAA poly(acrylic acid)

PAAm poly(acrylamide)

PAsp poly(aspartate)

P[Asp(DMEDA)] poly(aspartamide-*co*-*N,N*-dimethylethylenediamino aspartamide)

PB phosphate buffer

PBLA poly(β-benzyl $_{L}$-aspartate)

PCL poly(caprolactone)

PDI polydispersity index

pDNA plasmid DNA

PDT photodynamic therapy

PEI polyethyleneimine

PEO poly(ethylene oxide)

PGMA poly(glyceryl methacrylate)

PHEA poly(hydroxylethylacrylate)

PHPMA poly(*N*-2-(hydroxypropyl) methacrylamide)

PIC polyion complex

PMDETA N-N'-N'-N''-N''-pentamethyldiethylenetriamine

PNIPAM poly(isopropylacrylamide)

PSI poly(succinimide)

ROP ring opening polymerization

ROMP ring opening metathesis polymerization

SEC size exclusion chromatography

TBAB tetrabutyl ammonium bromide

TBPPI *tert*-butyl peroxypivalate

*t*Boc *tert*-butyoxycarbonyl

*t*BuMA *tert*-butyl methacrylate

TEA triethylamine

TFA trifluoroacetic acid

TEGDMA triethylene glycol dimethacrylate

THF tetrahydrofuran

TGA thermal gravimetric analysis

TMS-Br trimethylsilyl bromide

List of Figures

List of Tables

CHAPTER 1 - Introduction

Efforts to control drug delivery can be traced back to the late 1940s when the first sustained release drug using waxes was introduced.[1] In the past three decades, researchers have focused tremendously on developing novel drug delivery systems.[2-4] Major drawbacks for small-molecule drugs involve poor membrane permeability, short drug retention time and instabilities which lower the efficiency of drug delivery. The necessity of investigating polymeric carriers lies in the need for biocompatibility, enhancement of membrane permeability, enhanced stability, and sensitivity to pH and temperature, etc.[5]

Among different polymeric carriers, block copolymers have attracted significant attention due to their ability to form core-shell nanostructures in which drugs can be incorporated via covalent or non-covalent bonds.[6] Additionally, polymeric vesicles can be designed to facilitate site-specific drug delivery. Amphiphilic block copolymers are usually of interest since they contain both hydrophobic and hydrophilic parts that can load hydrophobic drugs and at the same time tune the solubility of the complexes.[7] Polyion complexes are of great importance in this field as well.[8] Polyion complexes consist of a block copolymer bearing a neutral hydrophilic block and an ionic block. In water, when substrates that bear complementary charges to the polyion block are introduced, the ionic species form a core of a nanostructure while the non-ionic water-soluble block will form a shell. In most cases, the counterions are biopharmaceuticals such as DNA, RNA, proteins or drugs. Due to electrostatic interactions between the ionic block and the counterions, charges are neutralized in these segments and they become hydrophobic, thus inducing micelle formation.[9]

In our initial work, we prepared poly(ethylene oxide) (PEO) and poly(acrylic acid) (PAA) block copolymers as polyion complexes for drug delivery.[10] The goal of this dissertation is to (1) design, synthesize and characterize graft copolymers containing phosphonate anions to enhance binding to inorganic cations; (2) understand relationships between phosphonic acid structure and binding to an antitumor drug, Carboplatin; (3) Functionalize the end group of poly(ethylene oxide)-b-poly(acrylic acid) copolymer to enable tracking and crosslinking capabilities.

Chapter 2 outlines a literature review on chemistry, properties and synthesis of (meth)acrylic phosphonates and PEO. It also covers synthesis and applications of a few representative PEO-containing polyion complexes for drug delivery systems.

Chapter 3 presents the synthesis of ammonium bisdiethylphosphonate acrylate and methacrylate monomers through a double aza-Michael addition of aminoalkyl alcohols in water followed by esterification. Conventional free radical copolymerizations of these monomers with acrylate-functional PEO macromonomers were carried out. It was found that copolymerizations with the methacrylate-functional ammonium phosphonate monomers incorporated both monomers efficiently while use of the acrylate-functional phosphonates produced heterogeneous blends of graft copolymers and homopolymers. These zwitterionic copolymers formed aggregates in water, likely due to electrostatic interchain attractions. Due to the biocompatibility, biodegradability and excellent binding capacities of the ammonium bisphosphonate methacrylate moieties, these graft copolymers might be employed as polymeric carriers for inorganic cations or metal-containing drugs and imaging agents for sustained drug release and real time tracking of drug distributions.

Chapter 4 describes synthesis and characterization of novel alkyl acrylamide phosphonate monomers. The amide linker between the vinyl bond and the phosphonate group possesses excellent hydrolytic stability which allows potential applications in dental adhesives. Again, conventional radical polymerization of the *n*-butylacrylamide phosphonate with acrylate-PEO yielded a statistical graft copolymer. The subsequent deprotection of the phosphonate ester groups was achieved leading to the poly(*n*-butylacrylamide phosphonic acid)-*g*-PEO copolymer. These phosphonic acid-containing copolymers are soluble in DMF, DMSO, methanol and water with adjusted pH. Further investigation on the self-assembly of the copolymer showed that it formed aggregates in DMF and DMSO, while only a small amount of aggregates were present in the copolymer/methanol or water solution. Binding properties of the *n*-butylacrylamide phosphonic acid to hydroxyapatite, the primary mineral on enamel, was investigated using a ^{13}C NMR approach. The novel phosphonic acid exhibited higher binding capacity to hydroxyapatite than acrylic acid which indicates promising potential of utilizing the *n*-butylacrylamide phosphonic acid in dental adhesives.

Chapter 5 describes the synthesis and characterization of amine functionalized PEO-*b*-PAA. A series of vinyl-PEO-OH with different molecular weights and low PDI's were synthesized using a double-metal cyanide catalyst. Post-functionalization of the hydroxyl group of the vinyl-PEO-OH led to a macroinitiator for ATRP. Utilization of the initiator for polymerization of *t*-butyl acrylate, then post-functionalization to form the amine and subsequent hydrolysis of the *t*-butyl esters yielded well-defined diblock copolymers, H_2N-PEO-*b*-PAA. The amine end-capped PEO-*b*-PAA can be employed for post-functionalization to achieve tracking and crosslinking purposes.

Our previous work[11] on encapsulating Carboplatin, an anticancer drug, into bisphosphonate copolymers showed remarkable anticancer efficacy against breast cancer cells. We hypothesized that this excellent property might be due to the replacement of ligand on Carboplatin by the phosphonate. Therefore, chapter 6 introduces the complexation of three model phosphonic acids with Carboplatin to understand the interaction between them. All of the three complexes showed some extent of covalent bonding to carboplatin, but only under acidic conditions. Further investigation might be conducted on characterization of the complexation products using UV-visible spectrometry and platinum NMR to obtain a more in-depth understanding of this complexation.

Chapter 7 concludes the work from the previous chapters and provides recommendations associated with this research.

1.1 References

1. Park, K.; Editor, *Controlled Drug Delivery: Challenges and Strategies*. ACS: 1997; p 629 pp.

2. Moses, M. A.; Brem, H.; Langer, R., Advancing the field of drug delivery: taking aim at cancer. *Cancer Cell* 2003, 4, 337-41.

3. Park, K., Facing the Truth about Nanotechnology in Drug Delivery. *ACS Nano* 2013, 7, 7442-7447.

4. Soppimath, K. S.; Aminabhavi, T. M.; Kulkarni, A. R.; Rudzinski, W. E., Biodegradable polymeric nanoparticles as drug delivery devices. *J. Controlled Release* 2001, 70, 1-20.

5. Timko, B. P.; Whitehead, K.; Gao, W.; Kohane, D. S.; Farokhzad, O.; Anderson, D.; Langer, R., Advances in drug delivery. *Annu. Rev. Mater. Res.* 2011, 41, 1-20.

6. Gaucher, G.; Dufresne, M.-H.; Sant, V. P.; Kang, N.; Maysinger, D.; Leroux, J.-C., Block copolymer micelles: preparation, characterization and application in drug delivery. *J. Controlled Release* 2005, 109, 169-188.

7. Miyata, K.; Christie, R. J.; Kataoka, K., Polymeric micelles for nano-scale drug delivery. *React. and Funct. Polym.* 2011, 71, 227-234.

8. Lee, Y.; Kataoka, K., Biosignal-sensitive polyion complex micelles for the delivery of biopharmaceuticals. *Soft Matter* 2009, 5, 3810-3817.

9. Kabanov, A. V.; Vinogradov, S. V.; Suzdaltseva, Y. G.; Alakhov, V. Y., Water-Soluble Block Polycations as Carriers for Oligonucleotide Delivery. *Bioconjugate Chem.* 1995, 6, 639-643.

10. Ranjan, A.; Pothayee, N.; Seleem, M.; Jain, N.; Sriranganathan, N.; Riffle, J. S.; Kasimanickam, R., Drug delivery using novel nanoplexes against a Salmonella mouse infection model. *J. Nanopart. Res.* 2010, 12, 905-914.

11. Pothayee, N.; Pothayee, N.; Hu, N.; Zhang, R.; Kelly, D. F.; Koretsky, A. P.; Riffle, J. S., Manganese graft ionomer complexes (MaGICs) for dual imaging and chemotherapy. *J. Mater. Chem. B* 2014, 2, 1087-1099.

CHAPTER 2 - Literature Review

2.1 Overview

The aim of our laboratory is to design core-shell nanostructures to carry both diagnostic and therapeutic agents. To achieve this goal, it is necessary to synthesize graft or block copolymers possessing biocompatibility and functional architectures to incorporate drugs and imaging agents. This literature review is focused on discussion directly related to these research topics and is divided into two sections. The first section covers an overview of phosphonate chemistry, synthesis and applications of methacrylic phosphonate monomers and polymers. The second section discusses properties and synthesis of PEO and PEO-containing polyions.

2.2 Chemistry, Synthesis and Applications of Phosphonate or Phosphonic acid-containing Monomers and Polymers

2.2.1 Phosphonate and Phosphonic acid

Interest in phosphorus-containing substrates has continued to expand in recent years. Phosphonates and phosphonic acids (Figure 2.1) represent a significant class of pentavalent organophosphorus compounds. They are well-known to be more hydrolytically stable than the phosphate derivatives due to the C-P bond compared to the C-O-P bond. Therefore, phosphonates and phosphonic acids have found their wide applications as flame retardants, adhesives, proton exchange membranes and in biomedicines.[1-4]

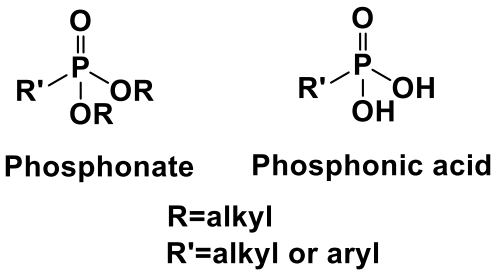

Figure 2.1 Structures of phosphonate and phosphonic acid

Phosphonic acids can be obtained by deprotection of phosphonates under various conditions.[5-8] However, the use of trimethylsilyl bromide[9] (TMS-Br) has dominated because of its high efficiency of deprotection without cleavage of hydrolytically-sensitive bonds, such as esters. This specific deprotection proceeds through a mechanism with silyl intermediates (Figure 2.2). Similar to phosphonates, the phosphorus in the phosphonic acid is sp^3 hybridized and thus the geometry of the molecule is close to tetrahedral. Phosphonic acids are diprotic as the pKa_1 ranges from 0.5 to 3 and pKa_2 is between 5 and 9.[10] The second dissociation constant lies in the physiological range. This might lead to pH-dependent drug release for phosphonic acid-containing drug carriers. In comparison with carboxylic acids, phosphonic acids share a number of similarities but also exhibit some differences from the carboxylic analogues.

a) Phosphorus is less electronegative than carbon which makes the P-O bond more polar than the C-O bond.

b) Phosphonic acids possess three oxygen atoms available for coordination while carboxylic acids only have two oxygen atoms. This increases possibilities of preparing more structurally varied compounds.

c) Phosphonic acids can be fully protonated, or single or doubly deprotonated while carboxylic acids can only be in the fully protonated or deprotonated form. This also allows phosphonic acids to have varied structures depending on pH.

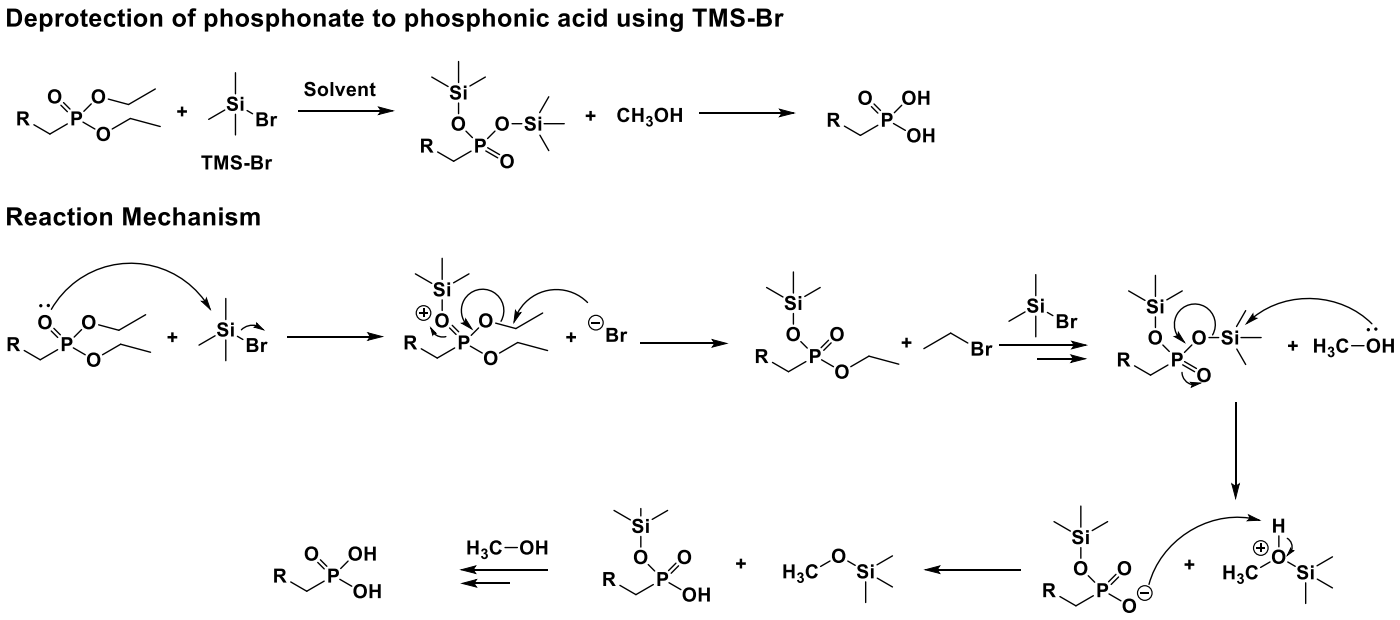

Figure 2.2 Deprotection and reaction mechanism of diethylphosphonate treated with TMS-Br

Due to their multidentate nature, phosphonic acids are able to bind to metal or metal oxide surfaces in different ways. Mutin *et al.* have proposed some possible binding modes (Figure 2.3) for interactions between phosphonic acids and titania (TiO_2) surfaces.[11] Phosphonic acids usually bind to the titanium oxide surface via a Ti-O-P bond which results from a condensation reaction of P-OH and Ti-OH groups and from coordination of phosphoryl oxygen to the titanium surface. This leads to a variety of bonding types including monodentate, bidentate and tridentate. The multidentate modes can be further divided into bridging and chelating. Bridging corresponds to oxygen atoms from one phosphonic acid group binding to different titanium atoms while chelating is oxygen atoms coordinating to the same titanium atom.

Additionally, phosphonic acid can interact with an adjacent phosphonic acid group, a hydroxyl group and an oxygen atom on the titania surface through hydrogen bonding. Some of these binding modes can possibly be extended to other phosphonic acid and metal or metal oxide systems.

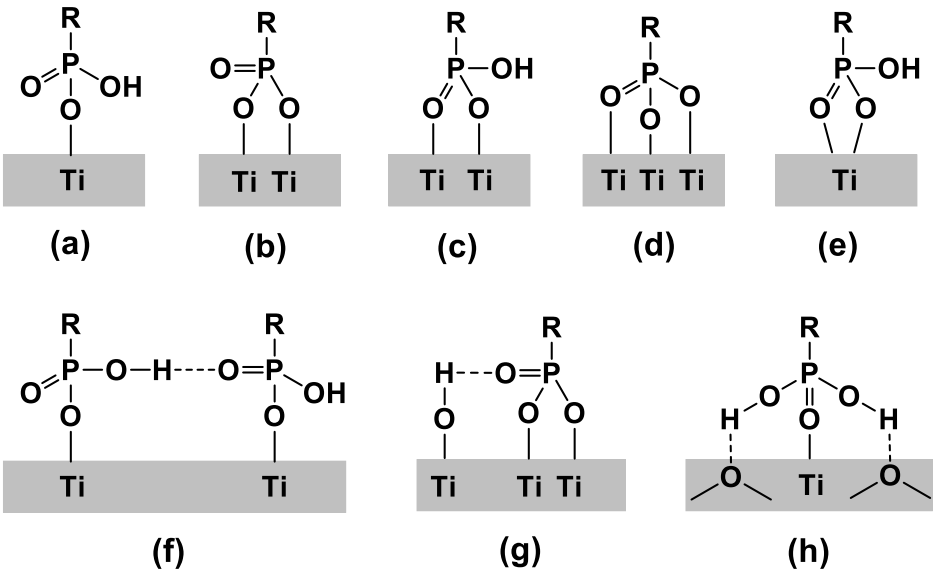

Figure 2.3 Schematic representation of some possible binding modes of phosphonic acid to a titania surface: (a) monodentate, (b,c) bridging bidentate, (d) bridging tridentate, (e) chelating bidentate, (f-h) additional hydrogen bonding interactions. Adapted from Mutin *et al.*[11] with modification

Geminal bisphosphonic acids (Figure 2.4) are among the most intensively studied phosphonic acids during the last four decades.[12-15] Their stability against acidic hydrolysis and their ability to chelate cations in solution enables these compounds to be employed in various biomedical applications. Geminal bisphosphonic acids are structural analogues of naturally occurred pyrophosphates (Figure 2.4) with a carbon replacing the oxygen in pyrophosphates. Inorganic pyrophosphate can be released from the hydrolysis of ATP to AMP in the body.[16] It

prevents calcification and regulates bone mineralization by inhibiting hydroxyapatite (HAP) deposition.[17, 18] Due to the P-O-P bond, pyrophosphate hydrolyzes under acidic conditions, thus limiting its application in oral medications. The more stable geminal phosphonic acids with a P-C-P bond were thus synthesized and investigated. Besides being alternatives for pyrophosphate, geminal phosphonic acids also act as inhibitors of bone resorption. Many bisphosphonic acids have been applied clinically to treat bone-related diseases, especially osteoporosis.[19] The first generation for this type of drugs included etidronate and clodronate (Figure 2.5). The second generation featured nitrogen-containing bisphosphonic acids (N-BPs) in which there is at least one nitrogen atom. Examples of these N-BPs are neridronate, alendronate, ibandronate, risedronate, zoledronate and minodronate (Figure 2.5). The second generation N-BPs have replaced the first generation in the market since the N-BPs exhibited higher anti-resorptive potency.[20] The N-BPs can inhibit farnesylpyrophosphate synthase, a key enzyme within osteoclast cells responsible for bone resorption. The phosphonate chelates the aspartate-rich part of the enzyme through a magnesium ion, while the nitrogen orients to hydrogen-bond with active hydroxyl and carbonyl groups of the enzyme.[21] A complete understanding of the inhibition behavior of the N-BPs remains under investigation, but it has been shown that the nitrogen on the side chain of the bisphosphonic acids is critical for this process.[22]

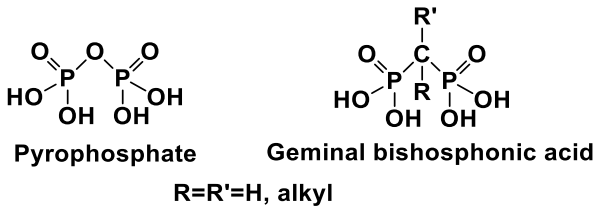

Figure 2.4 Structures of pyrophosphate and geminal bisphosphonic acids

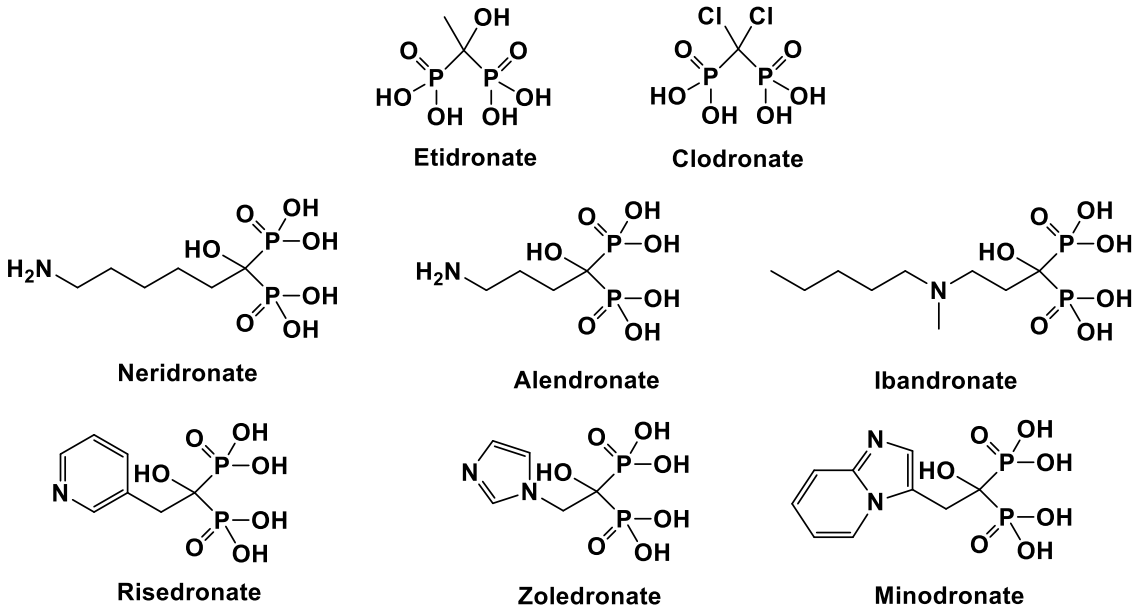

Figure 2.5 Clinically used bisphosphonic acids

Aminophosphonic acids (Figure 2.6) are phosphorus analogues of amino acids (Figure 2.6) which have also attracted tremendous attention. Horiguchi and Kandatsu first discovered and isolated 2-aminoethylphosphonic acid from living organisms in 1959.[23] Investigations of the synthesis and modifications of aminophosphonic acids accelerated greatly in the last 40 years due to their diverse potential for therapeutic and diagnostic applications.[24] Like the geminal bisphosphonic acids, aminophosphonic acids are also utilized as enzyme inhibitors. Various inhibition mechanisms have been proposed including direct coordination to the active sites of enzymes, mimicking the tetrahedral transition state of the substrate for enzymes, binding to the enzyme-substrate complex and other mechanisms.[25] Characterized by their inhibition properties, aminophosphonic acids exert their biological activities in antibiotics, antithrombotics, neuroactive agents and HIV protease inhibitors.[26]

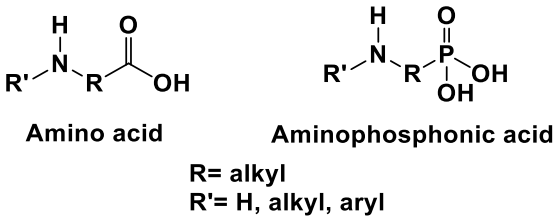

Figure 2.6 Structures of amino acids and aminophosphonic acid

2.2.2 Synthesis and Applications of Phosphonate Monomers and Polymers

Numerous investigations have been conducted on phosphonate monomers suitable for radical (co)polymerization including allyl-, styrenic-, vinyl- and (meth)acrylic-based phosphonates.[27-34] (Meth)acrylic phosphonates are of special interest due to their relatively high reactivity toward free radical polymerization. In this section, different synthetic approaches are reviewed regarding the preparation of (meth)acrylate and (meth)acrylamide phosphonate monomers (Figure 2.7) and their radical (co)polymerizations. The (meth)acrylate phosphonate monomers can be further categorized into phosphonate linked to the vinyl bond and phosphonate linked to the ester.

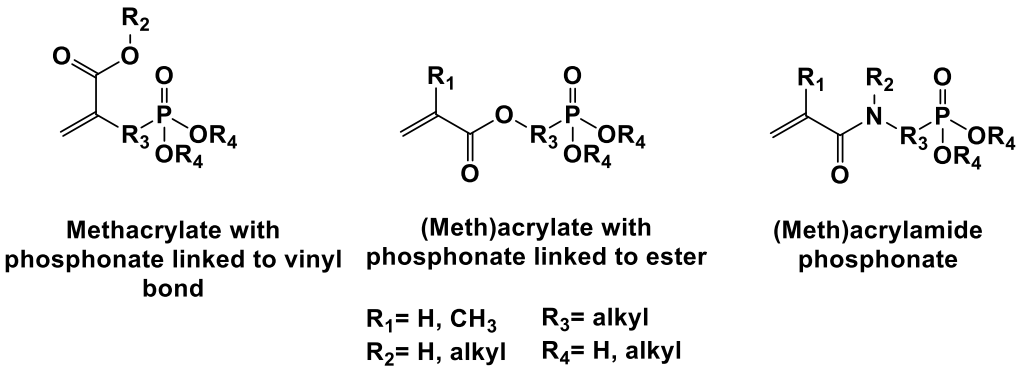

Figure 2.7 Structures of (meth)acrylate and (meth)acrylamide phosphonates

2.2.2.1 Synthesis of (Meth)acrylate Phosphonate Monomers and Polymers

2.2.2.1.1 (Meth)acrylates with Phosphonate Linked to the Vinyl Bond

Only a few papers have been published on this type of monomer.[35, 36] These monomers and the corresponding polymers are considered to be hydrolytically stable since the phosphonate is connected to the vinyl bond by an alkyl spacer. In case of hydrolysis, only the ester bond of the methacrylate would cleave while the phosphonic acid would remain linked to the vinyl bond or the backbone of the polymer. Moszner and coworkers[36] synthesized three methacrylate monomers with phosphonate linked to the vinyl bond through etherification of ethyl α-chloromethyl acrylate with hydroxyl bearing phosphonates (Figure 2.8). The phosphonates were then deprotected using TMS-Br to yield phosphonic acid monomers. Free radical polymerizations of these monomers were initiated by AIBN at 65°C in THF. Polymerization of the diacrylate phosphonates yielded crosslinked networks. These networks were found to be insoluble in solvents including methanol, THF and water/ethanol mixtures.

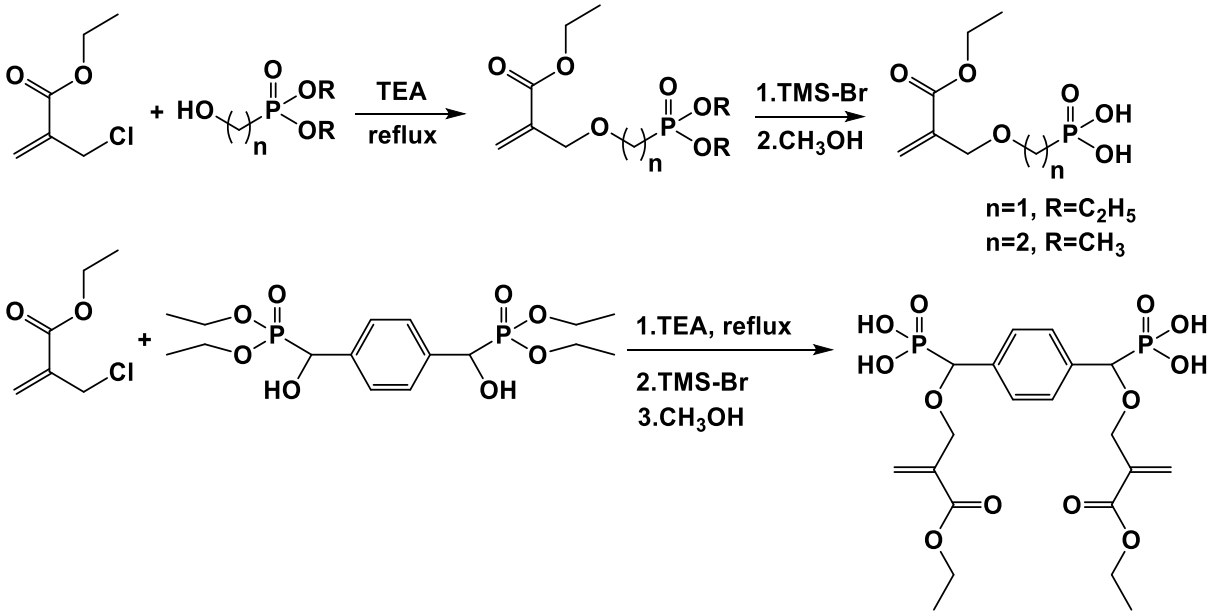

Figure 2.8 Synthesis of methacrylate monomers with phosphonate linked to the vinyl bond by etherification

Avci's group contributed more in-depth studies on the methacrylate monomers with phosphonates linked to the vinyl bond. They synthesized both alkyl and aromatic phosphonates through esterification and similar etherification reactions[35, 37, 38] (Figure 2.9) as in Moszner *et al*[36]. For the aromatic monomers, after deprotection of the phosphonates with TMS-Br, trifluoroacetic acid (TFA) was added to hydrolyze the *t*-butyl ester bond which resulted in methacrylate monomers with both phosphonic and carboxylic acid functionalities (Figure 2.9). All of the alkyl and aromatic phosphonate monomers were polymerized by thermal or photo-initiation. The aromatic monomers exhibited chain transfer behavior which was explained by abstraction of the α-methylene hydrogens. Due to the chain transfer, copolymers formed with the aromatic monomers and acrylamide had lower molecular weights than the acrylamide homopolymer. Avci and coworkers also developed a series of aminophosphonate-containing dimethacrylates by reaction of diethyl aminophosphonates with α-bromomethylacrylates (Figure 2.10).[39] Interestingly, these monomers were able to produce soluble cyclic polymers or insoluble crosslinked polymers depending on the monomer structures and polymerization conditions. Formation of cyclic units was attributed to the special 2,6-disubstituted 1,6-heptadiene structure which could undergo intramolecular cyclization in competition with intermolecular addition.[40] When the monomers were bulk polymerized, those with the longer alkyl spacers between the nitrogen and the phosphonate group cyclopolymerized more effectively.

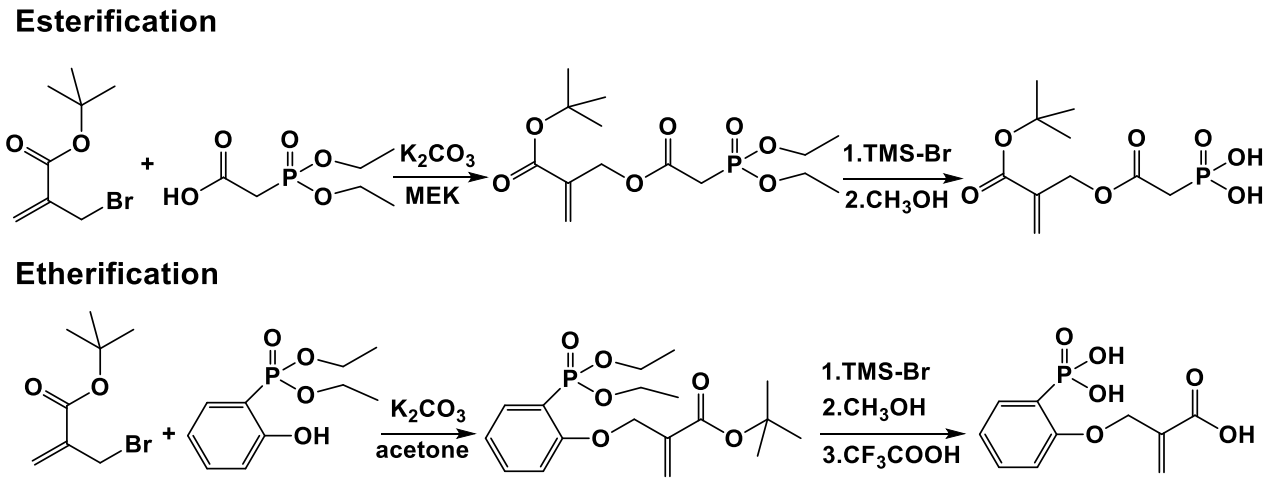

Figure 2.9 Synthesis of alkyl and aromatic phosphonates linked to the vinyl bond by esterification and etherification

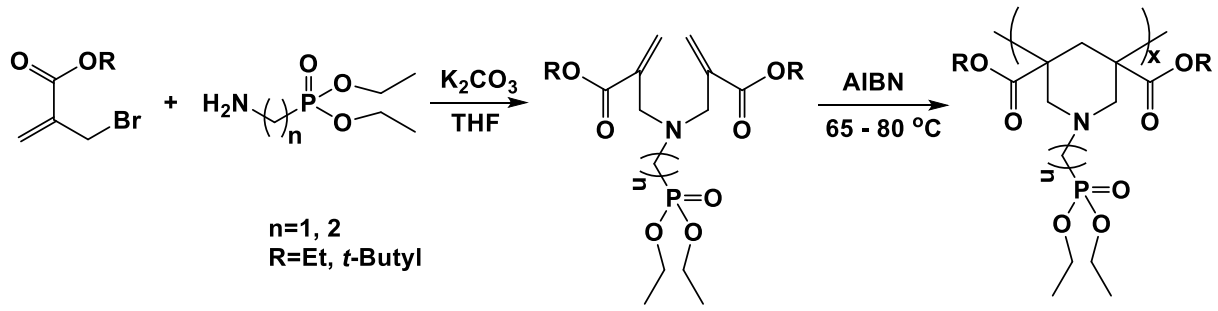

Figure 2.10 Synthesis and cyclopolymerization of aminophosphonate dimethacrylates

More recently, Avci *et al.* have prepared geminal bisphosphonate methacrylates[41, 42] using the same esterification and etherification approach (Figure 2.11). They conducted both homo- and copolymerizations with methacrylate-PEO. It was shown that conversion of the homopolymerization ranged from 22 to 34% in 3.5-5.0 h. The low conversion was attributed to the labile hydrogen on the carbon connecting the geminal bisphosphonates which might have undergone chain transfer. Copolymerizations of the monomers with methacrylate-PEO (M_n = 950 g mol^{-1}) was carried out in the presence of AIBN at 65°C in methanol. In all of those

copolymerizations, the methacrylate-PEO macromonomer incorporated into the copolymers quickly and approximately a 12 to 23 % higher PEO content was in the copolymers compared to the feed ratios. This indicated the methacrylate-PEO had a higher reactivity relative to the bisphosphonate methacrylates.

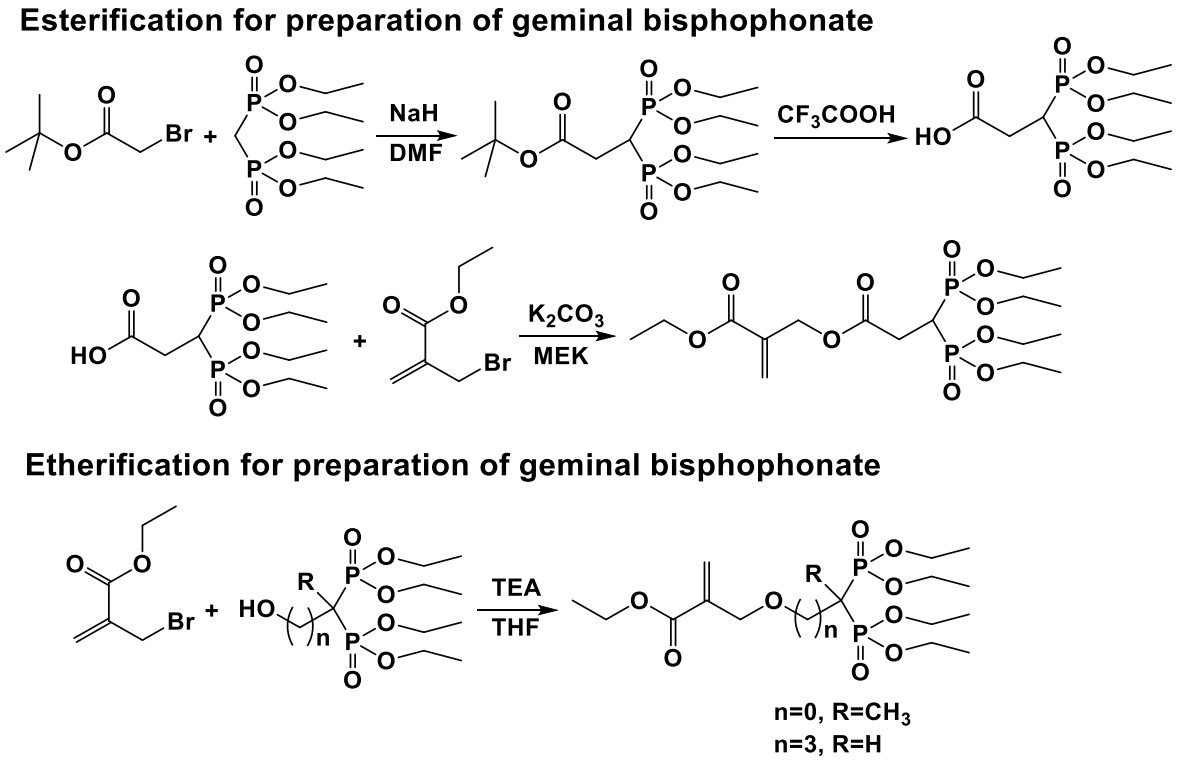

Figure 2.11 Synthesis of geminal bisphosphonate bearing methacrylates

2.2.2.1.2 (Meth)acrylates with Phosphonate Linked to the Ester

This class of (meth)acrylic phosphonate monomers has been extensively investigated. The early studies on these monomers date back to the 1970s.[43] Different reactions have been employed to synthesize this group of monomers including four major types: Michaelis-Arbuzov reaction,[44] free radical telomerization,[45] Kabachnik-Field reaction[46] and Michael addition.[47]

Most of the synthetic routes introduced in the following section utilize at least one of these reactions.

Boutevin and coworkers have played an important role in this field during the last two decades. Boutevin first synthesized two (meth)acrylate phosphonates with a thioether linker by a three-step procedure.[48, 49] The first step is a Michaelis-Arbuzov reaction using triethylphosphite and allyl bromide followed by a thiol-ene reaction and (meth)acrylation (Figure 2.12). To determine the reactivities, kinetic studies on copolymerization of the two phosphonate monomers with 2,3-epoxypropyl methacrylates were performed. Slight reactivity differences were observed between the epoxide methacrylate (r_1=1.1) and the methacrylate phosphonate monomer (r_2=0.9). However, the reactivity of epoxide methacrylate (r_1=2.4) was much higher than the acrylate phosphonate (r_2=0.9) probably because of the more reactive methacrylate moiety.

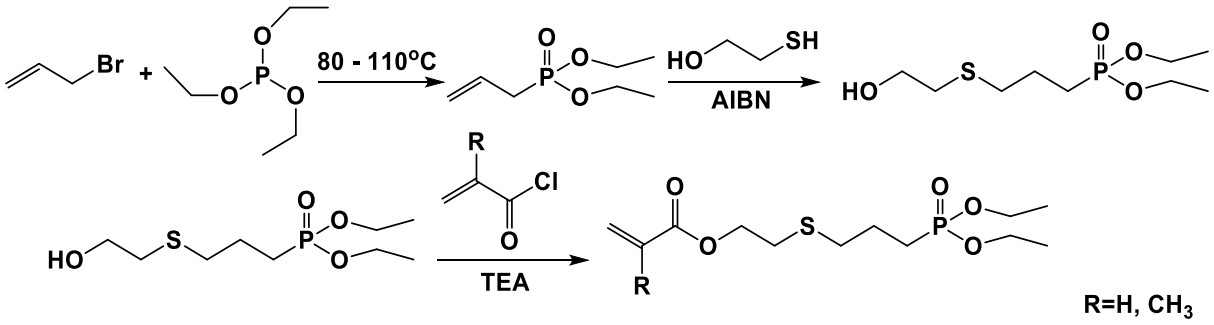

Figure 2.12 Synthesis of (meth)acrylate phosphonates with a thioether linker

Free radical telomerization was also conducted by Boutevin and coworkers followed by methacrylation to prepare methacrylate phosphonates with long alkyl spacers[50, 51] (Figure 2.13). The mechanism of telomerization includes generation of a phosphonyl radical by di-*tert*-butyl peroxide, propagation of the phosphonyl radical with vinyl alcohols and abstraction of a proton from the hydrogenphosphonate to the vinyl radical (Figure 2.13). Francová *et al*.[52, 53] employed a

similar method by changing the peroxide initiator to AIBN for synthesizing methacrylate phosphonates with two different alkyl spacers (C_3 and C_{11}).

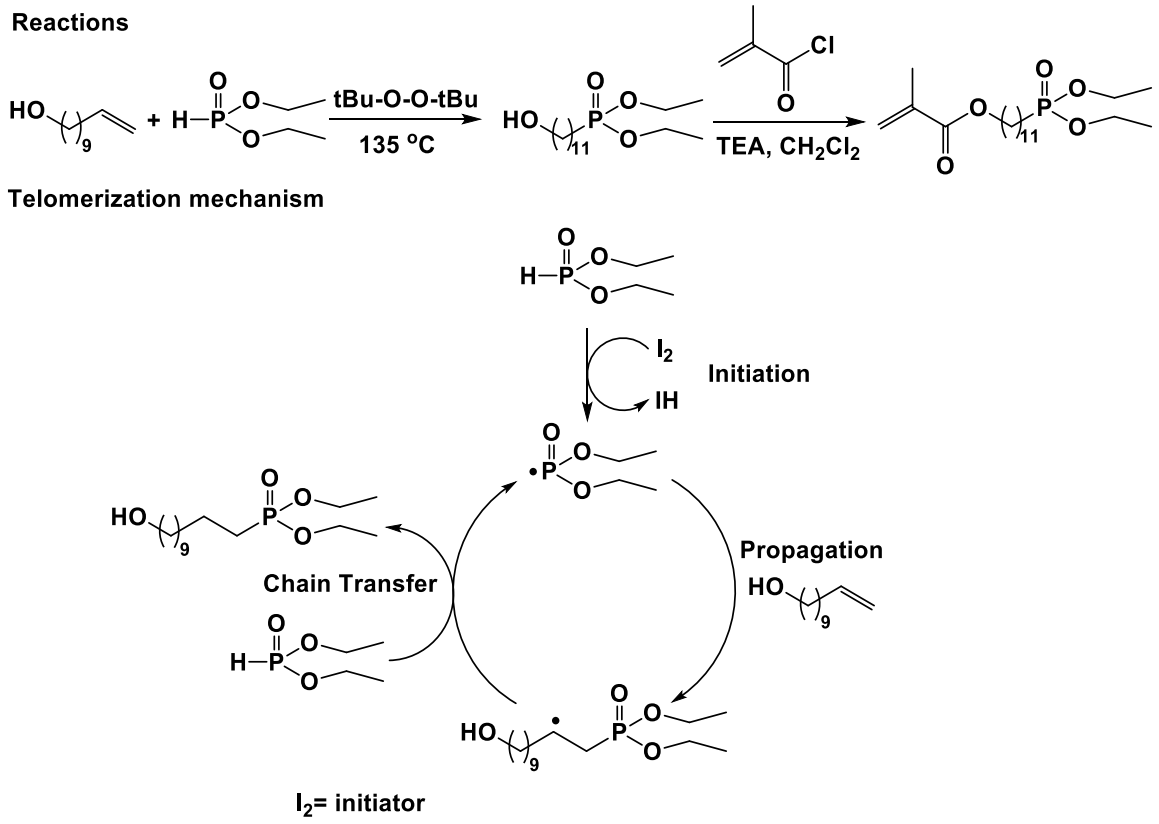

Figure 2.13 Synthesis of methacrylate phosphonate by telomerization

Despite the frequently used esterification reaction, Boutevin and coworkers also applied urethane chemistry to prepare (meth)acrylate phosphonate monomers.[54] The urethane-containing monomers can be obtained through the direct reaction of 2-isocyanatoethyl methacrylate with dimethyl hydroxy alkylphosphonate (Figure 2.14). To prevent formation of urea, the reactants were completely dried prior to reaction. Subsequent treatment with TMS-Br and methanol yielded phosphonic acid derivatives.

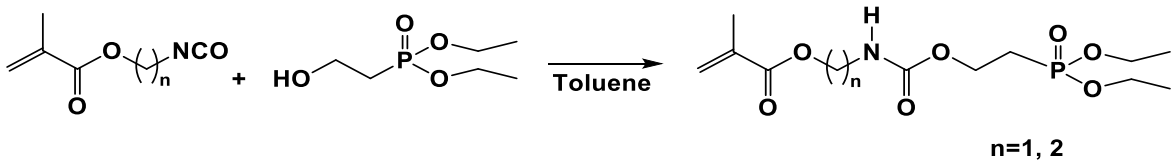

Figure 2.14 Synthesis of urethane-containing methacrylate phosphonate monomers

Another important reaction Boutevin and coworkers[28, 55, 56] utilized was the Kabachnik-Fields reaction. This approach requires a primary amine, a hydrogen phosphonate and an aldehyde. The aldehyde reacts with the amine by condensation and releases water leading to the formation of a C=N bond.[57] The hydrogen phosphonate adds to the C=N bond to generate a monophosphonate. The secondary amine can further react with excess aldehyde and hydrogen phosphonate to obtain an aminobisphosphonate with a hydroxyl end. Subsequent methacrylation leads to the aminobisphosphonate methacrylate monomers (Figure 2.15). The authors copolymerized the aminobisphosphonates with MMA initiated by AIBN in chloroform under reflux. The reactivity ratios calculated for the aminobisphosphonates (r_1) and the MMA (r_2) were 1.1-1.3 and 0.8, respectively. These values indicated that MAA only slightly tends to homopolymerize instead of copolymerize with the aminobisphosphonates. Therefore, statistical copolymers were formed during copolymerization but with a higher content of MMA.

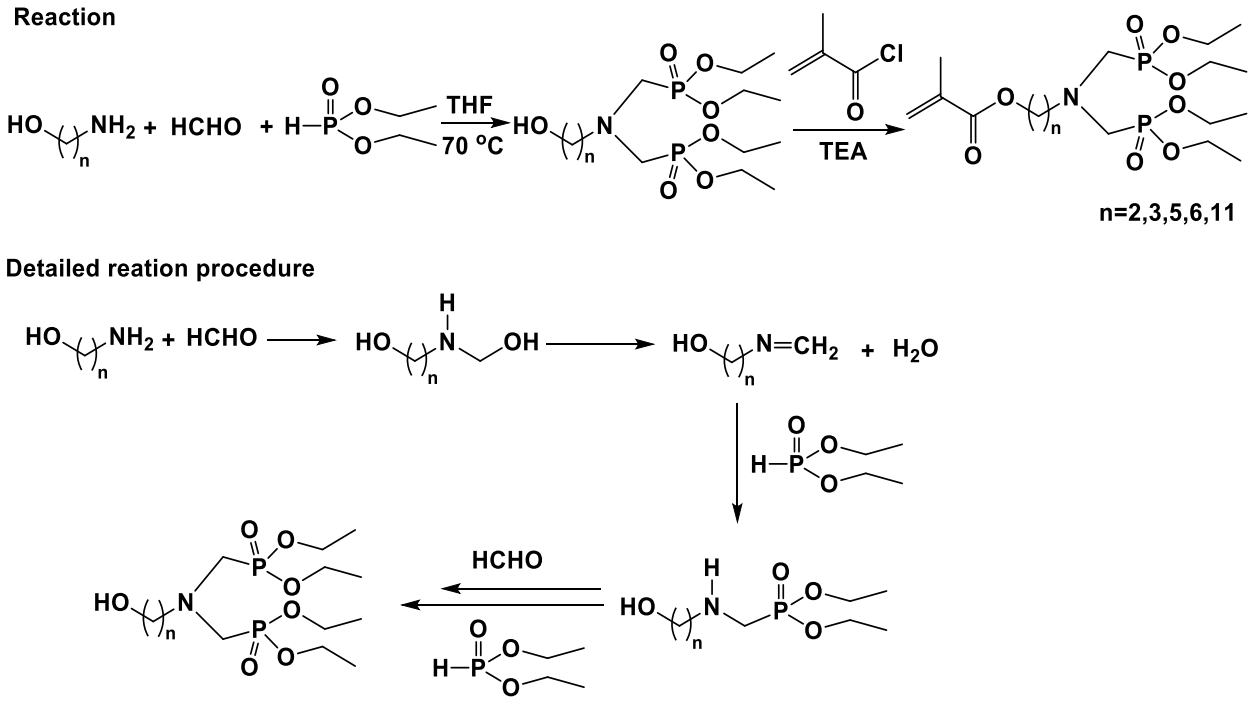

Figure 2.15 Synthesis of methacrylate aminobisphosphonates by the Kabachnik-Fields reaction

A methacrylate phosphonate synthesized through epoxide bearing compounds has been prepared (Figure 2.16) by Boutevin's group as well.[58] The first step included synthesis of an epoxide-phosphonate precursor. The second step was ring opening of the epoxide with methacrylic acid catalyzed by tetrabutylammonium bromide (TBAB). Copolymerization of MMA with this epoxide-based methacrylate phosphonate monomer was conducted in the presence of AIBN at 80°C in acetonitrile. The reactivity ratios of the phosphonate (r_1) and MMA (r_2) were determined as 1.19 and 0.80, respectively revealing the formation of statistical copolymers. Terpolymerization of the phosphonate (10 mol%), MMA (40 mol%) and *t*BuMA (50 mol%) was carried out in the presence of benzene thiol, a chain transfer agent. The molar ratio in the terpolymer was 8 mol%, 46 mol% and 46 mol% for the three monomers which was

in close agreement to that targeted. The terpolymer was then deprotected to yield a phosphonic acid-containing polymer as a component for anti-corrosive coatings.

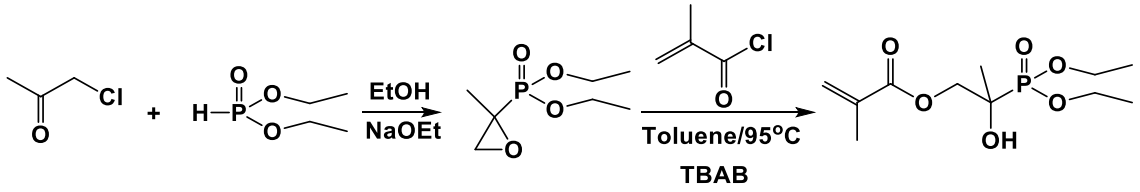

Figure 2.16 Synthesis of methacrylate phosphonate through epoxide

Avci's group has made contributions in this area as well. They synthesized aromatic phosphonates[59, 60] using the same hydroxyphenyl phosphonate precursor as for the ether linked methacrylate phosphonate.[38] The hydroxyl group was reacted with methacryloyl chloride to produce methacrylate phosphonates (Figure 2.17). Photocopolymerization of the two phosphonate monomers were carried out with 2,2-bis[4-(2-hydroxy-3-methacryloyloxy propyloxy) phenyl] propane (bis-GMA), a diacrylate used in dental applications. Conversion of the bis-GMA was increased in copolymerization with the phosphonate monomer compared to its homopolymerization.

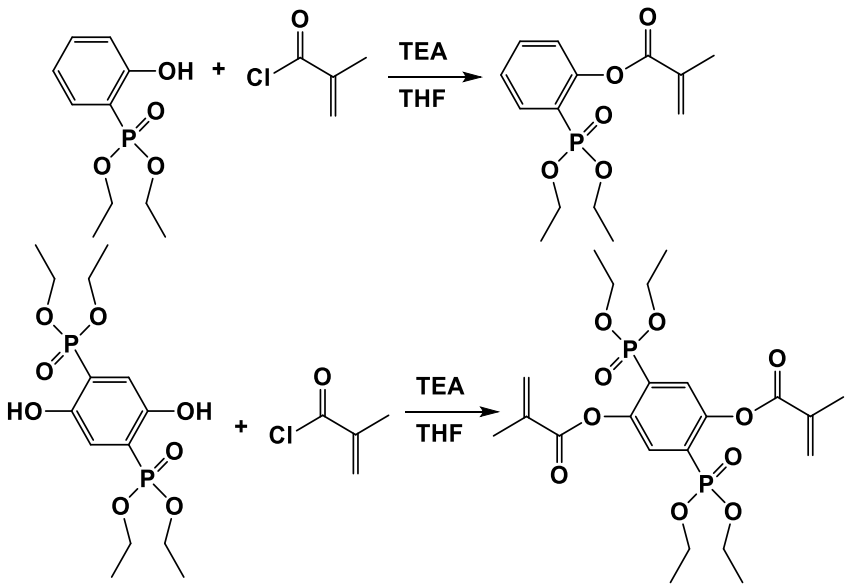

Figure 2.17 Synthesis of methacrylate phosphonates by hydroxylphenyl phosphonate

Employing similar chemistry as Boutevin[58] but using different compounds, Avci *et al.* prepared three methacrylate phosphonates synthesized from epoxides. The synthesis relied on either carboxylic phosphonate or hydroxyl phosphonate reacting with glycidyl methacrylate or bisphenol A diglycidylether catalyzed by a base (Figure 2.18). These monomers were copolymerized with glycerol dimethacrylate (GDMA), triethylene glycol dimethacrylate (TEGDMA) and bis-GMA through photopolymerization.

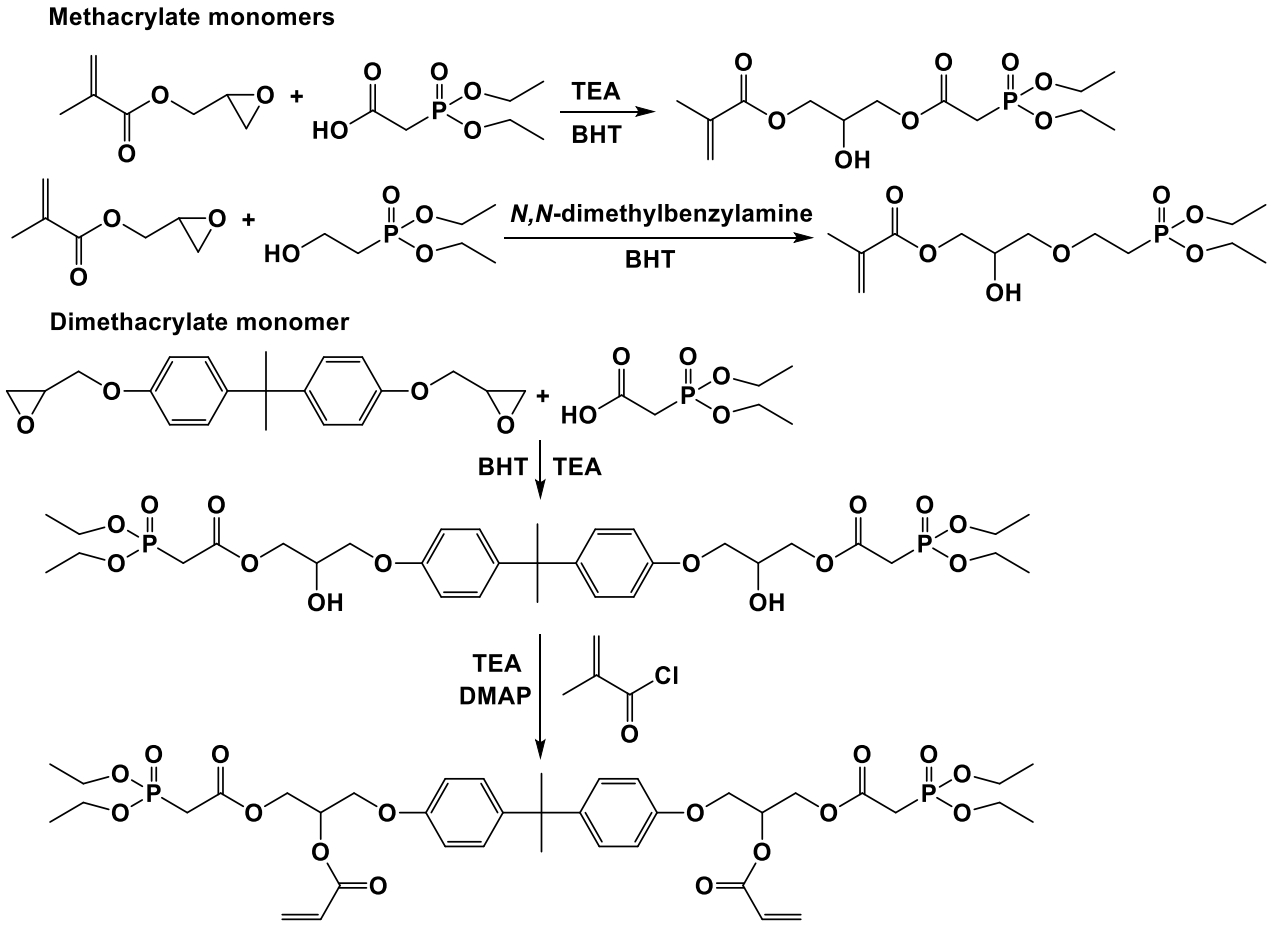

Figure 2.18 Synthesis of methacrylate and dimethacrylate phosphonate monomers by reaction of alcohols or carboxylic acids with epoxides.

Michael addition has also been employed by Avci and coworkers[39] to prepare two aminophosphonates. Diethyl aminophosphonate or diethyl 2-aminophosphonate was added to the vinyl bond of 3-(acryloyloxy)-2-hydroxypropyl methacrylate (AHM) (Figure 2.19). A second addition of the amine to another vinyl bond was not successful which was explained by the steric hindrance or electron withdrawing effect of the phosphonate group. Homopolymerization of these phosphonate monomers initiated by AIBN at 60 °C yielded cross-linked networks. This was attributed to possible hydrogen abstraction around the amine group inducing chain transfer.

The reactivity of these phosphonates was higher than the AHM precursor in photopolymerization which might be again due to the hydrogen-bonding capability of the amine group. Preorganization of monomers bearing amide, urethane and urea functionalities via hydrogen-bonding could make the double bonds closer to each other, thus accelerating the polymerization rate.[61]

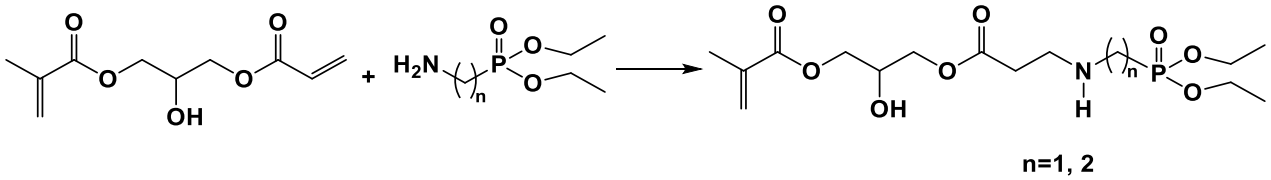

Figure 2.19 Synthesis of aminophosphonate monomers via Michael addition

Urea-containing methacrylate phosphonates were recently synthesized by Avci *et al*.[62] Two urea-bearing phosphonates were synthesized from aminophosphonates reacting with 2-isocyanatoethyl methacrylate (Figure 2.20). The aminophosphonates were obtained from two approaches. The first was aminolysis of diethyl phthalimidomethylphosphonate using hydrazine monohydrate in ethanol. The second included reaction of benzylaldehyde, ammonium carbonate and hydrogen phosphonate catalyzed by aluminum triflate. Copolymerization of the two phosphonates with HEMA and bis-GMA was conducted by photoinitiation. The enhancement by phosphonates of the polymerization rate of HEMA was probably due to the same hydrogen-bonding effect[61] stated in the last paragraph.

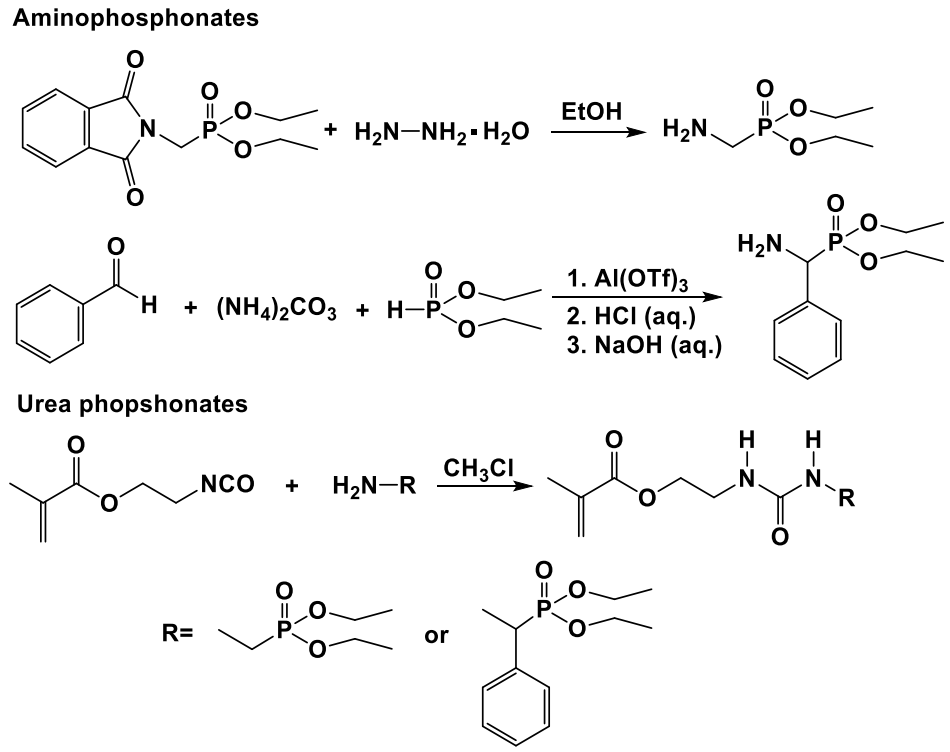

Figure 2.20 Synthesis of urea-containing methacrylate phosphonates

Ikemura's team[63-65] is another group who have designed syntheses of phosphonic acid monomers. They prepared phosphonic acid monomers with carboxylic acid functionalities in a two-step procedure (Figure 2.21). The first step was comprised of ring opening of β-propiolactone with triethylphosphite to produce 2-carboxyethylphosphonic acid. This compound was then reacted with hydroxyalkyl(meth)acrylates by esterification. The monomers were polymerized using initiators including benzoyl peroxide, *N,N*-di(hydroxyethyl)-*p*-toluidine and 1-benzyl-5-phenyl barbituric acid.

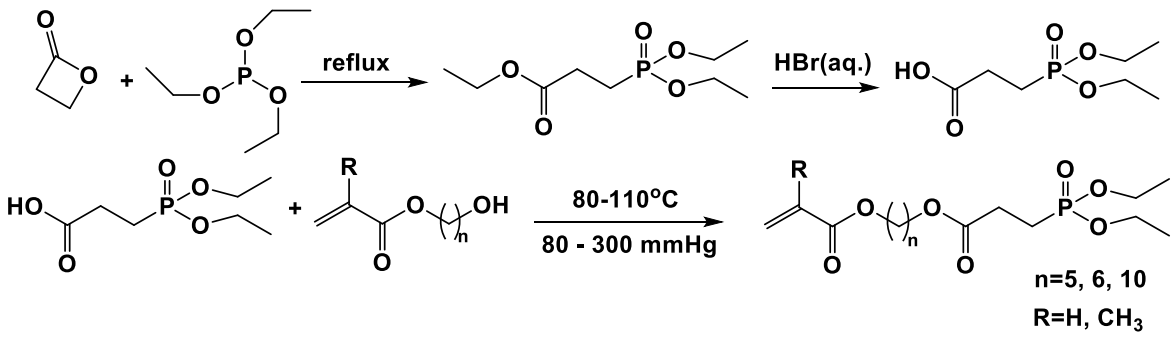

Figure 2.21 Synthesis of phosphonic acid monomers with carboxylic acid functionalities based on ring-opening reactions

2.2.2.2 Synthesis of (Meth)acrylamide Phosphonate Monomers and Polymers

(Meth)acrylamide phosphonate monomers and polymers are gaining more attention since they exhibit improved hydrolytic stability under acidic conditions compared to the methacrylate analogues.[66] Synthesis of (meth)acrylamide phosphonates usually includes preparation of amino alkylphosphonate and (meth)acrylation of the amine.

Xu *et al.* synthesized two methacrylamide phosphonic acid monomers (Figure 2.22).[67] The alkyl monomer was prepared by direct reaction of commercially available 2-aminoethylphosphonic acid with methacryloyl chloride. The aromatic monomer was obtained through a four-step procedure. After ring-opening of bisphenol A diglycidyl ether with ammonia, the amines were reacted with diethyl(2-bromoethyl)-phosphonate, followed by methacrylation and hydrolysis of the phosphonate group to yield the aromatic methacrylamide phosphonate monomer. The methacrylamidoethyl phosphonic acid was shown to be more hydrolytically stable than a reference compound, 2-methacryloyloxyethyl phosphoric acid by electrospray mass spectrometry.

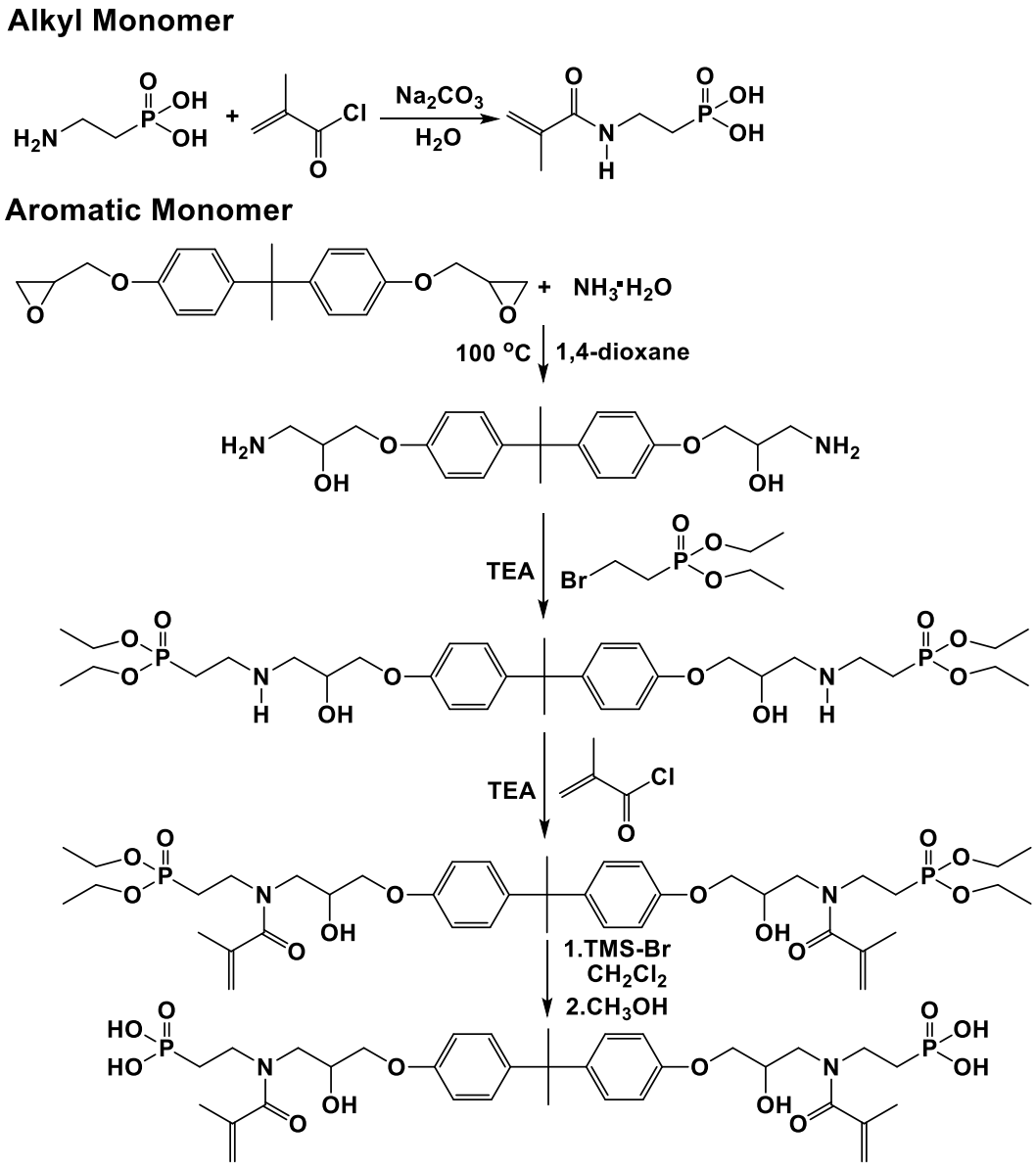

Figure 2.22 Synthesis of an alkyl and an aromatic acrylamide phosphonate monomer

Le Pluart and coworkers contributed in-depth investigations of synthesis and characterization of acrylamide phosphonates and phosphonic acids. They developed a four-step procedure (Figure 2.23) based on the Michaelis-Arbuzov reaction to prepare acrylamido phosphonic acid monomers with alkyl or ether spacers.[29, 68] Homopolymerizations of these monomers were carried out in water/ethanol mixtures due to the polar nature of the phosphonic

acid. This group also studied polymerization kinetics of the alkyl acrylamide phosphonate and phosphonic acid.[69, 70] The phosphonic acid monomers showed significant acceleration of polymerization rates while no significant rate increase was found for the phosphonate ester derivatives. This was explained by the increase of medium polarity in the presence of phosphonic acid.

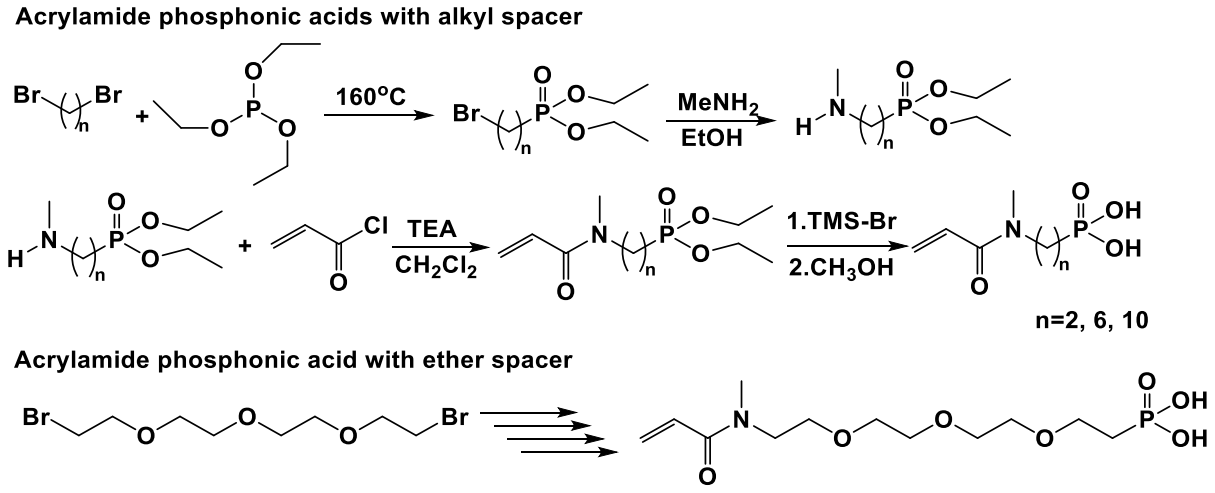

Figure 2.23 Synthesis of acrylamido phosphonic acids based on the Michaelis-Arbuzov reaction

Le Pluart's team also synthesized acrylamido geminal bisphosphonic acids (Figure 2.24) by two approaches.[68, 71] The first phosphonate functionality was introduced via the Michaelis-Arbuzov reaction. The second phosphonate were added using diethyl chlorophosphate catalyzed by a strong base, lithium diisopropylamine (LDA). The ether terminated geminal bisphosphonates were either converted to an aldehyde or an alcohol followed by treatment with amines to yield aminoalkyl bisphosphonates. Methacrylation and deprotection was carried out to yield the acrylamido bisphosphonic acid. All of these monomers were photopolymerized with a difunctional monomer *N,N'*-diethyl-1,3-bis(acrylamido)propane (DEBAAP).

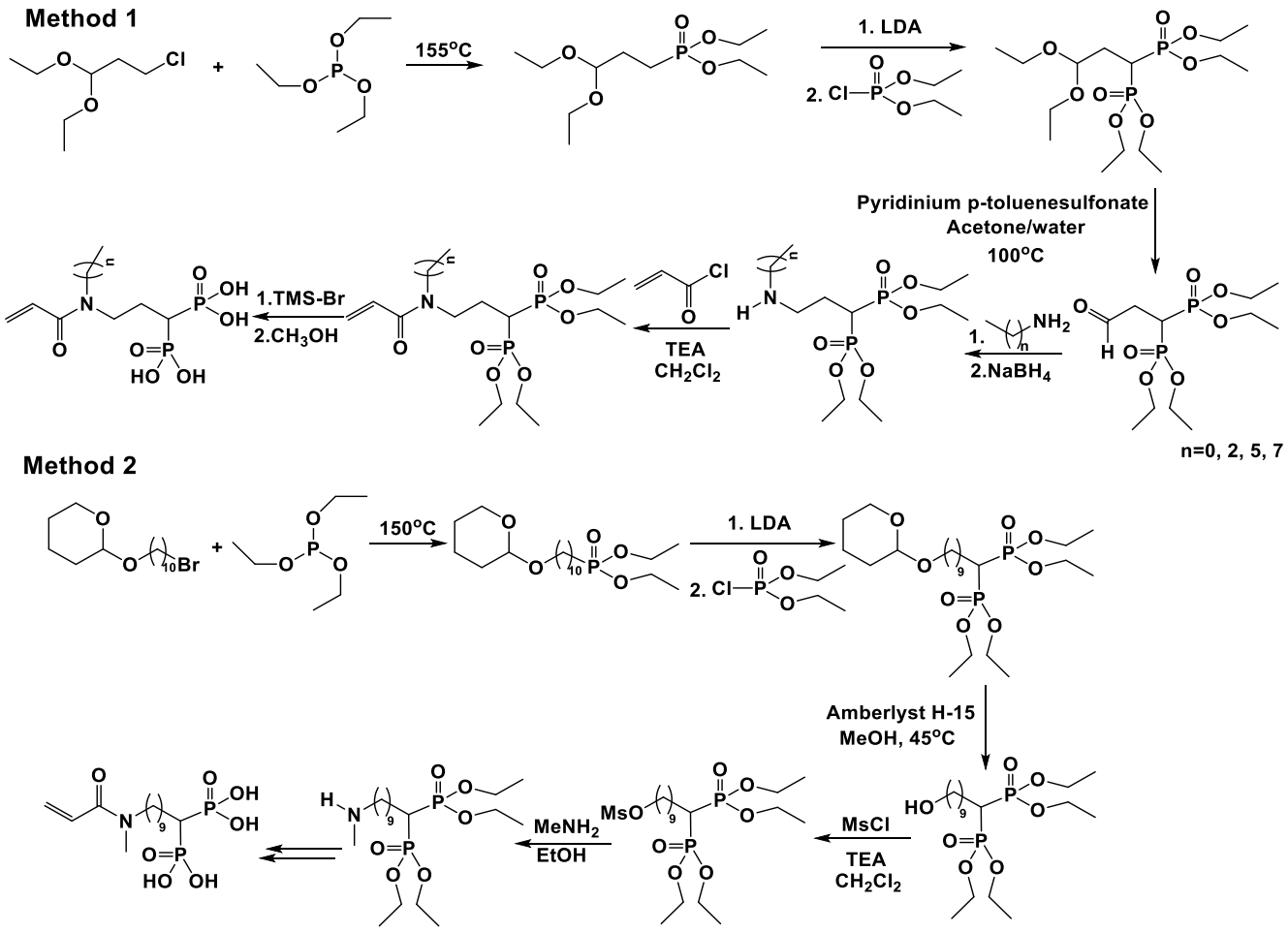

Figure 2.24 Synthesis of acrylamido geminal bisphosphonic acids based on the Michaelis-Arbuzov reaction

Klee and Lehmann[72] synthesized a series of acrylamido phosphonic acids via Michael-addition. The three-step procedure (Figure 2.25) included addition of amines to vinyl phosphonate, (meth)acrylation and hydrolysis of phosphonates. The addition reaction was achieved by two methods. The first was by reacting vinyl phosphonate with amines under reflux followed by (meth)acrylation. The second was by directly adding the vinyl phosphonate to (meth)acrylamides catalyzed by sodium hydride. The authors compared the hydrolytic stability

of the acrylamide, methacrylamide and methacrylate phosphonic acids. The stabilities were tested on phosphonic acid solutions stored at 50°C with detection of the degradation products, acrylic or methacrylic acids, using HPLC. The acrylamido phosphonate exhibited higher stability than the methacrylamide and methacrylate analogues. The hydrolysis percentage of the acrylamide, methacrylamide and methacrylate phosphonates in 42 days were 10%, 40% and 80%, respectively.

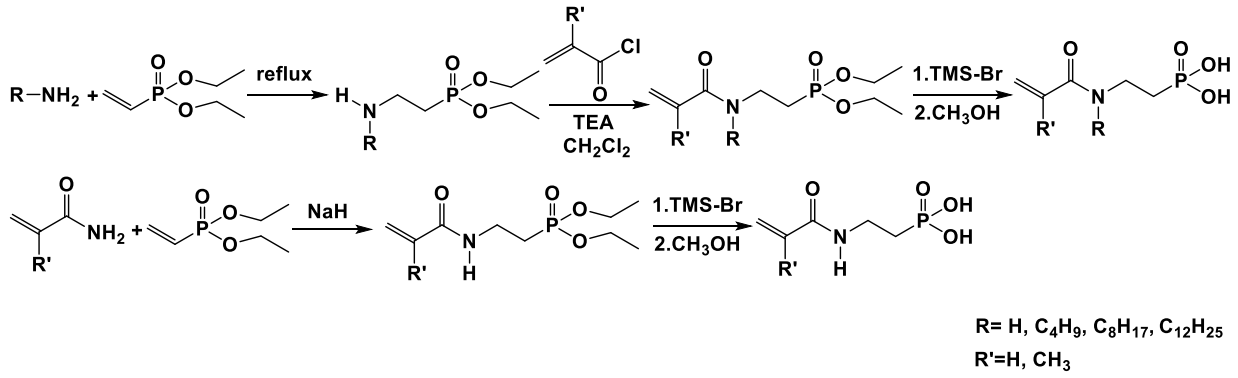

Figure 2.25 Synthesis of acrylamido phosphonic acids via Michael-addition

Avci and coworkers expanded exploration of acrylamido phosphonic acids as well. They prepared aminophosphonate precursors by applying similar methodology to that used for synthesizing the urea-containing methacrylate.[62] The aminophosphonates were then converted to (meth)acrylamido phosphonate monomers via esterification and this was followed by hydrolysis of the phosphonates (Figure 2.26).[73] The monomers were either thermally polymerized at 65 °C or photopolymerized. The group synthesized methacrylamide and diacrylamide geminal bisphosphonates (Figure 2.27).[74] The methacrylamido geminal bisphosphonate was prepared by reacting methacryloyl chloride with tetraethyl aminomethyl-bisphosphonate. The difunctional monomer was obtained in a four-step procedure. *t*-Butyl acrylate was reacted with an aldehyde to

produce a diacrylate precursor, then this was followed by hydrolysis and acylation. A diacryloyl chloride was reacted with tetraethyl aminomethyl-bisphosphonate to afford the dimethacrylamido geminal bisphosphonate.

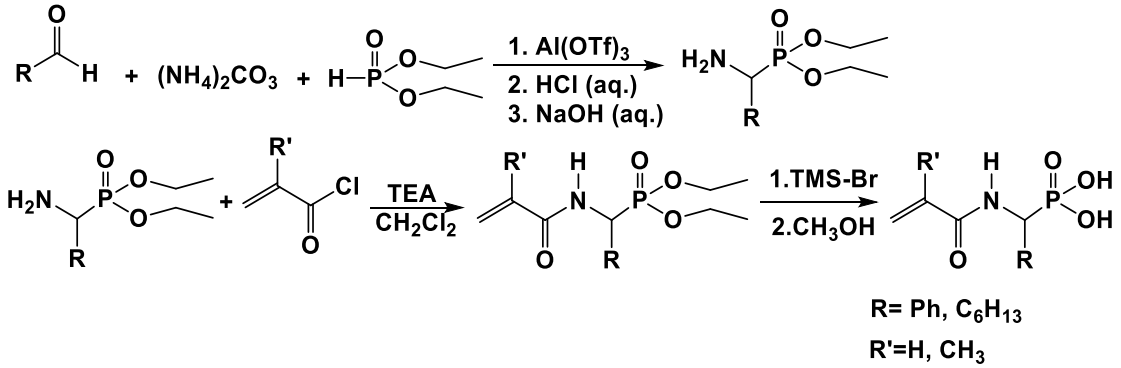

Figure 2.26 Synthesis of acrylamido phosphonates with aromatic and alkyl linkers

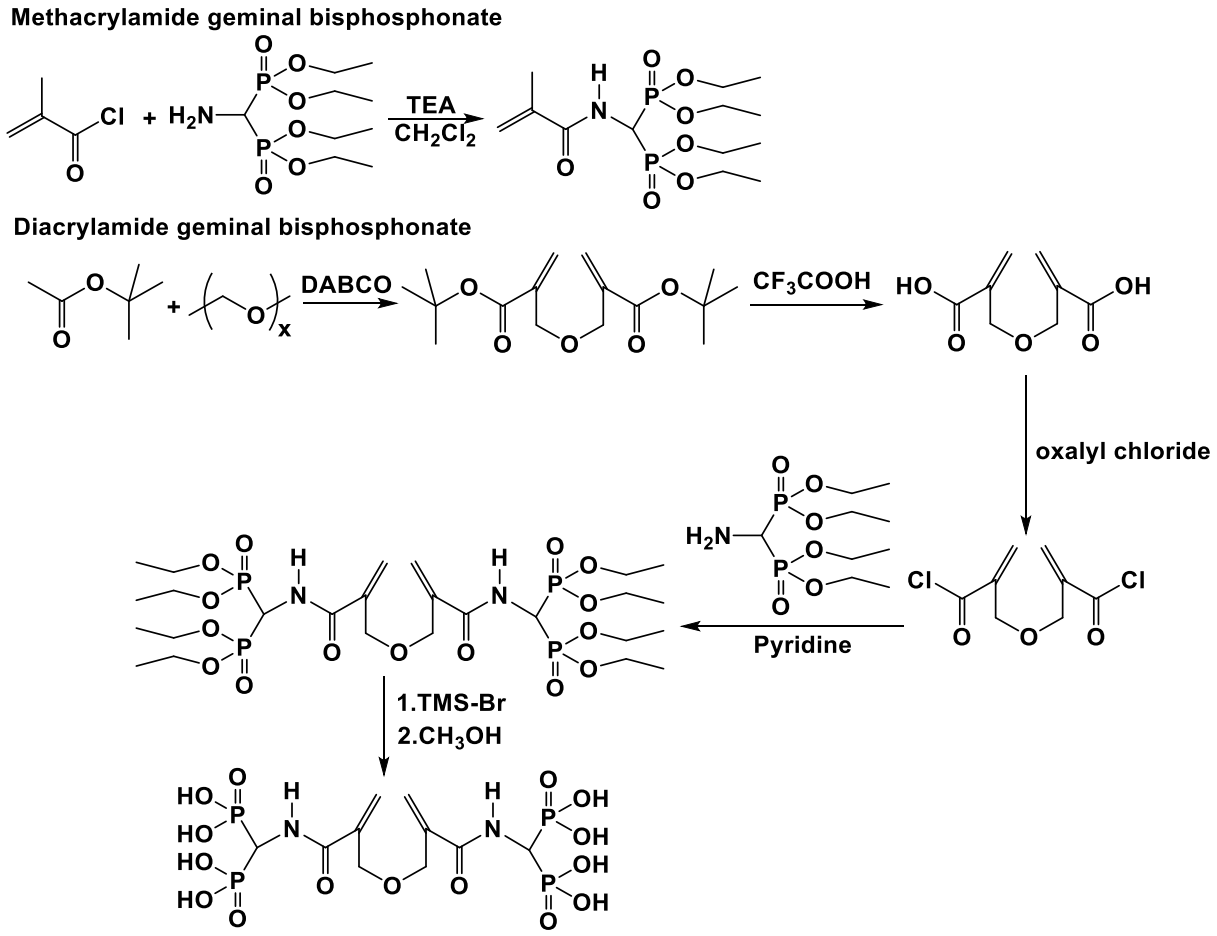

Figure 2.27 Synthesis of methacrylamido and diacrylamido geminal bisphosphonates

Robin *et al.* employed two approaches for synthesizing two (meth)acrylamido phosphonates which were polymerized by reversible addition-fragmentation transfer (RAFT) polymerization (Figure 2.28).[75, 76] The first step for synthesizing the acrylamide phosphonate monomer was via a Michaelis-Arbuzov reaction. The product bromide-functionalized phthalimide was deprotected with hydrazine monohydrate to afford 2-aminoethyl phosphonate. This compound was then reacted with acryloyl chloride to yield the acrylamide phosphonate. The methacrylamide was synthesized by a three-step procedure. Dimethylhydrogenphosphonate was added to undecylenic acid in the presence of *tert*-butyl peroxypivalate (TBPPI). The

carboxylic terminated phosphonate was then treated with sodium azide to give the aminophosphonate. The methacrylamido phosphonate was obtained by methacrylation of the aminophosphonate. Both the acrylamide phosphonate and the methacrylamide phosphonate monomers were polymerized in the presence of 2-cyano-2-propyl benzodithioate or 2-(dodecylthiocarbonothioylthio)-2-methylpropionic acid as chain transfer agents, respectively. The molecular weights that were obtained were in the range of 2,200 to 10,000 g mol^{-1} and the PDI values were 1.15 to 1.35. The acrylamide phosphonate was also polymerized using poly(*N*-*n*-propylacrylamide) (*Nn*PAAm) as a macro chain transfer agent which afforded block copolymers. The phosphonate block copolymers showed about the same low critical solution temperatures (LCST's) as the homopolymer of *Nn*PAAm while the deprotected phosphonic acid copolymer exhibited a higher LCST which was considered reasonable due to its increased hydrophilicity.

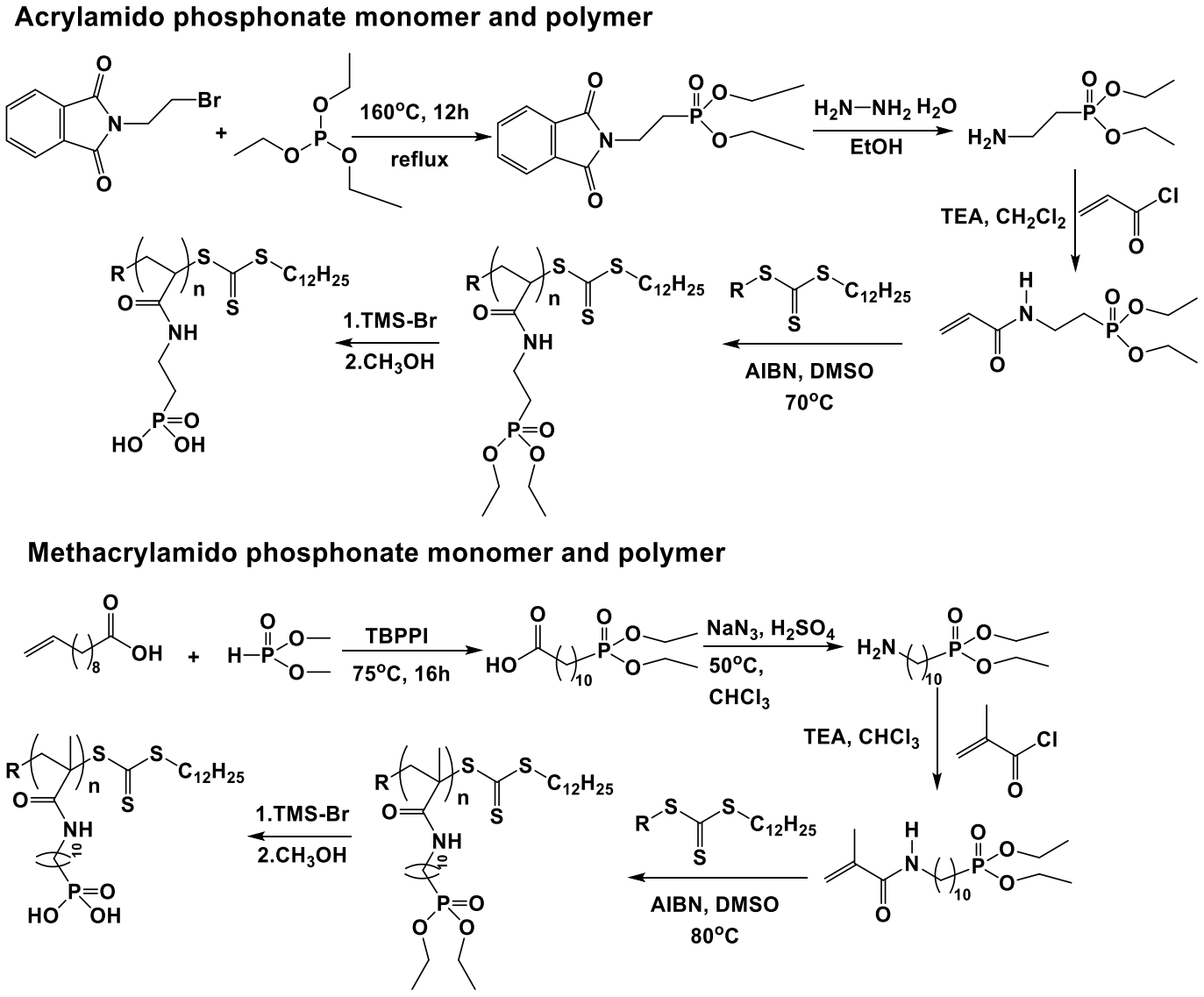

Figure 2.28 Synthesis of (meth)acrylamido phosphonate monomers and their RAFT polymerization

2.2.2.3 Applications of (Meth)acrylate and (Meth)acrylamide Phosphonate Monomers and Polymers

(Meth)acrylic phosphonate monomers and polymers have found applications in dental materials,[36, 37, 64, 68, 77, 78] as flame retardants[79, 80] and as anticorrosive coatings.[55, 58] Among these

applications, (meth)acrylic phosphonates have been largely considered as primers for self-etching dental adhesives. In general, these adhesives bond resinous composites onto enamel or dentin by demineralization of a weak "smear" layer on the dentin, and create an etched pattern on the enamel.[81] Then the photopolymerizable primers (carboxylic acid, phosphate or phosphonic acid monomers) infiltrate the demineralized areas.[68] These adhesives become mechanically interlocked within the pores of the enamel through polymerization of the primers.[82] The reason that the primers (acids) are able to etch the dentin or the enamel is that these acids chemically bind to the calcium ions from HAP, a component of the tooth surface.[83] The binding stability depends on the structures of the acids. (Meth)acrylic phosphonic acids have attracted more attention in applications as dental adhesives due to their biocompatibility, excellent capability for binding HAP, high reactivity in free radical polymerization and improved stability against hydrolysis as compared to phosphates.[81, 83]

2.3 Properties, Synthesis and PEO-containing Ionomers for Biomedical Applications

2.3.1 Properties of PEO

PEO is a clear, colorless liquid or white low-melting point solid depending on its molecular weight. It is inert to many chemicals and stable against hydrolysis. Biocompatibility, lack of toxicity and absence of immunogenicity[84, 85] makes PEO the most frequently selected component for biomedical applications. PEO has excellent solubility in water[86] as well as in many organic solvents. It is soluble in water at all compositions and molecular weights. PEO chains extend very well in water due to their remarkable solubility. Because of the hydrogen bonding between PEO and water, the chains are surrounded by a large amount of water molecules resulting in a large excluded volume.[87, 88] Owing to this characteristic, PEO excludes other macromolecules and nanoparticles in water. This is especially important for obtaining

resistance against protein adsorption.[89] According to thermodynamic theory, conjugation of PEO with proteins would lead to a decrease of freedom of the chains.[86] When a protein approaches a PEO chain in solution, it causes packing of the long polymer chain, thus decreasing the entropy (Figure 2.29).

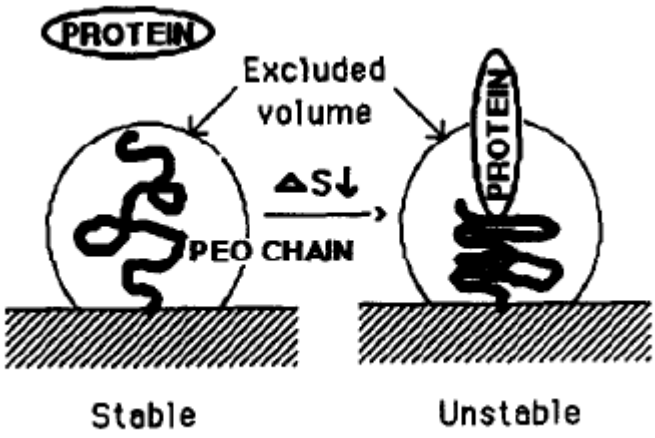

Figure 2.29 Prevention of protein absorption by PEO. Adapted from Lee *et al.*[86]

2.3.2 Synthesis of PEO

Most commercially available PEO is terminated with hydroxyl groups at both ends (HO-PEO-OH) or with one methoxy end group and the other a hydroxyl group (mPEO) (Figure 2.30). PEO can be prepared by anionic ring opening polymerization (ROP) of ethylene oxide (EO) with narrow molecular weight distributions. Ring opening polymerization is a widely used technique to produce well-defined structures with variable molecular weights.[90] Anionic ring opening polymerization of EO usually involves a hydroxide or alkoxide initiator attacking the methylene carbon of EO which leads to opening of the ring and subsequent propagating chains (Figure 2.31).[91]

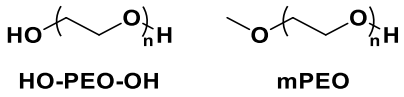

Figure 2.30 Structures of HO-PEO-OH and mPEO

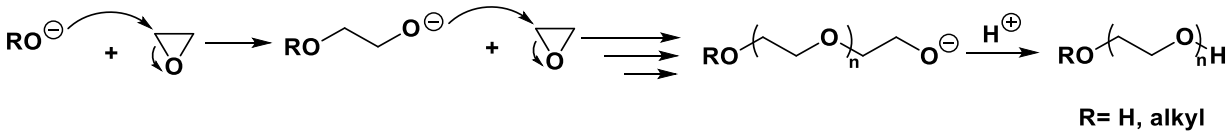

Figure 2.31 Anionic ring opening polymerization of EO initiated by hydroxide or alkoxide

Anionic ring-opening polymerization can be carried out in the presence of metal-based catalysts as well. Double metal cyanide (DMC) catalysts are commonly used in homo- and copolymerization of propylene oxide (PO) and EO. One example of a DMC is $Zn_3[Co(CN)_6]_2$ which has been employed in the copolymerization of EO and PO by Qi *et al*.[92, 93] The resulting copolymers with different compositions of EO and PO exhibited unimodal molecular weight distributions in the range of 1.21 to 1.55.

2.3.2.1 Synthesis and Applications of mPEO-(meth)acrylate

mPEO is one of the most commonly used forms of PEO. Numerous functionalities such as (meth)acrylate,[94, 95] azide,[96, 97] maleimide[98, 99] and thiol[100, 101] can be introduced by modifying the hydroxyl end group of mPEO. Functionalized mPEO can be utilized in protein- or peptide-conjugation, surfactants and surface modification.[102-106]

mPEO-(meth)acrylates are well-known as macromonomers for free radical polymers due to the relative high reactivity of the (meth)acrylate moieties. mPEO-(meth)acrylate can be prepared by simply reacting (meth)acryloyl chloride with mPEO in the presence of triethylamine or pyridine (Figure 2.32). Various small-molecule monomers including styrene, acrylamide,

NIPAM, methacrylic acid and ester have been copolymerized with mPEO-(meth)acrylates.[107-111] The reactivity of the mPEO-(meth)acrylate is lower than that of conventional small-molecule monomers which is might be attributed to the PEO polymer chain reducing the reactivity of its end groups. The detailed mechanism for this reduction is not yet clear, but it might be due to inductive or steric effects together with the solution properties of the PEO chain.[112]

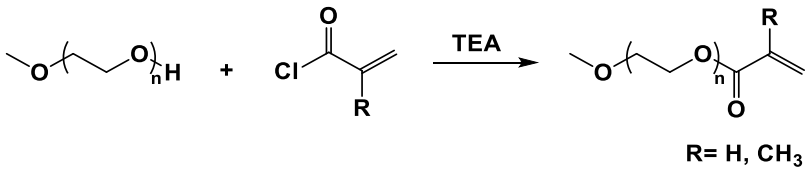

Figure 2.32 Synthesis of mPEO-(meth)acrylate

2.3.2.2 Synthesis and Applications of NH_2-PEO-OH

Heterobifunctional PEO's have the general structure of X-PEO-Y and have been well studied in the last two decades.[91, 113-116] Heterobifunctional PEO's usually bear two different reactive end groups that allow further modification to control and tune the properties of resulting materials. For example, one end group can be utilized to bind targeting groups whereas the other group serves as a coupling moiety or precursor for building copolymers.[113, 117] Two broad approaches have been used to synthesize heterobifunctional PEO's (Figure 2.33). The first method is using a heterobifunctional reagent to initiate anionic polymerization of EO followed by termination of the polymerization with another functional reagent. The second approach involves functionalization of PEO diols and isolation of the targeted heterobifunctional PEO's from the reaction mixture.[91]

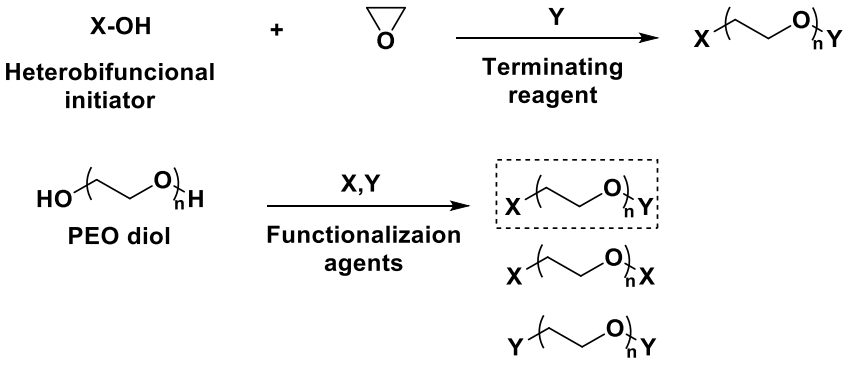

Figure 2.33 Two approaches for synthesis of heterobifunctional PEO's. Adapted from Riffle *et al.*[91] with modification

Primary amine terminated PEO oligomers are of great interest since amines exhibit higher reactivity in many organic reactions compared to hydroxyl groups. One example of a heterobifunctional PEO bearing a primary amine with a structure of NH_2-PEO-OH has been synthesized through different strategies. Some of these methods are reviewed in the following sections.

2.3.2.2.1 Synthesis of NH_2-PEO-OH via a Schiff Base-containing Initiator

To avoid reaction between amines and EO, amino groups in the initiators for EO polymerization are always protected. The protecting groups are removed after completion of polymerization. Amine groups can be protected by reaction with an aldehyde which coverts them to Schiff bases.[118, 119] Huang *et al.* prepared a Schiff base by reacting ethanolamine with benzaldehyde in the presence of sodium (Figure 2.34).[120] Polymerization of EO was initiated by this Schiff base and hydrochloric acid was added at the end of polymerization to terminate the propagating chain and at the same time to deprotect the Schiff base (Figure 2.34). These NH_2-PEO-OH oligomers were used as stabilizers for poly(vinyl benzyl chloride) latexes.

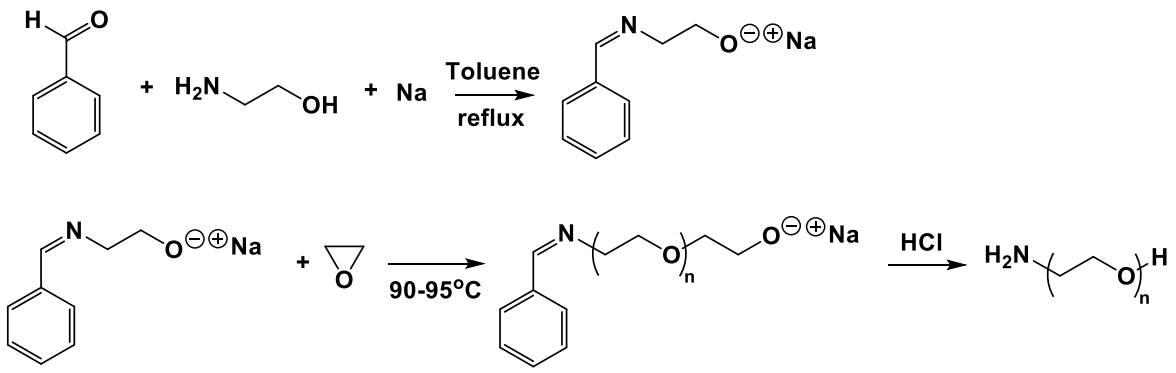

Figure 2.34 Synthesis of NH_2-PEO-OH via a Schiff base-containing initiator

2.3.2.2.2 Synthesis of NH_2-PEO-OH via Silyl or Sila Protected Amino Initiators

Yokoyama and coworkers synthesized NH_2-PEO-OH with different molecular weights via a potassium bis(trimethylsilyl)amide protected amino initiator (Figure 2.35).[121] Utilizing similar methodology, Kim *et al*. also prepared a heterobifunctional PEO by replacing the silyl initiator with a sila-based reagent, N-2-(2,2,5,5-tetramethyl-1-aza-2,5-disilacyclopentyl)-ethylmethylamine (Figure 2.35).[122] Polymerization of EO was initiated by these protected amino compounds in THF and terminated by addition of hydrochloric acid. Polymers were obtained from each method in quantitative yields and the molecular weights determined from SEC agreed well with the targeted values. Jia *et al.* employed the approach developed by Yokoyama and modified the resulting NH_2-PEO-OH to give PEO with sulfadiazine and chlorambucil end groups which are antitumor drugs as small molecules.[123] These polymer drugs with both sulfadiazine and chlorambucil showed higher antitumor activity against Lewis lung cancer than the polymer without sulfadiazine. Tessmar and coworkers also utilized the same method for preparing NH_2-PEO-OH which served as an initiator to polymerize lactide.[124] The amino-ended PEO-*b*-PLA showed potential to bind to bioactive molecules.

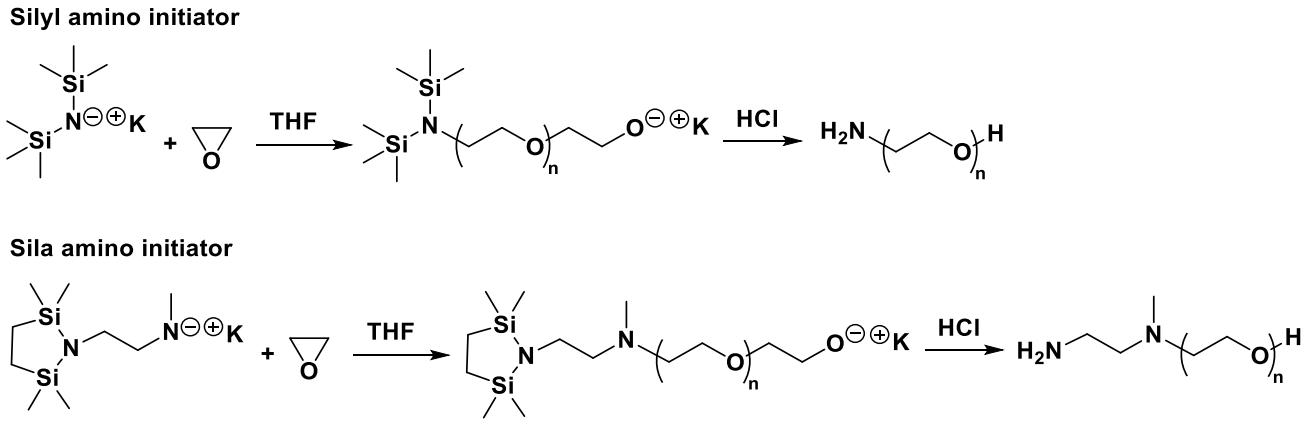

Figure 2.35 Synthesis of NH_2-PEO-OH via silyl or sila-based initiators

2.3.2.2.3 Synthesis of NH_2-PEO-OH via an Allyl Initiator

Cammas *et al.* developed a facile method to synthesize NH_2-PEO-OH with an allyl initiator (Figure 2.36).[85] This initiator was prepared through a two-step procedure. Potassium was reacted with naphthalene in THF to afford potassium naphthalide solution followed by adding this solution to allyl alcohol which led to formation of the initiator, allyl alcoholate. Polymerization of EO was terminated by acetic acid. The resulting polymer was treated with cysteamine hydrochloride through a radical reaction using AIBN as the radical initiator to yield the NH_2-PEO-OH. The non-modified and post-functionalized polymers both had controllable molecular weights and low PDI's (<1.08). This synthetic strategy can be extended by replacing cysteamine hydrochloride with other reagents (i.e. mercaptocarboxylic acids) to introduce various functionalities.

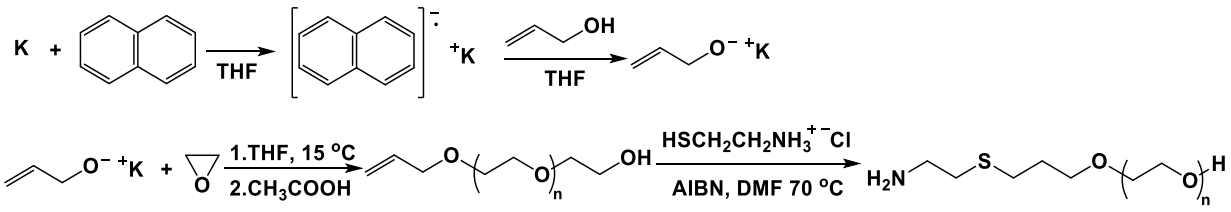

Figure 2.36 Synthesis of NH_2-PEO-OH via an allyl initiator

2.3.2.2.4 Synthesis of NH_2-PEO-OH via Cyano-based Initiators

Cyano groups can be converted to primary amines through reduction. Utilizing this reaction, Nagasaki *et al.* synthesized NH_2-PEO-OH via a cyano-based initiator (Figure 2.37).[125] Cyanomethyl potassium (CMP), the initiator, was prepared by a metalation reaction between acetonitrile and potassium naphthalide in THF. Polymerization of EO was initiated by CMP in the presence of 18-crown-6 to prevent formation of a dianion of acetonitrile. Deng *et al.* adapted a similar procedure to prepare PEO with a cyano group at one end and a potassium alkoxide on the other. This alkoxide initiated polymerization of ε-caprolactone (ε-CL). The resulting CN-PEO-PCL was converted to a primary amine end-capped PEO-PCL by reduction catalyzed with palladium on carbon or Raney nickel to avoid reduction of the labile ester bond in PCL. ROP of (γ-benzyl-$_L$-glutamic acid) (BLG) was carried out with NH_2-PEO-PCL as a macroinitiator to obtain a triblock copolymer, PBLG-PEO-PCL.

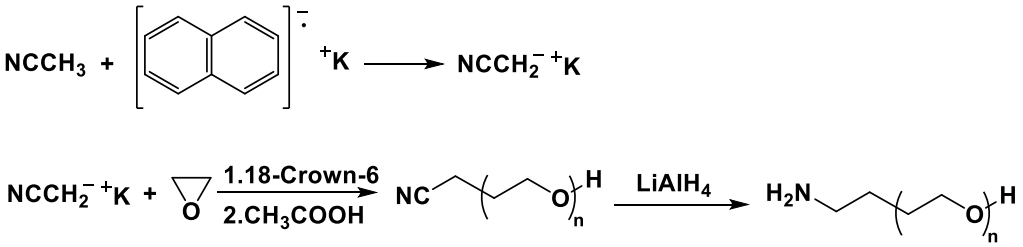

Figure 2.37 Synthesis of NH_2-PEO-OH via CMP

Schlaad and coworkers replaced the potassium alkoxide initiator with a phosphazene-containing compound, α-methylbenzyl cyanide/*t*BuP$_4$ (Figure 2.38), to initiate metal-free anionic polymerization of EO (Figure 2.39).[126] The use of [*t*BuP$_4$]$^+$ instead of a potassium cation led to a higher polymerization rate of EO. The bulky structure of [*t*BuP$_4$]$^+$ formed looser ion pairs with

the cyanide resulting in an accelerated polymerization rate.[127] The measured molecular weights of the heterobifunctional NH_2-PEO-OH were close to the expected ones and the polymers had low PDI values (<1.10)

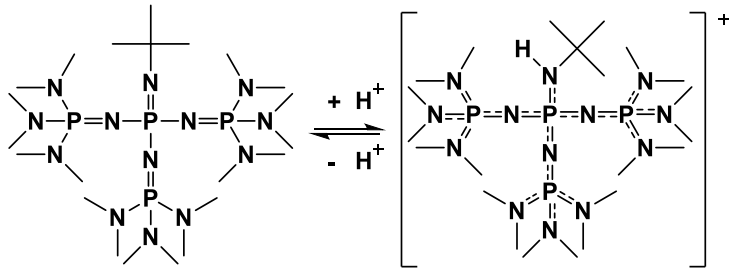

Figure 2.38 Structure of phosphazene *t*BuP$_4$ and its conjugate acid [*t*BuP$_4$]$^+$

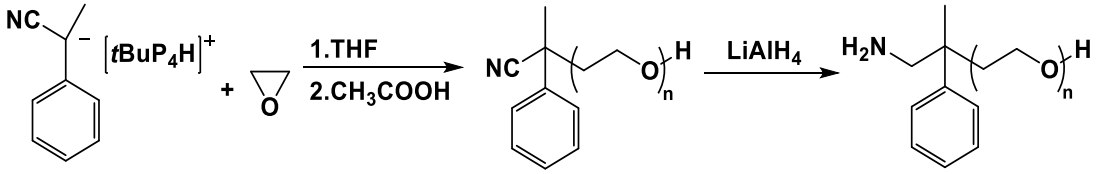

Figure 2.39 Synthesis of NH_2-PEO-OH via α-methylbenzyl cyanide/*t*BuP$_4$

2.3.3 Block and Graft Polyion Complexes

Polyion complex (PIC) micelles developed by Kataoka[128] and Kabanov[129] represent a frontier technology in the drug delivery field. PIC's are usually comprised of a block copolymer containing a neutral hydrophilic block and an ionic block loaded with counter-charged substrates containing the complementary charge. In most cases, the counter ions are biopharmaceuticals such as DNA, RNA, proteins or drugs. Due to electrostatic interactions between the ionic block and the counterions, charges are neutralized in these segments, they become hydrophobic and this induces micelle formation (Figure 2.40).[130, 131] The ionic block of the copolymer complexed with the cargo with complementary charge forms the core of the polyion micelle and the neutral

hydrophilic block forms the corona. The corona should be biocompatible and stable since it directly interacts with the outside biological environment. Both the ionic and the neutral blocks can be sensitive to biosignals (e.g., pH, ionic strength, temperature and electric field) which might trigger release of the cargo.

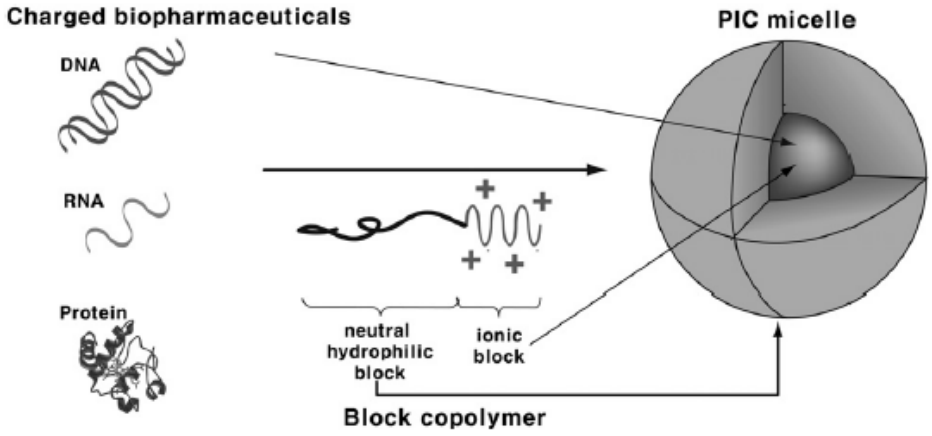

Figure 2.40 PIC micelle formation. Adapted from Kataoka *et al.*[131]

The ionic block can be either cationic or anionic depending on the biopharmaceutical counter ions. Anionic blocks such as poly(acrylic acid) (PAA)/poly(methacrylic acid) (PMAA) and poly(aspartate) (PAsp) (Figure 2.41) are able to encapsulate cationic drugs[132] and cationic proteins while cationic blocks of PIC including poly(L-lysine) (PLL), poly(amino aspartamide) and poly(amino methacrylate) can interact with DNA,[133] siRNA[134] and anionic drugs.[135] Various types of polymers have been used as the neutral hydrophilic segment including PEO, poly(acrylamide) (PAAm),[136] poly(isopropylacrylamide) (PNIPAM),[137] poly(*N*-2-(hydroxypropyl) methacrylamide) (PHPMA),[138] poly(hydroxylethylacrylate) (PHEA)[139] and poly(glyceryl methacrylate) (PGMA) (Figure 2.30).[140] Among these polymers, PEO is frequently selected as the neutral hydrophilic shell for its extraordinary properties discussed in section 2.3.1.

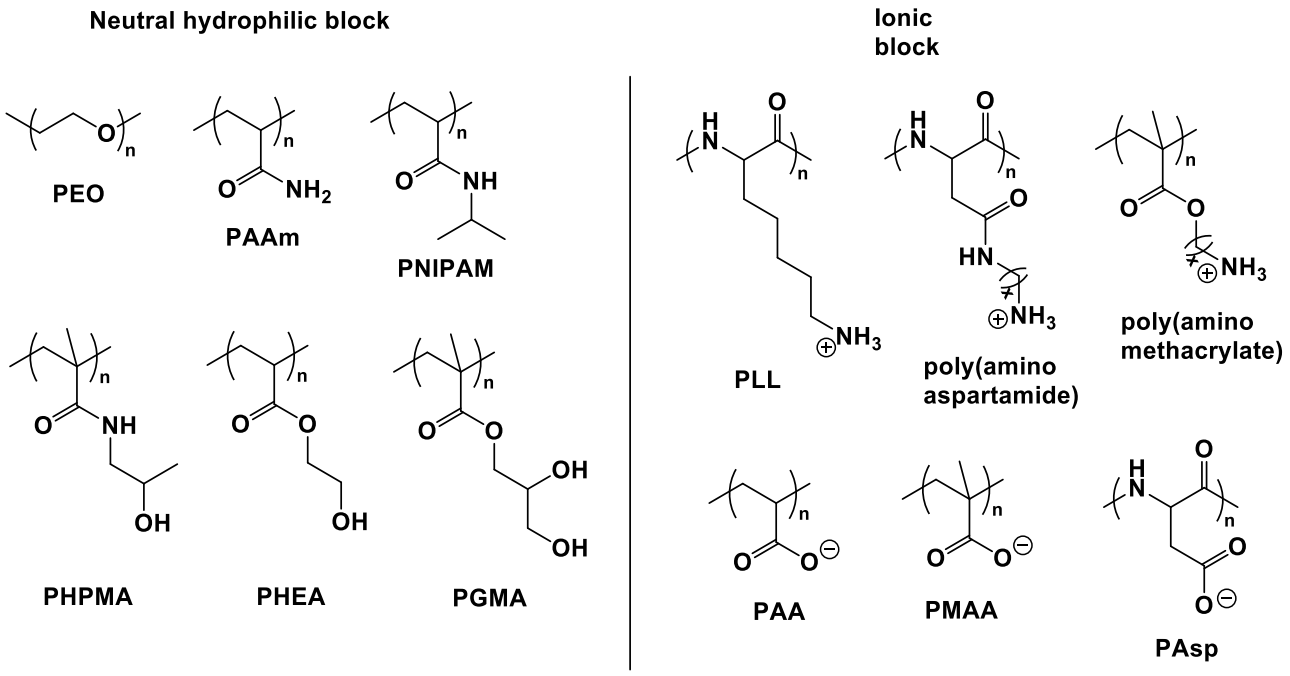

Figure 2.41 Polymers used for PIC

Graft copolymers have also been employed to prepare PIC's.[141-143] Different from block copolymers with two or more distinct segments, graft copolymers usually consist of a linear backbone with one composition and another one or more compositions as side chains randomly distributed along the backbone (Figure 2.42). The terms "grafting-through", "grafting-from" and "grafting-to" have been coined to describe three related synthetic approaches (Figure 2.43).[144] "Grafting-through" involves copolymerization of macromonomers carrying polymerizable end groups with small-molecule monomers. "Grafting-from" refers to growing side chains from monomers from a polymer backbone containing initiating moieties. "Grafting-to" is meant to describe a coupling approach between a polymer backbone and another oligomer or polymer. Random graft copolymers are easier to synthesize than the corresponding block copolymers while the major drawback is less control over the molecular structures. Well-defined graft

copolymers with controlled side chain length and grafting density can also be constructed through living polymerization techniques such as ROP, ROMP, ATRP and RAFT.[144]

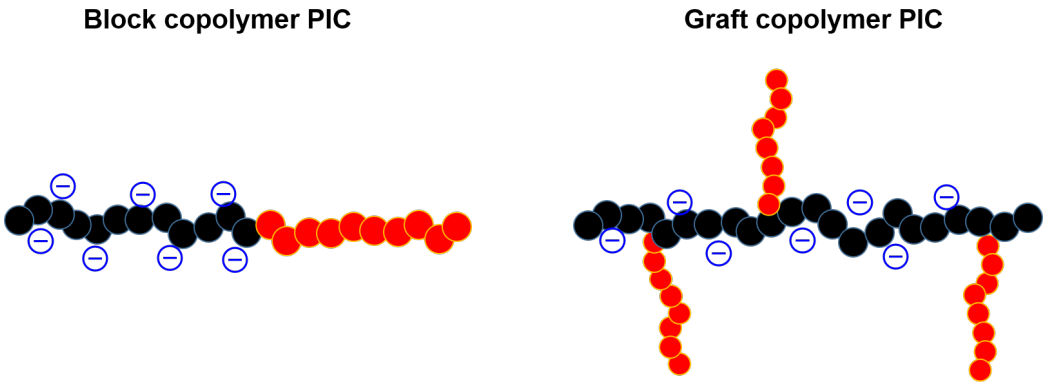

Figure 2.42 Structures of block and graft copolymer PIC's (shown as anionic copolymers)

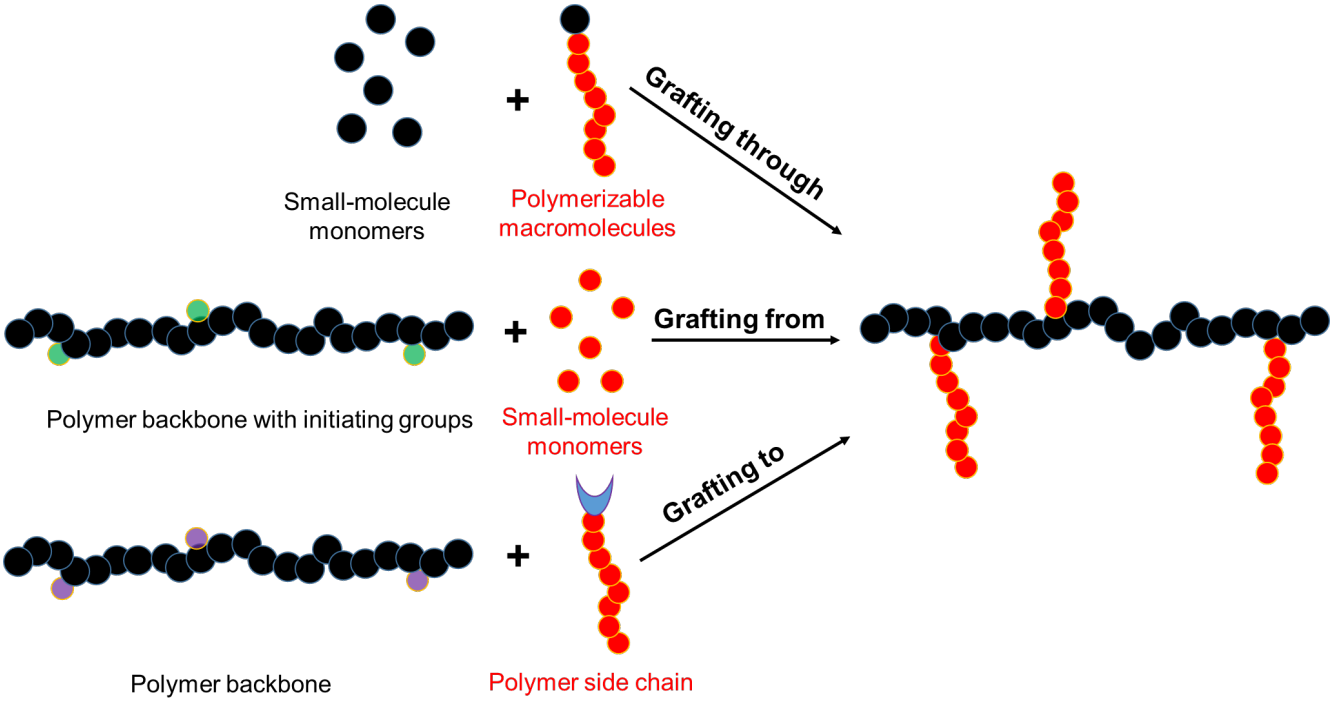

Figure 2.43 Three approaches for synthesis of graft copolymers

2.3.4 PEO-containing Ionomers as Therapeutic Agent Carriers

2.3.4.1 PEO-PAA or PEO-PMAA copolymers

Poly(acrylic acid) (PAA) is one of the most commonly used polyanions in drug delivery. The carboxylic acid can be either in protonated or deprotonated forms depending on the pH of the medium, and changes in pH can in some cases induce drug release.[145] PEO-PAA block copolymers have been prepared by ATRP.[146-148] Polymerization of an alkyl acrylate (e.g. *t*BuA) is initiated by bromo-2-methyl-propionate end-capped mPEO in the presence of a ligand and copper bromide in a solvent, then this is followed by deprotection (removal) of the ester alkyl groups using trifluoroacetic acid (TFA) (Figure 2.44). Alternatively, the block copolymer can be synthesized by RAFT.[149] Acrylic acids have been directly polymerized by RAFT using mPEO as a macromolecular chain transfer agent and AIBN as the initiator (Figure 2.44). Copolymers obtained from both ATRP and RAFT techniques exhibit well-controlled molecular weights and low PDI's.

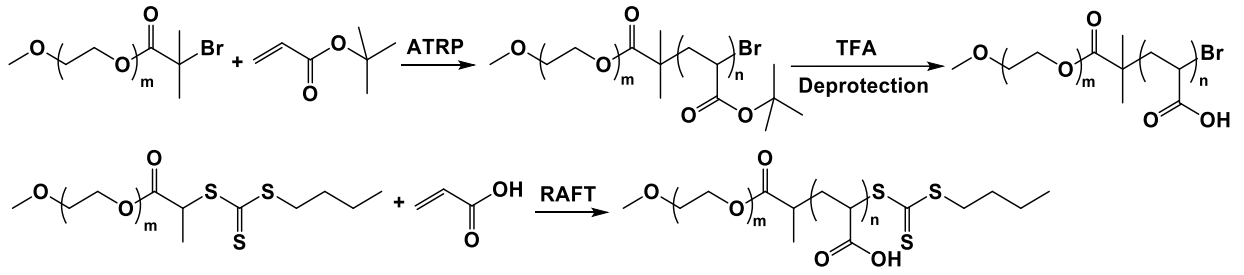

Figure 2.44 Synthesis of PEO-*b*-PAA by ATRP or RAFT. Adapted from Krieg *et al.*[149]

Employing the anionic nature of poly(methacrylic acid) (PMAA), Khanal *et al.* successfully incorporated cationic chitosan or methylglycolchitosan into PEO-*b*-PMAA copolymers. Chitosan, a derivative of the natural product chitin, was found to have antimicrobial and wound healing properties.[150] Partial neutralization of the PMAA block led to insolubilization

of PMAA that induced formation of core-shell "nanoaggregates" of the copolymer with PMAA in the core and PEO as the corona. The sizes of those aggregates in water ranged from 100 to 160 nm.

PIC networks can form hydrogels with charges confined inside. The encapsulated oppositely charged bioactive agents are thus protected from hostile media such as enzymes and low pH.[151] Oh *et al.* explored crosslinked PAA and PEO (PEO-*cl*-PAA) through copolymerization of acrylic acid and a crosslinker, PEO diacrylate (Figure 2.45).[152] Long PEO chains separated PAA chains and increased the space between adjacent PAA chains. This contributed to a higher loading capacity of drugs compared with linear copolymer analogues. A cationic protein, cytochrome C, was entrapped in the PEO-*cl*-PAA networks. Release of cytochrome C was triggered by exchange of competitive cations including calcium chloride, sodium chloride, or a polymeric cation, poly(*N*-ethyl-4-vinylpyridinium bromide) (PEVP). Comparisons of effects on release of adding different competitive cations with cross-linked PAA (*cl*-PAA) homopolymers and PEO-*cl*-PAA copolymers are shown in (Figure 2.46). In most cases, release of cytochrome C from PEO-*cl*-PAA was faster than from *cl*-PAA. Release behavior was studied in four media including NaCl, PBS, $CaCl_2$ and PEVP solutions. In NaCl solution (Figure 2.46a), release efficiency was lower compared to the other three systems indicating that addition of Na^+ alone did not promote release. In $CaCl_2$ solution (Figure 2.46c), calcium cations migrated through the network and enhanced release rate. Interestingly, for the PEVP system (Figure 2.46d), adding NaCl into the PEVP solution greatly accelerated the release rate for *cl*-PAA and PEO-*cl*-PAA (320). This is consistent with a polyion exchange mechanism.[153] Release of cytochrome C from PEO-*cl*-PAA (80) was not improved by PEVP. This probably resulted from

the increased ratio of PEO in the copolymer impeding the polyion exchange and inhibiting migration of PEVP inside the network.

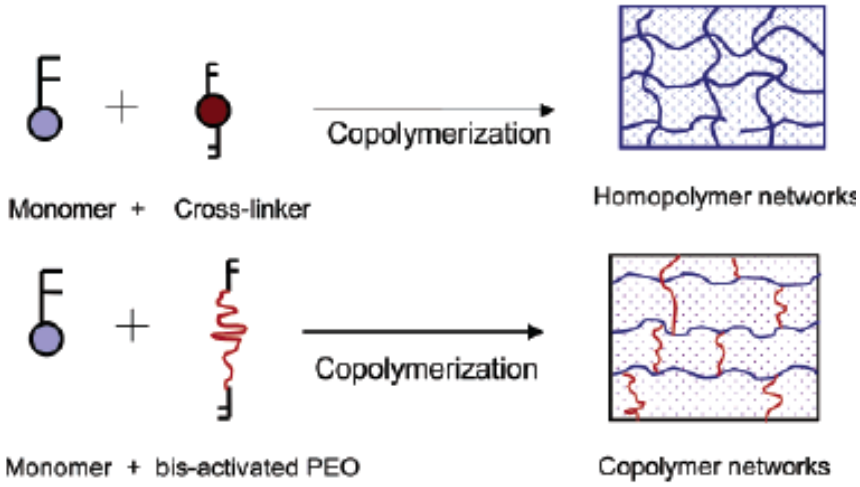

Figure 2.45 Formation of *cl*-PAA homopolymer and PEO-*cl*-PAA copolymer networks. Adapted from Oh *et al.*[152]

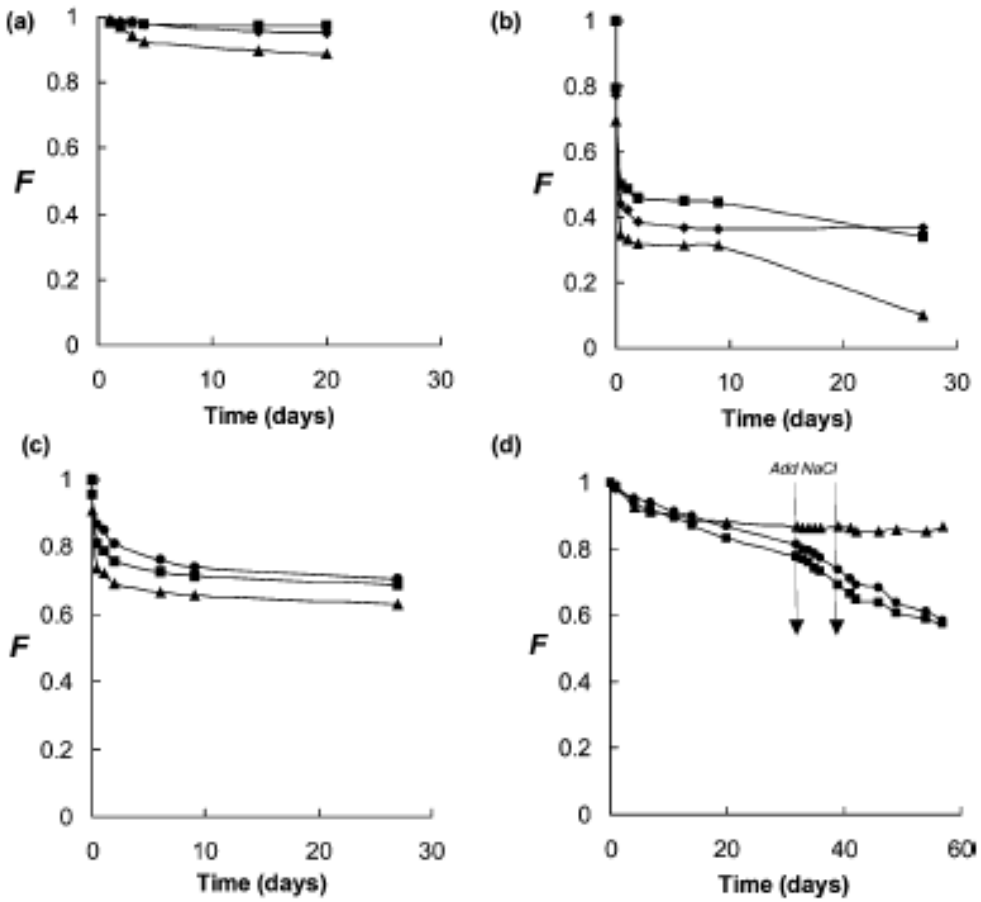

Figure 2.46 Release of cytochrome C in (●) *cl*-PAA; (■) PEO-*cl*-PAA (320); (▲)PEO-*cl*-PAA (80). 320 and 80 refer to the mole ratio of AA to bisacrylate PEO in PEO-*cl*-PAA (320) and PEO-cl-PAA (80), respectively. (a) 2mM NaCl; (b) PBS; (c) 1mM $CaCl_2$; (d) 0.2 mM PEVP. In (d), the vertical arrows indicate the points of addition of NaCl, and each data point between the arrows represents concentrations of NaCl of 2, 4, 6, 10 and 15 mM, increasing from left to right arrows, respectively. Adapted from Oh *et al*.[152]

2.3.4.2 PEO-PAsp copolymers

PEO-PAsp (PEO-polyaspartic acid) copolymers are among the earliest studied anionic copolymers for drug delivery systems.[154-156] In preparation of the copolymer, PEO-*b*-poly(β-

benzyl $_L$-aspartate) (PBLA) was synthesized as a precursor using a primary amine end-capped PEO as a macroinitiator to initiate ring-opening of a benzyl-protected *N*-carboxyanhydride monomer (Figure 2.47). The PEO-*b*-PBLA copolymer was deprotected under basic conditions to yield PEO-*b*-PAsp. It was reported that the selection of solvents significantly affected these polymerizations, and this was attributed to activities of the amino groups at the chain ends in solution. For instance, PBLA can exist in different conformations including an α-helix, β-sheet and random coil.[157, 158] These conformations restrict the mobility of the amino end groups in the chains during polymerization, and this can lead to different molecular weights and broader PDI's. It has been demonstrated that well-defined PEO-*b*-PBLA with 50 repeating units of PBLA can be prepared in organic solvents such as DMSO and DMF.[157]

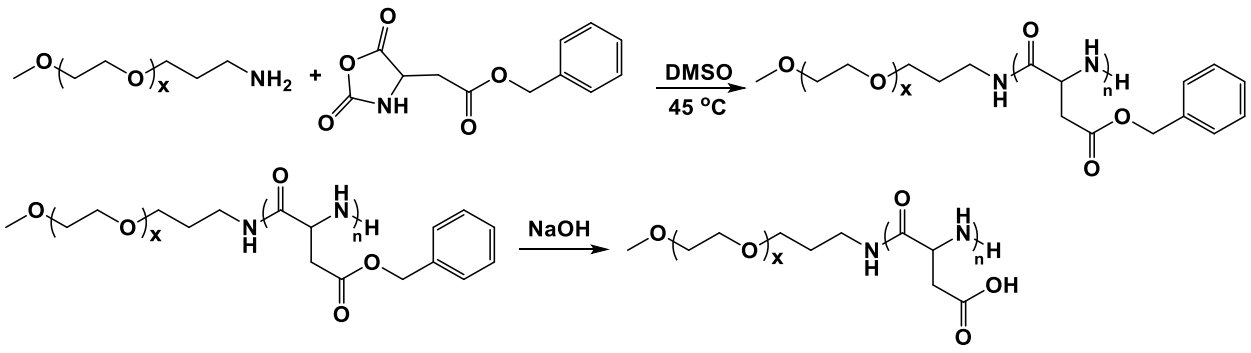

Figure 2.47 Synthesis of PEO-*b*-PAsp

Chemical modifications of the PAsp groups on such copolymers has also been demonstrated. For example, the amino end group of PBLA has been reacted with a carboxylic group from PAsp to form a grafted nanostructure. Networks were also obtained by using a diamine to crosslink the carboxylic acid groups.[159]

Deprotonation of carboxylic acid groups on PAsp can induce electrostatic interactions with cationic substrates. Bae and coworkers entrapped doxorubicin (DOX), an anthracyline

anticancer drug with an ionizable amine group, into an ionic PEO-*b*-PAsp copolymer ("Na-micelle"), a protonated PEO-*b*-PAsp ("H-micelle") and a hydrophobic PEO-*b*-PBLA copolymer ("Bz-micelle").[160] Both the "Na-micelles" and the "H-micelles" showed higher stability in solution for at least six months as opposed to the "Bz-micelles". Slower drug release rates were observed at pH 7.4 and 5.0 for the "Na-micelles" (Figure 2.48). These results indicated the potency of the ionic form of PEO-*b*-PAsp as a drug carrier. Besides positively-charged drugs, inorganic cations have also been encapsulated into PEO-*b*-PAsp copolymers. For instance, Kakizawa *et al.* designed calcium phosphate (CaP)/PEO-*b*-PAsp nanoparticles loaded with plasmid DNA (pDNA), oligodeoxynucleotide (ODN) or siRNA.[161, 162] CaP has an adsorptive capacity for nucleic acids which has been attributed to interactions between the calcium ion of CaP and phosphates from the backbone of the nucleic acids.[163] Therefore, CaP has been widely investigated in gene delivery vehicles.[164] However, a problem with CaP-based delivery systems is the fast growth of CaP crystals that induces precipitation of the complexes. The aspartic acid from PEO-*b*-PAsp can coat the CaP surface, thus preventing the growth of crystals. The resulting hybrid nanoparticles had good colloidal stability in 1.5 or 3.0 mM phosphate buffer with particle sizes in the range of 100 to 300 nm. The complexes also had high pDNA, ODN or siRNA encapsulation efficiencies. Specifically, enhanced cellular uptake was observed with the ODN loaded complexes.

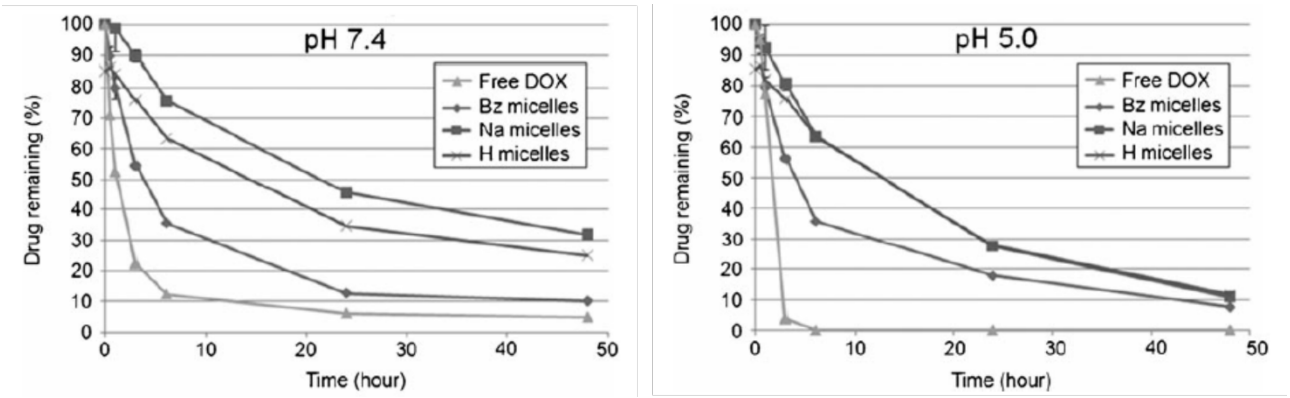

Figure 2.48 Drug release patterns of Bz/Na/H micelles at pHs 7.4 and 5.0 (37°C). Free DOX was used as a control to determine the dialysis efficiency and data normalization. Adapted from Bae *et al.*[160]

2.3.4.3 PEO-Poly(amino aspartamide) copolymers

Poly(amino aspartamide)s are derivatives of PBLA, the precursor for PAsp. PBLA can undergo aminolysis by treating the polymer with amino compounds such as diethylenetriamine (DET) under mild conditions (Figure 2.49).[165] The resulting polymer is cationic poly(amino aspartamide) with a low degree of crosslinking and some inter- or intramolecular isomerization to form β-aspartamide.[165] Specifically, the ethylenediamine unit is able to undergo protonation-deprotonation as a function of pH and this induced conformational changes (Figure 2.50). Due to this feature, these polymers that contained ethylenediamine such as polyethyleneimine (PEI) had buffering properties. The degree of protonation of PEI increases from about 20 to 45% as pH drops from 7 to 5.[166] The increased amount of protons together with chloride ions entering an endosome causes a rise of osmotic pressure and thus results in disruption of the endosome. This leads to transfection of the cationic polymers into the cytoplasm. This phenomenon is termed a "proton sponge" effect.[167-169] The underlying concept for designing PEO-poly(amino

aspartamide) is to employ this special characteristic of ethylenediamine for *in vivo* drug or gene delivery.

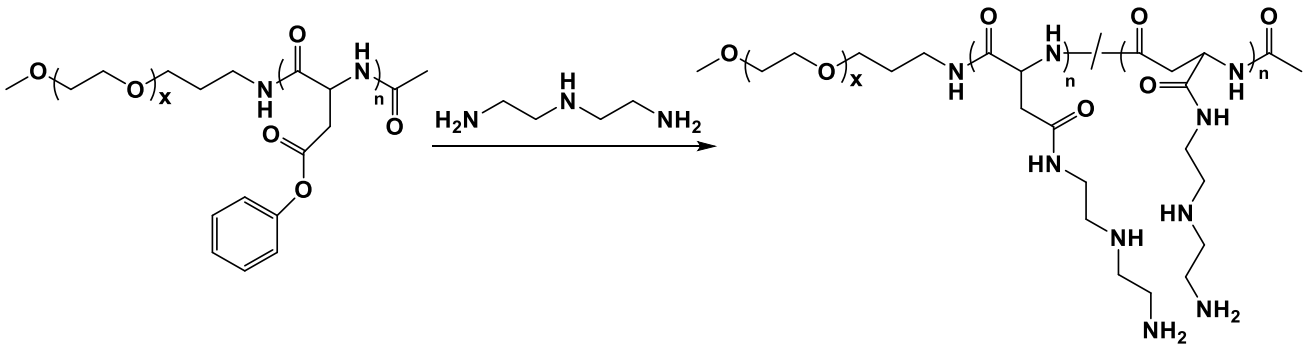

Figure 2.49 Synthesis of PEO-*b*-P[Asp(DET)] by aminolysis

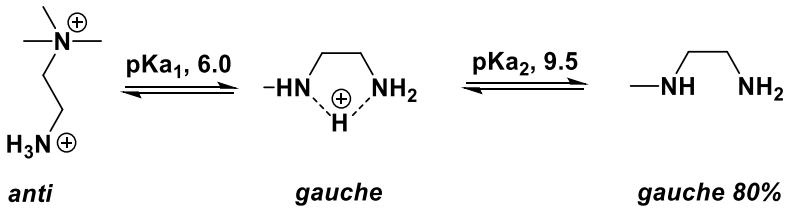

Figure 2.50 Protonation-deprotonation process of ethylenediamine at different pH's inducing conformational changes

Kataoka and coworkers investigated the properties, cytotoxicity and potential gene delivery potential of PEO-*b*-P[Asp(DET)] copolymers.[133, 165, 170-173] They primarily incorporated pDNA into the copolymer. They revealed the importance of possessing ethylenediamine moieties to enable high transfection efficiency and low gene toxicity of the PEO-*b*-P[Asp(DET)] copolymers.[171, 172] The copolymer loaded with pDNA was investigated in bone regeneration applications as well.[170] It showed good gene delivery efficiency which led to an enhancement of bone regeneration in a bone defect model *in vivo*. In addition, the researchers introduced a

disulfide linker between the PEO and the P[Asp(DET)] segments so that the PEO could be detached from the micelles through cleavage of the disulfide bond.[133] This carrier with the disulfide linker exhibited 1-3 orders of magnitude higher gene delivery efficiency than the regular PEO-*b*-P[Asp(DET)] due to release of the PEO in the endosomes.

Poly(amino aspartamide) with PEO grafts has been introduced to encapsulate drugs. Hu *et al.* synthesized PEO-*g*-poly(aspartamide-*co*-*N,N*-dimethylethylenediamino aspartamide) (PEO-*g*-P[Asp(DMEDA)]) by a two-step ring-opening polymerization of poly(succinimide) (PSI) (Figure 2.51).[174] An aminofunctional mPEO was reacted with some of the succinimide rings in the PSI to form PEO-*g*-PSI. The remaining succinimide units were ring opened by DMEDA leading to the PEO-*g*-P[Asp(DMEDA)] copolymer. Ammonium glycyrrhizinate (AMG), a drug with three carboxylate anions for treating chronic hepatitis C and inflammatory diseases,[175-177] was encapsulated into the graft copolymers. High loading capacity and sustained release of AMG from the polymeric micelles were observed through *in vitro* studies.

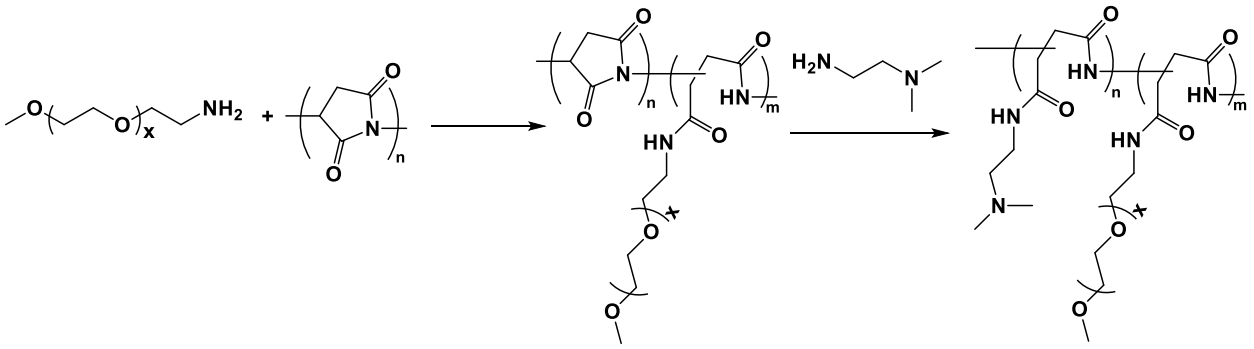

Figure 2.51 Synthesis of PEO-*g*-P[Asp(DMEDA)]

2.3.4.4 PEO-PLL copolymers

PEO-poly(L-lysine) (PLL) is another important member in the family of cationic PIC's. Similar to the synthesis of PAsp, PLL is prepared by ring opening of an *N*-carboxyanhydride of ε-(benzyloxycarbonyl)-$_L$-lysine using amine functionalized mPEO as a macroinitiator (Figure 2.52). This was followed by deprotection of the ε-(benzyloxycarbonyl) group.[128]

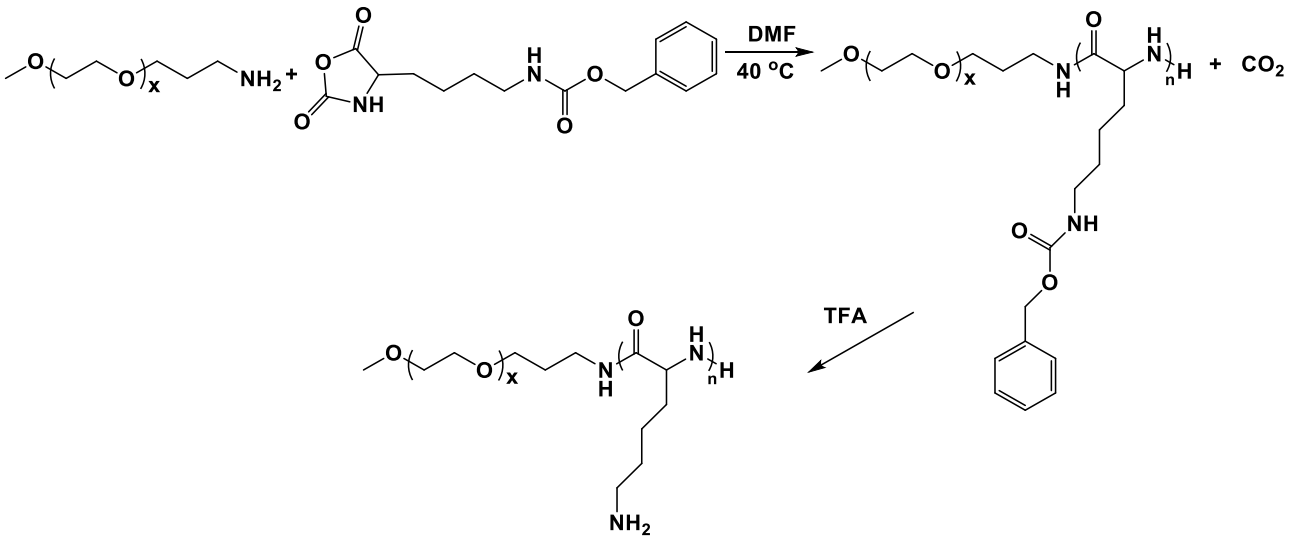

Figure 2.52 Synthesis of PEO-*b*-PLL

Kataoka *et al.* attempted to load negatively charged antisense-oligodeoxynucleotides (antisense-ODN) into PEO-*b*-PLL copolymers.[178] Antisense-ODN's can inhibit expression of special genes in cells by binding to a complementary mRNA sequence and thus blocking their translation.[179] Such biological activities can lead to treatment approaches for certain human diseases.[180] Problems with antisense-ODN's arise from their instabilities and poor capabilities for entering cells.[181] Therefore, cationic polymeric carriers for antisense-ODN's are desirable to improve their stability and cell permeability. Kataoka and coworkers encapsulated antisense-ODN's with different lengths into the PEO-*b*-PLL copolymers. The complexes that formed had

low PDI's (0.03 to 0.04) as measured by dynamic light scattering and well-defined sizes (23 to 37 nm). They also showed improved resistance to degradation by nucleases compared to free antisense ODN's. The same research group designed cross-linked PEO-*b*-PLL micelles as carriers for therapeutic siRNA as well.[134] The cross-linked complex had a 100-fold higher siRNA transfection efficiency than the linear polymer. This was attributed to the improved stability of the cross-linked network under physiological conditions.

Graft copolymers of PEO and PLL have also been designed to serve as gene delivery vehicles. The approach was to couple a functionalized mPEO with some of the amine groups on the side chains of PLL to afford grafted architectures.[182, 183] Kim *et al.* utilized an acyl chloride end-capped mPEO as the coupling agent to react with PEO-*g*-PLL (Figure 2.53).[182] They entrapped an anionic pDNA (pSV-β-gal), a reporter gene for monitoring gene expression, to the graft PEO-*g*-PLL copolymer. The complexes exhibited 5- to 30-fold higher transfection efficiencies compared to the drug loaded PLL carriers with Hep G2 cells, a human carcinoma cell line. Maruyama *et al.* also employed a PEO-*g*-PLL copolymer to incorporate Photofrin® (porfimer sodium), a photosensitizer with anionic carboxylates used in photodynamic therapy (PDT).[184] PDT is a treatment for cancer that utilizes photosensitizers with laser radiation to generate reactive oxygen species that can react with surrounding tumor cells or tissues.[185] A major side effect of Photofrin® is skin photosensitivity due to systemic delivery. The Photofrin® with PEO-*g*-PLL enhanced tumor localization about 2-fold compared to the free Photofrin® and this suppressed the side effect of skin photosensitivity.

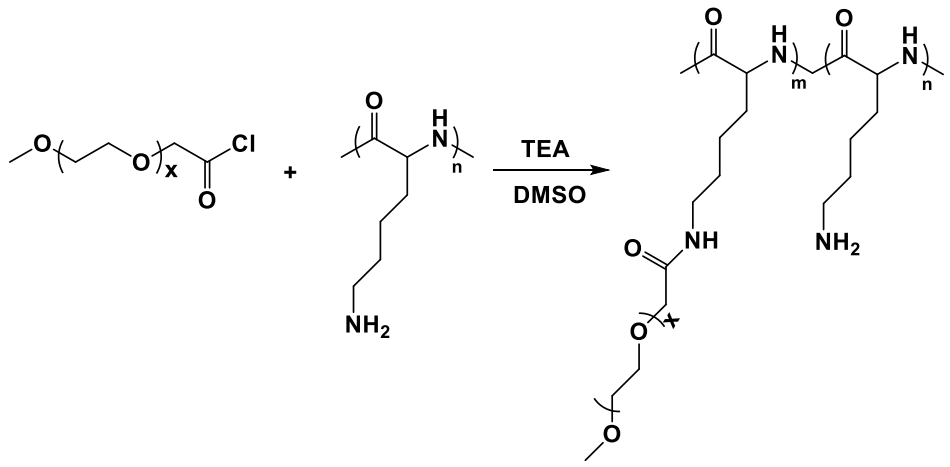

Figure 2.53 Synthesis of PEO-*g*-PLL via acyl chloride mPEO.

2.4 References

1. Kim, M.-J.; Jeon, I.-Y.; Seo, J.-M.; Dai, L.; Baek, J.-B., Graphene Phosphonic Acid as an Efficient Flame Retardant. *ACS Nano* 2014, 8, 2820-2825.

2. Stone, C.; Daynard, T. S.; Hu, L. Q.; Mah, C.; Steck, A. E., Phosphonic acid functionalized proton exchange membranes for PEM fuel cells. *J. New Mater. Electrochem. Syst.* 2000, 3, 43-50.

3. Tan, J.; Gemeinhart, R. A.; Ma, M.; Mark Saltzman, W., Improved cell adhesion and proliferation on synthetic phosphonic acid-containing hydrogels. *Biomaterials* 2005, 26, 3663-3671.

4. Xu, X.; Yu, H.; Gao, S.; Mao, H.-Q.; Leong, K. W.; Wang, S., Polyphosphoester microspheres for sustained release of biologically active nerve growth factor. *Biomaterials* 2002, 23, 3765-3772.

5. Aksnes, G.; Songstad, J., Alkaline hydrolysis of diethyl esters of alkylphosphonic acids and some chloro substituted derivatives. *Acta Chem. Scand.* 1965, 19, 893-7.

6. Hudson, R. F.; Keay, L., Hydrolysis of phosphonate esters. *J. Chem. Soc.* 1956, 2463-9.

7. Pfeiffer, F. R.; Mier, J. D.; Weisbach, J. A., Synthesis of phosphoric acid isoesters of 2-phospho-, 3-phospho-, and 2,3-diphosphoglyceric acid. *J. Med. Chem.* 1974, 17, 112-15.

8. Rabinowitz, R., The reactions of phosphonic acid esters with acid chlorides. A very mild hydrolytic route. *J. Org. Chem.* 1963, 28, 2975-8.

9. McKenna, C. E.; Higa, M. T.; Cheung, N. H.; McKenna, M. C., The facile dealkylation of phosphonic acid dialkyl esters by bromotrimethylsilane. *Tetrahedron Lett.* 1977, 155-8.

10. Zon, J.; Garczarek, P.; BiaLek, M., Chapter 6 Synthesis of Phosphonic Acids and Their Esters as Possible Substrates for Reticular Chemistry. In *Metal Phosphonate Chemistry: From Synthesis to Applications*, The Royal Society of Chemistry: 2012; pp 170-191.

11. Brodard-Severac, F.; Guerrero, G.; Maquet, J.; Florian, P.; Gervais, C.; Mutin, P. H., High-Field 17O MAS NMR Investigation of Phosphonic Acid Monolayers on Titania. *Chem. Mater.* 2008, 20, 5191-5196.

12. Rogers, M. J.; Crockett, J. C.; Coxon, F. P.; Mönkkönen, J., Biochemical and molecular mechanisms of action of bisphosphonates. *Bone* 2011, 49, 34-41.

13. Faisca Phillips, A. M.; Barros, M. T., Synthesis of geminal bisphosphonates via organocatalyzed enantioselective Michael additions of cyclic ketones and 4-piperidones. *Org. Biomol. Chem.* 2012, 10, 404-412.

14. Degenhardt, C. R.; Burdsall, D. C., Synthesis of ethenylidenebis(phosphonic acid) and its tetraalkyl esters. *J. Org. Chem.* 1986, 51, 3488-90.

15. Matczak-Jon, E.; Kurzak, B.; Kafarski, P.; Woźna, A., Coordination abilities of piperyd-1-yl-methane-1,1-diphosphonic acids towards zinc(II), magnesium(II) and calcium(II): Potentiometric and NMR studies. *J. Inorg. Biochem.* 2006, 100, 1155-1166.

16. Woodbury, C. P., Chapter 8 Basic Concepts in Metabolism. In *Biochemistry for the Pharmaceutical Sciences*, Sudbury, MA : Jones & Bartlett Learning: 2012.

17. Fleisch, H.; Russell, R. G. G.; Bisaz, S.; Termine, J. D.; Posner, A. S., Influence of pyrophosphate on the transformation of amorphous to crystalline calcium phosphate. *Calcified Tissue Res.* 1968, 2, 49-59.

18. De Rosa, G.; Misso, G.; Salzano, G.; Caraglia, M., Bisphosphonates and cancer: what opportunities from nanotechnology? *J. Drug Delivery* 2013, 637976, 17 pp.

19. Ebetino, F. H.; Hogan, A.-M. L.; Sun, S.; Tsoumpra, M. K.; Duan, X.; Triffitt, J. T.; Kwaasi, A. A.; Dunford, J. E.; Barnett, B. L.; Oppermann, U.; Lundy, M. W.; Boyde, A.; Kashemirov, B. A.; McKenna, C. E.; Russell, R. G. G., The relationship between the chemistry and biological activity of the bisphosphonates. *Bone* 2011, 49, 20-33.

20. Dunford, J. E.; Thompson, K.; Coxon, F. P.; Luckman, S. P.; Hahn, F. M.; Poulter, C. D.; Ebetino, F. H.; Rogers, M. J., Structure-activity relationships for inhibition of farnesyl diphosphate synthase in vitro and inhibition of bone resorption in vivo by nitrogen-containing bisphosphonates. *J. Pharmacol. Exp. Ther.* 2001, 296, 235-242.

21. Dunford, J. E.; Kwaasi, A. A.; Rogers, M. J.; Barnett, B. L.; Ebetino, F. H.; Russell, R. G. G.; Oppermann, U.; Kavanagh, K. L., Structure-Activity Relationships Among the Nitrogen Containing Bisphosphonates in Clinical Use and Other Analogues: Time-Dependent Inhibition of Human Farnesyl Pyrophosphate Synthase. *J. Med. Chem.* 2008, 51, 2187-2195.

22. Stresing, V.; Fournier, P. G.; Bellahcène, A.; Benzaïd, I.; Mönkkönen, H.; Colombel, M.; Ebetino, F. H.; Castronovo, V.; Clézardin, P., Nitrogen-containing bisphosphonates can inhibit angiogenesis in vivo without the involvement of farnesyl pyrophosphate synthase. *Bone* 2011, 48, 259-266.

23. Horiguchi, M.; Kandatsu, M., Isolation of 2-aminoethylphosphonic acid from rumen protozoa. *Nature (London, U. K.)* 1959, 184, 901-2.

24. Huang, J.; Chen, R., An overview of recent advances on the synthesis and biological activity of α-aminophosphonic acid derivatives. *Heteroatom Chem.* 2000, 11, 480-492.

25. Kafarski, P.; Lejczak, B., Biological activity of aminophosphonic acids. *Phosphorus, Sulfur Silicon Relat. Elem.* 1991, 63, 193-215.

26. Kukhar, V. P.; Hudson, H. R.; Editors, *Aminophosphonic and Aminophosphinic Acids: Chemistry and Biological Activity*. Wiley: 2000; p 634 pp.

27. David, G.; Boutevin, B.; Seabrook, S.; Destarac, M.; Woodward, G.; Otter, G., Radical telomerisation of vinyl phosphonic acid with a series of chain transfer agents. *Macromol. Chem. Phys.* 2007, 208, 635-642.

28. Chougrani, K.; Niel, G.; Boutevin, B.; David, G., Regioselective ester cleavage during the preparation of bisphosphonate methacrylate monomers. *Beilstein J. Org. Chem.* 2011, 7, 364-368, No 46.

29. Catel, Y.; Degrange, M.; Le Pluart, L.; Madec, P.-J.; Pham, T.-N.; Picton, L., Synthesis, photopolymerization and adhesive properties of new hydrolytically stable phosphonic acids for dental applications. *J. Polym. Sci., Part A: Polym. Chem.* 2008, 46, 7074-7090.

30. Boutevin, B.; Hervaud, Y.; Boulahna, A.; El Asri, M., Free-Radical Polymerization of Dimethyl Vinylbenzylphosphonate Controlled by Tempo. *Macromolecules* 2002, 35, 6511-6516.

31. Souzy, R.; Ameduri, B., Functional fluoropolymers for fuel cell membranes. *Prog. Polym. Sci.* 2005, 30, 644-687.

32. Steininger, H.; Schuster, M.; Kreuer, K. D.; Kaltbeitzel, A.; Bingoel, B.; Meyer, W. H.; Schauff, S.; Brunklaus, G.; Maier, J.; Spiess, H. W., Intermediate temperature proton conductors for PEM fuel cells based on phosphonic acid as protogenic group: A progress report. *Phys. Chem. Chem. Phys.* 2007, 9, 1764-1773.

33. Negrell-Guirao, C.; Boutevin, B.; David, G.; Fruchier, A.; Sonnier, R.; Lopez-Cuesta, J.-M., Synthesis of polyphosphorinanes Part II. Preparation, characterization and thermal properties of novel flame retardants. *Polym. Chem.* 2011, 2, 236-243.

34. Kosolapoff, G. M., Preparation of dibutyl allylphosphonate. *J. Am. Chem. Soc.* 1951, 73, 4040.

35. Avci, D.; Mathias, L. J., Synthesis and polymerization of phosphorus-containing acrylates. *J. Polym. Sci., Part A: Polym. Chem.* 2002, 40, 3221-3231.

36. Moszner, N.; Zeuner, F.; Fischer, U. K.; Rheinberger, V., Monomers for adhesive polymers, 2. Synthesis and radical polymerisation of hydrolytically stable acrylic phosphonic acids. *Macromol. Chem. Phys.* 1999, 200, 1062-1067.

37. Sahin, G.; Avci, D.; Karahan, O.; Moszner, N., Synthesis and photopolymerizations of new phosphonated methacrylates from alkyl α-hydroxymethacrylates and glycidyl methacrylate. *J. Appl. Polym. Sci.* 2009, 114, 97-106.

38. Sahin, G.; Albayrak, A. Z.; Bilgici, Z. S.; Avci, D., Synthesis and evaluation of new dental monomers with both phosphonic and carboxylic acid functional groups. *J. Polym. Sci., Part A: Polym. Chem.* 2009, 47, 1953-1965.

39. Bilgici, Z. S.; Ordu, O. D.; Isik, M.; Avci, D., Synthesis and polymerizations of six aminophosphonate-containing methacrylates. *J. Polym. Sci., Part A: Polym. Chem.* 2011, 49, 5042-5048.

40. Tsuda, T.; Mathias, L. J., Cyclopolymerization of ether dimers of α-(hydroxymethyl)acrylic acid and its alkyl esters: substituent effect on cyclization efficiency and microstructures. *Polymer* 1994, 35, 3317-3328.

41. Bilgici, Z. S.; Buyukgumus, O.; Altin, A.; Avci, D., Synthesis and polymerizations of novel bisphosphonate-containing methacrylates derived from alkyl α-hydroxymethacrylates. *Polym. Int.* 2014, 63, 427-434.

42. Bilgici, Z. S.; Turker, S. B.; Avci, D., Novel Bisphosphonated Methacrylates: Synthesis, Polymerizations, and Interactions with Hydroxyapatite. *Macromol. Chem. Phys.* 2013, 214, 2324-2335.

43. Misato, T.; Ko, K.; Honma, Y.; Takeda, M.; Konno, K.; Fuga, N. Ethylphosphonate analogs as bactericides and fungicides. JP51125750A, 1976.

44. Bhattacharya, A. K.; Thyagarajan, G., Michaelis-Arbuzov rearrangement. *Chem. Rev.* 1981, 81, 415-430.

45. Starks, C. M., *Free radical telomerization*. Academic Press: New York, 1974; p 198.

46. Fields, E. K., The synthesis of esters of substituted amino phosphonic acids. *J. Am. Chem. Soc.* 1952, 74, 1528-31.

47. Enders, D.; Saint-Dizier, A.; Lannou, M.-I.; Lenzen, A., The phospha-Michael addition in organic synthesis. *Eur. J. Org. Chem.* 2005, 29-49.

48. Boutevin, B.; Hamoui, B.; Parisi, J. P., New diethyl phosphonoalkyl acrylates and their reactivity in copolymerization. *Polym. Bull. (Berlin)* 1993, 30, 243-8.

49. Boutevin, B.; Hamoui, B.; Parisi, J. P., Synthesis and polymerizations of monomers bearing phosphonated groups. I. Applications on acrylates and methacrylates. *J. Appl. Polym. Sci.* 1994, 52, 449-456.

50. Senhaji, O.; Robin, J. J.; Achchoubi, M.; Boutevin, B., Synthesis and characterization of new methacrylic phosphonated surface active monomer. *Macromol. Chem. Phys.* 2004, 205, 1039-1050.

51. Gaboyard, M.; Robin, J.-J.; Hervaud, Y.; Boutevin, B., Free-radical graft copolymerization of phosphonated methacrylates onto low-density polyethylene. *J. Appl. Polym. Sci.* 2002, 86, 2011-2020.

52. Francova, D.; Kickelbick, G., Synthesis of methacrylate-functionalized phosphonates and phosphates with long alkyl-chain spacers and their self-aggregation in aqueous solutions. *Monatsh. Chem.* 2009, 140, 413-422.

53. Francova, D.; Kickelbick, G., Self-Assembly of Methacrylate-Functionalized Phosphonate and Phosphate Amphiphiles and their Conversion into Nanospheres. *Macromol. Chem. Phys.* 2009, 210, 2037-2045.

54. Rixens, B.; Boutevin, G.; Boulahna, A.; Hervaud, Y.; Boutevin, B., Synthesis of new phosphonated monomers. *Phosphorus, Sulfur Silicon Relat. Elem.* 2004, 179, 2617-2626.

55. Chougrani, K.; Boutevin, B.; David, G.; Seabrook, S.; Loubat, C., Acrylate based anticorrosion films using novel bis-phosphonic methacrylates. *J. Polym. Sci., Part A: Polym. Chem.* 2008, 46, 7972-7984.

56. Chougrani, K.; Boutevin, B.; David, G.; Boutevin, G., New N,N-amino-diphosphonate-containing methacrylic derivatives, their syntheses and radical copolymerizations with MMA. *Eur. Polym. J.* 2008, 44, 1771-1781.

57. Zefirov, N. S.; Matveeva, E. D., Catalytic Kabachnik-Fields reaction: new horizons for old reaction. *ARKIVOC (Gainesville, FL, U. S.)* 2008, 1-17.

58. Lam, O. A.; David, G.; Hervaud, Y.; Boutevin, B., High performance anticorrosive coatings based on new phosphonic methacrylate terpolymers. *J. Polym. Sci., Part A: Polym. Chem.* 2009, 47, 5090-5100.

59. Edizer, S.; Sahin, G.; Avci, D., Development of reactive phosphonated methacrylates. *J. Polym. Sci., Part A: Polym. Chem.* 2009, 47, 5737-5746.

60. Edizer, S.; Avci, D., Synthesis and Photo-Polymerization of an Aryl Diphosphonic Acid-Containing Dimethacrylate for Dental Materials. *Des. Monomers Polym.* 2010, 13, 337-347.

61. Jansen, J. F. G. A.; Dias, A. A.; Dorschu, M.; Coussens, B., Fast Monomers: Factors Affecting the Inherent Reactivity of Acrylate Monomers in Photoinitiated Acrylate Polymerization. *Macromolecules* 2003, 36, 3861-3873.

62. Altin, A.; Akgun, B.; Buyukgumus, O.; Sarayli Bilgici, Z.; Agopcan, S.; Asik, D.; Yagci Acar, H.; Avci, D., Synthesis and photopolymerization of novel, highly reactive phosphonated-urea-methacrylates for dental materials. *React. Funct. Polym.* 2013, 73, 1319-1326.

63. Ikemura, K.; Tay, F. R.; Nishiyama, N.; Pashley, D. H.; Endo, T., Multi-purpose bonding performance of newly synthesized phosphonic acid monomers. *Dent. Mater. J.* 2007, 26, 105-115.

64. Ikemura, K.; Endo, T.; Kadoma, Y., A review of the developments of multi-purpose primers and adhesives comprising novel dithiooctanoate monomers and phosphonic acid monomers. *Dent. Mater. J.* 2012, 31, 1-25.

65. Ikemura, K.; Tay, F. R.; Nishiyama, N.; Pashley, D. H.; Endo, T., Design of new phosphonic acid monomers for dental adhesives - synthesis of (Meth)acryloxyalkyl 3-phosphonopropionates and evaluation of their adhesion-promoting functions. *Dent. Mater. J.* 2006, 25, 566-575.

66. Nishiyama, N.; Suzuki, K.; Yoshida, H.; Teshima, H.; Nemoto, K., Hydrolytic stability of methacrylamide in acidic aqueous solution. *Biomaterials* 2004, 25, 965-969.

67. Xu, X.; Wang, R.; Ling, L.; Burgess, J. O., Synthesis and stability study of dental monomers containing methacrylamidoethyl phosphonic acids. *J. Polym. Sci., Part A: Polym. Chem.* 2006, 45, 99-110.

68. Catel, Y.; Fischer, U. K.; Moszner, N., Monomers for adhesive polymers: 11. Structure–adhesive properties relationships of new hydrolytically stable acidic monomers. *Polym. Int.* 2013, 62, 1717-1728.

69. Besse, V.; Le Pluart, L.; Cook, W. D.; Pham, T.-N.; Madec, P.-J., Polymerization kinetics of phosphonic acids and esters using an iodonium initiator. *J. Polym. Sci., Part A: Polym. Chem.* 2013, 51, 5046-5055.

70. Besse, V.; Le Pluart, L.; Cook, W. D.; Pham, T. N.; Madec, P. J., Synthesis and polymerization kinetics of acrylamide phosphonic acids and esters as new dentine adhesives. *J. Polym. Sci., Part A: Polym. Chem.* 2013, 51, 149-157.

71. Catel, Y.; Degrange, M.; Pluart, L. L.; Madec, P.-J.; Pham, T.-N.; Chen, F.; Cook, W. D., Synthesis, photopolymerization, and adhesive properties of new bisphosphonic acid monomers for dental application. *J. Polym. Sci., Part A: Polym. Chem.* 2009, 47, 5258-5271.

72. Klee, J. E.; Lehmann, U., N-alkyl-N-(phosphonoethyl) substituted (meth)acrylamides - new adhesive monomers for self-etching self-priming one part dental adhesive. *Beilstein J. Org. Chem.* 2009, 5, No. 72, No pp. given, No. 72.

73. Altin, A.; Akgun, B.; Sarayli Bilgici, Z.; Begum Turker, S.; Avci, D., Synthesis, photopolymerization, and adhesive properties of hydrolytically stable phosphonic acid-containing (meth)acrylamides. *J. Polym. Sci., Part A: Polym. Chem.* 2014, 52, 511-522.

74. Akgun, B.; Avci, D., Synthesis and evaluations of bisphosphonate-containing monomers for dental materials. *J. Polym. Sci., Part A: Polym. Chem.* 2012, 50, 4854-4863.

75. Graillot, A.; Monge, S.; Faur, C.; Bouyer, D.; Robin, J.-J., Synthesis by RAFT of innovative well-defined (co)polymers from a novel phosphorus-based acrylamide monomer. *Polym. Chem.* 2013, 4, 795-803.

76. Bouilhac, C.; Travelet, C.; Graillot, A.; Monge, S.; Borsali, R.; Robin, J.-J., Synthesis of fatty phosphonic acid based polymethacrylamide by RAFT polymerization and self-assembly in solution. *Polym. Chem.* 2014, 5, 2756-2767.

77. Mou, L.; Singh, G.; Nicholson, J. W., Synthesis of a hydrophilic phosphonic acid monomer for dental materials. *Chem. Commun. (Cambridge)* 2000, 345-346.

78. Moszner, N., New monomers for dental application. *Macromol. Symp.* 2004, 217, 63-75.

79. Quittmann, U.; Lecamp, L.; El Khatib, W.; Youssef, B.; Bunel, C., Synthesis of a New Phosphonated Dimethacrylate: Photocuring Kinetics in Homo- and Copolymerization, Determination of Thermal and Flame-Retardant Properties. *Macromol. Chem. Phys.* 2001, 202, 628-635.

80. Youssef, B.; Lecamp, L.; El Khatib, W.; Bunel, C.; Mortaigne, B., New phosphonated methacrylates: Synthesis, photocuring and study of their thermal and flame-retardant properties. *Macromol. Chem. Phys.* 2003, 204, 1842-1850.

81. Moszner, N.; Salz, U.; Zimmermann, J., Chemical aspects of self-etching enamel–dentin adhesives: A systematic review. *Dent. Mater.* 2005, 21, 895-910.

82. Van Meerbeek, B.; Yoshihara, K.; Yoshida, Y.; Mine, A.; J, D. M.; K.L, V. L., State of the art of self-etch adhesives. *Dent. Mater.* 2011, 27, 17-28.

83. Monge, S.; Canniccioni, B.; Graillot, A.; Robin, J.-J., Phosphorus-Containing Polymers: A Great Opportunity for the Biomedical Field. *Biomacromolecules* 2011, 12, 1973-1982.

84. Zalipsky, S., Functionalized Poly(ethylene glycols) for Preparation of Biologically Relevant Conjugates. *Bioconjugate Chem.* 1995, 6, 150-165.

85. Cammas, S.; Nagasaki, Y.; Kataoka, K., Heterobifunctional Poly(ethylene oxide): Synthesis of .alpha.-Methoxy-.omega.-amino and .alpha.-Hydroxy-.omega.-amino PEOs with the Same Molecular Weights. *Bioconjugate Chem.* 1995, 6, 226-230.

86. Lee, J. H.; Lee, H. B.; Andrade, J. D., Blood compatibility of polyethylene oxide surfaces. *Prog. Polym. Sci.* 1995, 20, 1043-1079.

87. Lasic, D. D.; Martin, F. J.; Gabizon, A.; Huang, S. K.; Papahadjopoulos, D., Sterically stabilized liposomes: a hypothesis on the molecular origin of the extended circulation times. *Biochim. Biophys. Acta, Biomembr.* 1991, 1070, 187-92.

88. Zalipsky, S.; Harris, J. M., Introduction to chemistry and biological applications of poly(ethylene glycol). *ACS Symp. Ser.* 1997, 680, 1-13.

89. Otsuka, H.; Nagasaki, Y.; Kataoka, K., Self-assembly of poly(ethylene glycol)-based block copolymers for biomedical applications. *Curr. Opin. Colloid Interface Sci.* 2001, 6, 3-10.

90. Nuyken, O.; Pask, S. D., Ring-opening polymerization - an introductory review. *Polymers (Basel, Switz.)* 2013, 5, 361-403, 43 pp.

91. Thompson, M. S.; Vadala, T. P.; Vadala, M. L.; Lin, Y.; Riffle, J. S., Synthesis and applications of heterobifunctional poly(ethylene oxide) oligomers. *Polymer* 2008, 49, 345-373.

92. Huang, Y. J.; Qi, G. R.; Chen, L. S., Effects of morphology and composition on catalytic performance of double metal cyanide complex catalyst. *Appl. Catal., A.* 2003, 240, 263-271.

93. Huang, Y.-J.; Qi, G.-R.; Chen, G.-X., Random copolymer of propylene oxide and ethylene oxide prepared by double metal cyanide complex catalyst. *Chin. J. Polym. Sci.* 2002, 20, 453-459.

94. Ito, K.; Tanaka, K.; Tanaka, H.; Imai, G.; Kawaguchi, S.; Itsuno, S., Poly(ethylene oxide) macromonomers. 7. Micellar polymerization in water. *Macromolecules* 1991, 24, 2348-2354.

95. Plank, J.; Pöllmann, K.; Zouaoui, N.; Andres, P. R.; Schaefer, C., Synthesis and performance of methacrylic ester based polycarboxylate superplasticizers possessing hydroxy terminated poly(ethylene glycol) side chains. *Cem. Concr. Res.* 2008, 38, 1210-1216.

96. Cernovska, K.; Koenig, B., Safe and Convenient Preparation of Azido-Methoxy Polyethylene glycol on an Azide-Anion Exchange Resin. *Synth. Commun.* 2003, 33, 3789-3794.

97. Deng, J.; Luo, Y.; Zhang, L.-M., PEGylated polyamidoamine dendron-assisted encapsulation of plasmid DNA into in situ forming supramolecular hydrogel. *Soft Matter* 2011, 7, 5944-5947.

98. Nho, K.; Hyun, C.; Lee, J.; Pak, Y. Preparation of polyethylene glycol maleimide derivatives. US20040225097A1, 2004.

99. Ananda, K.; Nacharaju, P.; Smith, P. K.; Acharya, S. A.; Manjula, B. N., Analysis of functionalization of methoxy–PEG as maleimide–PEG. *Anal. Biochem.* 2008, 374, 231-242.

100. Du, Y. J.; Brash, J. L., Synthesis and characterization of thiol-terminated poly(ethylene oxide) for chemisorption to gold surface. *J. Appl. Polym. Sci.* 2003, 90, 594-607.

101. Vidal, F.; Guyot, A., Thiol-ended polyethylene oxide as a stabilizer in styrene emulsion polymerization. *New J. Chem.* 1995, 19, 1081-8.

102. Dalsin, J. L.; Lin, L.; Tosatti, S.; Vörös, J.; Textor, M.; Messersmith, P. B., Protein Resistance of Titanium Oxide Surfaces Modified by Biologically Inspired mPEG−DOPA. *Langmuir* 2004, 21, 640-646.

103. Veronese, F. M., Peptide and protein PEGylation: a review of problems and solutions. *Biomaterials* 2001, 22, 405-417.

104. Veronese, F. M.; Pasut, G., PEGylation, successful approach to drug delivery. *Drug Discovery Today* 2005, 10, 1451-1458.

105. Roberts, M. J.; Bentley, M. D.; Harris, J. M., Chemistry for peptide and protein PEGylation. *Adv. Drug Delivery Rev.* 2012, 64, Supplement, 116-127.

106. Schulz, D. N.; Kaladas, J. J.; Maurer, J. J.; Bock, J.; Pace, S. J.; Schulz, W. W., Copolymers of acrylamide and surfactant macromonomers: synthesis and solution properties. *Polymer* 1987, 28, 2110-2115.

107. Restrepo, A. S.; Pinzón, N. M.; Ju, L.-K., Synthesis of pH-sensitive surfactants by the terpolymerization of methacrylic acid, methoxy poly(ethylene glycol) methacrylate, and lauryl methacrylate: Initiator effect and reactivity ratio study. *J. Polym. Sci., Part A: Polym. Chem.* 2004, 42, 2950-2959.

108. Xiao, H.; Pelton, R.; Hamielec, A., Preparation and kinetic characterization of copolymers of acrylamide and poly(ethylene glycol) (meth)acrylate macromonomers. *Polymer* 1996, 37, 1201-1209.

109. Smith, B. L.; Klier, J., Determination of monomer reactivity ratios for copolymerizations of methacrylic acid with poly (ethylene glycol) monomethacrylate. *J. Appl. Polym. Sci.* 1998, 68, 1019-1025.

110. Khousakoun, E.; Gohy, J.-F.; Jérôme, R., Self-association of double-hydrophilic copolymers of acrylic acid and poly(ethylene oxide) macromonomer. *Polymer* 2004, 45, 8303-8310.

111. Belleney, J.; Hélary, G.; Migonney, V., Terpolymerization of methyl methacrylate, poly(ethylene glycol) methyl ether methacrylate or poly(ethylene glycol) ethyl ether methacrylate with methacrylic acid and sodium styrene sulfonate: determination of the reactivity ratios. *Eur. Polym. J.* 2002, 38, 439-444.

112. Ito, K.; Tsuchida, H.; Hayashi, A.; Kitano, T.; Yamada, E.; Matsumoto, T., Reactivity of poly(ethylene oxide) macromonomers in radical copolymerization. *Polym. J. (Tokyo)* 1985, 17, 827-39.

113. Otsuka, H.; Nagasaki, Y.; Kataoka, K., PEGylated nanoparticles for biological and pharmaceutical applications. *Adv Drug Deliv Rev* 2012.

114. Scholz, C.; Iijima, M.; Nagasaki, Y.; Kataoka, K., Polymeric micelles as drug delivery systems: a reactive polymeric micelle carrying aldehyde groups. *Polym. Adv. Technol.* 1998, 9, 768-776.

115. La, S. B.; Nagasaki, Y.; Kataoka, K., Poly(ethylene glycol)-based micelles for drug delivery. *ACS Symp. Ser.* 1997, 680, 99-118.

116. Vadala, M. L.; Thompson, M. S.; Ashworth, M. A.; Lin, Y.; Vadala, T. P.; Ragheb, R.; Riffle, J. S., Heterobifunctional Poly(ethylene oxide) Oligomers Containing Carboxylic Acids. *Biomacromolecules* 2008, 9, 1035-1043.

117. Nakamura, T.; Nagasaki, Y.; Kataoka, K., Synthesis of Heterobifunctional Poly(ethylene glycol) with a Reducing Monosaccharide Residue at One End. *Bioconjugate Chem.* 1998, 9, 300-303.

118. Bedekar, A. N.; Naik, A. N.; Pise, A. C., Schiff base derivatives of 2-amino-2-deoxy-1,3,4,6-tetra-O-acetyl-β-D-glucopyranose. *Asian J. Chem.* 2009, 21, 6661-6666.

119. Culf, A. S.; Melanson, J. A.; Ouellette, R. J.; Briand, G. G., Bis-imine primary amine protection of the dialkyltriamine, norspermidine. *Tetrahedron Lett.* 2012, 53, 3301-3304.

120. Huang, Y.; Li, Z.; Morawetz, H., The kinetics of the attachment of polymer chains to reactive latex particles and the resulting latex stabilization. *J. Polym. Sci., Polym. Chem. Ed.* 1985, 23, 795-9.

121. Yokoyama, M.; Okano, T.; Sakurai, Y.; Kikuchi, A.; Ohsako, N.; Nagasaki, Y.; Kataoka, K., Synthesis of poly(ethylene oxide) with heterobifunctional reactive groups at its terminals by an anionic initiator. *Bioconjugate Chem.* 1992, 3, 275-276.

122. Kim, Y. J.; Nagasaki, Y.; Kataoka, K.; Kato, M.; Yokoyama, M.; Okano, T.; Sakurai, Y., Heterobifunctional poly(ethylene oxide). One pot synthesis of poly(ethylene oxide) with a primary amino group at one end and a hydroxyl group at the other end. *Polym. Bull. (Berlin)* 1994, 33, 1-6.

123. Jia, Z.; Zhang, H.; Huang, J., Synthesis of poly(Ethylene glycol) with sulfadiazine and chlorambucil end groups and investigation of its antitumor activity. *Bioorg. Med. Chem. Lett.* 2003, 13, 2531-2534.

124. Tessmar, J. K.; Mikos, A. G.; Goepferich, A., Amine-Reactive Biodegradable Diblock Copolymers. *Biomacromolecules* 2002, 3, 194-200.

125. Nagasaki, Y.; Iijima, M.; Kato, M.; Kataoka, K., Primary Amino-Terminal Heterobifunctional Poly(ethylene oxide). Facile Synthesis of Poly(ethylene oxide) with a Primary Amino Group at One End and a Hydroxyl Group at the Other End. *Bioconjugate Chem.* 1995, 6, 702-704.

126. Schlaad, H.; Kukula, H.; Rudloff, J.; Below, I., Synthesis of α,ω-Hetero-bifunctional Poly(ethylene glycol)s by Metal-Free Anionic Ring-Opening Polymerization. *Macromolecules* 2001, 34, 4302-4304.

127. Halasa, A. F., Anionic Polymerization: Principles and Practical Applications, by Henry L. Hsieh and Roderic P. Quirk. *Rubber Chem. Technol.* 1997, 70, G10.

128. Harada, A.; Kataoka, K., Formation of Polyion Complex Micelles in an Aqueous Milieu from a Pair of Oppositely-Charged Block Copolymers with Poly(ethylene glycol) Segments. *Macromolecules* 1995, 28, 5294-5299.

129. Kabanov, A. V.; Bronich, T. K.; Kabanov, V. A.; Yu, K.; Eisenberg, A., Soluble Stoichiometric Complexes from Poly(N-ethyl-4-vinylpyridinium) Cations and Poly(ethylene oxide)-block-polymethacrylate Anions. *Macromolecules* 1996, 29, 6797-6802.

130. Kabanov, A. V.; Vinogradov, S. V.; Suzdaltseva, Y. G.; Alakhov, V. Y., Water-Soluble Block Polycations as Carriers for Oligonucleotide Delivery. *Bioconjugate Chem.* 1995, 6, 639-643.

131. Lee, Y.; Kataoka, K., Biosignal-sensitive polyion complex micelles for the delivery of biopharmaceuticals. *Soft Matter* 2009, 5, 3810-3817.

132. Ranjan, A.; Pothayee, N.; Seleem, M.; Jain, N.; Sriranganathan, N.; Riffle, J. S.; Kasimanickam, R., Drug delivery using novel nanoplexes against a Salmonella mouse infection model. *J. Nanopart. Res.* 2010, 12, 905-914.

133. Takae, S.; Miyata, K.; Oba, M.; Ishii, T.; Nishiyama, N.; Itaka, K.; Yamasaki, Y.; Koyama, H.; Kataoka, K., PEG-Detachable Polyplex Micelles Based on Disulfide-Linked Block Catiomers as Bioresponsive Nonviral Gene Vectors. *J. Am. Chem. Soc.* 2008, 130, 6001-6009.

134. Matsumoto, S.; Christie, R. J.; Nishiyama, N.; Miyata, K.; Ishii, A.; Oba, M.; Koyama, H.; Yamasaki, Y.; Kataoka, K., Environment-Responsive Block Copolymer Micelles with a Disulfide Cross-Linked Core for Enhanced siRNA Delivery. *Biomacromolecules* 2009, 10, 119-127.

135. Yan, Y.; Li, J.; Zheng, J.; Pan, Y.; Wang, J.; He, X.; Zhang, L.; Liu, D., Poly(l-lysine)-based star-block copolymers as pH-responsive nanocarriers for anionic drugs. *Colloids Surf., B* 2012, 95, 137-143.

136. Voets, I. K.; de Keizer, A.; de Waard, P.; Frederik, P. M.; Bomans, P. H. H.; Schmalz, H.; Walther, A.; King, S. M.; Leermakers, F. A. M.; Cohen Stuart, M. A., Double-faced micelles from water-soluble polymers. *Angew. Chem., Int. Ed.* 2006, 45, 6673-6676.

137. Annaka, M.; Morishita, K.; Okabe, S., Electrostatic Self-Assembly of Neutral and Polyelectrolyte Block Copolymers and Oppositely Charged Surfactant. *J. Phys. Chem. B* 2007, 111, 11700-11707.

138. Scales, C. W.; Huang, F.; Li, N.; Vasilieva, Y. A.; Ray, J.; Convertine, A. J.; McCormick, C. L., Corona-Stabilized Interpolyelectrolyte Complexes of SiRNA with Nonimmunogenic, Hydrophilic/Cationic Block Copolymers Prepared by Aqueous RAFT Polymerization. *Macromolecules* 2006, 39, 6871-6881.

139. Sanson, N.; Bouyer, F.; Gerardin, C.; In, M., Nanoassemblies formed from hydrophilic block copolymers and multivalent ions. *Phys. Chem. Chem. Phys.* 2004, 6, 1463-1466.

140. Voets, I. K.; De Keizer, A.; Cohen Stuart, M. A.; De Waard, P., Core and Corona Structure of Mixed Polymeric Micelles. *Macromolecules* 2006, 39, 5952-5955.

141. Chiang, W.-H.; Huang, W.-C.; Chang, Y.-J.; Shen, M.-Y.; Chen, H.-H.; Chern, C.-S.; Chiu, H.-C., Doxorubicin-Loaded Nanogel Assemblies with pH/Thermo-triggered Payload Release for Intracellular Drug Delivery. *Macromol. Chem. Phys.* 2014, n/a-n/a.

142. Bisht, H. S.; Manickam, D. S.; You, Y.; Oupicky, D., Temperature-Controlled Properties of DNA Complexes with Poly(ethylenimine)-graft-poly(N-isopropylacrylamide). *Biomacromolecules* 2006, 7, 1169-1178.

143. Kim, S. H.; Mok, H.; Jeong, J. H.; Kim, S. W.; Park, T. G., Comparative Evaluation of Target-Specific GFP Gene Silencing Efficiencies for Antisense ODN, Synthetic siRNA, and siRNA Plasmid Complexed with PEI-PEG-FOL Conjugate. *Bioconjugate Chem.* 2006, 17, 241-244.

144. Feng, C.; Li, Y.; Yang, D.; Hu, J.; Zhang, X.; Huang, X., Well-defined graft copolymers: from controlled synthesis to multipurpose applications. *Chem. Soc. Rev.* 2011, 40, 1282-1295.

145. Grainger, S. J.; El-Sayed, M. E. H. In *Stimuli-sensitive particles for drug delivery*, World Scientific Publishing Co. Pte. Ltd.: 2010; pp 171-190.

146. Piogé, S.; Fontaine, L.; Gaillard, C.; Nicol, E.; Pascual, S., Self-Assembling Properties of Well-Defined Poly(ethylene oxide)-b-poly(ethyl acrylate) Diblock Copolymers. *Macromolecules* 2009, 42, 4262-4272.

147. Guo, L.; Ida, S.; Takashiba, A.; Daio, T.; Teramae, N.; Ishihara, T., Soft-templating method to synthesize crystalline mesoporous [small alpha]-Fe2O3 films. *New J. Chem.* 2014, 38, 1392-1395.

148. Sun, Y.; Peng, Z.; Liu, X.; Tong, Z., Synthesis and pH-sensitive micellization of doubly hydrophilic poly(acrylic acid)-b-poly(ethylene oxide)-b-poly(acrylic acid) triblock copolymer in aqueous solutions. *Colloid. Polym. Sci.* 2010, 288, 997-1003.

149. Krieg, A.; Pietsch, C.; Baumgaertel, A.; Hager, M. D.; Becer, C. R.; Schubert, U. S., Dual hydrophilic polymers based on (meth)acrylic acid and poly(ethylene glycol) - synthesis and water uptake behavior. *Polym. Chem.* 2010, 1, 1669-1676.

150. LeHoux, J. G.; Grondin, F., Some effects of chitosan on liver function in the rat. *Endocrinology (Baltimore)* 1993, 132, 1078-84.

151. Lee, V. H. L.; Li, V. H. K., Prodrugs for improved ocular drug delivery. *Adv. Drug Delivery Rev.* 1989, 3, 1-38.

152. Oh, K. T.; Bronich, T. K.; Kabanov, V. A.; Kabanov, A. V., Block Polyelectrolyte Networks from Poly(acrylic acid) and Poly(ethylene oxide): Sorption and Release of Cytochrome C. *Biomacromolecules* 2006, 8, 490-497.

153. Izumrudov, V. A.; Ortega Ortiz, H.; Zezin, A. B.; Kabanov, V. A., Temperature controllable interpolyelectrolyte substitution reactions. *Macromol. Chem. Phys.* 1998, 199, 1057-1062.

154. Yokoyama, M.; Fukushima, S.; Uehara, R.; Okamoto, K.; Kataoka*, K.; Sakurai, Y.; Okano, T., Characterization of physical entrapment and chemical conjugation of adriamycin in polymeric micelles and their design for in vivo delivery to a solid tumor. *J. Controlled Release* 1998, 50, 79-92.

155. Yokoyama, M.; Sugiyama, T.; Okano, T.; Sakurai, Y.; Naito, M.; Kataoka, K., Analysis of Micelle Formation of an Adriamycin-Conjugated Poly(Ethylene Glycol)–Poly(Aspartic Acid) Block Copolymer by Gel Permeation Chromatography. *Pharm. Res.* 1993, 10, 895-899.

156. Yokoyama, M.; Inoue, S.; Kataoka, K.; Yui, N.; Okano, T.; Sakurai, Y., Molecular design for missile drugs: synthesis of adriamycin conjugated with immunoglobulin G using poly(ethylene glycol)-block-poly(aspartic acid) as intermediate carrier. *Makromol. Chem.* 1989, 190, 2041-54.

157. Cammas, S.; Harada, A.; Nagasaki, Y.; Kataoka, K., Poly(ethylene oxide-co-β-benzyl l-aspartate) Block Copolymers: Influence of the Poly(ethylene oxide) Block on the Conformation of the Poly(β-benzyl l-aspartate) Segment in Organic Solvents. *Macromolecules* 1996, 29, 3227-3231.

158. Bae, Y.; Kataoka, K., Intelligent polymeric micelles from functional poly(ethylene glycol)-poly(amino acid) block copolymers. *Adv. Drug Delivery Rev.* 2009, 61, 768-784.

159. Lee, H. J.; Bae, Y., Cross-Linked Nanoassemblies from Poly(ethylene glycol)-poly(aspartate) Block Copolymers as Stable Supramolecular Templates for Particulate Drug Delivery. *Biomacromolecules* 2011, 12, 2686-2696.

160. Eckman, A. M.; Tsakalozou, E.; Kang, N. Y.; Ponta, A.; Bae, Y., Drug Release Patterns and Cytotoxicity of PEG-poly(aspartate) Block Copolymer Micelles in Cancer Cells. *Pharm. Res.* 2012, 29, 1755-1767.

161. Kakizawa, Y.; Kataoka, K., Block Copolymer Self-Assembly into Monodispersive Nanoparticles with Hybrid Core of Antisense DNA and Calcium Phosphate. *Langmuir* 2002, 18, 4539-4543.

162. Kakizawa, Y.; Furukawa, S.; Kataoka, K., Block copolymer-coated calcium phosphate nanoparticles sensing intracellular environment for oligodeoxynucleotide and siRNA delivery. *J. Controlled Release* 2004, 97, 345-356.

163. Giger, E. V.; Puigmarti-Luis, J.; Schlatter, R.; Castagner, B.; Dittrich, P. S.; Leroux, J.-C., Gene delivery with bisphosphonate-stabilized calcium phosphate nanoparticles. *J. Controlled Release* 2011, 150, 87-93.

164. Xie, Y.; Chen, Y.; Sun, M.; Ping, Q., A mini review of biodegradable calcium phosphate nanoparticles for gene delivery. *Curr. Pharm. Biotechnol.* 2014, 14, 918-25.

165. Kanayama, N.; Fukushima, S.; Nishiyama, N.; Itaka, K.; Jang, W.-D.; Miyata, K.; Yamasaki, Y.; Chung, U.-i.; Kataoka, K., A PEG-based biocompatible block catiomer with high buffering capacity for the construction of polyplex micelles showing efficient gene transfer toward primary cells. *ChemMedChem* 2006, 1, 439-444.

166. Akinc, A.; Thomas, M.; Klibanov, A. M.; Langer, R., Exploring polyethylenimine-mediated DNA transfection and the proton sponge hypothesis. *J. Gene Med.* 2005, 7, 657-663.

167. Boussif, O.; Lezoualc'h, F.; Zanta, M. A.; Mergny, M. D.; Scherman, D.; Demeneix, B.; Behr, J. P., A versatile vector for gene and oligonucleotide transfer into cells in culture and in vivo: polyethylenimine. *Proc. Natl. Acad. Sci. USA* 1995, 92, 7297-301.

168. Pollard, H.; Remy, J.-S.; Loussouarn, G.; Demolombe, S.; Behr, J.-P.; Escande, D., Polyethylenimine but not cationic lipids promotes transgene delivery to the nucleus in mammalian cells. *J. Biol. Chem.* 1998, 273, 7507-7511.

169. Behr, J.-P., Synthetic Gene Transfer Vectors II: Back to the Future. *Acc. Chem. Res.* 2012, 45, 980-984.

170. Itaka, K.; Ohba, S.; Miyata, K.; Kawaguchi, H.; Nakamura, K.; Takato, T.; Chung, U.-I.; Kataoka, K., Bone Regeneration by Regulated In Vivo Gene Transfer Using Biocompatible Polyplex Nanomicelles. *Mol. Ther.* 2007, 15, 1655-1662.

171. Han, M.; Bae, Y.; Nishiyama, N.; Miyata, K.; Oba, M.; Kataoka, K., Transfection study using multicellular tumor spheroids for screening non-viral polymeric gene vectors with low cytotoxicity and high transfection efficiencies. *J. Controlled Release* 2007, 121, 38-48.

172. Akagi, D.; Oba, M.; Koyama, H.; Nishiyama, N.; Fukushima, S.; Miyata, T.; Nagawa, H.; Kataoka, K., Biocompatible micellar nanovectors achieve efficient gene transfer to vascular lesions without cytotoxicity and thrombus formation. *Gene Ther.* 2007, 14, 1029-1038.

173. Miyata, K.; Oba, M.; Nakanishi, M.; Fukushima, S.; Yamasaki, Y.; Koyama, H.; Nishiyama, N.; Kataoka, K., Polyplexes from Poly(aspartamide) Bearing 1,2-Diaminoethane Side Chains Induce pH-Selective, Endosomal Membrane Destabilization with Amplified Transfection and Negligible Cytotoxicity. *J. Am. Chem. Soc.* 2008, 130, 16287-16294.

174. Yang, D.; Zhang, X.; Yuan, L.; Hu, J., PEG-g-poly(aspartamide-co-N,N-dimethylethylenediamino aspartamide): synthesis, characterization and its application as a drug delivery system. *Prog. Nat. Sci.* 2009, 19, 1305-1310.

175. Ploeger, B.; Mensinga, T.; Sips, A.; Seinen, W.; Meulenbelt, J.; DeJongh, J., The pharmacokinetics of glycyrrhizic acid evaluated by physiologically based pharmacokinetic modeling. *Drug Metab. Rev.* 2001, 33, 125-147.

176. Nakata, N.; Kira, Y.; Yabunaka, Y.; Takaoka, K., Prevention of venous thrombosis by preoperative glycyrrhizin infusion in a rat model. *J. Orthop. Sci.* 2008, 13, 456-462.

177. Kumada, H., Long-term treatment of chronic hepatitis C with glycyrrhizin [Stronger Neo-Minophagen C (SNMC)] for preventing liver cirrhosis and hepatocellular carcinoma. *Oncology* 2002, 62, 94-100.

178. Harada, A.; Togawa, H.; Kataoka, K., Physicochemical properties and nuclease resistance of antisense-oligodeoxynucleotides entrapped in the core of polyion complex micelles composed of poly(ethylene glycol)-poly(l-Lysine) block copolymers. *Eur. J. Pharm. Sci.* 2001, 13, 35-42.

179. Wagner, R. W., Gene inhibition using antisense oligodeoxynucleotides. *Nature (London)* 1994, 372, 333-5.

180. Bayever, E.; Iversen, P. L.; Bishop, M. R.; Sharp, J. G.; Tewary, H. K.; Arneson, M. A.; Pirruccello, S. J.; Ruddon, R. W.; Kessinger, A.; Zon, G.; et, a., Systemic administration of a phosphorothioate oligonucleotide with a sequence complementary to p53 for acute myelogenous leukemia and myelodysplastic syndrome: initial results of a phase I trial. *Antisense Res. Dev.* 1993, 3, 383-90.

181. Stein, C. A.; Cheng, Y. C., Antisense oligonucleotides as therapeutic agents - is the bullet really magical? *Science (Washington, D. C., 1883-)* 1993, 261, 1004-12.

182. Choi, Y. H.; Liu, F.; Kim, J.-S.; Choi, Y. K.; Park, J. S.; Kim, S. W., Polyethylene glycol-grafted poly-1-lysine as polymeric gene carrier. *J. Controlled Release* 1998, 54, 39-48.

183. Choi, S. W.; Yamayoshi, A.; Hirai, M.; Yamano, T.; Takagi, M.; Sato, A.; Kano, A.; Shimamoto, A.; Maruyama, A., Preparation of cationic comb-type copolymers having high density of PEG graft chains for gene carriers. *Macromol. Symp.* 2007, 249/250, 312-316.

184. Kano, A.; Taniwaki, Y.; Nakamura, I.; Shimada, N.; Moriyama, K.; Maruyama, A., Tumor delivery of Photofrin® by PLL-g-PEG for photodynamic therapy. *J. Controlled Release* 2013, 167, 315-321.

185. Usuda, J.; Kato, H.; Okunaka, T.; Furukawa, K.; Tsutsui, H.; Yamada, K.; Suga, Y.; Honda, H.; Nagatsuka, Y.; Ohira, T.; Tsuboi, M.; Hirano, T., Photodynamic Therapy (PDT) for Lung Cancers. *J. Thorac. Oncol.* 2006, 1, 489-493.

CHAPTER 3 - Synthesis of Ammonium Bisphosphonate Monomers and Polymers

Reprinted from Polymer, 54, N. Hu, L. M. Johnson, Nikorn Pothayee, Nipon Pothayee, Y. Lin, R. M. Davis and J. S. Riffle, Synthesis of Ammonium Bisphosphonate Monomers and Polymers, 3188-3197, Copyright (2013), with permission from Elsevier.

http://www.sciencedirect.com/science/article/pii/S0032386113003649

Nan Hu,[a,b] L. M. Johnson,[a] Nikorn Pothayee,[a] Nipon Pothayee,[a] Y. Lin,[a] R. M. Davis[a,c] and J. S. Riffle[a,b]

[a]Macromolecules and Interfaces Institute, [b]Department of Chemistry, [c]Department of Chemical Engineering, Virginia Tech, Blacksburg, VA 24061

3.1 Abstract

Ammonium bisdiethylphosphonate acrylate and methacrylate monomers were synthesized by an aza-Michael addition of 3-aminopropanol across the double bond of bisdiethylphosphonate, followed by acylation with (meth)acryloyl chloride. Free radical copolymerizations of the monomers with an acrylate-functional poly(ethylene oxide) (PEO) macromonomer produced graft copolymers. Quantitative deprotection of the alkylphosphonate groups, then adjustment of the pH to 7.74 ± 0.03, yielded graft copolymers with zwitterionic ammonium bisphosphonate backbones and PEO grafts. Copolymerization kinetic studies showed that the ammonium bisdiethylphosphonate methacrylate incorporated into the copolymers with PEO acrylate well, but that the corresponding acrylate monomer reacted too slowly. The zwitterionic copolymers spontaneously assembled into aggregates in aqueous media.

3.2 Introduction

Phosphorus-containing polymers have been widely investigated as flame retardants, adhesion promoters, components of dental resins, and as substrates for binding calcium or calcium phosphates.[1-4] Polymers containing phosphate and phosphonate pendent groups are of interest for potential orthopedic and dental applications. Stancu and coworkers[5] investigated copolymers of methacryloyloxyethyl phosphate with (2-diethylamino)ethyl methacrylate and found enhanced calcium binding capacity with increasing amounts of the phosphate-containing monomer. Mineralization of such substrates with calcium phosphates, however, was complicated and did not correlate well with calcium binding. Phosphoric and phosphonic acid bearing polymers have been studied as potential components of dental adhesives and resins, where their acidity can etch tooth enamel to increase adhesion of filler materials.[6, 7] Chougrani *et al.*[8, 9] reported a series of *N,N*-bis(methylene diphosphonate) methacrylate monomers as precursors for polymers that promote adhesion. Moszner *et al.*[6, 10] synthesized phosphonic acid-containing (meth)acrylamides and novel acrylic ether phosphonic acids for potential self-etching dental adhesives with increased hydrolytic stability over phosphorus-containing methacrylates.

Only a few investigations of block copolymers containing phosphonic acids and PEO have been carried out. Penczek et al. prepared PEO-polyglycidol diblock copolymers that were post-modified with phosphonates and carboxylates on the same pendent carbon.[11] This group also modified PEO-polyglycidol block copolymers with phosphate groups and showed that they could mediate crystallization of calcium carbonate.[12] Hollow spheres with hybrid calcium carbonate-polymer compositions comprised of layers of smaller spheres were formed with these materials.

Self-assembly of phosphonate and phosphate-containing monomers and polymers has been reported.[13-15] Francová *et al.*[16, 17] synthesized methacrylate-functional amphiphiles with alkyl spacers terminated with phosphonate and phosphate groups that formed micelles in water, then crosslinked the micelles in UV- or thermally initiated free radical polymerizations. Dynamic light scattering (DLS) measurements showed a distribution of spheres ranging from 30 to 400 nm in diameter. Tew *et al.*[18] prepared polyoxanorbornene copolymers where one block had pendent phosphonic acids and the other was relatively hydrophobic. A series of these materials had mean hydrodynamic radii ranging from 123 to 301 nm as measured by DLS.

This paper focuses on synthesis of ammonium bisdiethylphosphonate acrylates and methacrylates and their copolymerization with acrylate-functional PEO macromonomers to yield poly(ammonium bisdiethylphosphonate (meth)acrylate)-*g*-PEO copolymers. Subsequent removal of the ethyl groups on the phosphonates produced zwitterionic poly(ammonium bisphosphonate (meth)acrylate)-g-PEO copolymers. The properties of these copolymers in aqueous media are of interest because of their potential utility as components of drug delivery and bioimaging vehicles.

3.3 Experimental

3.3.1 Materials

Diethyl vinylphosphonate (Epsilon-Chimie, >98%) and dichloromethane (EMD Chemicals, anhydrous, 99.8%) were used as received. Methanol (99.9%), hexane (99.9%), dichloromethane (99.9%), chloroform (99.9%), magnesium sulfate (anhydrous, 98%), diethyl ether (anhydrous, 99.8%) and dialysis tubing (Spectra/Por, 3,500 MWCO), all from Fisher Scientific, were used as received. *N,N*-Dimethylformamide (DMF, anhydrous, 99.8%), methanol (anhydrous, 99.8%), sodium sulfate (anhydrous, 99%), 3-ammonium-1-propanol (>99%), triethylamine (>99.5%), sodium hydroxide (97%), poly(ethylene oxide) methyl ether (M_n= 5,085 and 2,100 g mol^{-1}),

2,2'-azobisisobutyronitrile (AIBN, 98%), sodium chloride (>99.5%) and benzoylated cellulose dialysis tubing (2,100 MWCO) were purchased from Sigma-Aldrich and used as received. Acryloyl chloride (97%), methacryloyl chloride (97%) and bromotrimethylsilane (TMSBr, 97.0%) were fractionally distilled before use.

3.3.2 Synthesis

3.3.2.1 Synthesis of Hydroxypropyl Ammonium Bisdiethylphosphonate

3-Aminopropanol (8.0 g, 0.11 mol), diethyl vinylphosphonate (36.0 g, 0.22 mol) and 200 mL of deionized water were charged to a 500-mL round-bottom flask with a magnetic stir bar and sealed with a septum. The reaction was placed in an oil bath and maintained at 60 °C for 24 h. The reaction mixture was extracted with dichloromethane (5 x 80 mL) at room temperature. The combined organic phase was washed with deionized water (2 x 25 mL), dried over anhydrous magnesium sulfate, then the solvent was evaporated to afford 3-hydroxypropylammonium bisdiethylphosphonate (**1**, 41 g, 95%).

3.3.2.2 Synthesis of an Ammonium Bisdiethylphosphonate Acrylate Monomer

1 (15 g, 37 mmol), triethylamine (4.1 g, 41 mmol), and 70 mL of anhydrous dichloromethane were charged to a flame-dried, 250-mL round-bottom flask equipped with a septum-sealed dropping funnel and placed in an ice bath. Acryloyl chloride (3.7 g, 41 mmol) was added drop-wise. The flask was removed from the ice bath and the reaction was stirred for 4 h at room temperature. The reaction mixture was washed with aq 0.1 N sodium hydroxide (3 x 150 mL) and the organic phase was dried over anhydrous sodium sulfate. The solvent was evaporated and the product (**2,** 11.4 g, 65%) was dried under vacuum at room temperature overnight.

3.3.2.3 Synthesis of an Ammonium Bisdiethylphosphonate Methacrylate Monomer

The ammonium bisdiethylphosphonate methacrylate monomer **3** (9.1 g, 78%) was synthesized in a similar manner to the analogous acrylate monomer using **1** (10.0 g, 25 mmol), triethylamine (2.9 g, 29 mmol), methacryloyl chloride (2.6 g, 29 mmol) and 50 mL of anhydrous dichloromethane. The monomer was dissolved in dichloromethane (18.2 mL) and stored in the refrigerator.

3.3.2.4 Synthesis of Acrylate-functional PEO

Poly(ethylene oxide) methyl ether (25 g, M_n = 5,085 g mol^{-1}, 4.9 mmol) was dried under vacuum at 50 °C overnight in a flame-dried 250-mL round bottom flask. Triethylamine (2.53 g, 25 mmol) and 70 mL of anhydrous dichloromethane were charged to the flask via syringe. Acryloyl chloride (2.3 g, 25 mmol) was added dropwise to the flask via syringe. The reaction mixture was stirred at room temperature overnight. The mixture was diluted with chloroform and washed 3 x 150 mL with an aqueous solution of sodium hydroxide (0.1 N). The organic phase was washed with water (2 x 100 mL), dried over anhydrous magnesium sulfate and concentrated by evaporation. The concentrated mixture was precipitated in hexane, filtered and dried under vacuum at room temperature to afford a pale yellow PEO-acrylate powder.

3.3.2.5 Synthesis of a 67:33 wt:wt Poly(ammonium bisdiethylphosphonate methacrylate)-*g*-PEO Copolymer

Dichloromethane in the ammonium bisdiethylphosphonate methacrylate monomer solution was removed by rotary evaporation. The monomer **3** (4.3 g, 9.1 mmol) was transferred to a flame-dried, 25-mL Schlenk flask equipped with a stir bar. An acrylate-PEO (2.15 g, 0.42 mmol) solution in degassed DMF (7 mL) was prepared in a 20-mL vial. AIBN (0.15 g, 0.9 mmol)

was dissolved in degassed DMF (5 mL) in a separate 20-mL vial. The acrylate-PEO solution and 1 mL of the freshly prepared AIBN solution in DMF were added to the Schlenk flask via syringe. After three freeze-pump-thaw cycles, the reaction mixture was heated at 70 °C for 7 h. The copolymer was precipitated in a cold mixture of 1:1 v:v anhydrous diethyl ether:hexane (2 x 400 mL). The resulting copolymer (**4**) was vacuum dried at room temperature overnight.

3.3.2.6 Deprotection of the 67:33 poly(ammonium bisdiethylphosphonate methacrylate)-*g*-PEO Copolymer

A flame-dried, round-bottom flask equipped with a stir bar was charged with dry poly(ammonium bisdiethylphosphonate methacrylate)-*g*-PEO (1.53 g, 8 meq of phosphonate), TMSBr (1.87 g, 12 mmol) and 10 mL of anhydrous dichloromethane. The reaction was stirred at room temperature for 15 h. Dichloromethane and the excess TMSBr were removed by rotary evaporation at 75 °C and the copolymer was dried under vacuum at room temperature for 1.5 h. Anhydrous methanol (10 mL) was added to the flask via syringe. After 12 h the reaction mixture was precipitated in cold ether (200 mL) and filtered. The copolymer was dissolved in 20 mL of methanol, transferred into 2,100 MWCO benzoylated cellulose dialysis tubing and dialyzed against 2 L methanol for 48 h. The solution was freeze-dried to obtain the poly(ammonium bisphosphonic acid)-*g*-PEO (**6**).

3.3.3 Kinetic Studies of Copolymerization

A poly(ammonium bisdiethylphosphonate acrylate)-*g*-PEO copolymer was synthesized as described above and aliquots were removed at known time intervals during the reaction. The copolymer samples were precipitated in a cold mixture of 1:1 v:v anhydrous diethyl ether:hexane (2 x 100 mL) to remove the unreacted ammonium bisdiethylphosphonate acrylate monomer. The

yellow solid was dissolved in THF, transferred to 3,500 MWCO dialysis tubing and dialyzed against 4 L of DI water for 48 h to remove unreacted acrylate-PEO.

Copolymers comprised of the ammonium bisdiethylphosphonate methacrylate monomer with the acrylate-PEO were prepared. Samples were taken at known time intervals during the reaction. Monomer conversions and copolymer compositions were measured by ^{1}H NMR.

3.3.4 Characterization

^{1}H NMR spectral analyses were performed on a Varian Unity 400 NMR, a JEOL Eclipse Plus 500 NMR or a Bruker Advance II-500 NMR operating at 399.95 MHz, 500 MHz or 500 MHz, respectively. ^{31}P NMR spectral analyses were obtained on a Varian Inova 400 NMR operating at 161.91 MHz. Parameters utilized for the ^{31}P NMR were a 45° pulse and 1 s relaxation delay with 128 scans. All spectra of the monomers and phosphonate polymers were obtained in $CDCl_3$. Spectra of the phosphonic acid polymers were obtained in D_2O by adjusting the pH to 7.74 with NaOD.

Thermogravimetric analysis (TGA) was conducted on a TGA Q500 (TA Instruments). All samples were held at 100 °C for 30 min prior to measurements to drive off excess moisture. Each sample was ramped from 50 to 600 °C at 10 °C /min in a nitrogen atmosphere. The mass remaining was recorded throughout the experiment.

Dynamic light scattering (DLS) measurements on the 67:33 wt:wt poly(ammonium bisphosphonic acid acrylate)-*g*-PEO copolymer and 67:33 poly(ammonium bisphosphonic acid methacrylate) copolymer were performed with a Zetasizer NanoZS particle analyzer (Malvern Instruments Ltd.) equipped with a solid-state He-Ne laser (λ= 633 nm) at a scattering angle of 173°. Intensity and volume average diameters were calculated with the Zetasizer Nano 4.2

software using an algorithm based on Mie theory that converts time-varying intensities to diameters. For DLS analysis, polymers were dissolved in DI water at concentrations of 0.5, 1.0, 1.5 and 2.0 mg mL^{-1}. The pH of the solution was adjusted to 7.74 ± 0.03 with addition of sodium hydroxide solution using a S47 SevenMulti pH meter (Mettler-Toledo International, Inc.) and the solution was sonicated for 1 min in a 75T VWR bath-type Ultrasonicator at 120 volts, then filtered through a 1.0 μm Teflon™ filter directly into a polystyrene cuvette for analysis.

3.4 Results and Discussion

3.4.1 Synthesis of Ammonium Bisdiethylphosphonate (Meth)acrylate Monomers

We have previously reported the formation of ammonium bisdiethylphosphonate end groups from primary amine-functional polymers via a double aza-Michael reaction of the terminal amine with diethyl vinylphosphonate in water.[19] Water promotes reaction of the unsaturated compound with the amine through hydrogen bonding.[20] Double addition of the amine onto diethyl vinylphosphonate was efficient with yields higher than 95%. Several researchers have synthesized ammonium bisphosphonates in organic solvents from aminoalcohols, formaldehyde, and dimethyl hydrogenphosphonate,[8] or by reacting aldehydes with amines and phosphites in the presence of a catalyst.[21, 22] In the present study, an aminoalcohol was simply reacted with diethyl vinylphosphonate in water to afford 3-hydroxypropyl ammonium bisdiethylphosphonate without the need for a catalyst. Subsequently, ammonium bisdiethylphosphonate-containing monomers were obtained by esterification of the hydroxypropyl ammonium bisdiethylphosphonate with acryloyl or methacryloyl chloride (Figure 3.1). The chemical structures of the new monomers were confirmed by ^{1}H NMR (Figure 3.2).

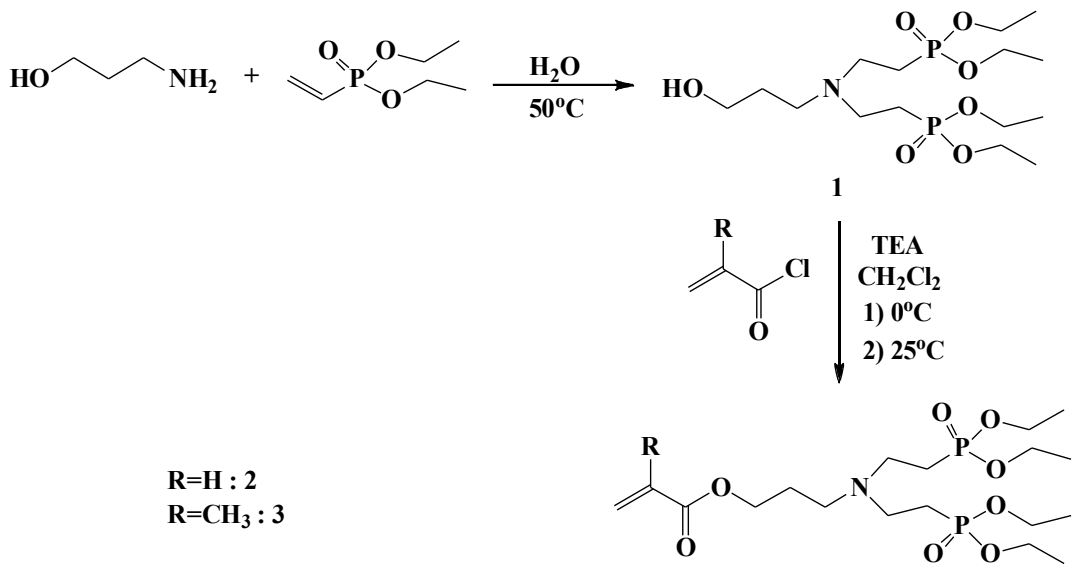

Figure 3.1 Synthesis of ammonium bisdiethylphosphonate (meth)acrylate monomers

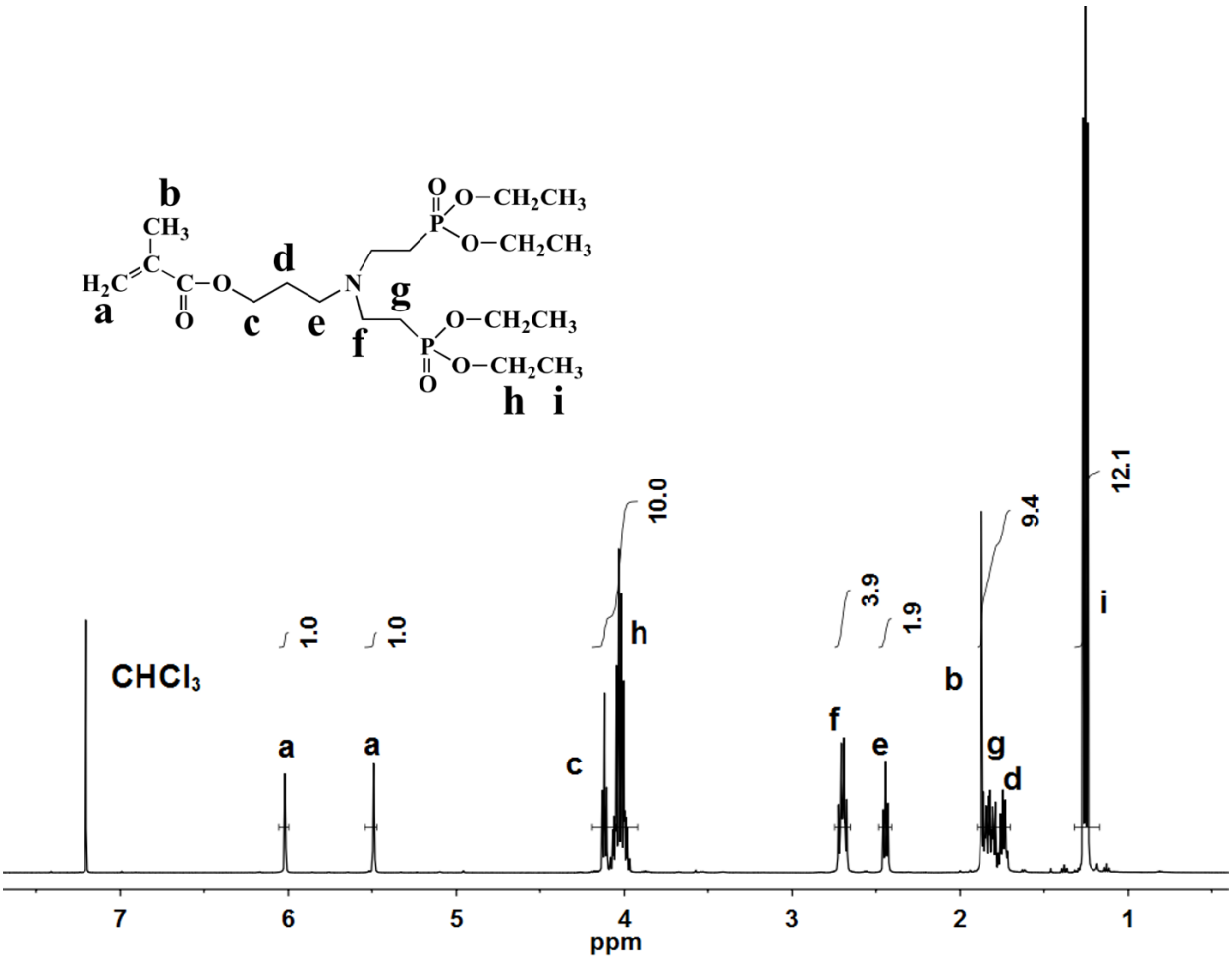

Figure 3.2 ^{1}H NMR spectrum of the ammonium bisdiethylphosphonate methacrylate monomer (**3**)

3.4.2 Synthesis of Poly(ammonium bisdiethylphosphonate (meth)acrylate)-*g*-PEO Copolymers

Free radical copolymerizations of methacrylate- or acrylate-functional PEO macromonomers with different methacrylate or acrylate derivatives have been carried out by several groups. Chougrani *et al.*[8] investigated kinetics of copolymerizations of related ammonium bisphosphonate methacrylate monomers with methyl methacrylate (MMA). The reactivity ratios (r_1's for the ammonium bisphosphonate monomers and r_2's for MMA) were approximately 1.1-1.3 and 0.8 respectively which indicated that the bisphosphonate groups could be incorporated into the methacrylate backbone in a statistical fashion. Neugebauer *et al.*[23] copolymerized PEO methyl ether methacrylate (MW = 1,100 g mol^{-1}) with PEO phenyl ether acrylate (MW = 324 g mol^{-1}). As expected, the methacrylate-PEO incorporated into the copolymer at a faster rate than the acrylate-PEO. Bencherif and coworkers[24, 25] synthesized star polymers using a PEO methyl ether methacrylate macromonomer, a heterobifunctional peptide end-capped acrylate-PEO and ethylene glycol dimethacrylate via ATRP. Anseth and coworkers[26] have prepared phosphate-containing PEO hydrogels by photocrosslinking ethylene glycol methacrylate phosphate with PEO diacrylates. These hydrogels were found to sequester the negatively charged cell adhesion protein osteopontin to promote adhesion and spreading of human mesenchymal stem cells. To our knowledge, few investigations have been conducted on copolymerization of acrylate-functional PEO with phosphonate-containing monomers. Herein we copolymerized acrylate-PEO macromonomers with ammonium bisdiethylphosphonate

acrylate (**2**) or ammonium bisdiethylphosphonate methacrylate monomers (**3**) to yield graft copolymers with (meth)acrylate-phosphonate backbones and PEO grafts (Figure 3.3). By varying the ratio of the ammonium bisdiethylphosphonate monomers relative to the acrylate-PEO, copolymers with the expected compositions were obtained. For targeted 67:33 and 50:50 wt:wt poly(ammonium bisdiethylphosphonate acrylate)-*g*-PEO copolymers, the experimental compositions after isolation of the materials were 64:36 and 49:51, respectively, as measured by ^{1}H NMR.

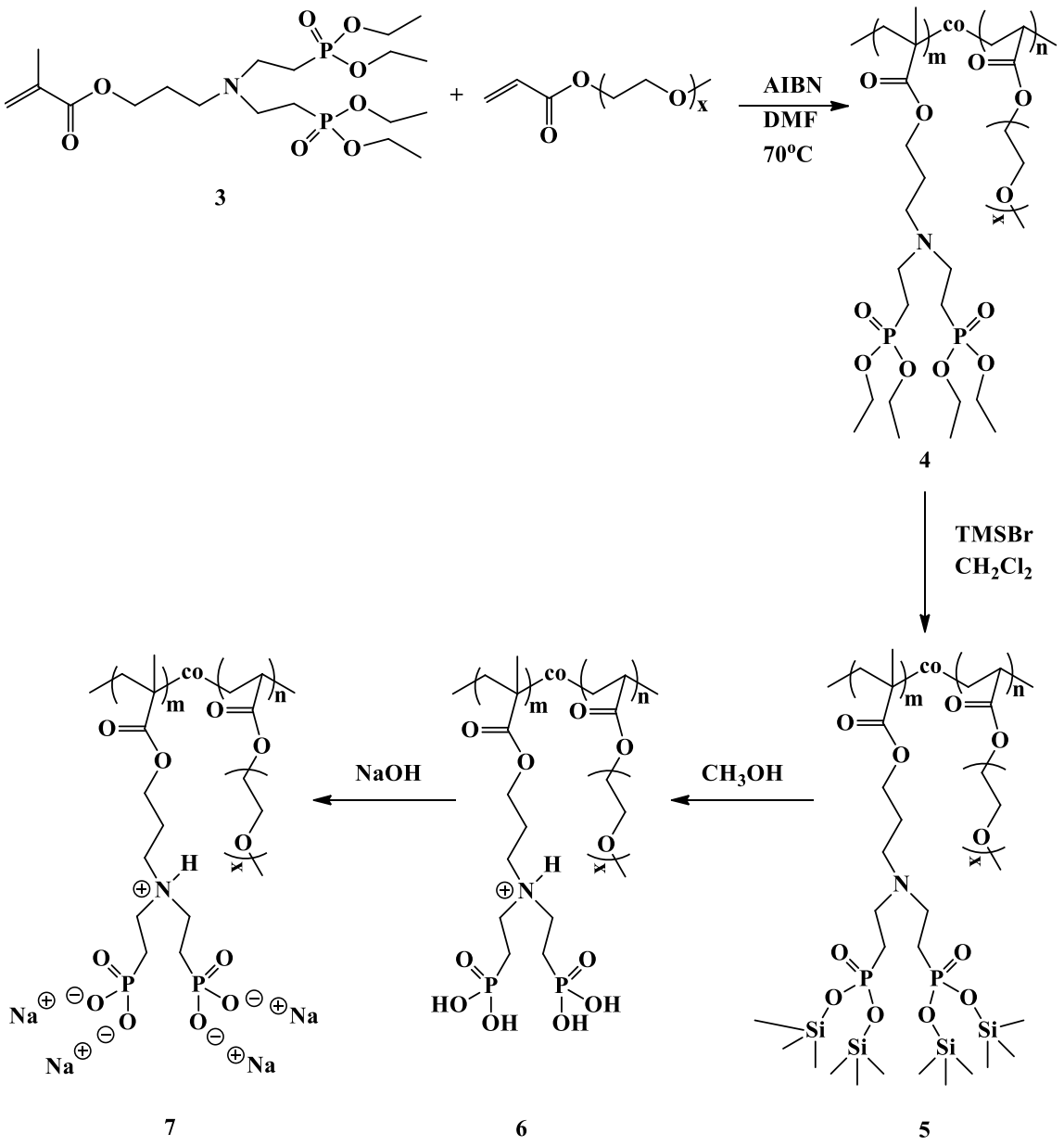

Figure 3.3 Synthesis of poly(ammonium bisdiethylphosphonate methacrylate)-*g*-PEO (**4**) and poly(ammonium bisphosphonate methacrylate)-*g*-PEO (**7**) copolymers

The relative rates of incorporation of the acrylate- and methacrylate-functional phosphonate monomers with the acrylate-PEO macromonomer into the copolymers were investigated to determine whether statistical graft copolymers formed. The molar feed ratio of

the phosphonate monomers relative to the acrylate-PEO macromonomer in these studies was 28 to 1. For cases where acrylate and methacrylate monomers were copolymerized, conversions of each monomer were directly measured by ^{1}H NMR of the reaction solutions by monitoring the vinyl peaks. For copolymerization of the ammonium bisdiethylphosphonate acrylate with acrylate-PEO, the overall conversions of both monomers were calculated by ^{1}H NMR, but measurement of individual conversions of each monomer by NMR was not possible due to overlap of the vinyl peaks. Thus, copolymers from aliquots of these reaction mixtures were isolated by precipitation and dialysis at early conversions so that the copolymer compositions could be analyzed.

Figure 3.4 shows a representative ^{1}H NMR spectrum of an ammonium bisdiethylphosphonate acrylate and acrylate-PEO copolymer that was isolated at 16% overall conversion. Only very small amounts of vinyl bonds resonating at 5.5-6.5 ppm from unreacted monomers remained. Integrals of the resonance at 3.6 ppm, assigned to the protons in the repeat units of PEO (M_n= 2,100 g mol^{-1}), were compared to the resonance at 4.1 ppm corresponding to the ammonium bisdiethylphosphonate acrylate in the copolymer. The resonance integral at 4.1 ppm was 31.33 (representing 10 protons per unit) relative to 198 for the PEO macromonomer at 3.6 ppm (representing one PEO unit of 2,100 g mol^{-1} M_n), and this corresponded to about three units of the ammonium bisdiethylphosphonate acrylate per PEO graft. This indicated that even though the functional group on both monomers was an acrylate, the acrylate-PEO macromonomer reacted much faster than the ammonium bisdiethylphosphonate acrylate. This, combined with the fact that only a small relative molar amount of the PEO was desirable, signified that the compositions of these copolymers were quite heterogeneous. Copolymers that formed early in these free radical reactions had high amounts of PEO, but the polymers formed

in the latter stages of this reaction were almost exclusively homopolymers of the ammonium bisdiethylphosphonate. Therefore, it was reasoned that these materials were actually blends of graft copolymers with poly(ammonium bisdiethylphosphonate acrylate) homopolymers. The reasons for the slow rate of polymerization of the phosphonate-containing monomers relative to the PEO remain unclear.

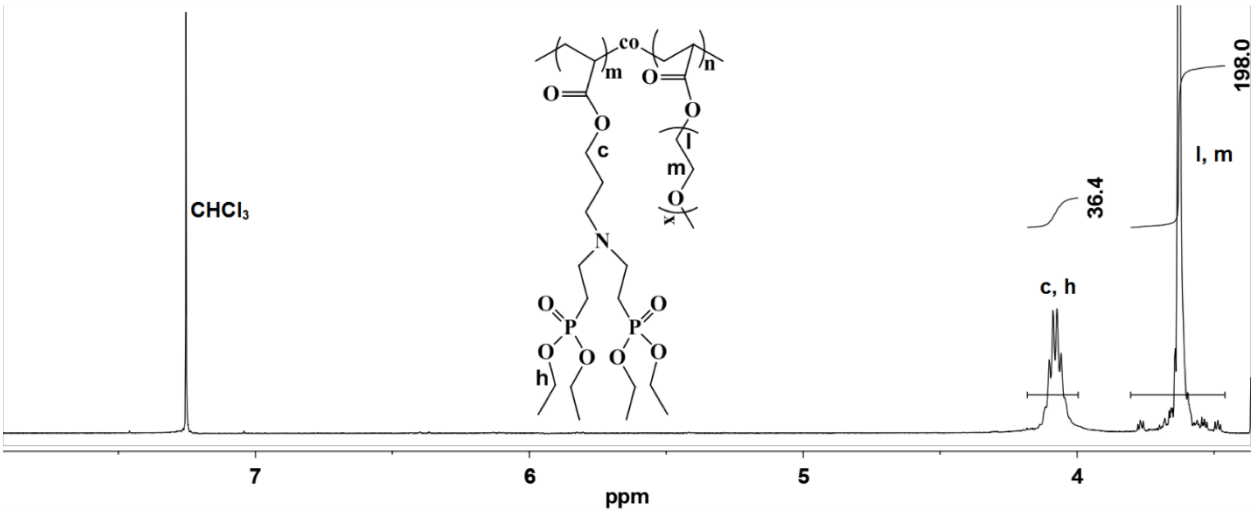

Figure 3.4 ^{1}H NMR of poly(ammonium bisdiethylphosphonate acrylate)-*g*-PEO separated at 16% total conversion of both ammonium bisdiethylphosphonate acrylate and acrylate-PEO monomers

Copolymerizations of ammonium bisdiethylphosphonate methacrylate with acrylate-PEO were investigated under similar conditions to the acrylate analogues. Figure 3.5 shows a representative ^{1}H NMR spectrum of a monomer mixture. The vinyl peaks of ammonium bisdiethylphosphonate methacrylate resonated at 5.5 and 6.0 ppm while the vinyl peaks on the acrylate-PEO were at 5.8, 6.1 and 6.4, and decreases in the peaks' intensities as the copolymerization proceeded were compared. Monomer conversions monitored early in a reaction showed much more efficient incorporation of the methacrylate-functional phosphonate monomer as compared to the acrylate-phosphonate (Figure 3.6). The ammonium

bisdiethylphosphonate methacrylate incorporated into the copolymer slightly faster than the acrylate-PEO macromonomer due to the higher reactivity of methacrylate relative to acrylate. At 7% and 4% individual conversion, the molar ratio of the ammonium bisdiethylphosphonate methacrylate to the acrylate-PEO in the copolymer was 49:1, about twice the feed molar ratio (28:1). Thus, while the compositions of the copolymers as the reaction progressed were somewhat heterogeneous, since the acrylate-PEO macromonomer that was present in a minor molar concentration was the slower to incorporate, graft copolymers formed continuously throughout these copolymerizations.

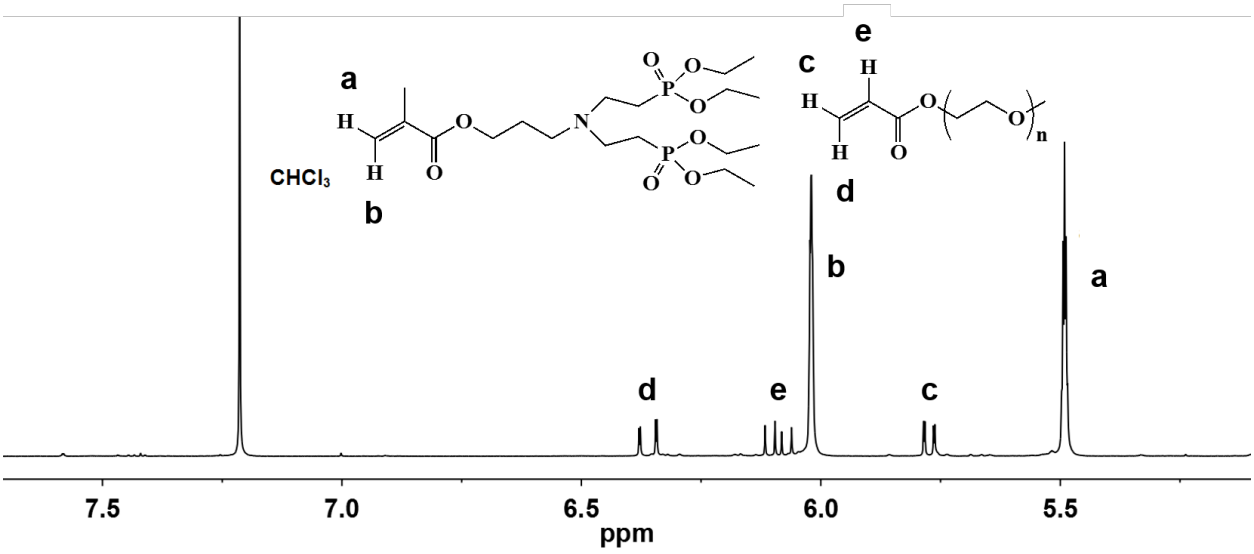

Figure 3.5 ^{1}H NMR of a monomer mixture comprised of ammonium bisdiethylphosphonate methacrylate and acrylate-PEO

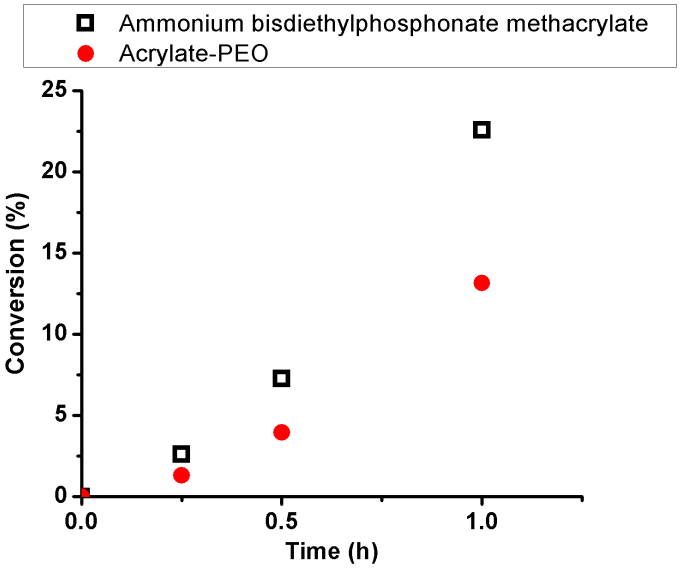

Figure 3.6 Monomer conversions during copolymerization of ammonium bisdiethylphosphonate methacrylate with acrylate-PEO

3.4.3 Deprotection of Poly(ammonium bisdiethylphosphonate (meth)acrylate)-*g*-PEO Copolymers

Different approaches have been utilized for deprotecting alkyl phosphonate esters to obtain phosphonic acid derivatives.[27] Several authors have hydrolyzed phosphonates under acidic conditions at elevated temperatures.[28, 29] Basic hydrolysis carried out at 20-50 °C in aqueous media has also been reported by Aksnes *et al.*[30] However, such acidic or basic conditions were not amenable to the present investigation since the ester groups connecting the polymer backbone with the pendent groups were sensitive to hydrolytic conditions.[10] Rabinowitz and coworkers[31] reported that reaction of diethyl β-cyanovinylphosphonate with trimethylchlorosilane and methanol led to phosphonic acid products but with limited conversion (<30%). McKenna *et al.*[32] replaced the trimethylchlorosilane with the more reactive trimethylbromosilane and the reactions with this reagent proceeded smoothly with quantitative

conversion of the phosphonate ester to the corresponding phosphonic acid. It was recently demonstrated by our group[19] and others[9, 16, 33] that deprotection of phosphonates can be achieved without cleavage of ester bonds utilizing the method developed by McKenna. Thus, the diethyl phosphonate pendent groups on the copolymers in the present study were removed by using an excess of TMSBr in anhydrous dichloromethane to form trimethylsilyl phosphonates (**5**), then the trimethylsilyl groups were reacted with methanol to form poly(ammonium bisphosphonic acid methacrylate)-*g*-PEO copolymers (**6**) (Figure 3.3). To avoid any side reactions with water, the precursor copolymers with bis(diethylphosphonate) pendent esters were dried under vacuum at 70 °C for 12 hours prior to the deprotection reaction. Residual TMSBr was also removed under vacuum before adding the methanol to avoid formation of significant HBr that might affect the (meth)acrylate ester bonds. ^{1}H NMR confirmed quantitative removal of the ethyl groups without cleavage of the esters between the polymer backbone and the pendent groups (Figure 3.7). The resonances at 1.2 and 4.1 ppm characterized the methyl and methylene groups in the bisdiethylphosphonates (Figure 3.7, top). The decrease of these resonances (Figure 3.7, bottom) compared to the PEO repeat unit protons at 3.6 ppm indicated complete removal of the ethyl groups without loss of the pendent ammonium bisphosphonates. The PEO oligomer depicted in the spectra in Figure 7 had an average degree of polymerization of 114.8 and at four protons per repeat unit, this totaled approximately 459 protons per graft. The integrations at 4.1 ppm were used to quantify the ester bonds in the polymers. Before deprotection the integration at 4.1 ppm was 187 relative to one PEO, and this resonance represented 10 protons per repeat unit including one methylene group adjacent to the ester bond and four methylene groups in the bisdiethylphosphonate (Figure 3.7, top). Thus, the integration of 187 corresponded to approximately 19 bisphosphonate units relative to one PEO graft. In the deprotected copolymer,

the integration at 4.1 ppm reduced to 36, corresponding to two protons remaining in each bisphosphonate repeat unit, so this ratio represented 18 units to one PEO (Figure 3.7, bottom). The close agreement of the numbers of acrylate repeat units confirmed that the ester bonds were retained after the deprotection reaction. Consistent with this data, only a single peak in the ^{31}P NMR spectra was observed for each of the protected (Figure 3.8, top) and deprotected (Figure 3.8, bottom) copolymers. The single ^{31}P resonance shifted from 31 to 16 ppm after deprotection which was similar to data obtained in our previous study with polymer end groups.[19]

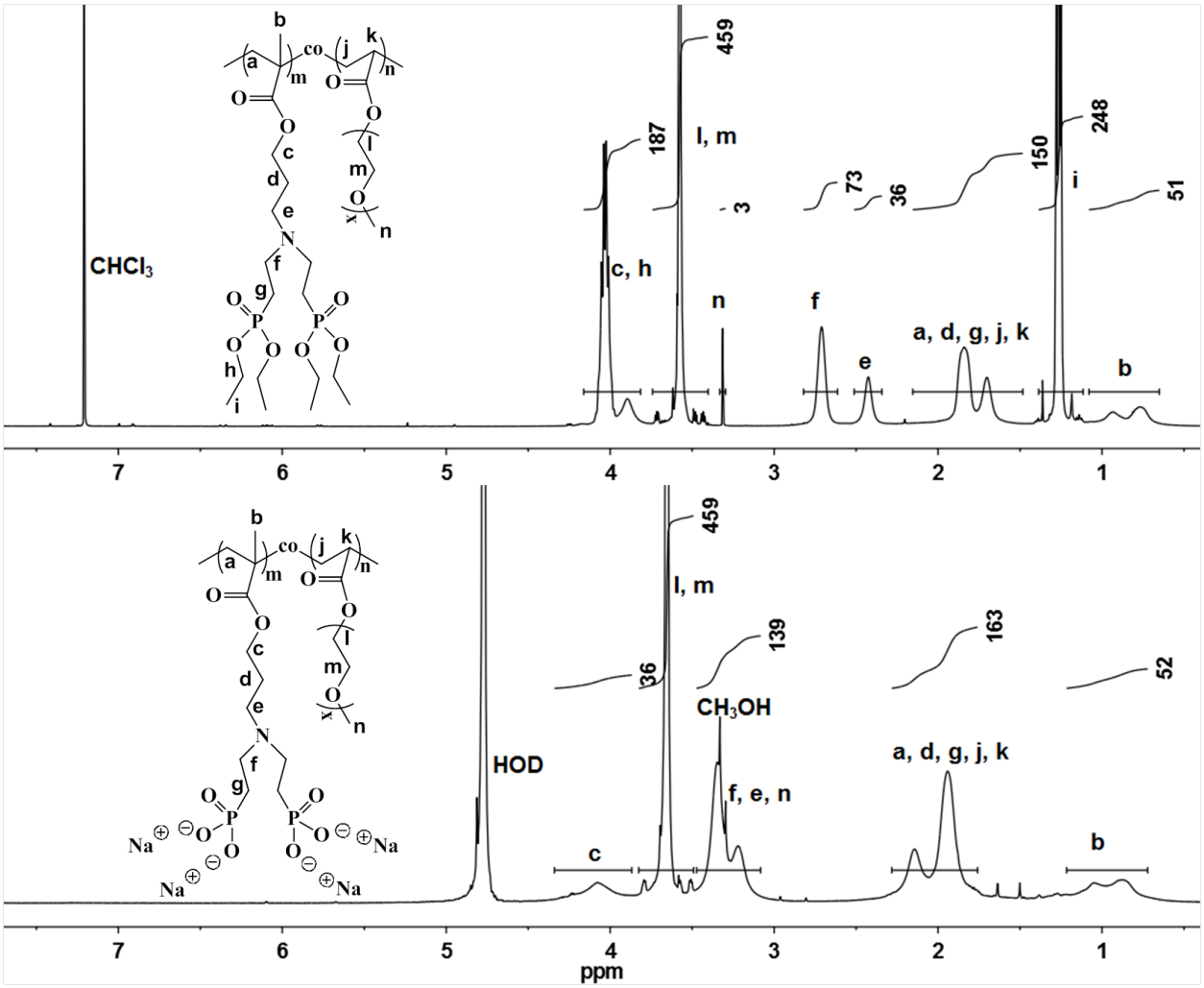

Figure 3.7 ^{1}H NMR spectra of a poly(ammonium bisdiethylphosphonate methacrylate)-*g*-PEO (**4**) and poly(ammonium bisphosphonate methacrylate)-*g*-PEO (**7**) copolymers at pH 7.74. The PEO oligomer in the acrylate-PEO macromonomer had M_n = 5085 g mol^{-1}

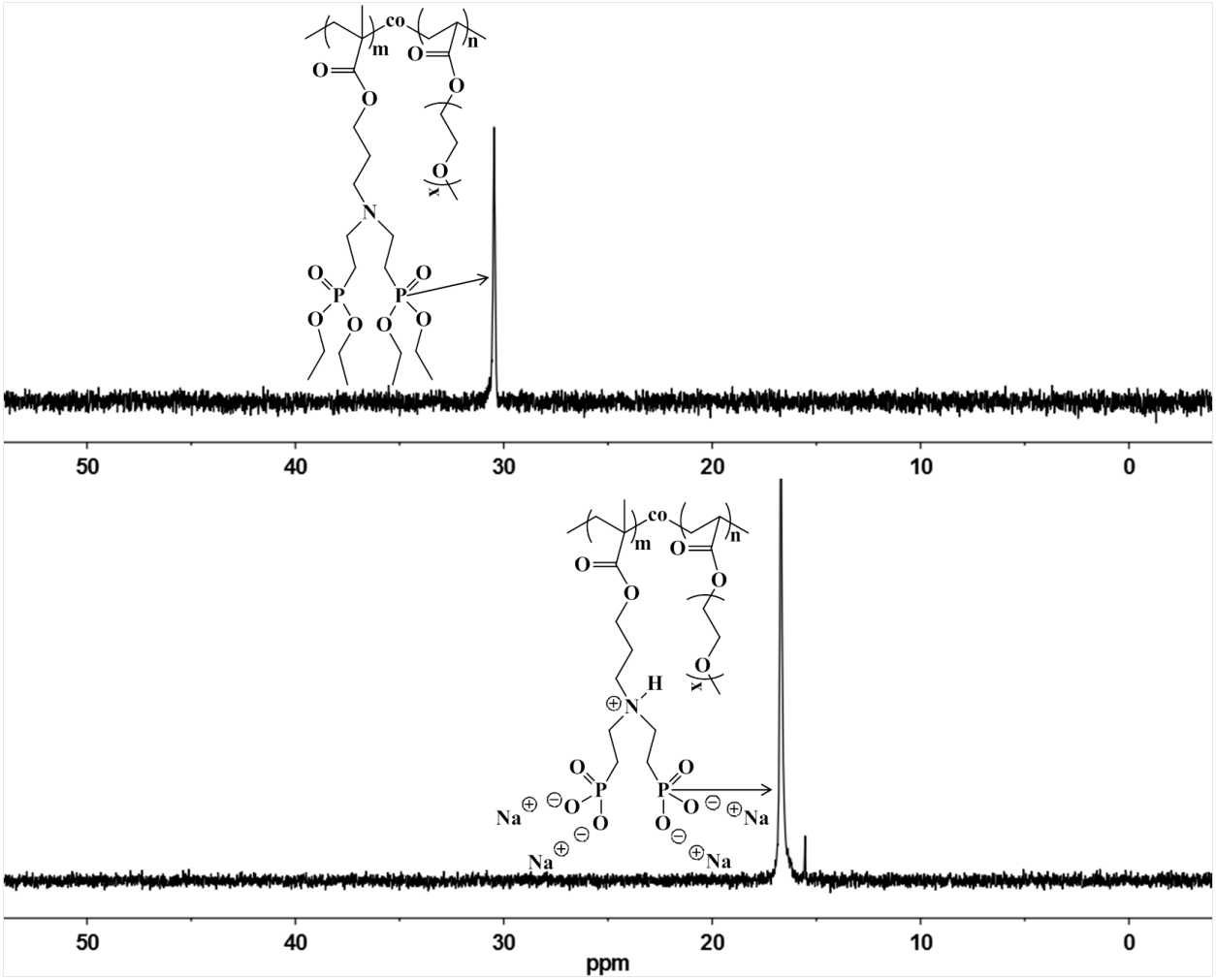

Figure 3.8 ^{31}P NMR spectra of a poly(ammonium bisdiethylphosphonate methacrylate)-*g*-PEO (**4**) and poly(ammonium bisphosphonate)-*g*-PEO (**7**) copolymers at pH 7.74

3.4.4 Thermal Properties of the Copolymers

TGA thermograms (Figure 3.9) of a poly(ammonium bisdiethylphosphonate acrylate) and poly(ammonium bisphosphonic acid acrylate) under nitrogen showed that weight loss of the two

homopolymers began at ~220 and ~190 °C, respectively, close to previously reported data for phosphonate- and phosphonic acid-containing polymers.[34, 35] In the present work, thermogravimetric analyses of the ammonium bisdiethylphosphonate and the ammonium bisphosphonic acid forms of the polymers corresponded to their compositions as determined by ^{1}H NMR. For example, the poly(ammonium bisdiethylphosphonate acrylate) homopolymer lost ~66% of its weight by 425 °C (Figure 3.9A, solid line), while the acrylate-functional PEO macromonomer completely degraded (Figure 3.9A, dotted line). The 50:50 wt:wt poly(ammonium bisdiethylphosphonate acrylate):PEO copolymer (Figure 3.9A, dash-dot line) lost ~83% of its weight by 425 °C. If one assumes that the backbone poly(ammonium bisdiethylphosphonate acrylate) portion would lose 66% of its weight and the PEO portion would completely decompose by this temperature, then the copolymer would be predicted to lose 33% plus 50% (total of 83%) of its weight. Thus, the weight loss of the copolymer was consistent with the copolymer composition. The 67:33 wt:wt backbone:graft copolymer (Figure 3.9A, dashed line) lost ~77% of its weight by 425 °C, again very close to the predicted amount that would be comprised of 33 wt% loss from the PEO plus 66% of the ammonium bisdiethylphosphonate backbone (i.e., 33% from PEO plus 44% from the backbone). The weight loss curves with temperature of the copolymers in the ammonium bisphosphonic acid form (Figure 3.9B) also corresponded well with the compositions. However, the poly(ammonium bisphosphonic acid acrylate) backbone (Figure 3.9B) lost significantly less weight than the corresponding polymers in their ammonium bisdiethylphosphonate forms (Figure 3.9A). This may be due to more efficient crosslinking at high temperatures through condensation of a –P-OH with another –P-OH on an adjacent chain when the materials are in their acid forms.

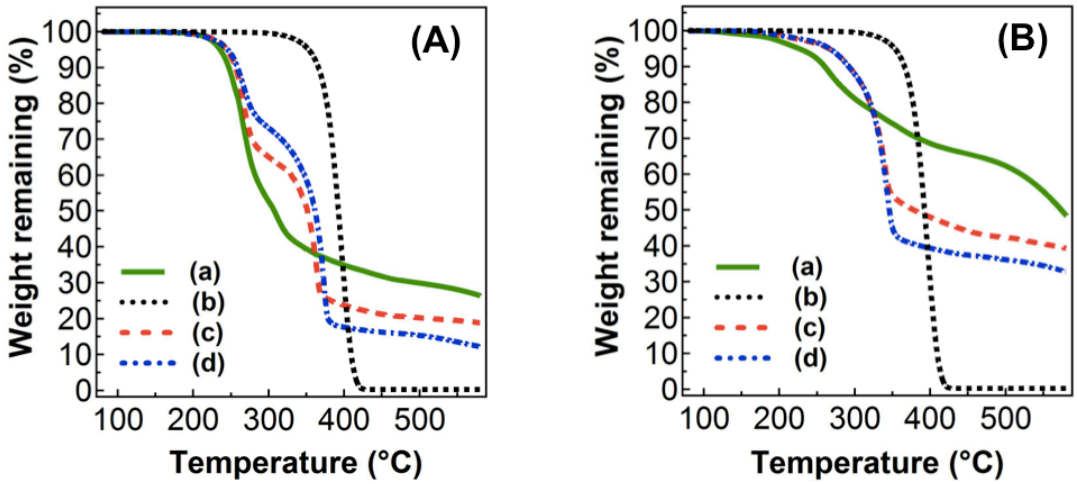

Figure 3.9 . TGA thermograms of (A) (a) poly(ammonium bisdiethylphosphonate acrylate) homopolymer, (b) PEO, (c) 67:33 wt:wt poly(ammonium bisdiethylphosphonate acrylate)-*g*-PEO, (d) 50:50 wt:wt poly(ammonium bisdiethylphosphonate acrylate)-*g*-PEO; (B) (a) poly(ammonium bisphosphonic acid acrylate) homopolymer, (b) PEO, (c) 67:33 wt:wt poly(ammonium bisphosphonic acid acrylate)-*g*-PEO, (d) 50:50 wt:wt poly(ammonium bisphosphonic acid acrylate)-*g*-PEO

3.4.5 Solution Properties of the Graft Copolymers

One objective of the present research is to develop complexes of these new polymers with drugs or nanoparticles that associate principally through electrostatic attractions, and that remain stable in physiological media long enough to enable sustained drug release. Thus, the solution properties of the copolymers in aqueous solutions were characterized. The poly(ammonium bisphosphonic acid acrylate)-*g*-PEO copolymer that was comprised of 57 wt% of the backbone and 43 wt% of the PEO grafts and the poly(ammonium bisphosphonic acid methacrylate)-*g*-PEO copolymer with 53% of the backbone and 47% of the PEO grafts was

dispersed in water, the pH was adjusted to 7.74 ± 0.03, and particle sizes were measured by DLS. This pH was close to the second proton dissociation constant (pK_2) for most ammonium-containing phosphonic acids which lie between 6.6 to 7.7.[36, 37] Thus, at the selected pH, it was reasoned that most of the bisphosphonic acid groups would be in their deprotonated ionic form. Figure 3.10(A-B) (open triangles) show that the intensity of scattered light as measured by DLS (in kilocounts per second) increased almost linearly with polymer concentration from 0.5 to 2.0 mg mL^{-1}. The linear increase of scattered light intensity with concentration is consistent with the premise that, over the concentration range probed, the copolymer formed aggregates with an almost constant size.[38] The poly(ammonium bisphosphonate acrylate)-*g*-PEO copolymer had intensity-average diameters of 156-161 nm with typical PDI values of 0.26. For the poly(ammonium bisphosphonate methacrylate)-*g*-PEO, the intensity-average diameters ranged from 212-242 nm with PDI values higher than 0.30. The reasons for these aggregates are not yet clear since both the backbone and the grafts are largely hydrophilic, but this is likely at least partially attributable to the zwitterionic nature of these polymers. It was reasoned that the zwitterions might cause interchain association through electrostatic interactions among complementary charges. Consistent with this result, Niu and coworkers also found that a zwitterionic polymer, poly(*N*,*N*-dimethyl(methacrylamido)propyl ammonium propiolactone) (Figure 3.11), formed aggregates in deionized water and they also attributed the aggregates to interchain zwitterionic interactions.[39] Other previously reported aggregates of phosphonic acid-based amphiphilic copolymers[17, 18] differed from the present materials in that they consisted of a hydrophobic segment as the core and the acid or charged groups as the shell and they were not zwitterions. Thus the formation of aggregates in those materials was attributed to the hydrophobic nature of the core segment. Another possible explanation for the aggregates

observed in the present work is that the combined nonpolar effect of the three methylene groups connecting the esters to the nitrogen plus the methylene groups connecting the nitrogen to the two phosphorus atoms made the backbone sufficiently hydrophobic to assemble into a micelle core in water.

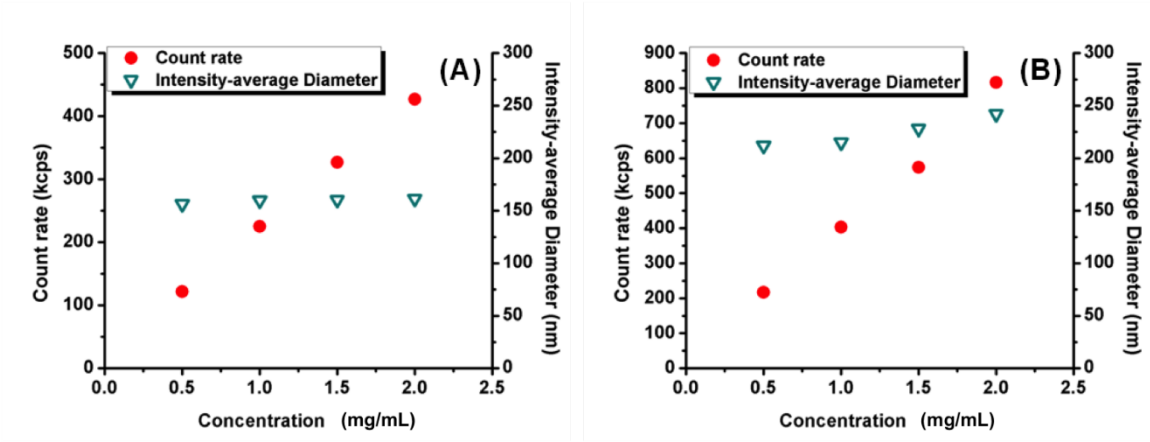

Figure 3.10 (A) Count rates and intensity-average diameters from DLS of (A) a poly(ammonium bisphosphonate acrylate)-*g*-PEO copolymer, and (B) a poly(ammonium bisphosphonate methacrylate)-*g*-PEO copolymer

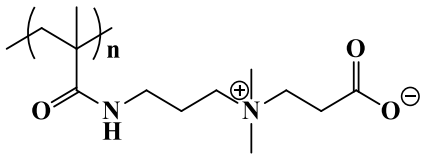

Figure 3.11 Poly(*N*,*N*-dimethyl(methacrylamido)propyl)ammonium propiolactone)

To determine whether the aggregates dissolved in the presence of added salt due to screening of electrostatic interchain interactions, solutions of sodium chloride and the copolymers in water at pH 7.74 were investigated. Figures 3.12(A-D) show the intensity (solid line) and volume (dashed line) size distributions of the copolymers in DI water with and without added salt. The volume-average diameters and the relative volumes of the aggregates versus

single chains with and without sodium chloride are summarized in Table 3.1. Only a single peak representing the aggregates was observed in both the intensity and volume size distributions of the copolymer solutions without salt. By contrast, the volume size distributions of the copolymers in 0.17 N sodium chloride were centered primarily at 5 and 19 nm, with only slight amounts of the aggregates remaining. This is likely indicative of aggregate dissociation as a result of screening of electrostatic attractions between phosphonate and ammonium groups on neighboring chains. It was reasoned that if hydrophobic interactions were driving the aggregate formation, addition of salt would have likely resulted in increased aggregate size. The areas under the DLS peaks in the intensity size distributions are proportional to the scattering intensity of each particle fraction, which is proportional to the sixth power of the radii. As a result, a small portion of large aggregates in the solution dominates the intensity size distribution.[40] Therefore, the intensity size distributions were transformed to the volume size distributions based on Mie theory for compositional analysis. It is not yet clear why small amounts of aggregates remain in the solutions with added salt.

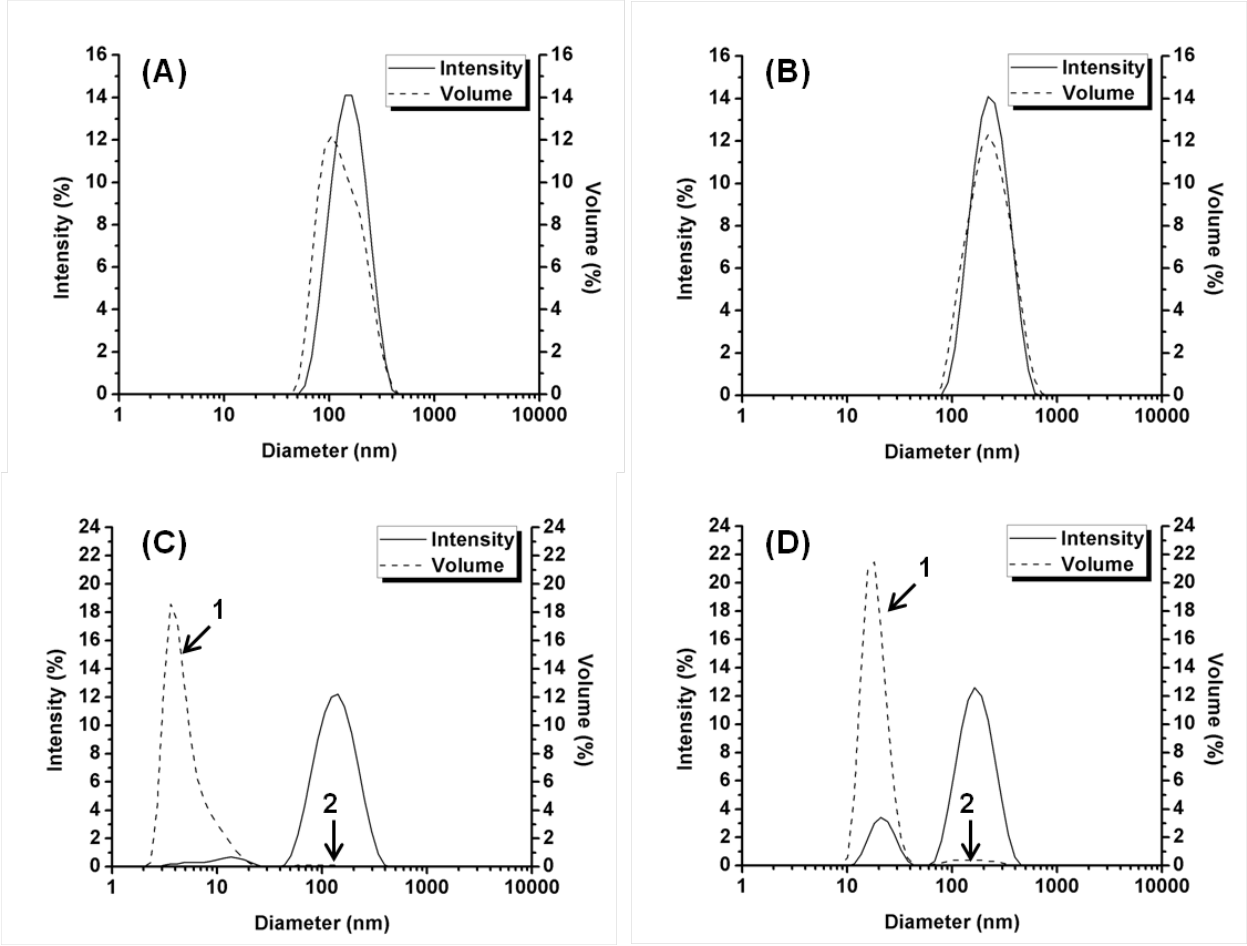

Figure 3.12 Intensity and volume size distributions measured by DLS at a concentration of 2 mg mL^{-1}: (A) Poly(ammonium bisphosphonate acrylate)-*g*-PEO copolymer in water; (B) Poly(ammonium bisphosphonate methacrylate)-*g*-PEO copolymer in water; (C) Poly(ammonium bisphosphonate acrylate)-*g*-PEO copolymer in water containing 0.17 N sodium chloride; (D) Poly(ammonium bisphosphonate methacrylate)-*g*-PEO copolymer in water containing 0.17 N sodium chloride

Table 3.1 Volume-average diameters of poly(ammonium bisphosphonate acrylate)-*g*-5K PEO and poly(ammonium bisphosphonate methacrylate)-*g*-5K PEO solutions with and without sodium chloride

DLS from Figure 12	Polymer solution	NaCl conc.	Peak 1 Volume ave. diameter (nm)	Peak 1 Volume	Peak 2 Volume ave. diameter (nm)	Peak 2 Volume
A	Poly(ammonium bisphosphonate acrylate)-g-PEO	-	141	100 %	-	-
B	Poly(ammonium bisphosphonate methacrylate)-g-PEO	-	245	100 %	-	-
C	Poly(ammonium bisphosphonate acrylate)-g-PEO	0.17 N	113	0.8%	5	99.2%
D	Poly(ammonium bisphosphonate methacrylate)-g-PEO	0.17 N	165	3.5%	19	96.5%

3.5 Conclusions

This investigation developed a facile and mild method for synthesizing ammonium bisdiethylphosphonate acrylate and methacrylate monomers through a double aza-Michael addition of aminoalkyl alcohols in water followed by esterification. It is reasoned that similar methodology can be extended to a range of aminoalkyl alcohols with varying hydrophobicity. Conventional free radical copolymerizations of the new monomers with acrylate-functional PEO macromonomers were conducted. It was found that copolymerizations with the methacrylate-functional ammonium phosphonate monomers incorporated both monomers efficiently while use of the acrylate-functional phosphonates produced heterogeneous blends of graft copolymers and

homopolymers. These zwitterionic copolymers formed aggregates in water, likely due to electrostatic interchain attractions. As a continuing effort in our group on developing core-shell nanoparticles as drug carriers and owing to the excellent binding property of bisphosphonates, we envision that the zwitterionic poly(ammonium bisphosphonate methacrylate)-*g*-PEO copolymers can be utilized to design drug-polymer complexes with sustained drug release.

3.6 Acknowledgements

The authors gratefully acknowledge the support of the National Science Foundation under contract numbers DMR 0805179, DMR 1106182 and DMR 0851662. Thanks are extended to Sharavanan Balasubramaniam for helpful discussions on DLS and Chen Qian for assistance in artwork.

3.7 References

1. Gentilhomme, A.; Cochez, M.; Ferriol, M.; Oget, N.; Mieloszynski, J. L., Thermal degradation of methyl methacrylate polymers functionalized by phosphorus-containing molecules-II: initial flame retardance and mechanistic studies. *Polym. Degrad. Stab.* 2003, 82, 347-355.

2. Nada, A. M. A.; Eid, M. A.; El Bahnasawy, R. M.; Khalifa, M. N., Preparation and characterization of cation exchangers from agricultural residues. *J. Appl. Polym. Sci.* 2002, 85, 792-800.

3. Narain, R. P.; Kumar, D., Synthesis of some adhesives containing Si-O-P linkages. *Int. J. Adhes. Adhes.* 1993, 13, 189-92.

4. Schartel, B., Phosphorus-based flame retardancy mechanisms - old hat or a starting point for future development? *Materials* 2010, 3, 4710-4745.

5. Stancu, I. C.; Filmon, R.; Cincu, C.; Marculescu, B.; Zaharia, C.; Tourmen, Y.; Basle, M. F.; Chappard, D., Synthesis of methacryloyloxyethyl phosphate copolymers and in vitro calcification capacity. *Biomaterials* 2004, 25, 205-13.

6. Moszner, N.; Salz, U.; Zimmermann, J., Chemical aspects of self-etching enamel-dentin adhesives: A systematic review. *Dent. Mater.* 2005, 21, 895-910.

7. Moszner, N.; Zeuner, F.; Fischer, U. K.; Rheinberger, V., Monomers for adhesive polymers. Part 2. Synthesis and radical polymerization of hydrolytically stable acrylic phosphonic acids. *Macromol. Chem. Phys.* 1999, 200, 1062-1067.

8. Chougrani, K.; Boutevin, B.; David, G.; Boutevin, G., New N,N-amino-diphosphonate-containing methacrylic derivatives, their syntheses and radical copolymerizations with MMA. *Eur. Polym. J.* 2008, 44, 1771-1781.

9. Chougrani, K.; Niel, G.; Boutevin, B.; David, G., Regioselective ester cleavage during the preparation of bisphosphonate methacrylate monomers. *Beilstein J. Org. Chem.* 2011, 7, 364-368.

10. Moszner, N., New monomers for dental application. *Macromol. Symp.* 2004, 217, 63-75.

11. Penczek, S.; Pretula, J.; Kaluzynski, K., Simultaneous introduction of phosphonic and carboxylic acid functions to hydroxylated macromolecules. *J. Polym. Sci., Part A Polym. Chem.* 2004, 42, 432-443.

12. Penczek, S.; Kaluzynski, K.; Pretula, J., Determination of copolymer localization in polymer-CaCO3 hybrids formed in mediated crystallization. *J. Polym. Sci., Part A Polym. Chem.* 2009, 47, 4464-4467.

13. Tosatti, S.; Michel, R.; Textor, M.; Spencer, N. D., Self-Assembled Monolayers of Dodecyl and Hydroxy-dodecyl Phosphates on Both Smooth and Rough Titanium and Titanium Oxide Surfaces. *Langmuir* 2002, 18, 3537-3548.

14. Brun, A.; Albouy, D.; Perez, E.; Rico-Lattes, I.; Etemad-Moghadam, G., Self-Assembly and Phase Behavior of New (α-Hydroxyalkyl)phosphorus Amphiphiles. *Langmuir* 2001, 17, 5208-5215.

15. Ariga, K.; Yuki, H.; Kikuchi, J.; Dannemuller, O.; Albrecht-Gary, A.-M.; Nakatani, Y.; Ourisson, G., Monolayer Studies of Single-Chain Polyprenyl Phosphates. *Langmuir* 2005, 21, 4578-4583.

16. Francova, D.; Kickelbick, G., Synthesis of methacrylate-functionalized phosphonates and phosphates with long alkyl-chain spacers and their self-aggregation in aqueous solutions. *Monatsh. Chem.* 2009, 140, 413-422.

17. Francova, D.; Kickelbick, G., Self-Assembly of Methacrylate-Functionalized Phosphonate and Phosphate Amphiphiles and their Conversion into Nanospheres. *Macromol. Chem. Phys.* 2009, 210, 2037-2045.

18. Eren, T.; Tew, G. N., Phosphonic acid-based amphiphilic diblock copolymers derived from ROMP. *J. Polym. Sci., Part A Polym. Chem.* 2009, 47, 3949-3956.

19. Pothayee, N.; Balasubramaniam, S.; Davis, R. M.; Riffle, J. S.; Carroll, M. R. J.; Woodward, R. C.; St. Pierre, T. G., Synthesis of 'ready-to-adsorb' polymeric nanoshells for

magnetic iron oxide nanoparticles via atom transfer radical polymerization. *Polymer* 2011, 52, 1356-1366.

20. Ranu, B. C.; Banerjee, S., Significant rate acceleration of the aza-Michael reaction in water. *Tetrahedron Lett.* 2007, 48, 141-143.

21. Azizi, N.; Saidi, M. R., Lithium perchlorate-catalyzed three-component coupling: A facile and general method for the synthesis of α-aminophosphonates under solvent-free conditions. *Eur. J. Org. Chem.* 2003, 4630-4633.

22. Wu, J.; Sun, W.; Sun, X.; Xia, H.-G., Expeditious approach to α-amino phosphonates via three-component solvent-free reactions catalyzed by NBS or CBr4. *Green Chem.* 2006, 8, 365-367.

23. Neugebauer, D.; Zhang, Y.; Pakula, T., Gradient graft copolymers derived from PEO-based macromonomers. *J. Polym. Sci., Part A Polym. Chem.* 2006, 44, 1347-1356.

24. Bencherif, S. A.; Gao, H.; Srinivasan, A.; Siegwart, D. J.; Hollinger, J. O.; Washburn, N. R.; Matyjaszewski, K., Cell-Adhesive Star Polymers Prepared by ATRP. *Biomacromolecules* 2009, 10, 1795-1803.

25. Bencherif, S. A.; Srinivasan, A.; Sheehan, J. A.; Walker, L. M.; Gayathri, C.; Gil, R.; Hollinger, J. O.; Matyjaszewski, K.; Washburn, N. R., End-group effects on the properties of PEG-co-PGA hydrogels. *Acta Biomater.* 2009, 5, 1872-1883.

26. Nuttelman, C. R.; Benoit, D. S. W.; Tripodi, M. C.; Anseth, K. S., The effect of ethylene glycol methacrylate phosphate in PEG hydrogels on mineralization and viability of encapsulated hMSCs. *Biomaterials* 2006, 27, 1377-1386.

27. Engel, R., Phosphonates as analogs of natural phosphates. *Chem. Rev.* 1977, 77, 349-67.

28. Pfeiffer, F. R.; Mier, J. D.; Weisbach, J. A., Synthesis of phosphoric acid isoesters of 2-phospho-, 3-phospho-, and 2,3-diphosphoglyceric acid. *J. Med. Chem.* 1974, 17, 112-15.

29. Hudson, R. F.; Keay, L., Hydrolysis of phosphonate esters. *J. Chem. Soc.* 1956, 2463-9.

30. Aksnes, G.; Songstad, J., Alkaline hydrolysis of diethyl esters of alkylphosphonic acids and some chloro substituted derivatives. *Acta Chem. Scand.* 1965, 19, 893-7.

31. Rabinowitz, R., The reactions of phosphonic acid esters with acid chlorides. A very mild hydrolytic route. *J. Org. Chem.* 1963, 28, 2975-8.

32. McKenna, C. E.; Higa, M. T.; Cheung, N. H.; McKenna, M. C., The facile dealkylation of phosphonic acid dialkyl esters by bromotrimethylsilane. *Tetrahedron Lett.* 1977, 155-8.

33. Carbonneau, C.; Frantz, R.; Durand, J.-O.; Granier, M.; Lanneau, G. F.; Corriu, R. J. P., Studies of the hydrolysis of ethyl and tert-butyl phosphonates covalently bonded to silica xerogels. *J. Mater. Chem.* 2002, 12, 540-545.

34. Inagaki, N.; Goto, K.; Katsuura, K., Thermal degradation of poly(diethyl vinylphosphonate) and its copolymer. *Polymer* 1975, 16, 641-4.

35. Jiang, D. D.; Yao, Q.; McKinney, M. A.; Wilkie, C. A., TGA/FTIR studies on the thermal degradation of some polymeric sulfonic and phosphonic acids and their sodium salts. *Polym. Degrad. Stab.* 1999, 63, 423-434.

36. Brown, H. C.; McDaniel, D. H.; Hafliger, O., Dissociation constants. *Determ. Org. Struct. Phys. Methods* 1955, 567-662.

37. Jose Sanchez-Moreno, M.; Gomez-Coca, R. B.; Fernandez-Botello, A.; Ochocki, J.; Kotynski, A.; Griesser, R.; Sigel, H., Synthesis and acid-base properties of (1H-benzimidazol-2-yl-methyl)phosphonate (Bimp2-). Evidence for intramolecular hydrogen-bond formation in aqueous solution between (N-1)H and the phosphonate group. *Org. Biomol. Chem.* 2003, 1, 1819-1826.

38. Kwaambwa, H. M.; Rennie, A. R., Interactions of surfactants with a water treatment protein from Moringa oleifera seeds in solution studied by zeta-potential and light scattering measurements. *Biopolymers* 2012, 97, 209-218.

39. Niu, A.; Liaw, D.-J.; Sang, H.-C.; Wu, C., Light-Scattering Study of a Zwitterionic Polycarboxybetaine in Aqueous Solution. *Macromolecules* 2000, 33, 3492-3494.

40. Pizones Ruiz-Henestrosa, V. M.; Martinez, M. J.; Patino, J. M. R.; Pilosof, A. M. R., A Dynamic Light Scattering Study on the Complex Assembly of Glycinin Soy Globulin in Aqueous Solutions. *J. Am. Oil Chem. Soc.* 2012, 89, 1183-1191.

CHAPTER 4 - Synthesis of Acrylamide Phosphonate Monomers and Polymers

Nan Hu, A. Peralta, S. Roy Choudrury, R. M. Davis and J. S. Riffle*

Macromolecules and Interfaces Institute, Virginia Tech, Blacksburg, VA 24061

Modified Chapter will be submitted to Polymer

4.1 Abstract

Three alkylacrylamide phosphonate monomers were synthesized through a two-step procedure. The first step involved an aza-Michael addition of an alkylamine onto the double bond of diethyl vinylphosphonate to afford a phosphonate ended secondary amine. This was subsequently reacted with acryloyl chloride to produce the alkyl acrylamide phosphonate. Free radical copolymerization of *n*-butylacrylamide phosphonate with an acrylate-functional PEO macromonomer yielded statistical graft copolymers. Removal of the ethyl groups from the phosphonate moieties led to poly(*n*-butylacrylamide phosphonic acid)-*g*-PEO copolymers. The poly(*n*-butylacrylamide phosphonic acid)-*g*-PEO copolymer comprising 56 wt% of the backbone and 44 wt% of the PEO grafts was soluble in DMF, DMSO, methanol and water at pH 7.4. This copolymer formed aggregates in DMF and DMSO while no significant amount of aggregates was observed in methanol or water at pH 7.4. Interaction of the phosphonic acid derivative of *n*-butylacrylamide phosphonate with hydroxyapatite (15 and 30 mg) showed 79.9% and 94.8% interacted amounts whereas those values of acrylic acid were 47.4% and 64.1%. The relatively hydrolytically stable acrylamide linker together with the excellent binding properties of the acrylamide phosphonic acid monomers and polymers might be potential candidates for applications in dental adhesives.

4.2 Introduction

Phosphonic acid-containing compounds have elicited great interest in the biomedical field. Geminal bis(phophonic acid)s, especially those containing nitrogen atoms, are well-known to be effective inhibitors of bone resorption due to their capability in binding calcium cation to target bone minerals and inhibit enzymes responsible for bone resorption.[1, 2] Polymerizable phosphonic acid monomers have been investigated as self-etching enamel-dentin adhesives.[3, 4] Phosphonic acid bearing polymers have also been reported to be potential substrates for applications in drug delivery[5-8] and tissue engineering.[9, 10] Recently, there has been growing interest in (meth)acrylamide phosphonate monomers and polymers since amides are more stable against hydrolysis than the corresponding esters.[11] Klee *et al.*[12] prepared *N*-alkyl-*N*-(phosphonoethyl) substituted mono-, bis- and tris-(meth)acrylamides by two different three-step reactions. The acrylamide phosphonic acids exhibited better hydrolytic stability than the acrylate and methacrylamide analogues. Le Pluart and coworkers synthesized a series of acrylamide phosphonic acid monomers that had ether or alkyl spacers. These monomers were homo- or copolymerized with *N,N'*-diethyl-1,3-bis(acrylamide)propane by photoinitiation.[13, 14] This group also investigated the polymerization kinetics of acrylamide containing phosphonic acids and esters.[15, 16] Rates of copolymerization of the acrylamide phosphonic acid monomers with *N,N'*-diethyl-1,3-bis(acrylamide)propane was significantly faster than homopolymerization of *N,N'*-diethyl-1,3-bis(acrylamide)propane, while no significant rate increase was found for the phosphonate ester derivatives. Reversible addition-fragmentation transfer (RAFT) polymerization of a diethyl-2-(acrylamide)ethyl phosphonate monomer was carried out by Monge *et al.*[17] Block copolymers consisting of this monomer and *N*-*n*-propylacrylamide maintained approximately the same lower critical solution temperature (LCST) as poly(*N*-*n*-

propylacrylamide) homopolymer. However, the LCST of the deprotected diblock copolymer containing the phosphonic acid and *N*-*n*-propylacrylamide was higher than for the homopolymer, and this was attributed to an increase in hydrophilicity.

Only a few investigations have been reported on the self-assembly behavior of monomers and polymers bearing phosphonic acids. Etemad-Moghadam and coworkers[18, 19] synthesized and studied the self-organization and phase behavior of a series of (α-hydroxyalkyl)phosphonic acids with long hydrocarbon substituents (C_8-C_{18}). The cetyltrimethylammonium salts of these compounds aggregated at low concentrations in water with different morphologies (vesicles, ribbons, tubules). Francová and Kickelbick[20, 21] prepared phosphonate- and phosphate-bearing methacrylates with alkyl spacers. These monomers formed micelles in water with the hydrophobic alkyl spacer in the core and the phosphonates or the phosphates as the shell. Subsequent crosslinking of the micelles by UV- or thermally-initiated free radical polymerizations led to formation of spheres ranging from 30 to 400 nm in diameter as measured by dynamic light scattering (DLS). Robin *et al.* described the synthesis of amphiphilic phosphonic acid methacrylamide homopolymers, poly((methacrylamido)decylphosphonic acid) by RAFT polymerization.[22] These homopolymers self-aggregated in water and acetonitrile. The hydrodynamic diameters were determined to be 2550 and 480 nm as measured by DLS in water and acetonitrile, respectively. This was attributed to their hydrophobic nature (74% hydrophobic groups). Tew and Eren[23] prepared diblock copolymers by ring-opening metathesis polymerization with one block containing phosphonic acid pendent groups and the other consisting of relatively hydrophobic polyoxanorbornene. Some of those compositions formed micelles in a THF:water 1:1 v:v mixed solvent with hydrodynamic radii ranging from 123 to 301 nm by DLS. Previously our group[24] investigated the solution properties of (meth)acrylate graft

polymers bearing phosphonic acids and poly(ethylene oxide) (PEO). These graft copolymers spontaneously formed aggregates in water due to complementary charges.

Herein we describe the synthesis of acrylamide monomers containing phosphonates and their copolymerization with acrylate-functional PEO macromonomers to yield poly(acrylamide phosphonate)-*g*-PEO copolymers. Subsequent removal of the ethyl groups on the phosphonates produced poly(acrylamide phosphonic acid)-*g*-PEO copolymers. The properties of these copolymers in organic solvents and aqueous media are discussed. Interaction of acrylamide phosphonic acids with hydroxyapatite, the primary mineral of tooth enamel, was also investigated to characterize the binding capacities of the phosphonic acid to calcium cations.

4.3 Experimental

4.3.1 Materials

Diethyl vinylphosphonate (Epsilon-Chimie, >98%), dimethyl sulfoxide (DMSO) and dichloromethane (EMD Chemicals, anhydrous, 99.8%) were used as received. Methanol (anhydrous, 99.9%), hexane (99.9%), dichloromethane (99.9%), chloroform (99.9%) and diethyl ether (anhydrous, 99.8%), all from Fisher Scientific, were used as received. *N,N*-Dimethylformamide (DMF, 99.9%), sodium sulfate (anhydrous, 99%), *n*-butylamine (>99%), triethylamine (>99.5%), sodium hydroxide (97%), poly(ethylene oxide) methyl ether (M_n=5,085), 2,2'-azobisisobutyronitrile (AIBN, 98%), sodium chloride (>99.5%), acrylic acid (99%) and hydroxyapatite (HAP, >97%) were purchased from Sigma-Aldrich and used as received. Acryloyl chloride (97%) and bromotrimethylsilane (TMSBr, 97.0%) were fractionally distilled before use. Acrylate-functional PEO was prepared according to a known procedure.[24]

4.3.2 Characterization

4.3.2.1 NMR analysis

^{1}H NMR spectral analyses were performed on a Bruker Advance II-500 NMR operating at 500 MHz. ^{13}C NMR spectral analyses were conducted on a Varian Unity Plus spectrometer operating at 100.56 MHz. ^{31}P NMR spectral analyses were obtained on a Varian Inova 400 NMR operating at 161.91 MHz. Parameters utilized for the ^{31}P NMR were a 45° pulse and 1 s relaxation delay with 128 scans. All ^{1}H, ^{13}C and ^{31}P NMR spectra of the protected and deprotected monomers and phosphonic acid polymers were obtained in D_2O. Spectra of the phosphonate polymers were obtained in $CDCl_3$.

4.3.2.2 Elemental analysis

Elemental analysis on the acrylamide phosphonate monomer was performed at Midwest Microlab, LLC (Indianapolis, IN). Four elements were tested including carbon, nitrogen hydrogen and phosphorus. Analysis on oxygen was not applicable due to the presence of phosphorus. Determination on carbon, nitrogen and hydrogen was carried out on a CE440 elemental analyzer. Phosphorus was analyzed manually by digesting the monomer into a micro bomb with appropriate reagents. The apparatus was sealed and heated in a flame for 60 s. The reaction mixture was purified and treated with appropriate reagents to afford acetone molybdiphosphate in which the phosphorus weight ratio was determined.

4.3.2.3 Dynamic light scattering (DLS)

DLS measurements on the poly(acrylamide phosphonic acid)-*g*-PEO copolymer were performed with a Zetasizer NanoZS particle analyzer (Malvern Instruments Ltd) equipped with a solid-state He-Ne laser (λ= 633 nm) at a scattering angle of 173°. Intensity and volume average

diameters were calculated with the Zetasizer Nano 4.2 software using an algorithm based on Mie theory that converts time-varying intensities to diameters. For DLS analysis, the polymers were dissolved in organic solvents (DMF, DMSO or methanol) or DI water at a concentration of 2.0 mg mL^{-1}. The polymer/organic solution was filtered through a 1.0 μm Teflon™ filter directly into a glass cuvette for analysis. The pH of the polymer/water solution was adjusted to 7.4 with addition of sodium hydroxide solution using a S47 SevenMulti pH meter (Mettler-Toledo International, Inc.) and the solution was sonicated for 1 min in a 75T VWR bath-type Ultrasonicator at 120 volts, then filtered and transferred into a polystyrene cuvette for analysis.

4.3.3 Synthesis

4.3.3.1 Synthesis of *n*-butylaminoethyl phosphonate

n-Butylamine (1.5 g, 20 mmol) and 0.3 mL of deionized water were charged to a 100-mL round-bottom flask with a magnetic stir bar and sealed with a septum. The flask was placed in an oil bath and heated to 70 °C. Diethyl vinylphosphonate (2.8 g, 17 mmol) was added dropwise to the flask. After 18 h the reaction mixture was cooled to room temperature and diluted with dichloromethane (20 mL). The diluted solution was dried over anhydrous sodium sulfate, filtered and the solvent was evaporated. The clear solution was then vacuum dried at 50 °C to afford a light yellow and viscous liquid, *n*-butylaminoethyl phosphonate (3.5 g, 88%).

4.3.3.2 Synthesis of an *n*-butylacrylamide phosphonate monomer

n-Butylaminoethyl phosphonate (3.5 g, 15 mmol), triethylamine (1.9 g, 19 mmol), and anhydrous dichloromethane (24 mL) were charged to a flame-dried, 100-mL, round-bottom flask and placed in an ice bath. Acryloyl chloride (1.7 g, 19 mmol) was added dropwise. The flask was removed from the ice bath and the reaction was stirred for 18 h at room temperature.

The reaction mixture was diluted with 30 mL of dichloromethane. The diluted solution was washed with 0.1 N aq. sodium hydroxide (3 x 30 mL), 0.2 N aq. hydrochloric acid (2 x 30 mL), DI water (2 x 30 mL) and the organic phase was dried over anhydrous sodium sulfate. The solvent was evaporated and the product, a bright yellow and viscous liquid was dried under vacuum at room temperature (yield 2.6 g, 61%).

4.3.3.3 Synthesis of a 67:33 wt:wt poly(*n*-butylacrylamide phosphonate)-*g*-PEO copolymer

The *n*-butylacrylamide phosphonate monomer (1.0 g, 3.4 mmol) was charged into a flame-dried, 25-mL Schlenk flask equipped with a stir bar. An acrylate-functional PEO (0.5 g, 0.1 mmol) solution in degassed DMSO (2 mL) was prepared in a 10-mL round-bottom flask. AIBN (38 mg, 0.23 mmol) was dissolved in degassed DMSO (5 mL) in a separate 10-mL flask. The acrylate-PEO solution and 1 mL of the freshly prepared AIBN solution in DMSO were added to the Schlenk flask via syringe. After three freeze-pump-thaw cycles, the reaction mixture was heated at 70 °C for 14.5 h. The reaction mixture was diluted with dichloromethane (20 mL) and washed with DI water (3 x 10 mL). The organic phase was dried over anhydrous sodium sulfate, filtered and the mixture was concentrated. The concentrated solution was then precipitated in a cold mixture of 50:50 v:v anhydrous diethyl ether:hexane (400 mL). The resulting yellow solid (1.13 g, 75%) was vacuum dried at room temperature overnight.

4.3.3.4 Deprotection of the 67:33 poly(*n*-butylacrylamide phosphonate)-*g*-PEO copolymer

A flame-dried round-bottom flask equipped with a stir bar was charged with dry poly(*n*-butylacrylamide phosphonate)-*g*-PEO (0.78 g, 1.8 meq of phosphonate), TMSBr (1.87 g, 5.4 mmol) and 7 mL of anhydrous dichloromethane. The reaction was stirred at room temperature for 24 h. Dichloromethane and the excess TMSBr were removed by rotary evaporation at 75 °C

and the copolymer was dried under vacuum at room temperature for 4 h. Anhydrous methanol (10 mL) was added to the flask via syringe. After 24 h the reaction mixture was precipitated in cold 50:50 v:v hexane and diethyl ether (300 mL). The copolymer was dissolved in 20 mL of methanol, transferred into dialysis tubing (1,000 $g.mol^{-1}$ MWCO) and dialyzed against 4 L of DI water for 48 h. The solution was freeze-dried to obtain the yellow solid, poly(*n*-butylacrylamide phosphonic acid)-*g*-PEO (0.53, 73%).

4.3.3.5 Kinetic studies of copolymerization

A poly(*n*-butylacrylamide phosphonate)-*g*-PEO copolymer was synthesized as described above and aliquots were removed at known time intervals during the reaction and dissolved directly in Chloroform-d for ^{1}H NMR analysis. Monomer conversions and copolymer compositions were measured by ^{1}H NMR according to the decrease of integrals of the vinyl bonds.

4.3.3.6 Deprotection of the *n*-butylacrylamide phosphonate monomer

Deprotection of the phosphonate monomer is similar to that of the copolymer. *n*-Butylacrylamide phosphonate (2.2 g, 7.6 mmol), TMS-Br (3.47 g, 22.7 mmol) and anhydrous dichloromethane (20 mL) were charged to a flame-dried, 100-mL round-bottom flask. The reaction was stirred for 24 h at room temperature. Dichloromethane and the excess TMSBr were removed by rotary evaporation at 75 °C and the precursor was dried under vacuum at room temperature for 4 h. Anhydrous methanol (16 mL) was added to the flask via syringe. After 24 h the reaction mixture was concentrated by rotary evaporation and precipitated in cold diethyl ether (2 x 600 mL). The yellow solid was collected and dried under vacuum for 12 h.

4.3.4 Interaction of *n*-butylacrylamide phosphonic acid or acrylic acid with HAP

4.3.4.1 Determination of the pKa values and ionization points of the *n*-butylacrylamide phosphonic acid or acrylic acid by ^{13}C NMR

pKa values and complete ionization points of phosphonic acid or acrylic acid were determined by ^{13}C NMR according to the method developed by Nishiyama *et al.*[25] For example, *n*-butylacrylamide phosphonic acid (28 mg, 0.11 mmol) was dissolved in 20 wt% deuterium oxide aqueous solution (1.0 g). Hydrochloric acid (5.0 N) or sodium hydroxide (1.0 N) solution was added to the phosphonic acid solution to adjust pH. The pH values were measured and ^{13}C NMR spectra were obtained. The two pKa values and two ionization points of the phosphonic acid were determined from the pH-dependent chemical shift of the α-methylene carbon attached to the phosphorus atom of the phosphonic acid group. For acrylic acid, the pH-dependent chemical shift curve was obtained from the carbonyl carbon of the carboxylic acid.

4.3.4.2 Interaction of the *n*-butylacrylamide phosphonic acid or acrylic acid with hydroxyapatite (HAP) determined by ^{13}C NMR

The extent of the *n*-butylacrylamide phosphonic acids or acrylic acids that interacted with HAP were determined by ^{13}C NMR according to the method given by Nishiyama *et al.*[25] A procedure for investigating the extent of interaction of the *n*-butylacrylamide phosphonic acid with HAP is provided as following. *n*-Butylacrylamide phosphonic acid (28 mg, 0.11 mmol) was dissolved in 20 wt% deuterium oxide aqueous solution (1.0 g). HAP (15 or 30 mg, 0.15 or 0.30 mmol of calcium ions) was added to the phosphonic acid solution to form a white suspension. The suspension was stirred at room temperature for 24 h. The pH values and the ^{13}C NMR spectra were obtained before and after addition of HAP. The percentage of the phosphonic acid that interacted with the calcium cations of HAP were determined by the chemical shift differences of the α-methylene carbon before and after mixing with HAP. Interaction of acrylic

acid (7.8 mg, 0.11mmol) with HAP (15 mg or 30 mg, 0.15 or 0.30 mmol of calcium ions) was studied using the same procedure.

4.4 Results and Discussion

4.4.1 Synthesis of acrylamide phosphonate monomers

We have previously reported ammonium bisphosphonate (meth)acrylate monomers and ammonium bisphosphonate functionalized polymers[24, 26] that were prepared via aza-Michael addition reactions in water. Water accelerates the addition rate of amines to α,β-unsaturated compounds through hydrogen bonding so that primary amine will react quantitatively with two moles of deithylvinylphosphonate under mild conditions.[27] Alkylamino phosphonates have also been reported by several other researchers through different synthetic routes. Catel *et al.*[14, 28] reacted dibromoalkane with triethylphosphite at 160°C and the reaction mixture was distilled under high vacuum to yield bromoalkyl phosphonates (60% yield). These precursors were then modified with amines to afford the corresponding alkylamino phosphonates. Monge and coworkers[17] followed a similar procedure for the first step by replacing the dibromoalkane with *N*-2-(bromoethyl)phthalimide to obtain the [2-(1,3-dioxo-1,3-dihydro-isoindol-2-yl)ethyl]phospohnic acid diethyl ester (80% yield). Aminolysis of this compound was achieved utilizing hydrazine monohydrate in ethanol to obtain the alkylamino phosphonate. Klee and Lehmann[12] synthesized *N*-alkyl-2-aminoethylphosphonates by refluxing alkyl amines with diethyl vinylphosphonate. In this paper, we simply reacted an aminoalkane with diethyl vinylphosphonate using water as a catalyst. Excess amine was used to ensure only one-fold addition to the vinyl bond. The unreacted residual amine was removed under reduced pressure with a yield of 88%. Subsequently, the acrylamide phosphonate monomers were obtained by reacting the alkylamino phosphonate with acryloyl chloride (Figure 4.1). The chemical structures

of the monomers were confirmed by ^{1}H NMR (Figure 4.2). Elemental analysis on the *n*-butylacrylamide phosphonate monomer also showed good agreement between the theoretical and experimental weight percentages (within ± 0.12%) of the tested elements that indicated high purity of the monomer. Table 4.1 summarizes the elemental analysis on the monomer.

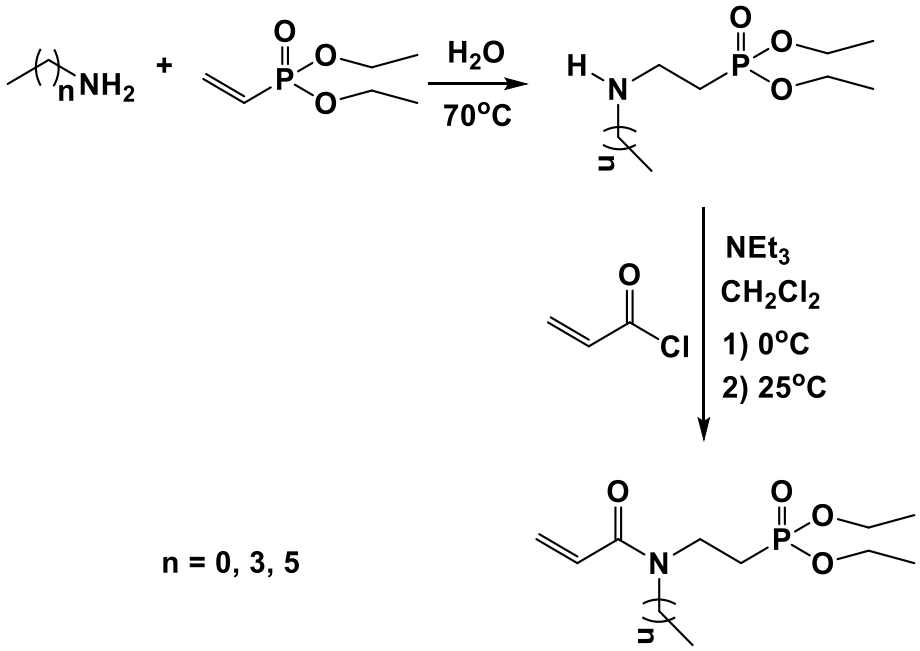

Figure 4.1 Synthesis of acrylamide phosphonate monomers

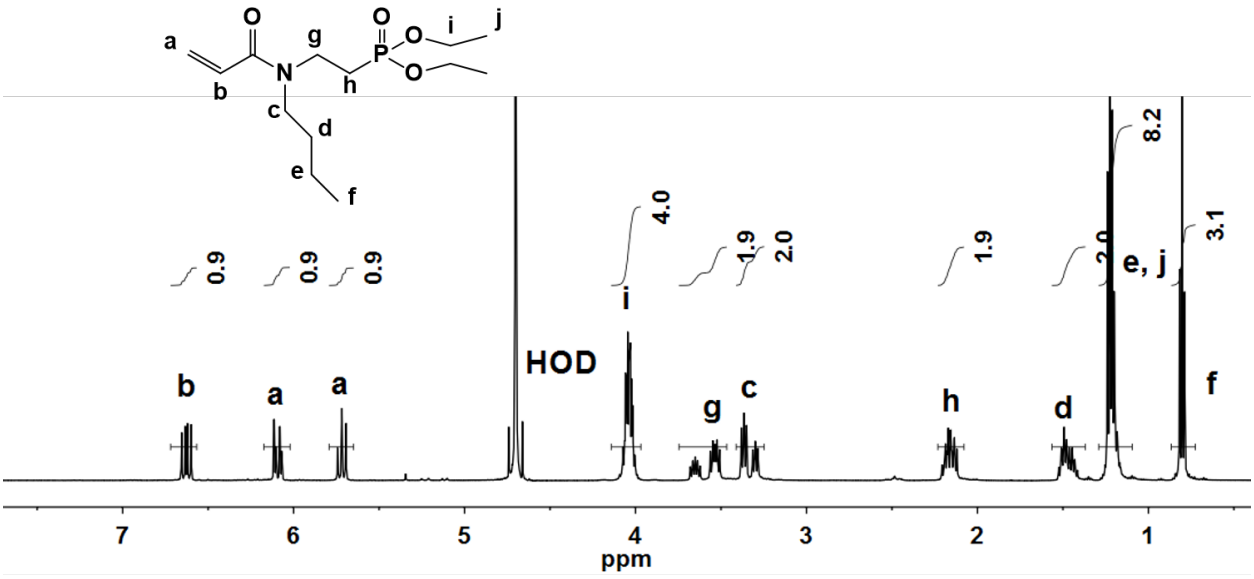

Figure 4.2. ^{1}H NMR spectrum of the *n*-butylacrylamide phosphonate monomer

Table 4.1 Summary of elemental analysis on the *n*-butylacrylamide phosphonate monomer

Element	Theoretical wt%	Found wt%
C	53.59	53.66
N	4.81	4.93
H	9.00	9.05
P	10.63	10.56

4.4.2 Synthesis of poly(*n*-butylacrylamide phosphonate)-*g*-PEO copolymers

A number of papers have been published on the free radical copolymerization of (meth)acrylate-functional PEO with other (meth)acrylates.[29-32] A few studies have been reported on copolymerizations of PEO macromonomers with (meth)acrylamide derivatives. Pelton *et al*. prepared and carried out kinetic studies on copolymerization of acrylamide with (meth)acrylate-functional PEO in aqueous solution.[33] The reactivity of the PEO macromonomer decreased with increasing PEO chain length (from M_n ~ 230 to 2,000 g mol^{-1}). Several research groups have investigated copolymerizations of *N*-isopropylacrylamide (NIPAM) with PEO macromonomers and the solution behavior of the PNIPAM-*g*-PEO graft copolymers.[34-37] Different compositions of the copolymer (5.9 - 48 wt% PEO) were obtained based on the corresponding feed ratios.[38, 39] When the temperature was increased through the LCST in water, the PNIPAM-*g*-PEO copolymers exhibited a "coil-to-globule" transition with a hydrophobic PNIPAM core and a hydrophilic PEO shell. To our knowledge, few studies have focused on copolymerizations of acrylamide-bearing phosphonate moieties with PEO. In the current study, we describe the synthesis of graft copolymers comprised of acrylamide phosphonate backbones and PEO

pendant chains (Figure 4.3). For a targeted 67:33 wt:wt acrylamide phosphonate to PEO ratio, the actual composition in the copolymer was found to be 63:37 by ^{1}H NMR after isolation.

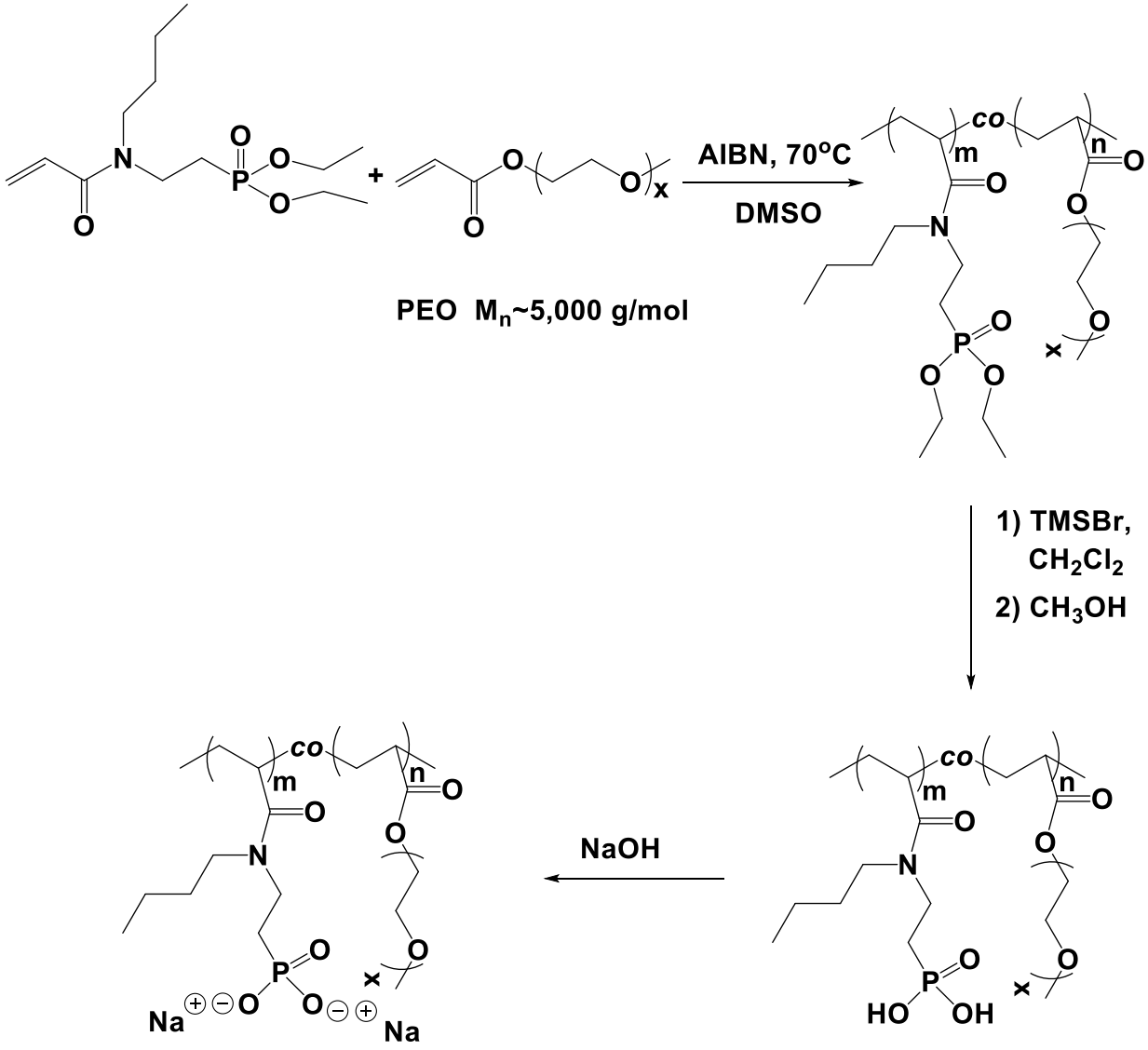

Figure 4.3 Synthesis of poly(*n*-butylacrylamide phosphonate)-*g*-PEO and poly(*n*-butylacrylamide phosphonic acid)-*g*-PEO copolymers

4.4.3 Kinetic studies of copolymerization

Kinetic studies on the copolymerization were carried out to estimate the microstructure of the graft copolymer. The feed molar ratio of the phosphonate monomer relative to the acrylate-PEO macromonomer was 28 to 1. Conversions of each monomer were directly measured by ^{1}H NMR of the reaction mixtures by monitoring the vinyl peaks. Figure 4.4 shows a representative ^{1}H NMR spectrum of a monomer mixture in deuterium oxide. The vinyl peaks of *n*-butylacrylamide phosphonate resonated at 5.7, 6.2 and 6.6 ppm while the vinyl peaks from the acrylate-functional PEO were at 5.9, 6.2 and 6.4 ppm. The intensity decrease of these vinyl peaks was converted to the conversion of each monomer. Figure 4.5 shows the comparison of the reaction rate of the *n*-butylacrylamide phosphonate monomer and the acrylate-PEO macromonomer with time, suggesting strongly that at this feed molar ratio, statistical copolymers formed. For example, at 9.1% and 9.4% conversion of phosphonate and acrylate-PEO respectively, the molar ratio of the *n*-butylacrylamide phosphonate to the acrylate-PEO in the copolymer was 27:1, very close to the feed molar ratio (28:1).

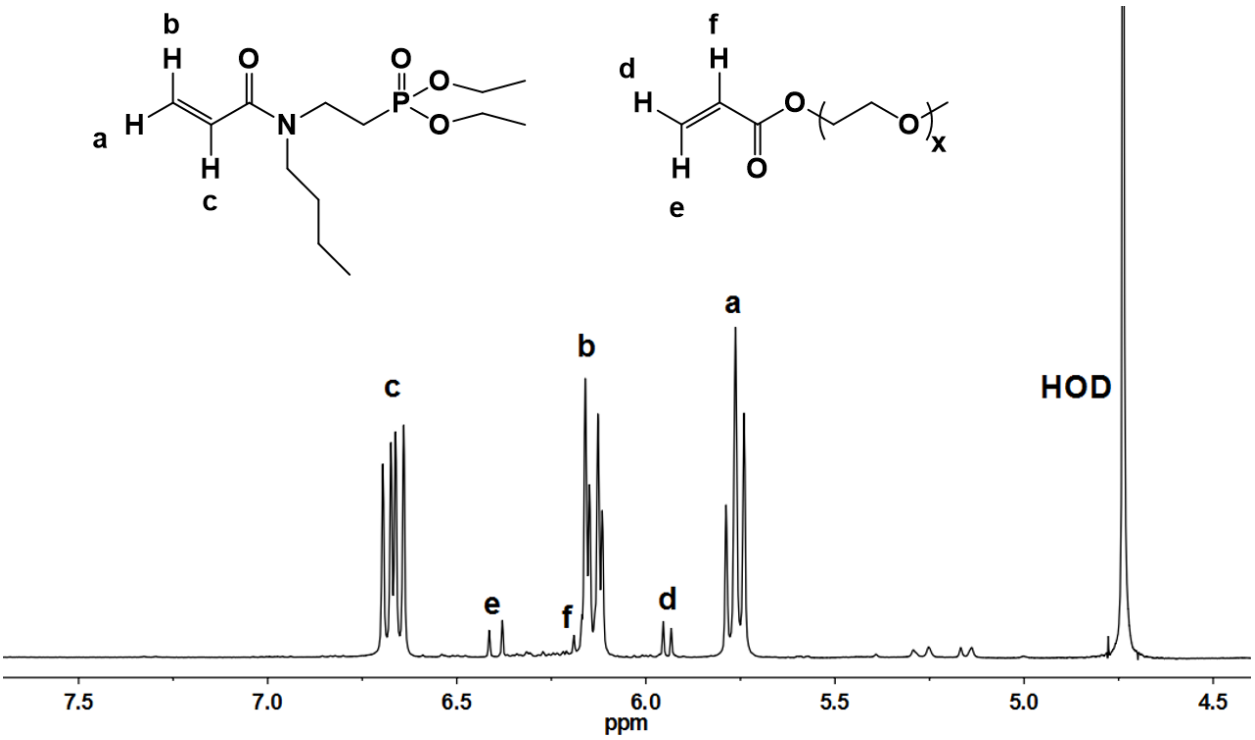

Figure 4.4 ^{1}H NMR of a monomer mixture comprised of *n*-butylacrylamide phosphonate and acrylate-PEO

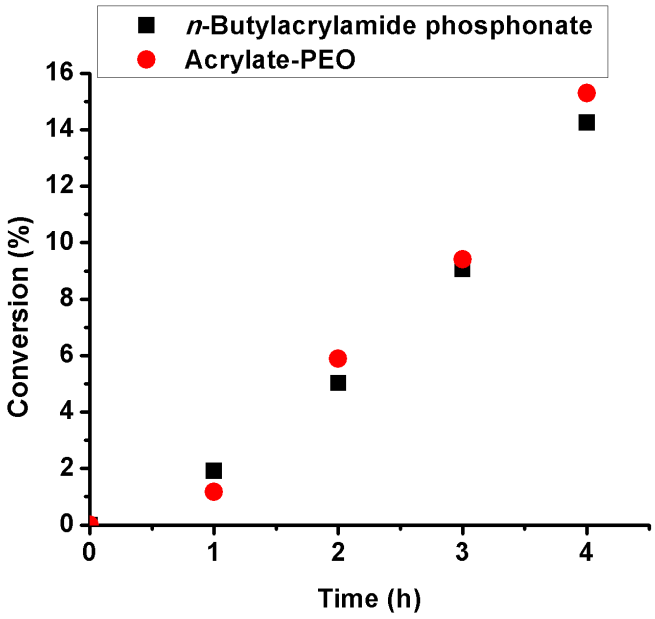

Figure 4.5 Monomer conversions during copolymerization of *n*-butylacrylamide phosphonate with acrylate-PEO at a feed molar ratio of 28 acrylamide phosphonates to 1 acrylate-PEO

4.4.4 Deprotection of poly(*n*-butylacrylamide phosphonate)-*g*-PEO copolymers

Deprotection of alkyl phosphonate esters lead to the corresponding phosphonic acids that can exhibit strong complexation properties with many substrates.[40] Various methods have been used for the deprotection including reactions under acidic or basic conditions.[41-44] Mild conditions have been employed by most researchers when unstable groups are present in the polymers.[20, 45, 46] In the present study, although the acrylamide bond is known to be relatively stable against hydrolysis, we used the mild deprotection approach developed by McKenna *et al.*[47] Dry poly(*n*-butylacrylamide phosphonate)-*g*-PEO copolymer was reacted with excess TMSBr in anhydrous dichloromethane. After 24 h, the solvent and the unreacted TMSBr were removed under reduced pressure to avoid any side reactions in the subsequent procedure. Methanol was added to convert the trimethylsilyl phosphonates into the corresponding phosphonic acids (Figure 4.3). ^{1}H NMR confirmed removal of the ethyl groups from phosphonate esters (Figure 4.6). The resonances at 1.2 and 4.1 ppm characterized the methyl and methylene groups in the phosphonates (Figure 6, top). The decrease of these resonances (Figure 6, bottom) compared to the PEO repeating unit protons at 3.6 ppm indicated complete removal of the ethyl groups. The single peak shifted from 31 to 20 ppm in the ^{31}P NMR spectrum (Figure 4.7) also suggested the successful deprotection of poly(*n*-butylacrylamide phosphonate)-*g*-PEO to the poly(*n*-butylacrylamide phosphonic acid)-*g*-PEO copolymer.

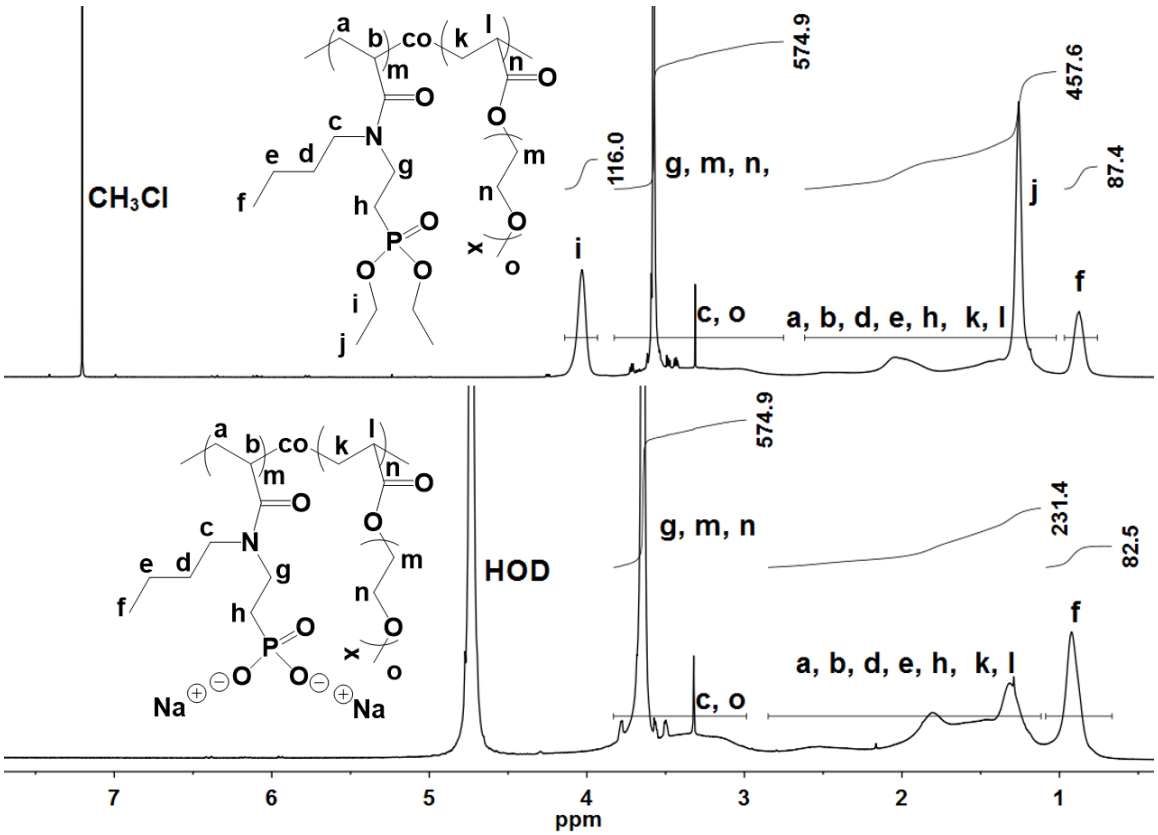

Figure 4.6 ^{1}H NMR spectra of a poly(*n*-butylacrylamide phosphonate)-*g*-PEO and poly(*n*-butylacrylamide phosphonic acid)-*g*-PEO copolymers at pH 7.4. The PEO oligomer in the acrylate-PEO macromonomer had M_n = 5085 g mol^{-1}

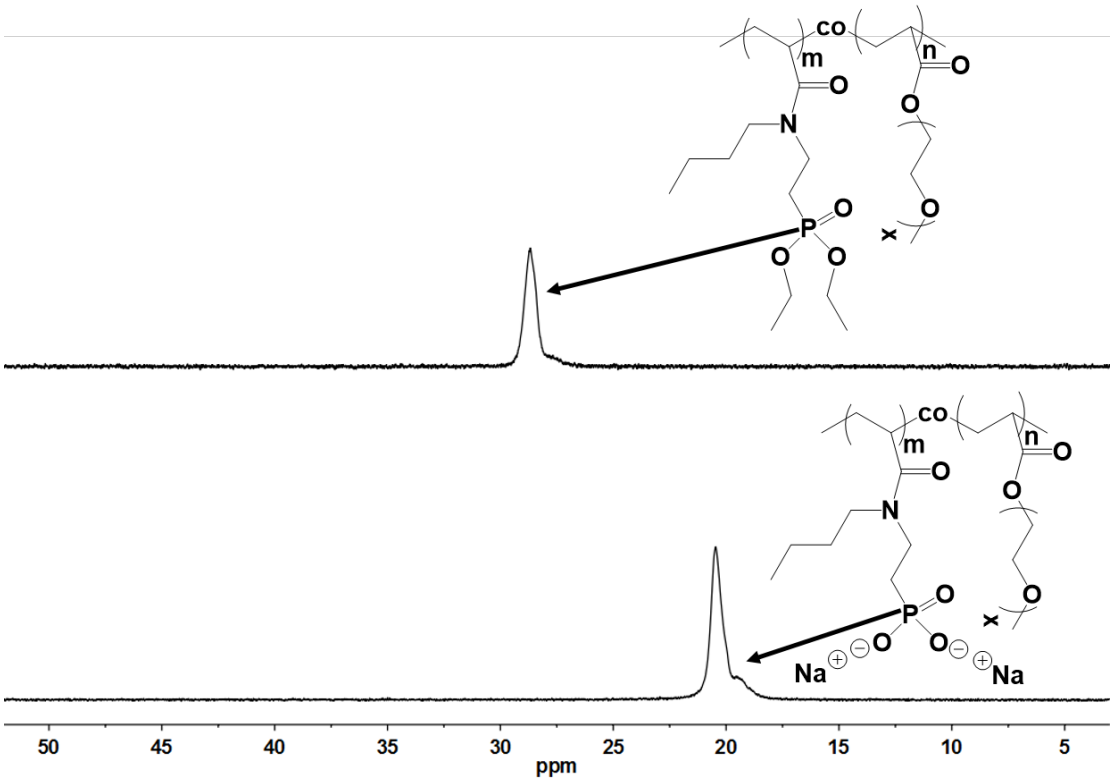

Figure 4.7 ^{31}P NMR spectra of a poly(*n*-butylacrylamide phosphonate)-*g*-PEO and poly(*n*-butylacrylamide phosphonic acid)-*g*-PEO copolymers at pH 7.4.

4.4.5 Solution properties of the graft copolymers

One of the objectives of designing phosphonic acid-containing copolymers in our research is to complex them with cationic or metal-containing drugs and nanoparticles through coordination or electrostatic interactions. Hence it is of great importance to investigate the solution properties of these copolymers to provide guidelines for developing complexes. The poly(*n*-butylacrylamide phosphonic acid)-*g*-PEO copolymer comprised of 56 wt% of the backbone and 44 wt% of the PEO grafts was soluble in DMF, DMSO, methanol and water at pH 7.4. It showed improved solubility in organic solvents compared to the previously synthesized poly(ammonium bisphosphonic acid (meth)acrylate)-*g*-PEO copolymers that could only be

dissolved in aqueous media (pH 7.74).[24] This was attributed to the increased hydrophobicity contributed by the *n*-butyl group, the mono phosphonic acid nature of the acrylamide copolymer, and also to the fact that these new polymers were anionic as opposed to zwitterionic.

To investigate the solution behavior of the poly(*n*-butylacrylamide phosphonic acid)-*g*-PEO, a copolymer concentration of 2 mg mL^{-1} was prepared in all of the solvents for DLS measurements. Volume size distributions were transformed from intensity size distributions based on Mie theory for compositional analysis. Figure 4.8(A-E) shows the volume size distributions of the copolymer in DMF, DMSO, methanol and water with and without added salt. Table 4.2 summarizes the volume-average sizes and the relative volume ratios of the aggregates versus single polymer chains. Only one peak, indicating formation of aggregates, was observed in the size distributions for the copolymer solutions in DMF and DMSO (Figure 4.8(A) and 4.8(B)). The volume-average diameters of these aggregates were 220 and 301 nm with PDI values (from DLS) lower than 0.29. In contrast, the copolymer showed a bimodal size distribution in methanol (Figure 4.8(C)). The large peak centered at 19 nm is indicative of the single polymer chains, while the small peak is attributed to aggregates. The reasons for the aggregation in DMF and DMSO and dissociation of aggregates in methanol are not yet clear. Acrylamides are known to form strong hydrogen bonds.[48] Pophristic and coworkers[49] have investigated hydrogen bonding in several *ortho*-substituted arylamides. There were two types of hydrogen bonds in their study: R-O···H-N and C=O···H-N. These hydrogen bonds were conserved in an aprotic environment (chloroform) but were significantly disrupted in protic solvents (methanol and water). In our case, instead of N-H bonds phosphonic acid groups with H-O bonds were in the copolymer. Therefore, one possible explanation is that the interchain hydrogen-bonding of the phosphonic acid with the amide groups lead to the aggregation in

aprotic solvents i.e. DMF and DMSO (Figure 4.9, left). Most of the aggregates dissociated in protic solvents such as methanol due to the capability of the solvent itself to form hydrogen bonds with the amide and the phosphonic acids (Figure 4.9, right).

Table 4.2 Volume-average diameters of poly(*n*-butylacrylamide phosphonate)-*g*-PEO and poly((*n*-butylacrylamide phosphonate)-*g*-PEO in DMF, DMSO, methanol and water solution.

DLS from Figure 4.8	**Solvent**	**NaCl (conc.)**	**Peak 1 Volume ave. diameter**	**Peak 1 Volume (%)**	**Peak 2 Volume ave. diameter**	**Peak 2 Volume (%)**
A	DMF	-	220	100	-	-
B	DMSO	-	301	100	-	-
C	MeOH	-	19	89.2	171	10.8
D	H_2O	-	18	88.7	212	11.3
E	H_2O	0.17 N	18	95.9	129	4.1

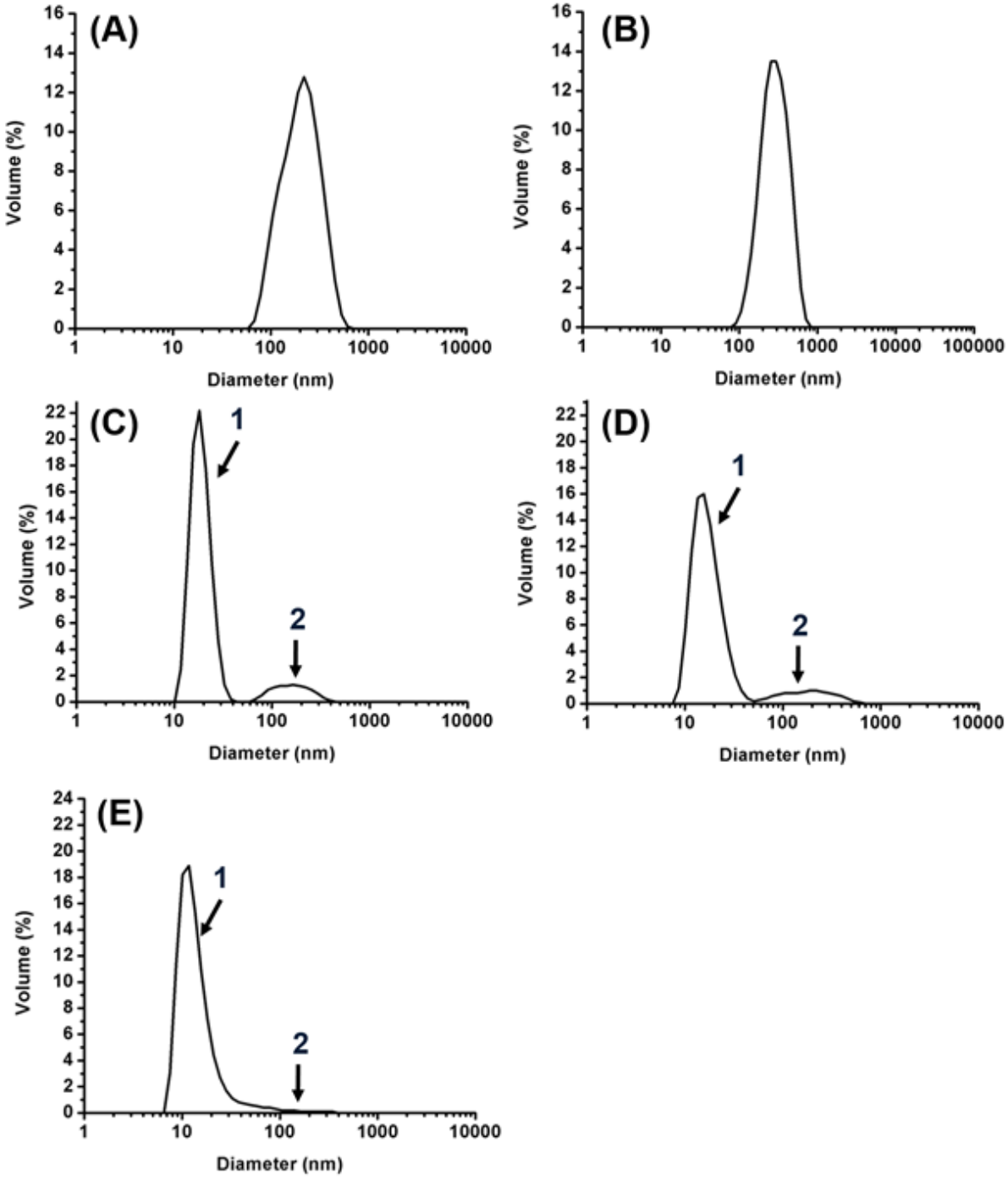

Figure 4.8 Volume size distributions measured by DLS of poly(*n*-butylacrylamide phosphonic acid)-*g*-PEO at a concentration of 2 mg mL^{-1} in: (A) DMF; (B) DMSO; (C) methanol; (D) water at pH 7.4; (E) water with 0.17 N sodium chloride at pH 7.4

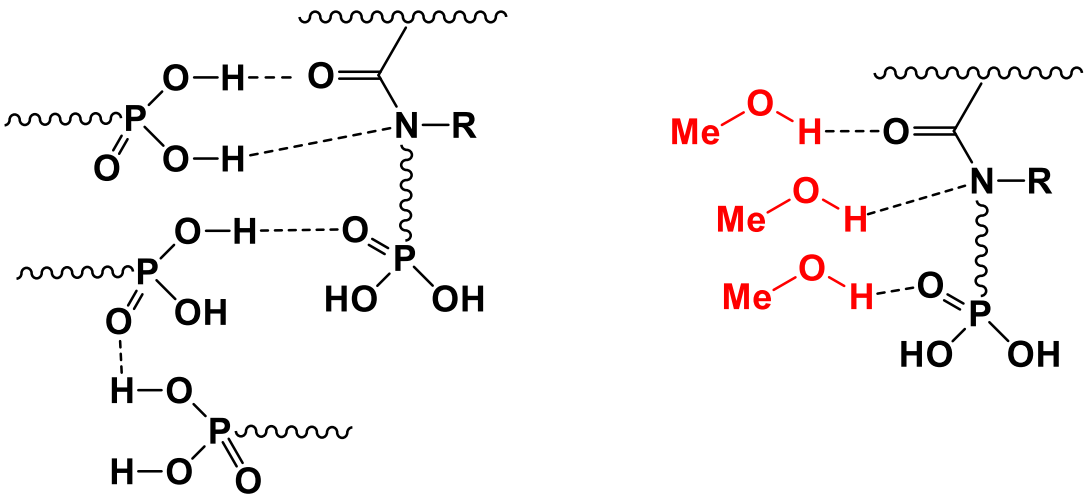

Figure 4.9 Illustration of hydrogen bonding of the poly(*n*-butylacrylamide phosphonic acid)-*g*-PEO copolymer in protic (methanol) and aprotic (DMF and DMSO) solvents

Similar bimodal size distributions (Figure 4.8(D)) were also observed in aqueous media at pH 7.4. This pH was chosen since it is close to the physiological condition. There was a large peak centered at 18 nm and a small peak at 212 nm. To explain this phenomenon, besides the breaking of hydrogen bonds by water, there might be electrostatic repulsion as well. At the selected pH, the phosphonic acids were partially ionized and formed phosphonate anions. The negative charges might induce interchain repulsion. Figure 4.8(E) shows the size distribution in an aqueous solution containing sodium chloride (0.17 N). Approximately 7 % more aggregates dissociated and about 5 % of the aggregates were still present in the solution. Therefore, this indicated that the addition of salt disrupted the aggregates to some extent, but not completely.

4.4.6 Interaction of the *n*-butylacrylamide phosphonic acid or acrylic acid monomers with hydroxyapatite (HAP)

HAP, with a formula of $Ca_5(PO_4)_3(OH)$, is found in calcified hard tissues of teeth and bone.[50] Adhesion of acid monomers to teeth is generally attributed to binding of the acid

functionalities to the calcium cation of HAP. Thus, several researchers have studied interactions of carboxylic or phosphonic acid-containing acrylic materials with HAP because of their potential applications in dental adhesives.[51-55] Herein we investigated binding of the phosphonic acid-containing *n*-butylacrylamide monomer to HAP and compared this with binding of acrylic acid. Since in dental adhesives acid monomers are applied as primers on teeth followed by photo-curing, we deprotected *n*-butylacrylamide phosphonate using TMSBr to afford the phosphonic acid for the investigation (Figure 4.10).

We employed a ^{13}C NMR method developed by Nishiyama and coworkers[25] to measure the ionization profiles of the acids and to evaluate their extents of interaction with HAP. This method was chosen since the chemical shift of the ^{13}C NMR peak is more sensitive to changes of chemical environment compared with pH changes upon titration. The chemical shift of the α-methylene carbon adjacent to the phosphorus atom in the phosphonic acid was pH-dependent. Figure 4.11 shows ^{13}C NMR spectra of the *n*-butylacrylamide phosphonic acid at pH 1.072 and 11.400, respectively. The chemical shift of the α-methylene carbon "e" moved downfield upon increasing the pH. By titrating each acid solution with aqueous sodium hydroxide (0.5 N), pH-dependent chemical shift curves (Figure 4.12) were established that reflected ionization of the diprotic phosphonic acid and the monoprotic carboxylic acid. Figure 4.12(A) shows the lower (at 28.71 ppm) and upper plateau (at 30.10 ppm) corresponding to the first and second dissociations of the acidic protons of the phosphonic acid. The chemical shift differences were 1.74 and 1.39 ppm for the two dissociations. pKa values were determined to be 1.3 and 7.1 for the two acidic protons and it was noted that these were very close to those of methacryloyl-2-aminoethyl phosphonic acid (pKa_1=1.8, pKa_2=7.1).[25] The pH-dependent chemical shift curve of the carbonyl carbon of acrylic acid showed a single plateau (at 175.41 ppm) corresponding to dissociation of

the proton from the carboxylic acid (Figure 4.12(B)). The chemical shift difference was 5.12 ppm and the pKa was measured as 4.2.

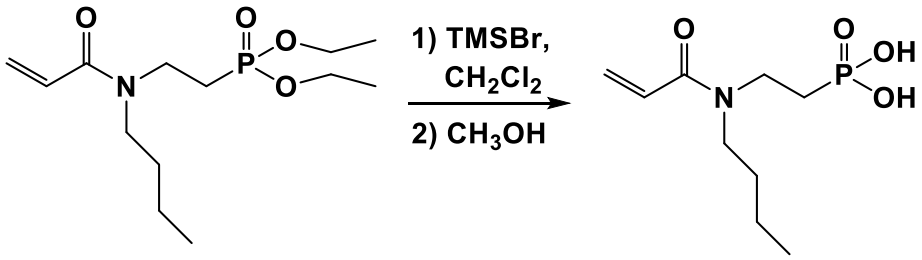

Figure 4.10 Deprotection of the *n*-butylacrylamide phosphonate monomer

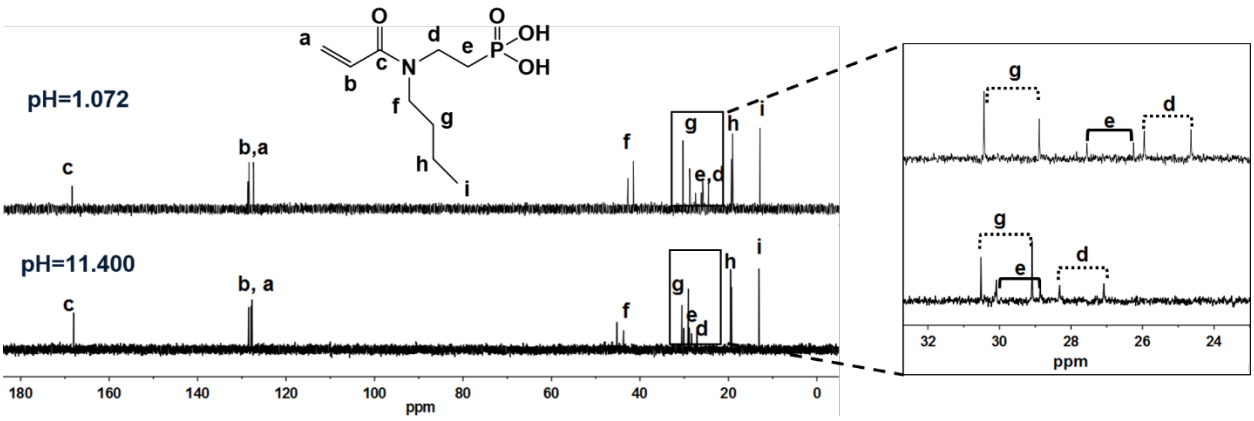

Figure 4.11 ^{13}C NMR of *n*-butylacrylamide phosphonic acid at pH 1.072 (top) and 11.400 (bottom)

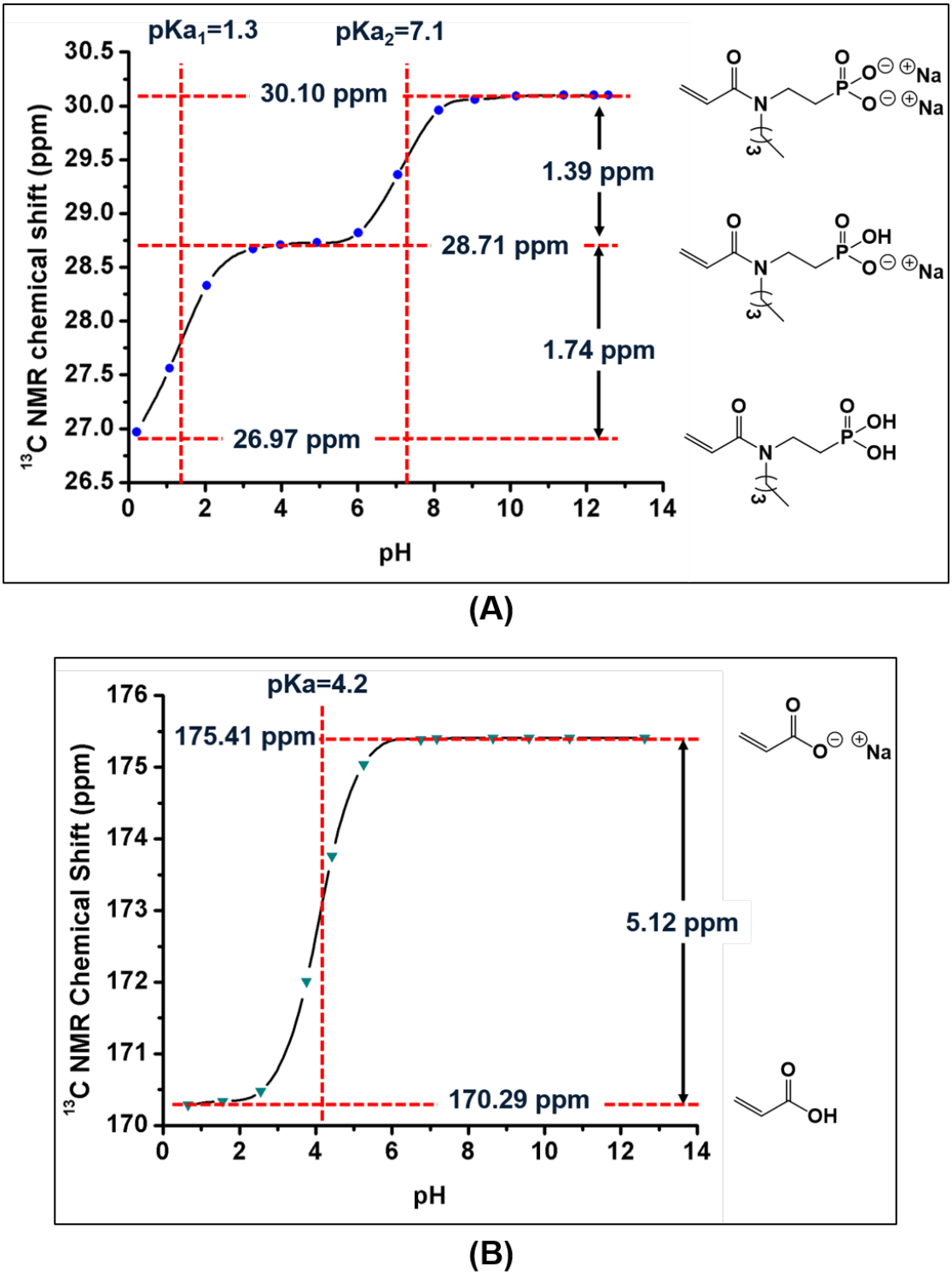

Figure 4.12 pH-dependent chemical shift curve of (A) α-methylene carbon "e" of *n*-butyl acrylamide phosphonic acid, and (B) carbonyl carbon of acrylic acid

To compare interactions of the phosphonic acid and acrylic acid with HAP, excess molar amounts of HAP (15 mg and 30 mg, 0.15 mmol and 0.30 mmol of calcium cations) were added to the acid solution. Figure 4.13(A-B) shows the ^{13}C NMR spectra of *n*-butylacrylamide phosphonic acid and acrylic acid with and without added HAP. In both cases, the pH of the acid solution increased when HAP was added, thus indicating interactions of the phosphonate or carboxylate anions with the calcium cation. The percentage of each acid that reacted with HAP was calculated by dividing the chemical shift difference before and after the addition of HAP by the difference of complete dissociation of the first proton from the phosphonic acid or the acrylic acid proton.[25, 51, 56, 57] For example, the chemical shift difference upon adding 15 mg HAP to the *n*-butylacrylamide phosphonic acid was 1.39 ppm and the difference for complete dissociation was 1.74 ppm. Thus the extent to which the phosphonic acid reacted with HAP was determined to be 79.9%. Table 4.3 summarizes the extents of interaction of the phosphonic acid-containing monomer and acrylic acid with HAP at two excess HAP concentrations. The *n*-butylacrylamide phosphonic acid exhibited 1.5-1.7 times higher binding capacity to HAP compared with that of the acrylic acid at both HAP concentrations (15 mg or 30 mg HAP). This is probably due to the lower pKa of the phosphonic acid (pKa=1.8) relative to acrylic acid (pKa=4.2) which allows the phosphonic acid to reach higher degree of dissociation under these relatively low pH conditions.

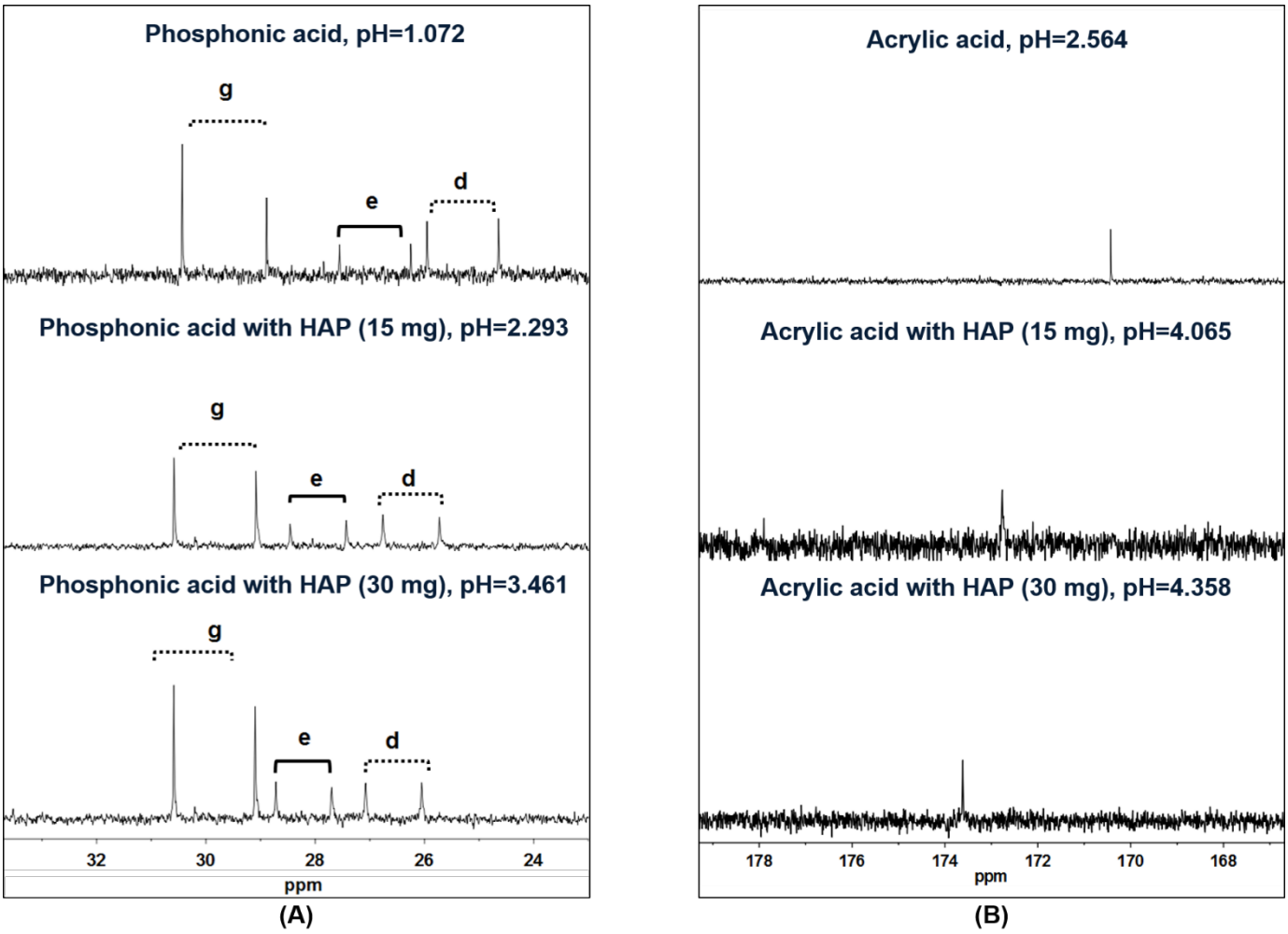

Figure 4.13 Expanded ^{13}C NMR spectra of (A) *n*-butylacrylamide phosphonic acid with and without added HAP (B) acrylic acid with and without added HAP

Table 4.3 Extent of binding of phosphonic acid and acrylic acid with HAP

	HAP (mg)	pH	Chemical shift difference (ppm)	% of acids associated with HAP
Phosphonic acid	15	2.293	1.39	79.9
Phosphonic acid	30	3.461	1.65	94.8
Acrylic acid	15	4.056	2.43	47.4

Acrylic acid	30	4.358	3.28	64.1

4.5 Conclusions

Alkyl acrylamide phosphonate monomers were prepared in two steps through aza-Michael addition followed by esterification. This simple methodology might be extended using other primary amines. Conventional radical polymerization of the *n*-butylacrylamide phosphonate with acrylate-functional PEO macromonomers yielded a statistical graft copolymer. Subsequent deprotection of the phosphonate ester groups was achieved leading to the poly(*n*-butylacrylamide phosphonic acid)-*g*-PEO copolymer. This phosphonic acid-containing copolymer is soluble in DMF, DMSO, methanol and water with adjusted pH. Further investigation on the self-assembly of the copolymer showed that it formed aggregates in DMF and DMSO, while only small amounts of aggregates were observed in the copolymer/methanol or water solutions. With respect to the phosphonic acid interactions with HAP as compared to those of carboxylic acid, the *n*-butylacrylamide phosphonic acid had a higher extent of binding compared to that of acrylic acid. These findings indicate that the phosphonate monomers and polymers may be good potential candidates in various biomedical applications such as drug delivery and dental adhesives.

4.6 Acknowledgements

The authors gratefully acknowledge the support of the National Science Foundation under contract numbers DMR 0805179, DMR 1106182 and DMR 0851662.

4.7 References

1. Ebetino, F. H.; Hogan, A.-M. L.; Sun, S.; Tsoumpra, M. K.; Duan, X.; Triffitt, J. T.; Kwaasi, A. A.; Dunford, J. E.; Barnett, B. L.; Oppermann, U.; Lundy, M. W.; Boyde, A.;

Kashemirov, B. A.; McKenna, C. E.; Russell, R. G. G., The relationship between the chemistry and biological activity of the bisphosphonates. *Bone* 2011, 49, 20-33.

2. Rogers, M. J.; Crockett, J. C.; Coxon, F. P.; Mönkkönen, J., Biochemical and molecular mechanisms of action of bisphosphonates. *Bone* 2011, 49, 34-41.

3. Moszner, N.; Zeuner, F.; Fischer, U. K.; Rheinberger, V., Monomers for adhesive polymers. Part 2. Synthesis and radical polymerization of hydrolytically stable acrylic phosphonic acids. *Macromol. Chem. Phys.* 1999, 200, 1062-1067.

4. Moszner, N.; Salz, U.; Zimmermann, J., Chemical aspects of self-etching enamel-dentin adhesives: A systematic review. *Dent. Mater.* 2005, 21, 895-910.

5. Troev, K.; Tsatcheva, I.; Koseva, N.; Georgieva, R.; Gitsov, I., Immobilization of aminothiols on poly(oxyethylene H-phosphonate)s and poly(oxyethylene phosphate)s—An approach to polymeric protective agents for radiotherapy of cancer. *J. Polym. Sci., Part A: Polym. Chem.* 2007, 45, 1349-1363.

6. Gitsov, I.; Johnson, F. E., Synthesis and hydrolytic stability of poly(oxyethylene-H-phosphonate)s. *J. Polym. Sci., Part A: Polym. Chem.* 2008, 46, 4130-4139.

7. Xu, X.; Yu, H.; Gao, S.; Mao, H.-Q.; Leong, K. W.; Wang, S., Polyphosphoester microspheres for sustained release of biologically active nerve growth factor. *Biomaterials* 2002, 23, 3765-3772.

8. Xu, X.; Yee, W.-C.; Hwang, P. Y. K.; Yu, H.; Wan, A. C. A.; Gao, S.; Boon, K.-L.; Mao, H.-Q.; Leong, K. W.; Wang, S., Peripheral nerve regeneration with sustained release of poly(phosphoester) microencapsulated nerve growth factor within nerve guide conduits. *Biomaterials* 2003, 24, 2405-2412.

9. Tan, J.; Gemeinhart, R. A.; Ma, M.; Mark Saltzman, W., Improved cell adhesion and proliferation on synthetic phosphonic acid-containing hydrogels. *Biomaterials* 2005, 26, 3663-3671.

10. Yin, Y. J.; Luo, X. Y.; Cui, J. F.; Wang, C. Y.; Guo, X. M.; Yao, K. D., A Study on Biomineralization Behavior of N-Methylene Phosphochitosan Scaffolds. *Macromol. Biosci.* 2004, 4, 971-977.

11. Nishiyama, N.; Suzuki, K.; Yoshida, H.; Teshima, H.; Nemoto, K., Hydrolytic stability of methacrylamide in acidic aqueous solution. *Biomaterials* 2004, 25, 965-969.

12. Klee, J. E.; Lehmann, U., N-alkyl-N-(phosphonoethyl) substituted (meth)acrylamides - new adhesive monomers for self-etching self-priming one part dental adhesive. *Beilstein J. Org. Chem.* 2009, 5, No. 72, No pp. given.

13. Catel, Y.; Degrange, M.; Pluart, L. L.; Madec, P.-J.; Pham, T.-N.; Chen, F.; Cook, W. D., Synthesis, photopolymerization, and adhesive properties of new bisphosphonic acid monomers for dental application. *J. Polym. Sci., Part A: Polym. Chem.* 2009, 47, 5258-5271.

14. Catel, Y.; Degrange, M.; Le Pluart, L.; Madec, P.-J.; Pham, T.-N.; Picton, L., Synthesis, photopolymerization and adhesive properties of new hydrolytically stable phosphonic acids for dental applications. *J. Polym. Sci., Part A: Polym. Chem.* 2008, 46, 7074-7090.

15. Besse, V.; Le Pluart, L.; Cook, W. D.; Pham, T.-N.; Madec, P.-J., Polymerization kinetics of phosphonic acids and esters using an iodonium initiator. *J. Polym. Sci., Part A: Polym. Chem.* 2013, 51, 5046-5055.

16. Besse, V.; Le Pluart, L.; Cook, W. D.; Pham, T. N.; Madec, P. J., Synthesis and polymerization kinetics of acrylamide phosphonic acids and esters as new dentine adhesives. *J. Polym. Sci., Part A: Polym. Chem.* 2013, 51, 149-157.

17. Graillot, A.; Monge, S.; Faur, C.; Bouyer, D.; Robin, J.-J., Synthesis by RAFT of innovative well-defined (co)polymers from a novel phosphorus-based acrylamide monomer. *Polym. Chem.* 2013, 4, 795-803.

18. Al-Ali, F.; Brun, A.; Rodrigues, F.; Etemad-Moghadam, G.; Rico-Lattes, I., New Catanionic Amphiphiles Derived from the Associative Systems (α-Hydroxyalkyl)-phosphinic or (α-Hydroxyalkyl)-phosphonic Acid/Cetyltrimethylammonium Hydroxide. Preparation, Characterization, and Self-Organization Properties. *Langmuir* 2003, 19, 6678-6684.

19. Brun, A.; Albouy, D.; Perez, E.; Rico-Lattes, I.; Etemad-Moghadam, G., Self-Assembly and Phase Behavior of New (α-Hydroxyalkyl)phosphorus Amphiphiles. *Langmuir* 2001, 17, 5208-5215.

20. Francova, D.; Kickelbick, G., Synthesis of methacrylate-functionalized phosphonates and phosphates with long alkyl-chain spacers and their self-aggregation in aqueous solutions. *Monatsh. Chem.* 2009, 140, 413-422.

21. Francova, D.; Kickelbick, G., Self-Assembly of Methacrylate-Functionalized Phosphonate and Phosphate Amphiphiles and their Conversion into Nanospheres. *Macromol. Chem. Phys.* 2009, 210, 2037-2045.

22. Bouilhac, C.; Travelet, C.; Graillot, A.; Monge, S.; Borsali, R.; Robin, J.-J., Synthesis of fatty phosphonic acid based polymethacrylamide by RAFT polymerization and self-assembly in solution. *Polym. Chem.* 2014, 5, 2756-2767.

23. Eren, T.; Tew, G. N., Phosphonic acid-based amphiphilic diblock copolymers derived from ROMP. *J. Polym. Sci., Part A Polym. Chem.* 2009, 47, 3949-3956.

24. Hu, N.; Johnson, L. M.; Pothayee, N.; Pothayee, N.; Lin, Y.; Davis, R. M.; Riffle, J. S., Synthesis of ammonium bisphosphonate monomers and polymers. *Polymer* 2013, 54, 3188-3197.

25. Nishiyama, N.; Fujita, K.; Ikemi, T.; Maeda, T.; Suzuki, K.; Nemoto, K., Efficacy of varying the NMEP concentrations in the NMGly–NMEP self-etching primer on the resin-tooth bonding. *Biomaterials* 2005, 26, 2653-2661.

26. Pothayee, N.; Balasubramaniam, S.; Davis, R. M.; Riffle, J. S.; Carroll, M. R. J.; Woodward, R. C.; St, P. T. G., Synthesis of 'ready-to-adsorb' polymeric nanoshells for magnetic iron oxide nanoparticles via atom transfer radical polymerization. *Polymer* 2011, 52, 1356-1366.

27. Ranu, B. C.; Banerjee, S., Significant rate acceleration of the aza-Michael reaction in water. *Tetrahedron Lett.* 2007, 48, 141-143.

28. Catel, Y.; Fischer, U. K.; Moszner, N., Monomers for adhesive polymers: 11. Structure–adhesive properties relationships of new hydrolytically stable acidic monomers. *Polym. Int.* 2013, 62, 1717-1728.

29. Smith, B. L.; Klier, J., Determination of monomer reactivity ratios for copolymerizations of methacrylic acid with poly (ethylene glycol) monomethacrylate. *J. Appl. Polym. Sci.* 1998, 68, 1019-1025.

30. Restrepo, A. S.; Pinzón, N. M.; Ju, L.-K., Synthesis of pH-sensitive surfactants by the terpolymerization of methacrylic acid, methoxy poly(ethylene glycol) methacrylate, and lauryl methacrylate: Initiator effect and reactivity ratio study. *J. Polym. Sci., Part A: Polym. Chem.* 2004, 42, 2950-2959.

31. Jones, J. A.; Novo, N.; Flagler, K.; Pagnucco, C. D.; Carew, S.; Cheong, C.; Kong, X. Z.; Burke, N. A. D.; Stöver, H. D. H., Thermoresponsive copolymers of methacrylic acid and poly(ethylene glycol) methyl ether methacrylate. *J. Polym. Sci., Part A: Polym. Chem.* 2005, 43, 6095-6104.

32. Ito, K.; Tsuchida, H.; Hayashi, A.; Kitano, T.; Yamada, E.; Matsumoto, T., Reactivity of poly(ethylene oxide) macromonomers in radical copolymerization. *Polym. J. (Tokyo)* 1985, 17, 827-39.

33. Xiao, H.; Pelton, R.; Hamielec, A., Preparation and kinetic characterization of copolymers of acrylamide and poly(ethylene glycol) (meth)acrylate macromonomers. *Polymer* 1996, 37, 1201-1209.

34. Chen, H.; Li, J.; Ding, Y.; Zhang, G.; Zhang, Q.; Wu, C., Folding and Unfolding of Individual PNIPAM-g-PEO Copolymer Chains in Dilute Aqueous Solutions. *Macromolecules* 2005, 38, 4403-4408.

35. Cheng, V.; Lee, B. H.; Pauken, C.; Vernon, B. L., Poly(N-isopropylacrylamide-co-poly(ethylene glycol))-acrylate simultaneously physically and chemically gelling polymer systems. *J. Appl. Polym. Sci.* 2007, 106, 1201-1207.

36. Singh, D.; Kuckling, D.; Koul, V.; Choudhary, V.; Adler, H.-J.; Dinda, A. K., Studies on copolymerization of N-isopropylacrylamide with poly(ethylene glycol) methacrylate. *Eur. Polym. J.* 2008, 44, 2962-2970.

37. Liang, D.; Song, L.; Zhou, S.; Zaitsev, V. S.; Chu, B., Poly(N-isopropylacrylamide)-g-poly(ethyleneoxide) for high resolution and high speed separation of DNA by capillary electrophoresis. *Electrophoresis* 1999, 20, 2856-2863.

38. Chen, H.; Zhang, Q.; Li, J.; Ding, Y.; Zhang, G.; Wu, C., Formation of Mesoglobular Phase of PNIPAM-g-PEO Copolymer with a High PEO Content in Dilute Solutions. *Macromolecules* 2005, 38, 8045-8050.

39. Qiu, X.; Wu, C., Study of the Core−Shell Nanoparticle Formed through the "Coil-to-Globule" Transition of Poly(N-isopropylacrylamide) Grafted with Poly(ethylene oxide). *Macromolecules* 1997, 30, 7921-7926.

40. Svara, J.; Weferling, N.; Hofmann, T., Phosphorus Compounds, Organic. In *Ullmann's Encyclopedia of Industrial Chemistry*, Wiley-VCH Verlag GmbH & Co. KGaA: 2000.

41. Aksnes, G.; Songstad, J., Alkaline hydrolysis of diethyl esters of alkylphosphonic acids and some chloro substituted derivatives. *Acta Chem. Scand.* 1965, 19, 893-7.

42. Hudson, R. F.; Keay, L., Hydrolysis of phosphonate esters. *J. Chem. Soc.* 1956, 2463-9.

43. Moszner, N., New monomers for dental application. *Macromol. Symp.* 2004, 217, 63-75.

44. Pfeiffer, F. R.; Mier, J. D.; Weisbach, J. A., Synthesis of phosphoric acid isoesters of 2-phospho-, 3-phospho-, and 2,3-diphosphoglyceric acid. *J. Med. Chem.* 1974, 17, 112-15.

45. Carbonneau, C.; Frantz, R.; Durand, J.-O.; Granier, M.; Lanneau, G. F.; Corriu, R. J. P., Studies of the hydrolysis of ethyl and tert-butyl phosphonates covalently bonded to silica xerogels. *J. Mater. Chem.* 2002, 12, 540-545.

46. Chougrani, K.; Niel, G.; Boutevin, B.; David, G., Regioselective ester cleavage during the preparation of bisphosphonate methacrylate monomers. *Beilstein J. Org. Chem.* 2011, 7, 364-368, No 46.

47. McKenna, C. E.; Higa, M. T.; Cheung, N. H.; McKenna, M. C., The facile dealkylation of phosphonic acid dialkyl esters by bromotrimethylsilane. *Tetrahedron Lett.* 1977, 155-8.

48. Huang, S.-Y.; Lipp, D. W.; Farinato, R. S., Acrylamide Polymers. In *Encyclopedia of Polymer Science and Technology*, John Wiley & Sons, Inc.: 2002; Vol. 1, p 44.

49. Liu, Z.; Remsing, R. C.; Liu, D.; Moyna, G.; Pophristic, V., Hydrogen Bonding in ortho-Substituted Arylamides: The Influence of Protic Solvents. *J. Phys. Chem. B* 2009, 113, 7041-7044.

50. Koutsopoulos, S., Synthesis and characterization of hydroxyapatite crystals: A review study on the analytical methods. *J. Biomed. Mater. Res.* 2002, 62, 600-612.

51. Albayrak, A. Z.; Bilgici, Z. S.; Avci, D., Influence of Structure on Polymerization Rates and Ca-Binding of Phosphorus-Containing 1,6-Dienes. *Macromol. React. Eng.* 2007, 1, 537-546.

52. Nishiyama, N.; Suzuki, K.; Takahashi, K.; Nemoto, K., The pKa effects of the carboxylic acid in N-methacryloyl-omega-amino acid on the demineralization and bond strengths to the teeth. *Biomaterials* 2004, 25, 5441-5447.

53. Yoshihara, K.; Yoshida, Y.; Hayakawa, S.; Nagaoka, N.; Torii, Y.; Osaka, A.; Suzuki, K.; Minagi, S.; Van Meerbeek, B.; Van Landuyt, K. L., Self-etch Monomer-Calcium Salt Deposition on Dentin. *J. Dent. Res.* 2011, 90, 602-606.

54. Nishiyama, N.; Suzuki, K.; Asakura, T.; Nakai, H.; Yasuda, S.; Nemoto, K., The effects of pH on N-methacryloyl glycine primer on bond strength to acid-etched dentin. *J. Biomed. Mater. Res.* 1996, 31, 379.

55. Nishiyama, N.; Asakura, T.; Suzuki, K.; Sato, T.; Nemoto, K., Adhesion mechanisms of resin to etched dentin primed with N-methacryloyl glycine studied by 13C-NMR. *J. Biomed. Mater. Res.* 1998, 40, 458-463.

56. Bilgici, Z. S.; Turker, S. B.; Avci, D., Novel Bisphosphonated Methacrylates: Synthesis, Polymerizations, and Interactions with Hydroxyapatite. *Macromol. Chem. Phys.* 2013, 214, 2324-2335.

57. Sahin, G.; Albayrak, A. Z.; Bilgici, Z. S.; Avci, D., Synthesis and evaluation of new dental monomers with both phosphonic and carboxylic acid functional groups. *J. Polym. Sci., Part A: Polym. Chem.* 2009, 47, 1953-1965.

CHAPTER 5 - Synthesis of Amine End-capped Poly(ethylene oxide-*b*-acrylic acid)

Nan Hu,[a,b] Nikorn Pothayee,[a] Nipon Pothayee,[a] Y. Lin,[a] R. M. Davis[a,c] and J. S. Riffle[a,b]

[a]Macromolecules and Interfaces Institute, [b]Department of Chemistry, [c]Department of Chemical Engineering, Virginia Tech, Blacksburg, VA 24061

5.1 Abstract

Heterobifunctional poly(ethylene oxide) (PEO) polymers with three different molecular weights were synthesized. Modification of one of these PEO afforded a macroinitiator with a bromide on one end and a protected amine on the other end for atom transfer radical polymerization (ATRP). Polymerization of *tert*-butyl acrylate (*t*BuA) in the presence of this initiator and copper (I) bromide (CuBr) catalyst yielded a diblock copolymer. The copolymer was deprotected by trifluoroacetic acid (TFA) and formed an amine terminated PEO-*b*-PAA.

5.2 Introduction

Polyion complex micelles developed by Kataoka[1] and Kabanov[2] represent a frontier technology in the drug delivery field. Polyion complexes are usually comprised of a block copolymer containing a neutral hydrophilic block and an ionic block loaded with substrates containing the complementary charge. In most cases, the counterions are biopharmaceuticals such as DNA, RNA, proteins or drugs. Due to electrostatic interactions between the ionic block and the counterions, charges are neutralized in these segments. They become hydrophobic and this induces micelle formation.[3, 4] Poly(ethylene oxide) and poly(acrylic acid) block copolymers (PEO-*b*-PAA) are an important class of anionic copolymers in the polyion complex family. PEO is extensively selected as the neutral hydrophilic block for polyion complexes because of its

biocompatibility, excellent solubility in water and organic solvents, and lack of toxicity and immunogenicity.[5-7] PAA contains carboxylic acid units which can be converted to carboxylate anions to interact with drugs.

Controlled radical polymerization provides possibilities for designing well-defined block copolymers with control of molecular weights and polydispersity. Normal controlled radical polymerization techniques involve nitroxide-mediated radical polymerization (NMRP),[8] atom transfer radical polymerization (ATRP)[9] and reversible addition-fragmentation transfer polymerization (RAFT).[10] PEO-*b*-PAA block copolymers have been prepared exclusively by ATRP.[11-15] An ester of acrylic acid (i.e. *t*-butyl acrylate) is polymerized by initiation of bromide-functionalized methoxy-PEO (mPEO-Br) in the presence of CuBr to afford PEO-*b*-P*t*BuA. Subsequent removal of the *tert*-butyl group under acidic conditions leads to the formation of PEO-*b*-PAA.

Heterobifunctional PEO oligomers (X-PEO-Y) are a special class of PEO that bear different moieties at each chain ends.[16] Both of these moieties can be reactive (e.g. HOOC-PEO-OH) or in some cases, only one of them is able to undergo modification (e.g. mPEO-OH). Heterobifunctional PEO oligomers that are end-capped with two reactive groups allow for tuning properties on both ends, thus leading to versatile applications of the resulting materials.[17-20] For instance, Tessmar *et al.* synthesized a heterobifunctional PEO with an amino group and a hydroxyl group on the ends (H_2N-PEO-OH).[18] The amine group was reacted with acetic acid to form an ammonium salt, then the hydroxyl group initiated ring opening polymerization of $_{D,L}$-lactide with catalysis from stannous 2-ethylhexanoate to form a block copolymer of PEO and poly($_{D,L}$-lactic acid) (H_2N-PEO-*b*-PLA-OH after neutralization). To establish that the amine was

present, it was derivatized with an amine-reactive fluorescent dye, then an increase in UV absorption was observed by SEC. It was reasoned that a variety of substrates, such as bioactive molecules, inorganic nanoparticles and cross-linkers could be reacted with the amine group and, thus, such diblock copolymers have promising potential for biomimic materials and drug delivery systems.

To our knowledge, few investigations have been conducted on preparation of end-group functionalized PEO-*b*-PAA copolymers. Herein we describe the synthesis of amine end-capped H_2N-PEO-*b*-PAA. This could undergo chemical modification for potential application in drug delivery systems with tracking and crosslinking capabilities.

5.3 Experimental

5.3.1 Materials

Dichloromethane (EMD Chemicals, anhydrous, 99.8%), toluene (EMD Chemicals, anhydrous, 99.8%), 3-chloropropylchlorodimethylsilane (Gelest Inc.) and trifluoroacetic acid (Alfa Aesar, 99%) were used as received. Hexane (99.9%), dichloromethane (99.9%), chloroform (99.9%), toluene (99.9%), tetrahydrofuran (THF, 99.99%) magnesium sulfate (anhydrous, 98%), sodium bicarbonate (99%), diethyl ether (anhydrous, 99.8%) and dialysis tubing (Spectra/Por, 3,500 MWCO), all from Fisher Scientific, were used as received. *N,N*-Dimethylformamide (DMF, anhydrous, 99.8%), 1,4-dioxane (99.8%), vinyl magnesium bromide (1.0 M in THF), acetone (99.99%), acetic acid (99.99%), sodium sulfate (anhydrous, 99%), ammonium chloride (99.99%), triethylamine (TEA, >99.5%), sodium hydroxide (97%), cysteamine hydrochloride (>98%), di-*tert*-butyl dicarbonate (99%), $_{D,L}$-dithiothreitol (>99%), *N,N*-diethylethanolamine (>99.5%) 2,2'-azobisisobutyronitrile (AIBN, 98%),

hexamethylphosphoramide (HMPA, 99%), sodium iodide (NaI, >99.5%), sodium chloride (>99.5%), 2-bromoisobutyryl bromide (98%), *N,N,N′,N″,N″*-pentamethyl-diethylenetriamine (PMDETA, 99%), CuBr (98%) and hydrochloric acid solution (1.0 N) were purchased from Sigma-Aldrich and used as received. THF was refluxed over sodium with benzophenone as an indicator until the solution turned deep purple, then it was fractionally distilled into a flame-dried round-bottom flask prior to polymerization. A double-metal cyanide catalyst, ($Zn_3[Co(CN)_6]_2$), graciously donated by Bayer, was dried at room temperature for 24 h under vacuum and diluted with distilled THF to yield a dispersion. Ethylene oxide packaged in a lecture bottle (EO, Sigma Aldrich, 99.5%) was distilled directly into a Parr pressure reactor for polymerization. *t*-Butyl acrylate (99%, Alfa Aesar) was passed through a basic alumina column to remove the inhibitor and distilled under reduced pressure before polymerization.

5.3.2 Synthesis

5.3.2.1 Synthesis of PEO with a Vinylsilylpropoxy Group at One End and a Hydroxyl Group at the other End (vinyl-PEO-OH)

PEO oligomers with controlled molecular weights were synthesized using 3-hydroxypropyldimethylvinylsilane (3-HPMVS) as an initiator. The initiator was prepared according to a method developed by our group.[21] A representative polymerization procedure is provided. EO (14.6 g, 0.332 mol) was distilled from a lecture bottle into a 300-mL high-pressure Parr reactor that was cooled in a dry ice bath. In a separate flame-dried, 50-mL round-bottom flask, 3-HPMVS (1.08 g, 7.5 mmol), THF (10 mL), and the double-metal cyanide catalyst (zinc hexcyanocobaltate, 13 mg, 500 ppm) were aged for 24 h. This solution was added to a stirring reaction mixture in the Parr reactor via syringe. The cooling bath was removed and the reaction mixture was heated to 90 °C. The reaction occurred after 15 min with an immediate increase of

temperature from 90 to 180 °C and the pressure increased from 110 psi to a maximum of 280 psi. After the sudden increase, the temperature and the pressure dropped to 95 °C and 60 psi, respectively. The reaction was maintained for 12 h. The reaction was allowed to cool to room temperature and was purged with N_2 for 1 h to remove any residual monomer. The reaction mixture was diluted with dichloromethane (100 mL) and transferred to a 600-mL beaker. The diluted reaction mixture was filtered through Celite twice to remove the double-metal cyanide catalyst. The solvent was removed by rotary evaporation and the resulting white solid (vinyl-PEO-OH) (14.5 g, 92%) was dried at 50 °C under vacuum overnight.

5.3.2.2 Synthesis of PEO with a *t*Boc Protected Amine Group at One End and a Hydroxyl Group at the other End (*t*BocNH-PEO-OH)

Vinyl-PEO-OH was reacted with *N*-(*tert*-butoxycarbonyl)-2-amino-ethanethiol via a thiol-ene reaction. *N*-(*tert*-Butoxycarbonyl)-2-amino-ethanethiol was prepared according to a procedure reported by Winger *et al.*[22] Vacuum dried vinyl-PEO-OH (2 g, 0.8 mmol), *N*-(*tert*-butoxycarbonyl)-2-amino-ethanethiol (0.43 g, 2.4 mmol) and AIBN (98.5 mg, 0.6 mmol) were dissolved in deoxygenated DMF (7 mL) in a 100-mL round bottom flask equipped with a stir bar. The round-bottom flask was placed in an oil bath and heated at 80 °C for 24 h. The reaction mixture was cooled to room temperature and diluted with dichloromethane (70 mL). The mixture was washed with DI water (4 x 50 mL) and precipitated in a hexane:ether (1:1 v:v) mixture (3 x 500 mL). The precipitate was collected by redissolving in dichloromethane. The solvent was evaporated and the white solid, *t*Boc-PEO-OH (1.89 g, 88%) was dried at 50 °C under vacuum overnight.

5.3.2.3 Synthesis of PEO with a *t*Boc Protected Amine Group at One End and a Bromide Group at the other End (*t*BocNH-PEO-Br)

Vacuum dried *t*BocNH-PEO-OH (1.93 g, 0.72 mmol) was charged in a 100-mL round bottom flask with a stir bar. THF (20 mL) and TEA (0.13 g, 1.3 mmol) was added to the flask. The flask was cooled in an ice bath. 2-Bromoisobutyryl bromide (0.3 g, 1.3 mmol) was slowly added to the flask via syringe. The ice bath was removed after 30 min and the reaction was conducted at room temperature. After 24 h, the reaction mixture was diluted with dichloromethane (70 mL) and washed with saturated sodium chloride solution (3 x 50 mL). The organic phase was dried over sodium sulfate and concentrated by rotary evaporation. The concentrated solution was precipitated in a hexane:ether (1:1 v:v) mixture (3 x 500 mL). The precipitates were collected by redissolving in dichloromethane. The solvent was evaporated and the white solid, *t*BocNH-PEO-Br (1.67 g, 81%) was dried at room temperature under vacuum overnight.

5.3.2.4 Synthesis of *t*BocNH-PEO-*b*-P*t*BuA using *t*BocNH-PEO-Br as a Macroinitiator by ATRP

*t*BocNH-PEO-Br (2.37 g, 0.84 mmol) and toluene (15 mL) were charged into a 100-mL round-bottom flask. The mixture was nitrogen purged for 15 min. In a 50-mL flask, *t*BuA (10.1 g, 79 mmol), PMDETA (0.145 g, 0.84 mmol) and toluene (1 mL) were mixed and nitrogen purged for 15 min. CuBr (0.12 g, 0.84 mmol) was quickly added to a flame dried 100-mL Schlenk flask. The Schlenk flask was vacuum dried for 15 min. The *t*BuA/toluene solution with PMDETA and the *t*BocNH-PEO-Br/toluene solution was transferred to the Schlenk flask under nitrogen. The Schlenk flask was nitrogen purged for 30 min followed by three freeze-pump-thaw cycles. The Schlenk flask was then placed in an oil bath preheated to 75 °C. After 18 h, the reaction mixture was allowed to cool to room temperature, diluted with dichloromethane (80 mL), and filtered

through a neutral alumina column to remove the catalyst. The solvent was evaporated and the pale yellow solid, *t*BocNH-PEO-*b*-P*t*BuA (10.5 g, 73%) was dried under vacuum at 50 ^{o}C overnight.

5.3.2.5 Synthesis of H_2N-PEO-*b*-PAA copolymer

The *t*Boc group on one terminus and the *t*-butyl ester groups of *t*BocNH-PEO-*b*-P*t*BuA were hydrolyzed simultaneously with trifluoroacetic acid (TFA). Briefly, *t*BocNH-PEO-*b*-P*t*BuA (0.9 g, 0.072 mmol) was dissolved in dichloromethane (6 mL) in a 50-mL round-bottom flask. TFA (3.2 g, 28 mmol) was slowly added to the flask and the reaction was maintained at room temperature for 24 h. The reaction mixture was then concentrated by evaporating the solvent, and the concentrated mixture was precipitated in cold hexane (2 x 200 mL). The precipitated H_2N-PEO-*b*-PAA was redissolved in THF and water mixture, transferred into 3,500 MWCO dialysis tubing and dialyzed against 2 L of DI water for 48 h, then lyophilized for 3 days. The yielded pale yellow solid (0.47 g, 81%) was stored in the refrigerator.

5.3.3 Characterization

^{1}H NMR spectral analyses were performed on a Varian Unity 400 NMR or a JEOL Eclipse Plus 500 NMR operating at 399.95 or 500 MHz, respectively. All spectra of the small-molecule compounds and heterobifunctional PEO and PEO-*b*-P*t*BuA copolymers were obtained in $CDCl_3$. Spectra of the PEO-*b*-PAA copolymers were obtained in d_6-DMSO.

Molecular weights were analyzed by size exclusion chromatography (SEC). A Waters Alliance model 2690 chromotograph with a Viscotek T60A dual viscosity detector and laser refractometer equipped with four Waters Styragel HR columns (HR4 7.8 x 300 mm, HR3 7.8 x

300 mm, HR2 7.8 x 300 mm, and HR0.5 7.8 x 300 mm) was used to obtain the chromatograms. HPLC grade chloroform was employed as the mobile phase at 30°C and a flow rate of 1.0 mL/min. Polystyrene standards were used to construct a universal calibration to determine absolute molecular weights. Samples (15 – 25 mg) were dissolved in HPLC grade chloroform (10 mL) and passed through a 0.45-μm Teflon® syringe filter before each measurement.

5.4 Results and Discussion

5.4.1 Synthesis of vinyl-PEO-OH

Previously our group developed a facile method for synthesizing vinylsilyl alcohols as initiators for polymerization of epoxide monomers.[21] The initiators were prepared by a three-step procedure beginning with a Grignard reaction of vinylmagnesium chloride with 3-chloropropyldimethylchlorosilane. This was followed by substitution reactions of the chloride group by iodide and then of a hydroxyl group for the iodide. Herein we replaced vinylmagnesium chloride with a more reactive bromide derivative (Figure 5.1).

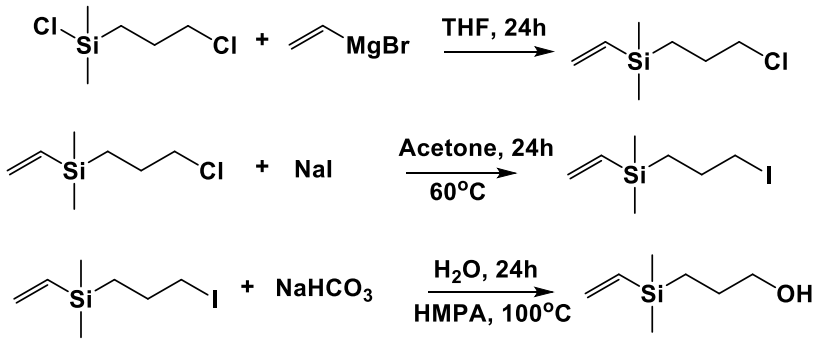

Figure 5.1 Synthesis of 3-HPMVS as an initiator for polymerization of EO

Polymerization of EO was initiated by 3-HPMVS in the presence of a heterogeneous double-metal cyanide catalyst (Figure 5.2). It has been shown by our group and others that this catalyst can afford PEO with expected molecular weights and low PDI values.[23-25] A series of

vinyl-PEO-OH oligomers with targeted molecular weights of ~1100, 2000, 3600 g mol^{-1} were synthesized and characterized by ^1H NMR and SEC (Table 5.1). A representative ^1H NMR spectrum of the polymer with a targeted molecular weight of 1100 g mol^{-1} is shown in Figure 5.3. The molecular weight was determined by normalizing the integration of the protons from the two methyl groups on the silicon as 6. The integration on the repeating unit of EO was then 113 and the calculated molecular weight was about 1200 g mol^{-1}. The SEC result of the same vinyl-PEO-OH (Figure 5.4) showed a molecular weight of 970 g mol^{-1} and a PDI value of 1.01.

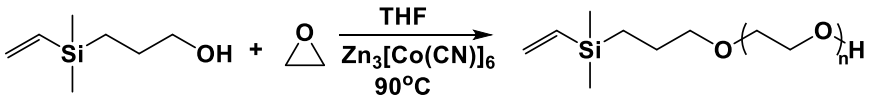

Figure 5.2 Synthesis of vinyl-PEO-OH by 3-HPMVS

Table 5.1 Characterization of vinyl-PEO-OH

Targeted Molecular Weight (g mol^{-1})	M_n (g mol^{-1})		PDI
	^1H NMR	SEC	
1100	1200	970	1.01
2000	2500	2500	1.05
3600	4100	3300	1.10

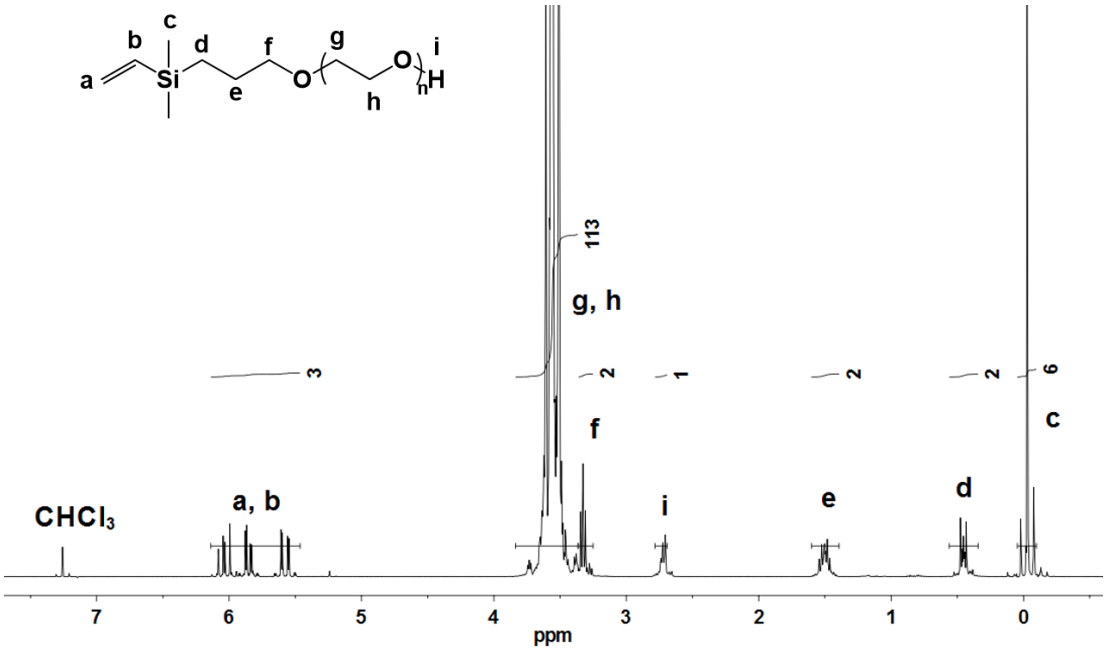

Figure 5.3 ^{1}H NMR of a vinyl-PEO-OH (targeted M_n=1100 g mol^{-1})

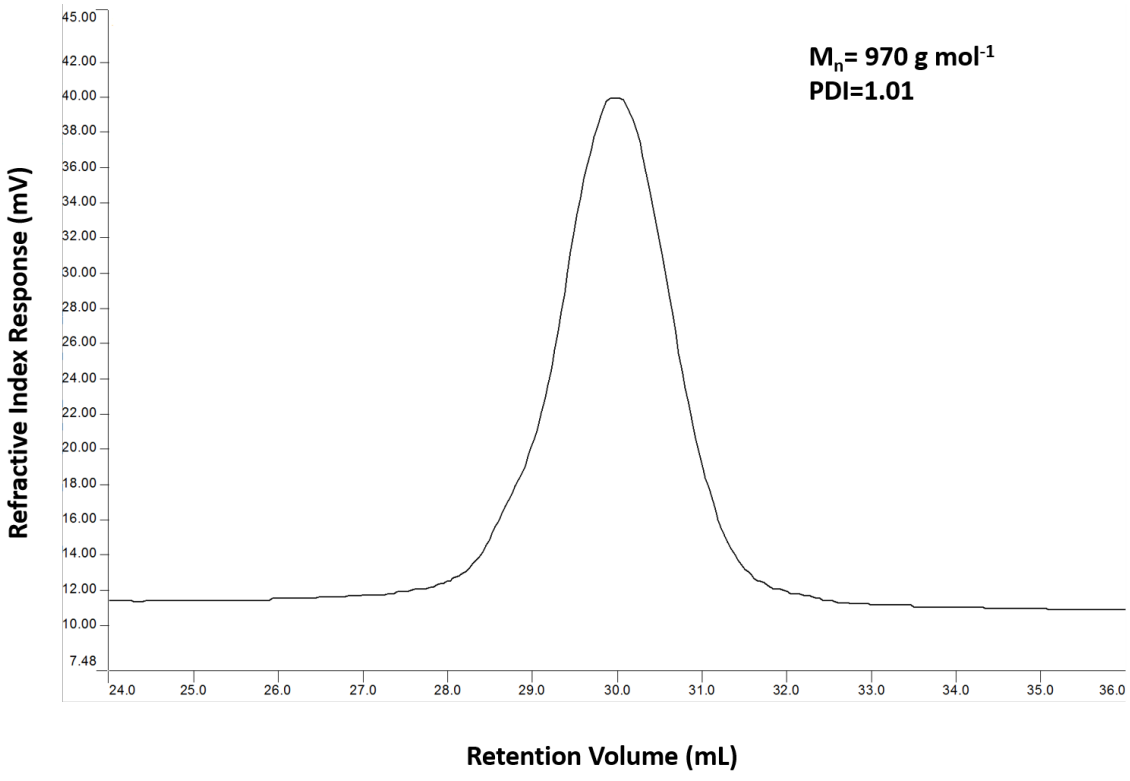

Figure 5.4 SEC trace of a vinyl-PEO-OH (targeted M_n=1100 g mol^{-1})

5.4.2 Synthesis of *t*BocNH-PEO-OH

The use of 3-HPMVS as the initiator produced PEO oligomers with a hydroxyl group on the terminal end and a vinylsilyl functionality on the initiator end. These two groups provide possibilities for versatile post-functionalization of PEO. The "click"-like thiol-ene reaction[26] is one of the most commonly used modification methods for PEO.[7, 27-30] Previously our group has employed this technique to introduce amine and carboxylic acid moieties.[21, 25] Herein we converted the vinylsilyl end group to a protected amine to prevent the amine from reacting with reagents in subsequent modifications. The protecting group was removed in the last step to yield amine functionalized block copolymers. The reaction proceeded through a free radical mechanism in the presence of *t*Boc-cysteamine-SH and vinyl-PEO-OH initiated by AIBN (Figure 5.5). The vinyl-PEO-OH did not polymerize because of the low reactivity of vinylsilyl double bonds toward free radical polymerization.[25] ^{1}H NMR (Figure 5.6) confirmed the addition of *t*Boc-cysteamine-SH to the vinyl bond of the PEO (M_n=2500 g mol^{-1}). The disappearance of the vinyl bond from 5.5 to 6.1 ppm and the corresponding appearance of a peak at ~1.4 ppm representing the *tert*-butyl group indicated the formation of *t*BocNH-PEO-OH (M_n=2680 g mol^{-1}).

Figure 5.5 Synthesis of *t*BocNH-PEO-OH

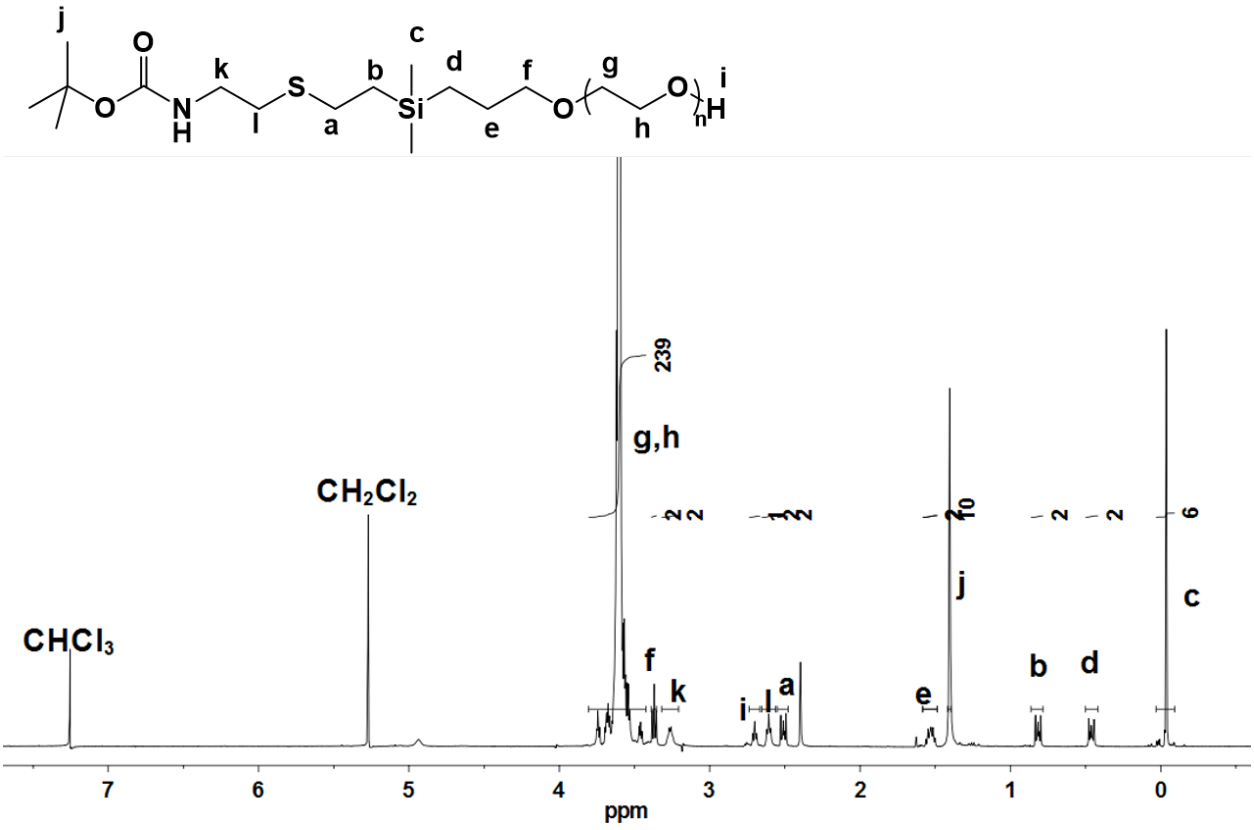

Figure 5.6 ^{1}H NMR of *t*BocNH-PEO-OH

5.4.3 Synthesis of *t*BocNH-PEO-Br

Numerous publications have covered the modification of mPEO-OH by 2-bromoisobutyryl bromide to convert the PEO to an ATRP initiator.[31-34] We adapted the same approach and it did not affect the protected amine group (Figure 5.7). ^{1}H NMR indicated the successful functionalization of the *t*BocNH-PEO-OH (M_n=2680 g mol^{-1}) with the acyl bromide to afford a bromoalkane end group (Figure 5.8). The peak at 1.95 ppm is due to the protons on the methyl groups from the isobutyryl moiety indicating the formation of *t*BocNH-PEO-Br (M_n=2830 g mol^{-1}). The integral for the peak at around 1.4 ppm representing the *tert*-butyl group from *t*Boc remained ~ 9. This suggested that the *t*Boc group was almost intact after bromination.

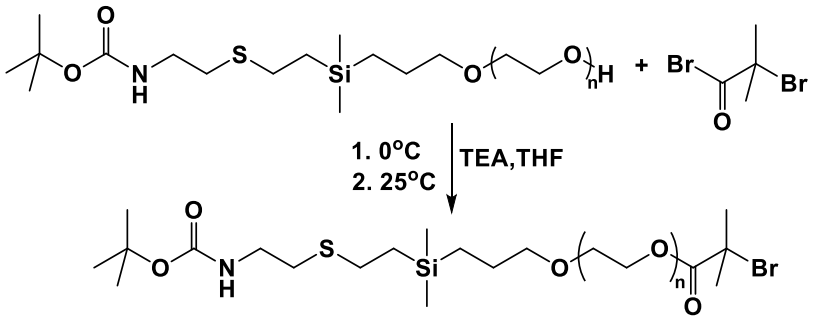

Figure 5.7 Synthesis of *t*BocNH-PEO-Br

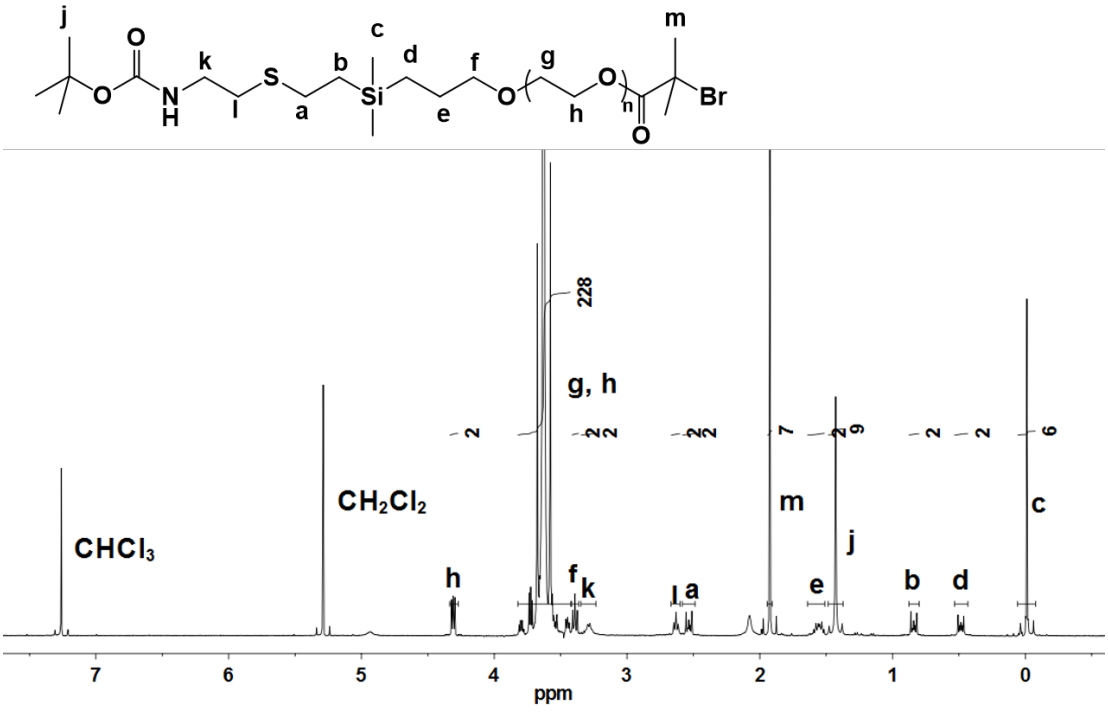

Figure 5.8 ^{1}H NMR of *t*BocNH-PEO-Br

5.4.4 Synthesis of the Block Copolymer and Deprotection of *t*BocNH-PEO-*b*-P*t*BuA

We employed ATRP conditions to prepare the block copolymer. *t*BocNH-PEO-Br served as the initiator to polymerize *t*-butyl acrylate in the presence of cuprous bromide as the activator and pentamethyldiethylenetriamine as the ligand to complex and disperse the copper in toluene

(Figure 5.9). ^{1}H NMR showed that the block copolymer, *t*BocNH-PEO-*b*-P*t*BuA polymerized as expected (Figure 5.10, top). The integral of the peak at around 0.0 ppm representing the protons from the methyl groups on silicon was again assigned as 6. A peak centered at about 2.2 ppm were the protons from the CH group in the backbone of the poly(*t*-butyl acrylate) block and the integration was 87 which indicated an average of 87 repeating units per chain. The calculated molecular weight for the poly(*t*-butyl acrylate) block from ^{1}H NMR was then 11,100 g mol^{-1}, and this was very close to the targeted molecular weight in this case of 12,000 g mol^{-1}. The total molecular weight of the diblock copolymer was thus 14,800 g mol^{-1}. A somewhat higher molecular weight (15,300 g mol^{-1}) was measured from SEC analysis using a Universal Calibration curve (Figure 5.11). Narrow molecular weight distribution (PDI=1.27) confirmed a well-defined structure of the diblock copolymer.

Removal of the *tert*-butyl groups from both the poly(*t*-butyl acrylate) block and the *t*Boc end group on the PEO under anhydrous acidic conditions, followed by dialysis and lyophilization afforded the NH_2-PEO-*b*-PAA copolymer. The reduction of the NMR peak integral at about 1.4 ppm attributed to the *tert*-butyl protons (Figure 10, bottom) clearly indicated complete removal. Moreover, the peak originally at ~3.25 ppm representing the methylene protons next to the nitrogen of the end group shifted upfield to ~3.00 ppm, and this provided evidence for the successful removal of the *t*Boc end group as well.

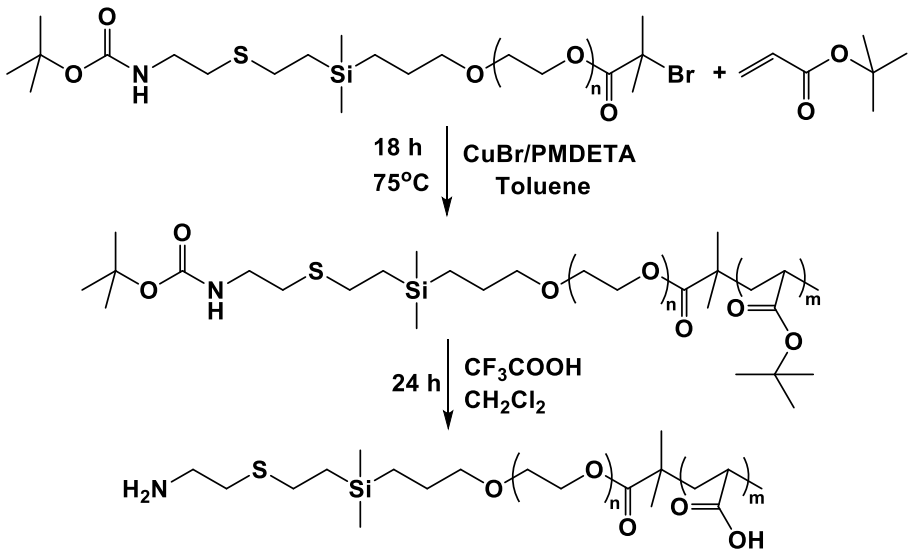

Figure 5.9 Synthesis and deprotection of *t*BocNH-PEO-*b*-P*t*BuA

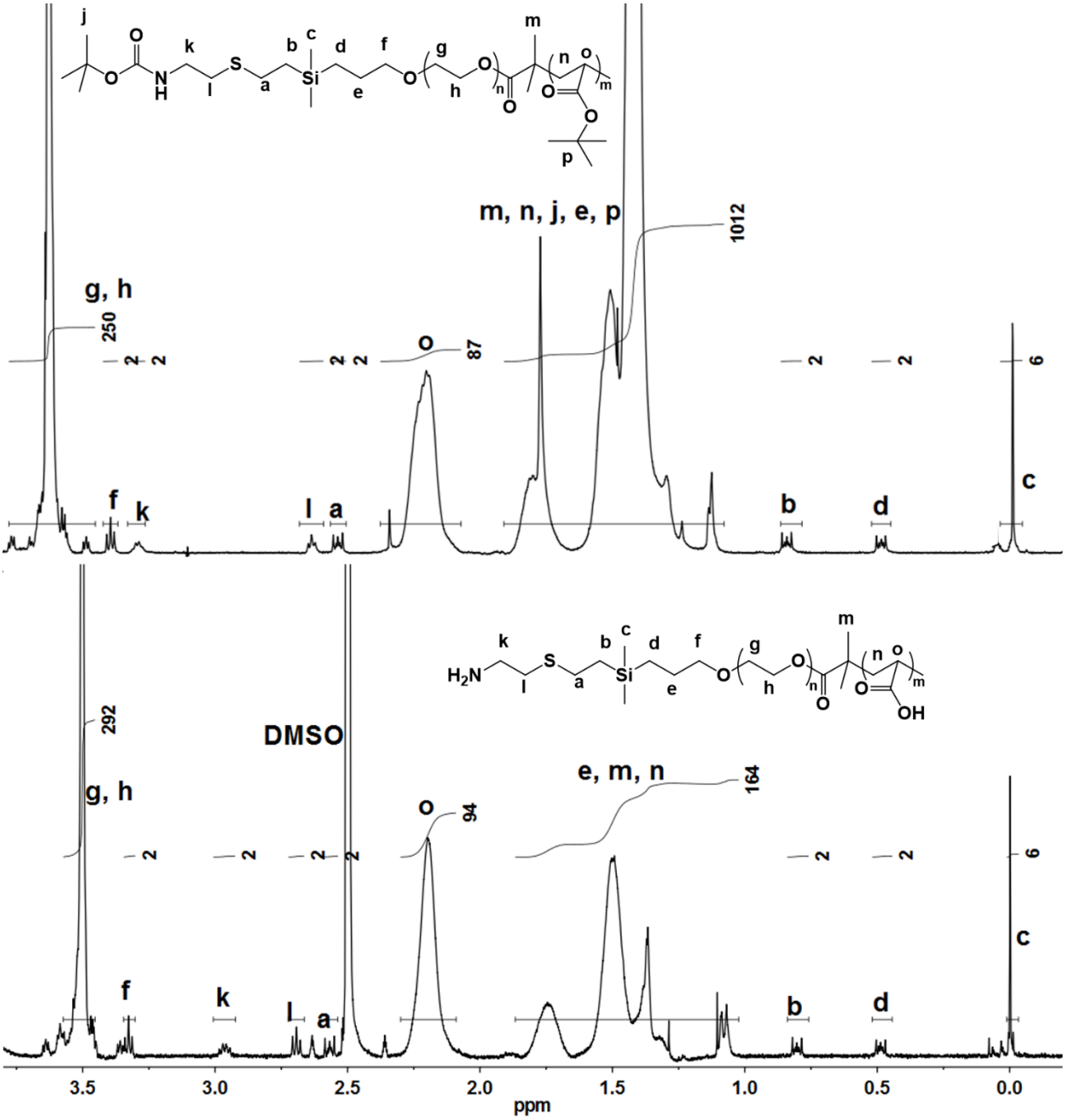

Figure 5.10 [1]H NMR of *t*BocNH-PEO-*b*-P*t*BuA before and after deprotection

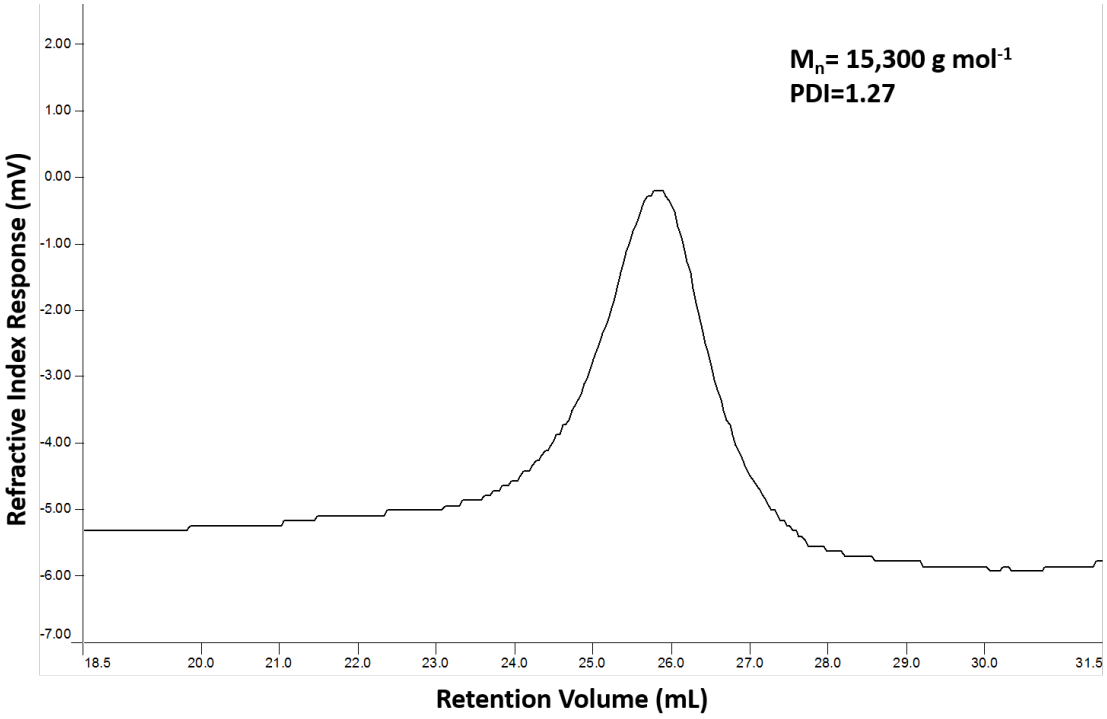

Figure 5.11 SEC trace of *t*BocNH-PEO-*b*-P*t*BuA

5.5 Conclusions

A series of vinyl-PEO-OH oligomers with different molecular weights and narrow molecular weight distributions were synthesized using a heterogeneous double-metal cyanide catalyst. Post-functionalization of the hydroxyl group on vinyl-PEO-OH with an acyl bromide functionalization of the vinylsilyl end with a protected cysteamine produced a macroinitiator for ATRP with a protected amine on the other end. Utilization of the initiator for polymerization of *t*-butyl acrylate and then subsequent hydrolysis to deprotect the initiator and remove the *tert*-butyl groups yielded well-defined diblock copolymers, H_2N-PEO-*b*-PAA. Due to the ionizable nature of the PAA block and the protein-resistant characteristic of PEO, this copolymer has potential to form a core-shell carrier for drugs and imaging agents. In addition, due to the high reactivity of the amine endgroup in various organic reactions, the amine functionality on the

surface of the shell can likely be further functionalized with tracking agents or it could serve as cross-linking sites. While introduction of all of these features requires several synthetic steps, such materials may become quite valuable for a large number of promising biomedical applications.

5.6 References

1. Harada, A.; Kataoka, K., Formation of Polyion Complex Micelles in an Aqueous Milieu from a Pair of Oppositely-Charged Block Copolymers with Poly(ethylene glycol) Segments. *Macromolecules* 1995, 28, 5294-5299.

2. Kabanov, A. V.; Bronich, T. K.; Kabanov, V. A.; Yu, K.; Eisenberg, A., Soluble Stoichiometric Complexes from Poly(N-ethyl-4-vinylpyridinium) Cations and Poly(ethylene oxide)-block-polymethacrylate Anions. *Macromolecules* 1996, 29, 6797-6802.

3. Kabanov, A. V.; Vinogradov, S. V.; Suzdaltseva, Y. G.; Alakhov, V. Y., Water-Soluble Block Polycations as Carriers for Oligonucleotide Delivery. *Bioconjugate Chem.* 1995, 6, 639-643.

4. Lee, Y.; Kataoka, K., Biosignal-sensitive polyion complex micelles for the delivery of biopharmaceuticals. *Soft Matter* 2009, 5, 3810-3817.

5. Lee, J. H.; Lee, H. B.; Andrade, J. D., Blood compatibility of polyethylene oxide surfaces. *Prog. Polym. Sci.* 1995, 20, 1043-1079.

6. Zalipsky, S., Functionalized Poly(ethylene glycols) for Preparation of Biologically Relevant Conjugates. *Bioconjugate Chem.* 1995, 6, 150-65.

7. Cammas, S.; Nagasaki, Y.; Kataoka, K., Heterobifunctional Poly(ethylene oxide): Synthesis of .alpha.-Methoxy-.omega.-amino and .alpha.-Hydroxy-.omega.-amino PEOs with the Same Molecular Weights. *Bioconjugate Chem.* 1995, 6, 226-230.

8. Hawker, C. J.; Bosman, A. W.; Harth, E., New Polymer Synthesis by Nitroxide Mediated Living Radical Polymerizations. *Chem. Rev.* 2001, 101, 3661-3688.

9. Matyjaszewski, K.; Xia, J., Atom Transfer Radical Polymerization. *Chem. Rev.* 2001, 101, 2921-2990.

10. Moad, G.; Rizzardo, E.; Thang, S. H., Radical addition-fragmentation chemistry in polymer synthesis. *Polymer* 2008, 49, 1079-1131.

11. Sun, Y.; Peng, Z.; Liu, X.; Tong, Z., Synthesis and pH-sensitive micellization of doubly hydrophilic poly(acrylic acid)-b-poly(ethylene oxide)-b-poly(acrylic acid) triblock copolymer in aqueous solutions. *Colloid. Polym. Sci.* 2010, 288, 997-1003.

12. Piogé, S.; Fontaine, L.; Gaillard, C.; Nicol, E.; Pascual, S., Self-Assembling Properties of Well-Defined Poly(ethylene oxide)-b-poly(ethyl acrylate) Diblock Copolymers. *Macromolecules* 2009, 42, 4262-4272.

13. Guo, L.; Ida, S.; Takashiba, A.; Daio, T.; Teramae, N.; Ishihara, T., Soft-templating method to synthesize crystalline mesoporous [small alpha]-Fe2O3 films. *New J. Chem.* 2014, 38, 1392-1395.

14. Krieg, A.; Pietsch, C.; Baumgaertel, A.; Hager, M. D.; Becer, C. R.; Schubert, U. S., Dual hydrophilic polymers based on (meth)acrylic acid and poly(ethylene glycol) - synthesis and water uptake behavior. *Polym. Chem.* 2010, 1, 1669-1676.

15. Guillemet, B.; Faatz, M.; Gröhn, F.; Wegner, G.; Gnanou, Y., Nanosized Amorphous Calcium Carbonate Stabilized by Poly(ethylene oxide)-b-poly(acrylic acid) Block Copolymers. *Langmuir* 2006, 22, 1875-1879.

16. Thompson, M. S.; Vadala, T. P.; Vadala, M. L.; Lin, Y.; Riffle, J. S., Synthesis and applications of heterobifunctional poly(ethylene oxide) oligomers. *Polymer* 2008, 49, 345-373.

17. Zayed, G. M. S.; Tessmar, J. K. V., Heterobifunctional Poly(ethylene glycol) Derivatives for the Surface Modification of Gold Nanoparticles Toward Bone Mineral Targeting. *Macromol. Biosci.* 2012, 12, 1124-1136.

18. Tessmar, J. K.; Mikos, A. G.; Goepferich, A., Amine-Reactive Biodegradable Diblock Copolymers. *Biomacromolecules* 2002, 3, 194-200.

19. Yamamoto, Y.; Nagasaki, Y.; Kato, M.; Kataoka, K., Surface charge modulation of poly(ethylene glycol)-poly(D,L-lactide) block copolymer micelles: conjugation of charged peptides. *Colloids Surf., B* 1999, 16, 135-146.

20. Yasugi, K.; Nakamura, T.; Nagasaki, Y.; Kato, M.; Kataoka, K., Sugar-Installed Polymer Micelles: Synthesis and Micellization of Poly(ethylene glycol)-Poly(D,L-lactide) Block Copolymers Having Sugar Groups at the PEG Chain End. *Macromolecules* 1999, 32, 8024-8032.

21. Vadala, M. L.; Thompson, M. S.; Ashworth, M. A.; Lin, Y.; Vadala, T. P.; Ragheb, R.; Riffle, J. S., Heterobifunctional Poly(ethylene oxide) Oligomers Containing Carboxylic Acids. *Biomacromolecules* 2008, 9, 1035-1043.

22. Winger, T. M.; Ludovice, P. J.; Chaikof, E. L., A convenient route to thiol terminated peptides for conjugation and surface functionalization strategies. *Bioconjug Chem* 1995, 6, 323-6.

23. Huang, Y.-J.; Qi, G.-R.; Chen, G.-X., Random copolymer of propylene oxide and ethylene oxide prepared by double metal cyanide complex catalyst. *Chin. J. Polym. Sci.* 2002, 20, 453-459.

24. Huang, Y. J.; Qi, G. R.; Chen, L. S., Effects of morphology and composition on catalytic performance of double metal cyanide complex catalyst. *Appl. Catal., A.* 2003, 240, 263-271.

25. Huffstetler, P. P., Synthesis and Characterization of Well-Defined Heterobifunctional Polyethers for Coating of Magnetite and their Applications in Biomedicine and Magnetic Resonance Imaging. *Dissertation* 2009.

26. Lowe, A. B., Thiol-ene "click" reactions and recent applications in polymer and materials synthesis. *Polym. Chem.* 2010, 1, 17-36.

27. Pale-Grosdemange, C.; Simon, E. S.; Prime, K. L.; Whitesides, G. M., Formation of self-assembled monolayers by chemisorption of derivatives of oligo(ethylene glycol) of structure HS(CH2)11(OCH2CH2)mOH on gold. *J. Am. Chem. Soc.* 1991, 113, 12-20.

28. Ishii, T.; Yamada, M.; Hirase, T.; Nagasaki, Y., New synthesis of heterobifunctional poly(ethylene glycol) possessing a pyridyl disulfide at one end and a carboxylic acid at the other end. *Polym. J. (Tokyo, Jpn.)* 2005, 37, 221-228.

29. Akiyama, Y.; Otsuka, H.; Nagasaki, Y.; Kato, M.; Kataoka, K., Selective Synthesis of Heterobifunctional Poly(ethylene glycol) Derivatives Containing Both Mercapto and Acetal Terminals. *Bioconjugate Chem.* 2000, 11, 947-950.

30. Tong, X.; Lai, J.; Guo, B.-H.; Huang, Y., A new end group structure of poly(ethylene glycol) for hydrolysis-resistant biomaterials. *J. Polym. Sci., Part A: Polym. Chem.* 2011, 49, 1513-1516.

31. Sun, X.; Zhang, H.; Zhang, L.; Wang, X.; Zhou, Q.-F., Synthesis of Amphiphilic Poly(ethylene oxide)-b-Poly(methyl methacrylate) Diblock Copolymers via Atom Transfer Radical Polymerization Utilizing Halide Exchange Technique. *Polym. J.* 2005, 37, 102-108.

32. Mahajan, S.; Renker, S.; Simon, P. F. W.; Gutmann, J. S.; Jain, A.; Gruner, S. M.; Fetters, L. J.; Coates, G. W.; Wiesner, U., Synthesis and Characterization of Amphiphilic Poly(ethylene oxide)-block-poly(hexyl methacrylate) Copolymers. *Macromol. Chem. Phys.* 2003, 204, 1047-1055.

33. Wu, T.; Mei, Y.; Xu, C.; Byrd, H. C. M.; Beers, K. L., Block Copolymer PEO-b-PHPMA Synthesis Using Controlled Radical Polymerization on a Chip. *Macromol. Rapid Commun.* 2005, 26, 1037-1042.

34. Hou, S.; Chaikof, E. L.; Taton, D.; Gnanou, Y., Synthesis of Water-Soluble Star-Block and Dendrimer-like Copolymers Based on Poly(ethylene oxide) and Poly(acrylic acid). *Macromolecules* 2003, 36, 3874-3881.

CHAPTER 6 - Complexation of Phosphonic Acids with Carboplatin

Nan Hu,[a,b] and J. S. Riffle[a,b]

[a]Macromolecules and Interfaces Institute, [b]Department of Chemistry,

Virginia Tech, Blacksburg, VA 24061

6.1 Abstract

Three compounds, vinylphosphonic acid, 3-hydroxypropyl ammonium bisphosphonic acid and 2-hydroxyethyl ammonium phosphonic acid were complexed with carboplatin under either acidic or neutral conditions. Covalent bonding of these acids to carboplatin was only observed under acidic pH. The covalently bonded percentage was 17%, 37% and 34%, respectively. A more in-depth investigation is necessary to understand this complexation behavior.

6.2 Introduction

Carboplatin, cis-diammine(cyclobutane-1,1-dicarboxylato)-platinum (II) or [Pt(CBDCA-O,O)$(NH_3)_2$], is a second generation platinum-containing anticancer drug (Figure 6.1).[1] It is a derivative of Cisplatin, cis-diamminedichloroplatinum (Figure 6.1). Cisplatin exerts itself as an important substrate in cancer chemotherapy.[2] Cisplatin-based drugs have been employed to treat a variety of cancers such as lung, head-and-neck, bladder, and breast cancer.[3-6] However, the clinical use of Cisplatin has been precluded by severe side effects including neurotoxicity, nephrotoxicity, ototoxicity and gastrointestinal toxicity.[7] As an alternative to Cisplatin, Carboplatin exhibits reduced toxicity, especially toward the kidneys and nervous system, while it retains comparable antitumor activities.[6]

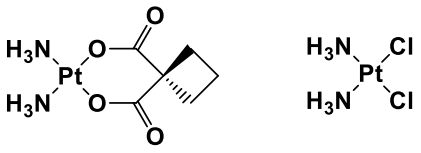

Carboplatin Cisplatin

Figure 6.1 Structures of Carboplatin and Cisplatin

With toxicity issues and side effects of Cisplatin, Carboplatin and other Pt-containing drugs, intrinsic and acquired drug resistance of tumors hinders the effectiveness of these drugs in cancer treatment as well. Hence, great effort has been made to improve efficacy of the platinum drugs. One extensively investigated area is complexation of platinum drugs with polymeric carriers.[8-12] Polymeric nanoparticles are of particular interest since they are capable of passively targeting tumor cells through the enhanced permeation and retention (EPR) effect.[13] With respect to the delivery of Carboplatin, various types of (co)polymers including polyanhydrides,[14] poly(methacrylic acid),[15] poly($_{L}$-lactide) or poly($_{D, L}$-lactide-co-glycolide),[16-20] polysaccharides,[21] and Pluronics[22] have been employed to form drug-polymer nanoparticles. Previously our group has utilized novel phosphonic acid-containing copolymers to incorporate Carboplatin. The resulting complexes exhibited excellent anticancer activity against MCF-7 breast cancer cells.[23] We hypothesized that the remarkable efficacy of these polymer-drug complexes might be due to ligand exchange of the dicarboxylate group of Carboplatin with the phosphonic acid moieties in the copolymer. Therefore, this investigation is focused on understanding binding behavior of phosphonic acids to Carboplatin. Three small-molecule phosphonic acids including vinylphosphonic acid, 3-hydroxypropyl ammonium bisphosphonic acid and 2-hydroxyethyl ammonium phosphonic acid were used as model compounds to react with Carboplatin.

6.3 Experimental

6.3.1 Materials

Diethyl vinylphosphonate (Epsilon-Chimie, >98%), phosphate bufferred saline (Mediatech), methanol (Fisher Scientific, 99.9%), dichloromethane (Fisher Scientific, 99.9%), and diethyl ether (Fisher Scientific, anhydrous, 99.8%) were used as received. Methanol (anhydrous, 99.8%), sodium sulfate (anhydrous, 99%), 3-amino-1-propanol (>99%), 2-(methylamino)ethanol (>98%), vinylphosphonic acid (97%) and Carboplatin were purchased from Sigma-Aldrich and used as received. Bromotrimethylsilane (Sigma-Aldrich, TMS-Br, 97.0%) was fractionally distilled before use.

6.3.2 Synthesis

6.3.2.1 Synthesis of phosphonate compounds

Synthesis of 3-hydroxypropyl ammonium bisdiethylphosphonate followed a procedure previously developed by our group.[24] Briefly, 3-aminopropanol (8.0 g, 0.11 mol), diethyl vinylphosphonate (36.0 g, 0.22 mol) and 200 mL of DI water were charged to a 500-mL round-bottom flask with a magnetic stir bar. The flask was placed in an oil bath and maintained at 60 °C for 24 h. The reaction mixture was extracted with dichloromethane. The combined organic phase was washed with DI water, dried over anhydrous sodium sulfate and the solvent was evaporated to afford 3-hydroxypropylammonium bisdiethylphosphonate.

Synthesis of 2-hydroxyethyl ammonium ethylphosphonate was similar to the method described above. 2-(Methylamino)ethanol (3.0 g, 0.04 mol) and diethyl vinylphosphonate (6.72 g, 0.041 mol) was reacted in water at 60 °C. The clear liquid obtained after isolation was 2-hydroxyethyl ammonium ethylphosphonate.

6.3.2.2 Synthesis of phosphonic acid derivatives

Converting the phosphonate group to phosphonic acid was achieved under mild conditions using TMS-Br. The molar ratio of TMS-Br to each phosphonate group was 3.75:1. A representative procedure to deprotect 3-hydroxypropylammonium bisdiethylphosphonate is provided. 3-Hydroxypropylammonium bisdiethylphosphonate (3.77 g, 9.34 mmol) was charged into a 100-mL flask with a stir bar and vacuum dried overnight. Anhydrous dichloromethane (30 mL) was added to dissolve the phosphonate. TMS-Br (10.72 g, 70 mmol) was slowly injected via syringe, then the reaction was conducted at room temperature for 24 h. Most of the solvent and TMS-Br were rotary evaporated. The reaction mixture was vacuum dried at room temperature for 4 h to remove any residual TMS-Br. Anhydrous methanol (20 mL) was added to the flask. After another 24 h the reaction mixture was precipitated in cold ether (500 mL). The precipitates were collected by redissolving into methanol and the solvent was removed by rotary evaporation. The viscous, pale yellow liquid was vacuum dried at 60 °C overnight.

6.3.3 Complexation

Complexation of vinylphosphonic acid, 3-hydroxypropyl ammonium bisphosphonic acid, 2-hydroxyethyl ammonium phosphonic acid with Carboplatin were conducted using the same procedure. For each complexation, the molar ratio of phosphonic acid groups or the sodium salt derivatives relative to Carboplatin (3.43:1, same ratio to that of the phosphonate polymer-Carboplatin complex)[23] was kept the same. For example, 3-hydroxypropyl ammonium bisphosphonic acid (6.8 mg, 34.1 μmol), corresponding to 46.2 μmol phosphonic acid, in DI water (2 mL) was charged into a 5-mL vial. Carboplatin (5 mg, 13.4 μmol) was dissolved in DI water (0.6 mL) with stirring and sonication until a clear solution was obtained. The Carboplatin/water solution was added drop-wise to the phosphonic acid solution. The vial was

sealed, sonicated for 2 min and stirred at room temperature. After 24 h, the reaction was stopped and samples were taken from the reaction mixture for NMR analysis.

6.3.4 Characterization

^{1}H NMR spectral analyses were performed on a Bruker Advance II-500 NMR operating at 500 MHz. Samples for the complexation study were prepared by removing 0.1 mL of the reaction mixture and adding this to 1.1 mL of D_2O. The NMR integrals for either α and β or γ methylene protons from the cyclobutane ring of Carboplatin were normalized at 4 or 2, respectively, to serve as an internal chemical shift reference.

6.4 Results and Discussion

Cisplatin exhibits antitumor properties by undergoing hydrolysis and then releasing the active species (Figure 6.2) which binds to DNA. This leads to DNA bending out of the preferred conformation and inhibits DNA replication and transcription, thus resulting in prevention of cancer cell proliferation.[6, 25] Carboplatin resembles the structure of Cisplatin but replaces the two chloride leaving ligands with a bidentate dicarboxylate group, and this significantly lowers the hydrolysis rate. The slow substitution rate of Carboplatin likely excludes the possibility of activating the drug by hydrolysis.[26] Several researchers have suggested that carbonate ions that are relatively abundant in the blood plasma trigger the antitumor activities of Carboplatin.[26-28] Dabrowiak *et al.* have made significant contributions in this area. They investigated possible reactions of Carboplatin in carbonate buffer.[28-32] Considering the similarities between carbonates and phosphonates, we wondered if complexation of phosphonic acid or phosphonate with Carboplatin might undergo similar reactions (Figure 6.3). The first step is the ring opening reaction of Carboplatin leading to the formation of intermediate **1**. Once formed, **1** might

generate a series of platinum-based products (Figure 6.3) together with the ligand, CBCDA. According to findings of Dabrowiak and coworkers, if Carboplatin releases CBCDA or covalently complexes with phosphonate or phosphonic acid, the methylene protons (α, β, γ) from the four-membered ring of CBCDA will become α' or α'', β' or β''and γ' or γ'', respectively.[30] This leads to a chemical shift in the ^{1}H NMR spectra since the chemical environment around those methylene groups are different from the original condition. Thus, we have employed ^{1}H NMR as a means to probe the binding properties of phosphonic acid or phosphonate with Carboplatin.

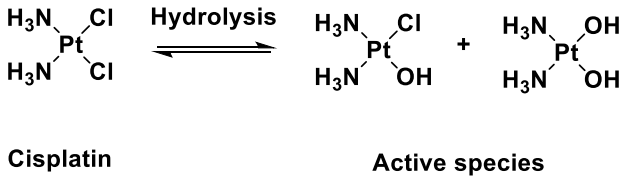

Figure 6.2 Hydrolysis reaction of Cisplatin releasing active species

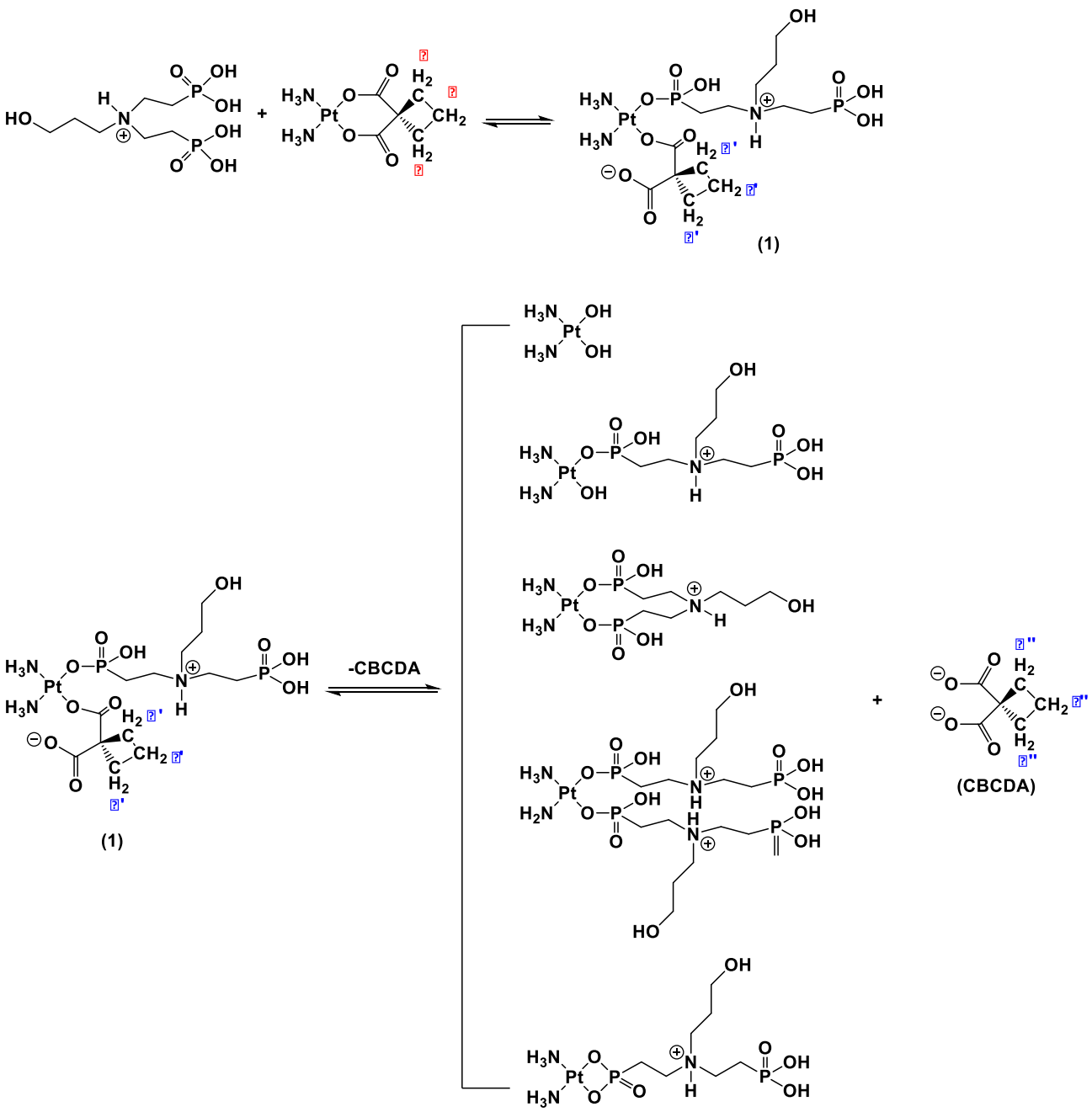

Figure 6.3 Possible complexation reactions between 3-hydroxypropyl ammonium bisphosphonic acid and Carboplatin

The three compounds utilized here were vinylphosphonic acid, 3-hydroxypropyl ammonium bisphosphonic acid and 2-hydroxyethyl ammonium phosphonic acid (Figure 6.4) which corresponds to a monophosphonic acid, bisphosphonic acids with a nitrogen atom and monophosphonic acid with a nitrogen atom, respectively. Complexation reactions were conducted under either acidic (pH ~ 2.0) or neutral (pH ~ 7.4) conditions with a fixed molar ratio (3.43:1) of phosphonic acid to Carboplatin. ^{1}H NMR spectra of the complexed products from vinylphosphonic acid and Carboplatin are shown in Figure 6.5. Peaks at 1.75 and 2.73 ppm correspond to the γ, then α and β methylene protons, respectively. Interestingly, no changes were observed at pH 7.4 while a new set of peaks appeared at about 1.85 and 2.41 ppm at pH 2.0. These peaks were related to the γ’ or γ’’, and the α’ or α’’and β’ or β’’ methylene protons of ring opened products of Carboplatin or CBCDA which in turn indicated the occurrence of covalent bonding between phosphonic acid and Carboplatin. Based on the integrals, there was about 17% of phosphonic acid covalently bonded to the Carboplatin when these were exposed to the acidic conditions. Similar binding behavior was observed from complexation of 3-hydroxypropyl ammonium bisphosphonic acid and Carboplatin (Figure 6.6). The percentage of covalently bound 3-hydroxypropyl ammonium bisphosphonic acid to the Carboplatin increased to 37%. The 20% increase might be due to the structure differences between vinylphosphonic acid and 3-hydroxypropyl ammonium bisphosphonic acid. Vinylphosphonic acid is a monophosphonic acid without nitrogen atoms while 3-hydroxypropyl ammonium bisphosphonic acid contains two phosphonic acid moieties and a nitrogen. To confirm this, complexation with a monophosphonic acid with a nitrogen atom was also carried out under acidic conditions. Again, similar complexation properties were observed from ^{1}H NMR (Figure 6.7). The calculated percentage was 34% which was close to the 37% of the bisphosphonic acid. This suggested that the nitrogen

atom played an important role in covalent bonding of phosphonic acid with Carboplatin. A complete comparison of the compound and complexation properties were summarized in Table 6.1.

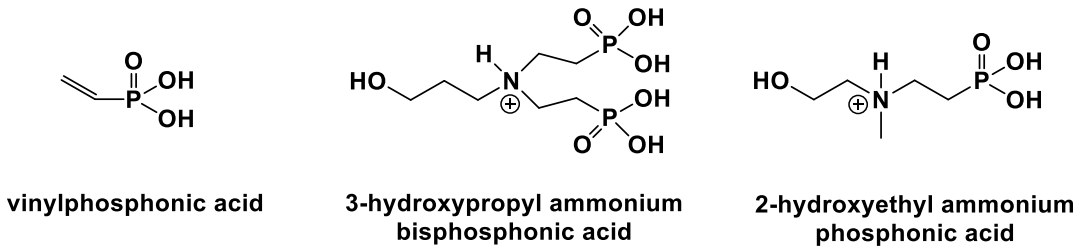

Figure 6.4 Structures of the three model phosphonic acids

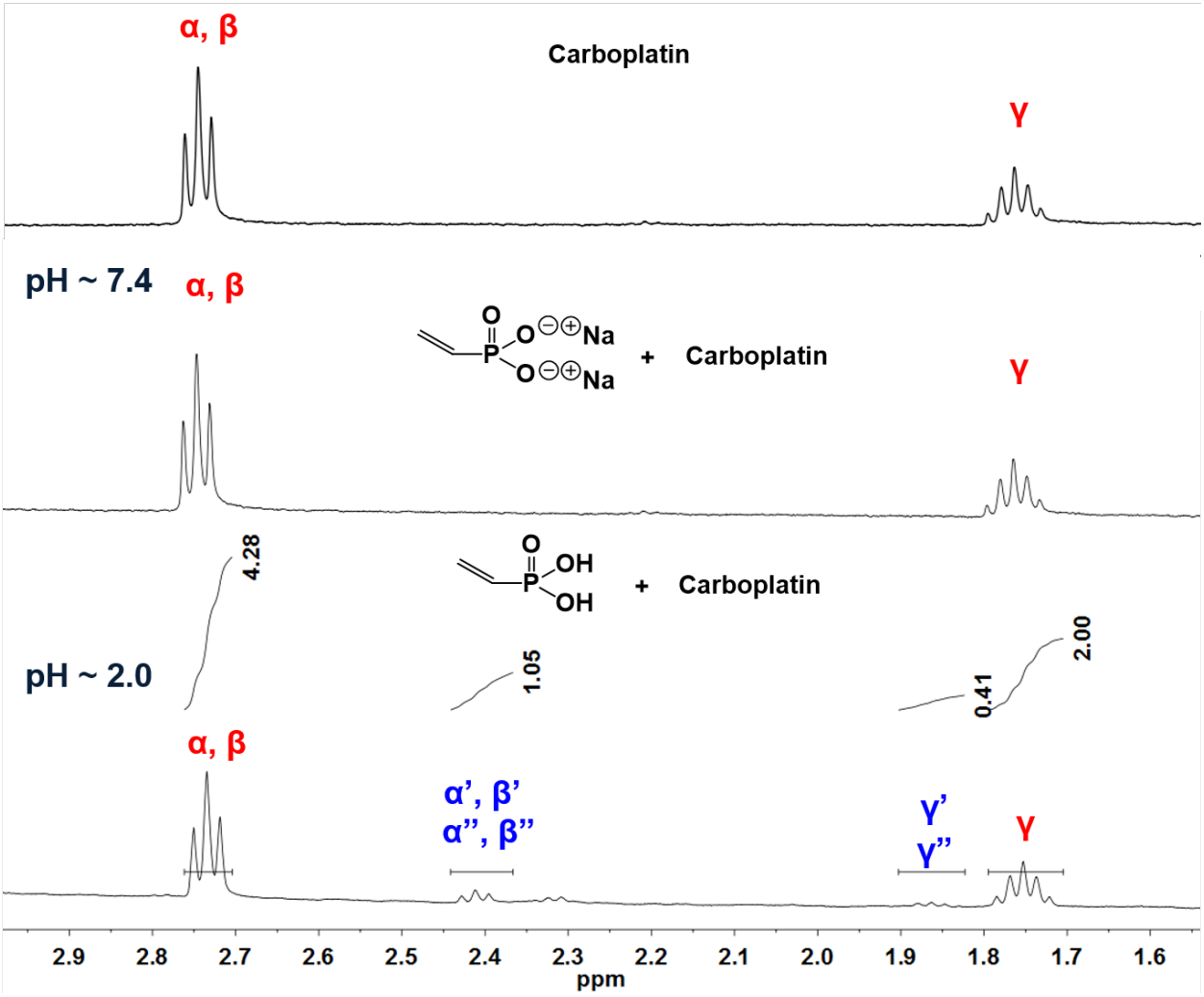

Figure 6.5 ^{1}H NMR spectra of Carboplatin (top) and the complexed products from vinylphosphonic acid and Carboplatin under neutral (middle) and acidic (bottom) conditions

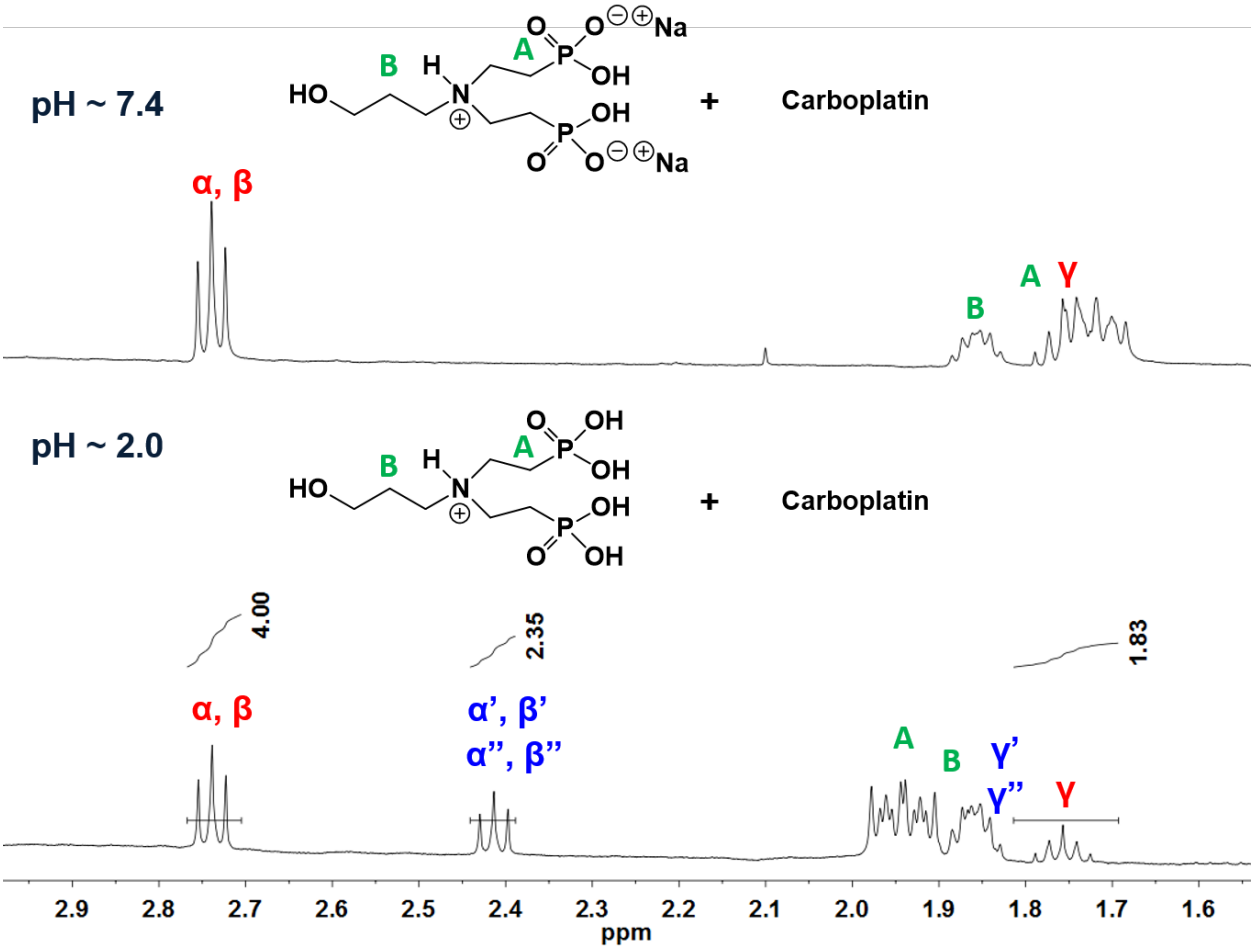

Figure 6.6 ^{1}H NMR spectra of the complexed products from 3-hydroxypropyl ammonium bisphosphonic acid and Carboplatin under neutral (top) and acidic (bottom) conditions

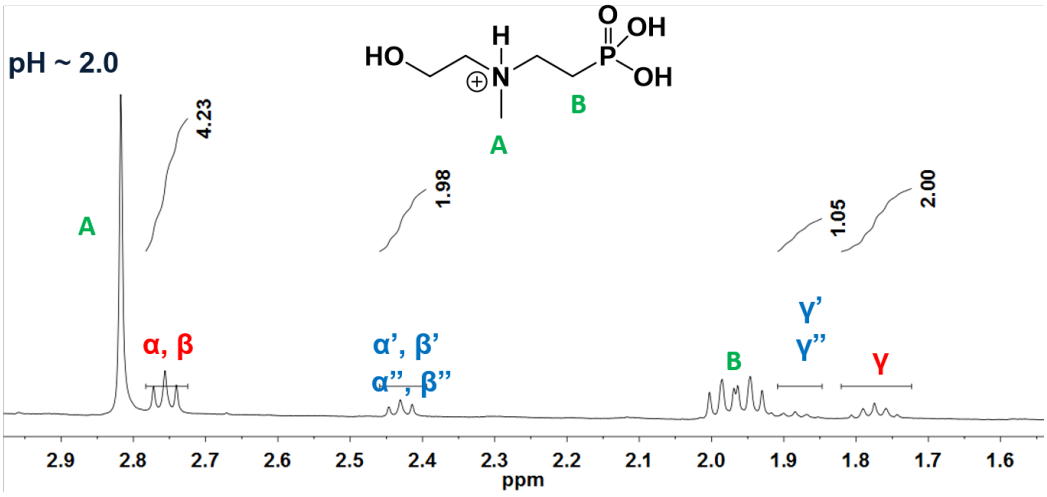

Figure 6.7 ^{1}H NMR spectra of the complexed products from 2-hydroxyethyl ammonium phosphonic acid and Carboplatin under acidic conditions

Table 6.1 Summary of compound and complexation properties

Compounds	Monophosphonic acid	Bisphosphonic acid	Nitrogen atom	Covalent bond percentage (%)
Vinylphosphonic acid	Yes	No	No	17
3-Hydroxypropyl ammonium bisphosphonic acid	No	Yes	Yes	37
2-Hydroxyethyl ammonium phosphonic acid	Yes	No	Yes	34

The reasons why covalent bonds between the phosphonic acids and Carboplatin are only present under acidic condition are not yet clear. In fact, our results are contrary to what others have reported on the complexation of Carboplatin with carbonate. A couple of investigations have indicated that covalent bonding usually occurs when most of the carboxylic acids are in their anionic form.[30, 31] In our case, under acidic conditions the phosphonic acids are almost fully protonated while they are partially deprotonated under neutral conditions. However, the partially deprotonated phosphonic acids did not facilitate the covalent bonding to Carboplatin. This leads

to a hypothesis that the special structure of the phosphonic acid might be part of the reason in forming covalent bonds.

6.5 Conclusions

We complexed three different phosphonic acids with Carboplatin, and all of them showed some extent of covalent bonding to Carboplatin, but only under acidic conditions. The reason for this phenomenon remains unclear. Further investigation should be conducted to characterize the complexed products using UV-visible spectrometry and platinum NMR to obtain a more in-depth understanding of this complexation. Theoretical calculation based on computational analysis of the phosphonic acid-platinum binding might be another powerful tool to study the complexation behavior as well.

6.6 References

1. Canetta, R.; Rozencweig, M.; Carter, S. K., Carboplatin: the clinical spectrum to date. *Cancer Treat. Rev.* 1985, 12, Supplement A, 125-136.

2. Florea, A.-M.; Büsselberg, D., Cisplatin as an Anti-Tumor Drug: Cellular Mechanisms of Activity, Drug Resistance and Induced Side Effects. *Cancers* 2011, 3, 1351-1371.

3. Boulikas, T.; Vougiouka, M., Recent clinical trials using cisplatin, carboplatin and their combination chemotherapy drugs (review). *Oncol. Rep.* 2004, 11, 559-595.

4. Boulikas, T.; Vougiouka, M., Cisplatin and platinum drugs at the molecular level (review). *Oncol. Rep.* 2003, 10, 1663-1682.

5. Hill, J. M.; Speer, R. J., Organo-platinum complexes as antitumor agents (review). *Anticancer Res* 1982, 2, 173-86.

6. Boulikas, T.; Pantos, A.; Bellis, E.; Christofis, P., Designing platinum compounds in cancer: structures and mechanisms. *Cancer Therapy* 2007, 5, 537-583.

7. Wong, E.; Giandomenico, C. M., Current Status of Platinum-Based Antitumor Drugs. *Chem. Rev. (Washington, D. C.)* 1999, 99, 2451-2466.

8. Bontha, S.; Kabanov, A. V.; Bronich, T. K., Polymer micelles with cross-linked ionic cores for delivery of anticancer drugs. *J. Controlled Release* 2006, 114, 163-174.

9. Haxton, K. J.; Burt, H. M., Polymeric drug delivery of platinum-based anticancer agents. *J. Pharm. Sci.* 2009, 98, 2299-2316.

10. Sood, P.; Thurmond, K. B., II; Jacob, J. E.; Waller, L. K.; Silva, G. O.; Stewart, D. R.; Nowotnik, D. P., Synthesis and Characterization of AP5346, a Novel Polymer-Linked Diaminocyclohexyl Platinum Chemotherapeutic Agent. *Bioconjugate Chem.* 2006, 17, 1270-1279.

11. Huynh, V. T.; Chen, G.; Souza, P. d.; Stenzel, M. H., Thiol-yne and Thiol-ene "Click" Chemistry as a Tool for a Variety of Platinum Drug Delivery Carriers, from Statistical Copolymers to Crosslinked Micelles. *Biomacromolecules* 2011, 12, 1738-1751.

12. Rice, J. R.; Gerberich, J. L.; Nowotnik, D. P.; Howell, S. B., Preclinical Efficacy and Pharmacokinetics of AP5346, A Novel Diaminocyclohexane-Platinum Tumor-Targeting Drug Delivery System. *Clin. Cancer Res.* 2006, 12, 2248-2254.

13. Greish, K., Enhanced permeability and retention (EPR) effect for anticancer nanomedicine drug targeting. *Methods Mol. Biol. (Totowa, NJ, U. S.)* 2010, 624, 25-37.

14. Olivi, A.; Ewend, M. G.; Utsuki, T.; Tyler, B.; Domb, A. J.; Brat, D. J.; Brem, H., Interstitial delivery of carboplatin via biodegradable polymers is effective against experimental glioma in the rat. *Cancer Chemother. Pharmacol.* 1996, 39, 90-96.

15. Huynh, V. T.; Quek, J. Y.; de Souza, P. L.; Stenzel, M. H., Block Copolymer Micelles with Pendant Bifunctional Chelator for Platinum Drugs: Effect of Spacer Length on the Viability of Tumor Cells. *Biomacromolecules* 2012, 13, 1010-1023.

16. Mittal, A.; Kurapati, P.; Chitkara, D.; Kumar, N., In vitro release behavior of paclitaxel and carboplatin from poly(-lactide) microspheres dispersed in thermosensitive biodegradable gel for combination therapy. *Int. J. Drug Delivery* 2011, 3, 245-259.

17. Chen, W.; Lu, D. R., Carboplatin-loaded PLGA microspheres for intracerebral injection: formulation and characterization. *J. Microencapsulation* 1999, 16, 551-563.

18. Chen, W.; He, J.; Olson, J. J.; Lu, D. R., Direct intracerebral delivery of carboplatin from PLGA microspheres against experimental malignant glioma in rats. *Drug Delivery* 1998, 5, 101-110.

19. Chen, W.; He, J.; Olson, J. J.; Lu, D. R., Carboplatin-loaded PLGA microspheres for intracerebral implantation: in vivo characterization. *Drug Delivery* 1997, 4, 301-311.

20. Sadhukha, T.; Prabha, S., Encapsulation in Nanoparticles Improves Anti-cancer Efficacy of Carboplatin. *AAPS PharmSciTech* 2014, Ahead of Print.

21. Nanjwade, B. K.; Singh, J.; Parikh, K. A.; Manvi, F. V., Preparation and evaluation of carboplatin biodegradable polymeric nanoparticles. *Int. J. Pharm.* 2010, 385, 176-180.

22. Exner, A. A.; Krupka, T. M.; Scherrer, K.; Teets, J. M., Enhancement of carboplatin toxicity by Pluronic block copolymers. *J. Controlled Release* 2005, 106, 188-197.

23. Pothayee, N.; Pothayee, N.; Hu, N.; Zhang, R.; Kelly, D. F.; Koretsky, A. P.; Riffle, J. S., Manganese graft ionomer complexes (MaGICs) for dual imaging and chemotherapy. *J. Mater. Chem. B* 2014, 2, 1087-1099.

24. Hu, N.; Johnson, L. M.; Pothayee, N.; Pothayee, N.; Lin, Y.; Davis, R. M.; Riffle, J. S., Synthesis of ammonium bisphosphonate monomers and polymers. *Polymer* 2013, 54, 3188-3197.

25. Jamieson, E. R.; Lippard, S. J., Structure, recognition, and processing of cisplatin-DNA adducts. *Chem. Rev. (Washington, D. C.)* 1999, 99, 2467-2498.

26. Ciancetta, A.; Coletti, C.; Marrone, A.; Re, N., Activation of carboplatin by carbonate: a theoretical investigation. *Dalton Trans.* 2012, 41, 12960-12969.

27. Mauldin, S. K.; Plescia, M.; Richard, F. A.; Wyrick, S. D.; Voyksner, R. D.; Chaney, S. G., Displacement of the bidentate malonate ligand from (d,l-trans-1,2-diaminocyclohexane)malonatoplatinum(II) by physiologically important compounds in vitro. *Biochem. Pharmacol.* 1988, 37, 3321-33.

28. Di Pasqua, A. J.; Centerwall, C. R.; Kerwood, D. J.; Dabrowiak, J. C., Formation of Carbonato and Hydroxo Complexes in the Reaction of Platinum Anticancer Drugs with Carbonate. *Inorg. Chem.* 2009, 48, 1192-1197.

29. Di Pasqua, A. J.; Kerwood, D. J.; Shi, Y.; Goodisman, J.; Dabrowiak, J. C., Stability of carboplatin and oxaliplatin in their infusion solutions is due to self-association. *Dalton Trans.* 2011, 40, 4821-4825.

30. Di Pasqua, A. J.; Goodisman, J.; Kerwood, D. J.; Toms, B. B.; Dubowy, R. L.; Dabrowiak, J. C., Role of Carbonate in the Cytotoxicity of Carboplatin. *Chem. Res. Toxicol.* 2007, 20, 896-904.

31. Di Pasqua, A. J.; Goodisman, J.; Kerwood, D. J.; Toms, B. B.; Dubowy, R. L.; Dabrowiak, J. C., Activation of Carboplatin by Carbonate. *Chem. Res. Toxicol.* 2006, 19, 139-149.

32. Di Pasqua, A. J.; Goodisman, J.; Dabrowiak, J. C., Understanding how the platinum anticancer drug carboplatin works: From the bottle to the cell. *Inorg. Chim. Acta* 2012, 389, 29-35.

CHAPTER 7 - Conclusions and Recommendations

We have developed facile methods for synthesizing and characterizing block and graft copolymers that have potential to be used as carriers for drug delivery systems. First, ammonium bisphosphonate methacrylate[1] and acrylamide phosphonate monomers and statistical graft copolymers with PEO grafts have been synthesized. Studies on the solution properties of these graft copolymers in different solvents provided guidelines for preparing complexes with drugs and MRI imaging agents.[2] In collaboration with Dr. Nipon Pothayee in our research group, we have developed a series of manganese graft ionomer complexes containing poly(ammonium bisphosphonate methacrylate)-*g*-PEO copolymer and manganese ions as T_1-weighted contrast agents for MRI.[2] T_1 relaxivities of those complexes were 2-10 times higher than that of a commercially available MRI contrast agent, manganese dipyridoxyl diphosphate (Teslascan®). Anticancer drugs including doxorubicin, cisplatin and carboplatin were encapsulated into the manganese ionomer complexes with high efficiency. Complexes loaded with carboplatin exhibited excellent antiproliferative efficacies against MCF-7 breast cancer cells.

Secondly, a series of heterobifunctional PEO oligomers with different molecular weights and low PDI's were synthesized and subsequently functionalized to yield PEO's with one protected amine and one hydroxyl end group. The hydroxyl group was converted to an alkyl bromide and was utilized as a macroinitiator for ATRP of *t*-butyl acrylate. The resultant diblock copolymers were then deprotected to afford amino functional poly(ethylene oxide-b-acrylic acid) (H_2N-PEO-PAA-Br) diblock copolymers. In collaboration with Dr. Nipon Pothayee, these were utilized to form core-shell nanostructures with magnetite imaging agents bound to the anionic block in the core and with the non-ionic PEO extending outward into water or buffers to stabilize

dispersions of these complexes.[3, 4] The amine groups on the outer termini of the PEO segments were subsequently reacted with a fluorescent dye, fluorescein isothiocyanate (FITC) for assessment of cell uptake.[3] The FITC labeled polymer was complexed with magnetite and encapsulated with gentamicin, a cationic antibiotic. The cell uptake of those drug-loaded complexes were measured by the fluorescent intensity using flow cytometry. Significant cell uptake of the complexes at all concentrations were observed. Alternatively, the amine groups were also utilized to react with multi-functional acrylates to form larger aggregates.[4] For cases where the cargo was comprised of magnetite nanoparticles, when the larger aggregates formed, they were found to have greatly enhanced T_2-weighted NMR relaxivities, and this feature correlates directly with improved image contrast for MRI.

Finally, small-molecule complexation of phosphonic acids with an anticancer drug, Carboplatin, was studied. Three different phosphonic acids were complexed with Carboplatin, and all of them showed some extent of covalent bonding to Carboplatin, but only under acidic conditions.

Further investigation should be carried out on complexation of small-molecule phosphonic acids with Carboplatin at pH 5.5 to assess the complexation behavior through the physiological range (pH 5.5 to pH 7.4). Studies also can be extended to characterize complexation of phosphonic acid-containing model compounds with Carboplatin using UV-visible spectroscopy and platinum NMR to obtain a more in-depth understanding. UV-visible spectroscopy can provide assessment of the progress of the complexation reaction. By analyzing the UV-visible spectra of samples taken at different time intervals, a qualitative estimate of the proceeding of the reaction can be obtained. Conducting platinum NMR on the complexation products might enable detailed understanding of the binding properties. The chemical shift of the

platinum atom in the platinum NMR changes upon replacement of ligands attached onto it. In the case of structure-property relationship of the phosphonic acids/Carboplatin complexes, especially for studying the effect of nitrogen-containing phosphonic acids on the complexation, theoretical calculation based on computational analysis of the phosphonic acid-platinum binding might be another powerful tool as well. Theoretical calculation might provide insight for the conformation and geometry of the binding between the phosphonic acids and Carboplatin.

Another interesting recommendation would be to copolymerize the acrylamide phosphonate with *N*-isopropylacrylamide (NIPAM). Poly(NIPAM) is a well-known thermally responsive polymer.[5] Aqueous solutions of poly(NIPAM) exhibit a lower critical solution temperature (LCST) around 33 °C that is close to body temperature. As the temperature is raised above the LCST, a coil to globule transition occurs, resulting in loss of water that might lead to expulsion of a drug from polymeric carriers in the case of drug delivery. Both the acrylamide phosphonate monomer and NIPAM bear the acrylamido functionality. If a small amount of the acrylamidophosphonate was copolymerized with NIPAM, followed by deprotection of the phosphonate, the resulting copolymer would be poly(NIPAM) with phosphonic anions statistically placed within the backbone (Figure 7.1). This copolymer could serve as a potential drug and imaging agent carrier with thermal sensitivity to trigger drug release. For example, the phosphonate could provide anions to chelate with magnetite and interact with drugs (Figure 7.2). The magnetite could serve as an MRI imaging. Such complexes could also be exposed to alternating current magnetic fields to induce a temperature rise caused by response of the magnetic magnetite nanoparticles.[6] The poly(NIPAM) might also be thermally responsive to induce release of drugs.

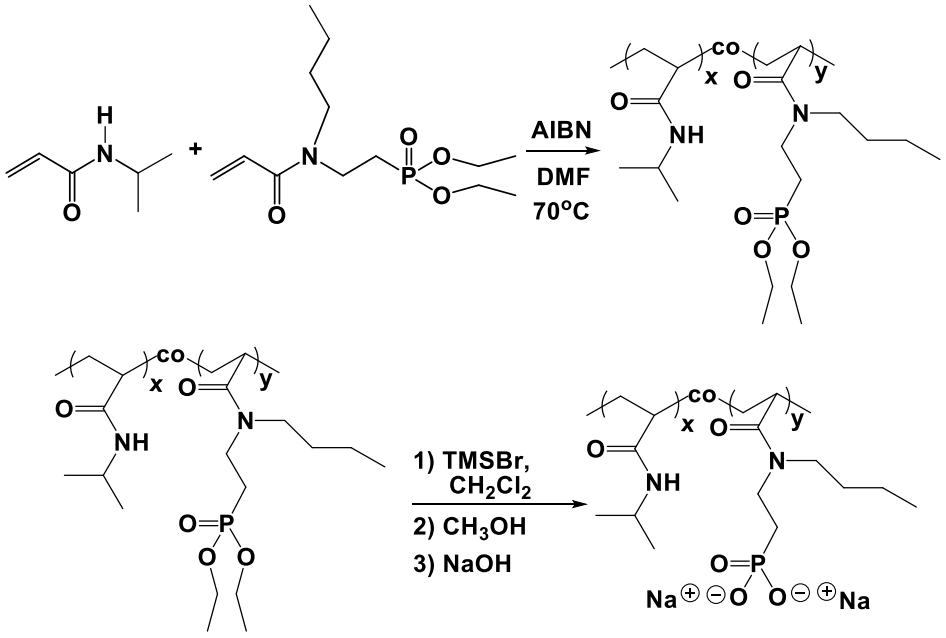

Figure 7.1 Copolymerization of NIPAM with *n*-butylacrylamide phosphonate

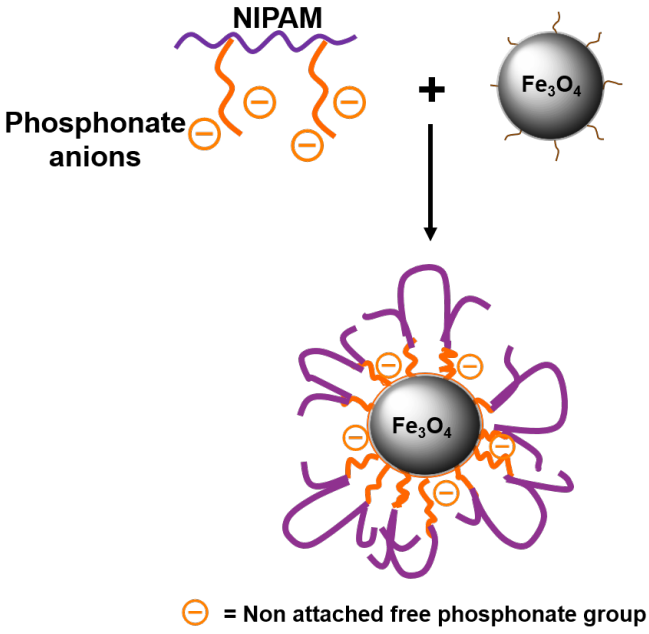

Figure 7.2 Illustration of possible poly(NIPAM)-*g*-poly(*n*-butylacrylamide phosphonate) carriers for drugs and magnetite

References

1. Hu, N.; Johnson, L. M.; Pothayee, N.; Pothayee, N.; Lin, Y.; Davis, R. M.; Riffle, J. S., Synthesis of ammonium bisphosphonate monomers and polymers. *Polymer* 2013, 54, 3188-3197.

2. Pothayee, N.; Pothayee, N.; Hu, N.; Zhang, R.; Kelly, D. F.; Koretsky, A. P.; Riffle, J. S., Manganese graft ionomer complexes (MaGICs) for dual imaging and chemotherapy. *J. Mater. Chem. B* 2014, 2, 1087-1099.

3. Pothayee, N.; Pothayee, N.; Jain, N.; Hu, N.; Balasubramaniam, S.; Johnson, L. M.; Davis, R. M.; Sriranganathan, N.; Riffle, J. S., Magnetic Block Ionomer Complexes for Potential Dual Imaging and Therapeutic Agents. *Chem. Mater.* 2012, 24, 2056-2063.

4. Pothayee, N.; Balasubramaniam, S.; Pothayee, N.; Jain, N.; Hu, N.; Lin, Y.; Davis, R. M.; Sriranganathan, N.; Koretsky, A. P.; Riffle, J. S., Magnetic nanoclusters with hydrophilic spacing for dual drug delivery and sensitive magnetic resonance imaging. *J. Mater. Chem. B* 2013, 1, 1142-1149.

5. Schild, H. G., Poly(N-isopropylacrylamide): experiment, theory and application. *Prog. Polym. Sci.* 1992, 17, 163-249.

6. Hayashi, K.; Ono, K.; Suzuki, H.; Sawada, M.; Moriya, M.; Sakamoto, W.; Yogo, T., High-Frequency, Magnetic-Field-Responsive Drug Release from Magnetic Nanoparticle/Organic Hybrid Based on Hyperthermic Effect. *ACS Appl. Mater. Interfaces* 2010, 2, 1903-1911.